

Status of Big Skate (*Beringraja binoculata*) Off the U.S. Pacific Coast in 2019



Ian G. Taylor¹
Vladlena Gertseva¹
Andi Stephens²
Joseph Bizzarro³

¹Northwest Fisheries Science Center, U.S. Department of Commerce, National Oceanic and Atmospheric Administration, National Marine Fisheries Service, 2725 Montlake Boulevard East, Seattle, Washington 98112

²Northwest Fisheries Science Center, U.S. Department of Commerce, National Oceanic and Atmospheric Administration, National Marine Fisheries Service, 2032 S.E. OSU Drive Newport, Oregon 97365

³Southwest Fisheries Science Center, U.S. Department of Commerce, National Oceanic and Atmospheric Administration, National Marine Fisheries Service, 110 Shaffer Road, Santa Cruz, California 95060

DRAFT SAFE

Disclaimer: This information is distributed solely for the purpose of pre-dissemination peer review under applicable information quality guidelines. It has not been formally disseminated by NOAA Fisheries. It does not represent and should not be construed to represent any agency determination or policy.

This report may be cited as:

Taylor, I.G., Gertseva, V., Stephens, A. and Bizzarro, J. Status of Big Skate (*Beringraja binoculata*) Off the U.S. West Coast, 2019. Pacific Fishery Management Council, Portland, OR. Available from <http://www.pfcouncil.org/groundfish/stock-assessments/>

Acronyms used in this Document

ABC	Allowable Biological Catch
ACL	Annual Catch Limit
AFSC	Alaska Fisheries Science Center
CDFW	California Department of Fish and Wildlife
DFO	Canada's Department of Fisheries and Oceans
DW	Disk Width
IFQ	Individual Fishing Quota
IPHC	International Pacific Halibut Commission
ISW	Interspiracular Width
NMFS	National Marine Fisheries Service
NWFSC	Northwest Fisheries Science Center
ODFW	Oregon Department of Fish and Wildlife
OFL	Overfishing Limit
OY	Optimum Yield
PacFIN	Pacific Fisheries Information Network
PFMC	Pacific Fishery Management Council
SPR	Spawning Potential Ratio
SSC	Scientific and Statistical Committee
SWFSC	Southwest Fisheries Science Center
TL	Total Length
VAST	Vector Autoregressive Spatio-Temporal Package
WCGBT	West Coast Groundfish Bottom Trawl Survey
WCGOP	West Coast Groundfish Observer Program
WDFW	Washington Department of Fish and Wildlife

Status of Big Skate (*Beringraja binoculata*) Off the U.S. Pacific Coast in 2019

Contents

Executive Summary	i
Stock	i
Catches	ii
Data and Assessment	iv
Stock Biomass	v
Recruitment	vii
Exploitation Status	ix
Reference Points	xii
Ecosystem Considerations	xiii
Management Performance	xiii
Unresolved Problems and Major Uncertainties	xiv
Scientific uncertainty	xiv
Decision Table	xiv
Projected Landings, OFLs and Time-varying ACLs	xv
Research and Data Needs	xix
1 Introduction	1
1.1 Biology	1
1.2 Distribution and Life History	2
1.3 Ecosystem Considerations	3
1.4 Fishery Information	4
1.5 Stock Status and Management History	4
1.6 Fisheries Off Alaska, Canada and Mexico	5
1.6.1 Alaska	5
1.6.2 Canada	6
1.6.3 Mexico	6

2 Fishery Data	7
2.1 Data	7
2.2 Fishery Landings and Discards	7
2.2.1 Washington Commercial Skate Landings Reconstruction	7
2.2.2 Oregon Commercial Skate Landings Reconstruction	8
2.2.3 California Catch Reconstruction	9
2.2.4 Tribal Catch in Washington	10
2.2.5 Fishery Discards	10
3 Fishery-Independent Data Sources	11
3.1 Indices of abundance	11
3.1.1 Alaska Fisheries Science Center (AFSC) Triennial Shelf Survey	11
3.1.2 Northwest Fisheries Science Center West Coast Groundfish Bottom Trawl Survey	12
3.1.3 Index Standardization	12
3.1.4 International Pacific Halibut Commission Longline Survey	13
4 Biological Parameters and Data	15
4.1 Measurement Details and Conversion Factors	15
4.2 Fishery dependent length and age composition data	15
4.3 Survey length and age composition data	16
4.4 Environmental or Ecosystem Data Included in the Assessment	17
5 Assessment	18
5.1 Previous Assessments	18
5.2 Model Description	18
5.2.1 Modeling Software	18
5.2.2 Summary of Data for Fleets and Areas	18
5.2.3 Other Specifications	19
5.2.4 Data Weighting	19
5.2.5 Priors	20
5.2.6 Estimated Parameters	23
5.2.7 Fixed Parameters	25
5.3 Model Selection and Evaluation	26

5.3.1	Key Assumptions and Structural Choices	26
5.3.2	Alternate Models Considered	26
5.3.3	Convergence	26
5.4	Response to the Current STAR Panel Requests	27
5.5	Base Case Model Results	30
5.5.1	Parameter Estimates	30
5.5.2	Fits to the Data	31
5.5.3	Uncertainty and Sensitivity Analyses	32
5.5.4	Retrospective Analysis	37
5.5.5	Likelihood Profiles	37
5.5.6	Reference Points	39
6	Harvest Projections and Decision Tables	40
7	Regional Management Considerations	41
8	Research and Data Needs	42
9	Acknowledgments	43
10	References	44
11	Tables	50
11.1	Data Tables	50
11.2	Model Results Tables	56
12	Figures	72
12.1	Data Figures	72
12.2	Biology Figures	87
12.3	Model Results Figures	95
12.3.1	Growth and Selectivity	95
12.3.2	Fits to the Data	101
12.3.3	Time Series Figures	111
12.3.4	Sensitivity Analyses and Retrospectives	116
12.3.5	Likelihood Profiles	128
12.3.6	Reference Points and Forecasts	137

Appendix A. Detailed fits to length composition data	A-1
Appendix B. Figures associated with responses to STAR Requests	B-1
Appendix C. Auxiliary files	B-16

Executive Summary

Stock

This assessment reports the status of the Big Skate (*Beringraja binoculata*) resource in U.S. waters off the West Coast using data through 2018. A map showing the area of the U.S. West Coast Exclusive Economic Zone covered by this stock assessment is provided in Figure a.



Figure a: U.S. West Coast Exclusive Economic zone covering the area in which this stock assessment is focused.

Catches

The majority of Big Skate catch was discarded prior to 1995 when markets for Big Skate and Longnose Skate developed, landings increased, and discarding decreased. The majority of the discards were unrecorded and the landings were in the unspecified skates category. The landings from prior to 1995 were reconstructed separately in each of the three coastal states for this assessment. In general the methods all relied on differences in depth distribution of the different skates species (primarily Big Skate and Longnose Skate). Discards during this period prior to 1995 were estimated outside the model based on an assumption that the average discard rate during the period 1950–1994 was equal to that for Longnose Skate. The current fishery, beginning in 1995, has less uncertainty in landings, lower discard rates, and more data on discards. The discards are estimated within the model for this period using a time-varying retention function. Big Skate have only been landed in their own species category in the past few years (starting in 2015).

In the current fishery (since 1995), annual total landings of Big Skate have ranged between 135-528 mt, with landings in 2018 totaling 173 mt.

Table a: Recent Big Skate landings (mt)

Year	Landings
2008	366.0
2009	205.7
2010	196.2
2011	268.4
2012	269.6
2013	135.0
2014	372.4
2015	331.5
2016	411.5
2017	277.6
2018	172.6

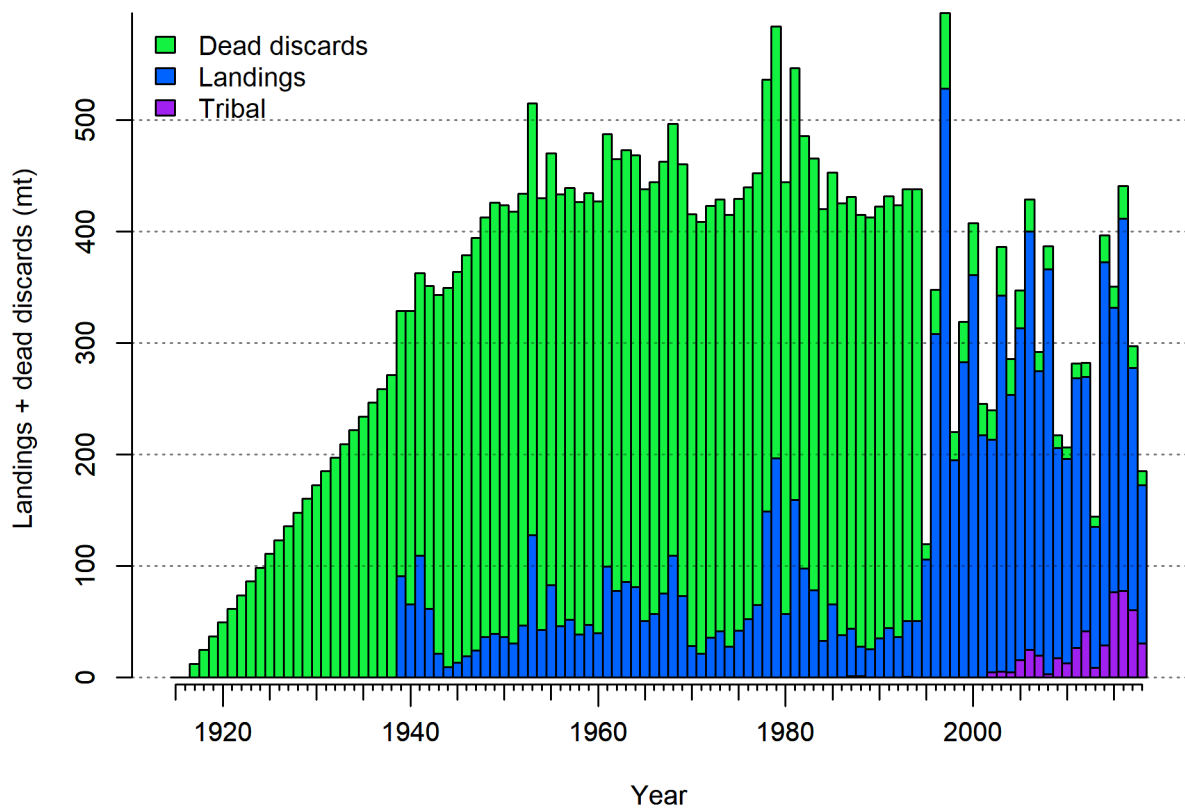


Figure b: Estimated catch history of Big Skate. Discards prior to 1995 were estimated outside the model while those from 1995 onward are estimated internally based on a time-varying retention function.

Data and Assessment

This the first full assessment for Big Skate. It is currently managed using an OFL which was based on a proxy for F_{MSY} and the average survey biomass for the years 2010–2012. This assessment uses the newest version of Stock Synthesis available prior to the review meeting (3.30.13.02). The model begins in 1916, and assumes the stock was at an unfished equilibrium that year. The choice of 1916 is based on the first year of the California catch reconstruction.

The assessment relies on two bottom trawl survey indices of abundance, the Triennial Survey from which an index covering the period 1980–2004 was used here and the West Coast Groundfish Bottom Trawl (WCGBT) Survey, which began in 2003 and for which data is available through 2018. The triennial survey shows an increasing trend over the 25 year period it covers, which the model is not able to fit as this includes the period when trawl fishing in this area was at its most intense and the model stock is expected to have been declining. The WCGBT Survey also shows an increasing trend, with the 5 most recent observations (2014–2018) all falling in the top 6 ever observed (2004 was the 5th highest observation). The model estimates an increasing trend during this period but the slope is more gradual than the trend in the survey observations. The misfit to these survey indices could be due to some combination of incorrect estimation of the catch history, variability in recruitment which is not modeled here, or biological or ecological changes which are also not represented in the model.

Length composition data from the fishery is available starting in 1995 but is sparse until the most recent 10 years. Most of the ages are also from 2008 onward. This limits the ability of the model to estimate any changes in composition of the population during the majority of the history of the fishery. Estimates of discard rates and mean body weight of discards are available for the years 2002 onward and discard length compositions are available starting in 2010.

The age and length data provide evidence for growth patterns and sex-specific differences in selectivity that are unusual among groundfish stocks that have been assessed within the U.S. West Coast and are not found in Longnose Skate, where the data show little difference between the sexes. Growth appears to be almost linear and similar between females and males up to about age 7 or over 100 cm at which point male growth appears to stabilize while females continue to grow. However, in spite of the similar growth pattern for ages prior to 7, males are observed more frequently in the length bins associated with these ages, with the 70–100 cm length bins showing more than 60% males in many years. Sex-specific differences in selectivity were included in the model in order to better match patterns in the sex ratios in the length composition data and a new “growth cessation model” was used to model growth as it provided much better fits than the von Bertalanffy growth function. The length and age data do not cover enough years or show enough evidence of distinct cohorts to reliably estimate deviations in recruitment around the stock-recruit curve, so recruitment in the final model is based directly on the Beverton-Holt stock-recruit curve. Steepness of

this stock-recruit curve was not well-informed by the model so was fixed at the 0.4 value used in a previous Longnose Skate stock assessment.

The final model has 44 estimated parameters, most of which are related to selectivity (including sex-specific differences), time-varying retention, and growth (including sex-specific differences). The remaining 7 parameters include natural mortality, equilibrium recruitment, an extra survey uncertainty parameter for each of the two surveys, and three catchability parameters, where the Triennial Survey is assumed to have a change in catchability starting in 1995 due to changes in survey design.

The scale of the population is not reliably informed by the data due to the combination of surveys that show trends which can't be matched by the structure of the model, and length and age data which inform growth and selectivity but provide relatively little information about changes in stock structure over time. Therefore, a prior on catchability of the WCGBT Survey (centered at 0.701) was applied in order to provide more stable results.

Although the assessment model requires numerous simplifying assumptions, it represents an improvement over the simplistic status-quo method of setting management limits, which relies on average survey biomass and an assumption about F_{MSY} . The use of an age-structured model with estimated growth, selectivity, and natural mortality likely provides a better estimate of past dynamics and the impacts of fishing in the future than the status-quo approach.

Stock Biomass

The 2019 estimated spawning biomass relative to unfished equilibrium spawning biomass is above the target of 40% of unfished spawning biomass at 79.2% (95% asymptotic interval: $\pm 65.5\%-92.9\%$) (Figure c and Table b). Approximate confidence intervals based on the asymptotic variance estimates show that the uncertainty in the estimated spawning biomass is high, although even the lower range of the 95% interval for fraction unfished is above the 40% reference point, and all sensitivity analyses explored also show the stock to be at a relatively high level.

Table b: Recent trend in beginning of the year spawning biomass and fraction unfished (spawning biomass relative to unfished equilibrium spawning biomass)

Year	Spawning Biomass (mt)	~ 95% confidence interval	Fraction Unfished	~ 95% confidence interval
2010	1938.7	(507.5-3369.9)	0.768	(0.616-0.92)
2011	1952.3	(519.8-3384.9)	0.773	(0.624-0.922)
2012	1960.1	(527.3-3393)	0.776	(0.628-0.924)
2013	1969.0	(535.8-3402.1)	0.780	(0.634-0.926)
2014	1991.1	(556-3426.2)	0.789	(0.648-0.93)
2015	1990.4	(556.3-3424.5)	0.788	(0.647-0.929)
2016	1992.8	(559.1-3426.6)	0.789	(0.649-0.929)
2017	1984.9	(552.5-3417.3)	0.786	(0.645-0.927)
2018	1987.9	(555.4-3420.4)	0.787	(0.647-0.927)
2019	1999.3	(565.7-3433)	0.792	(0.655-0.929)

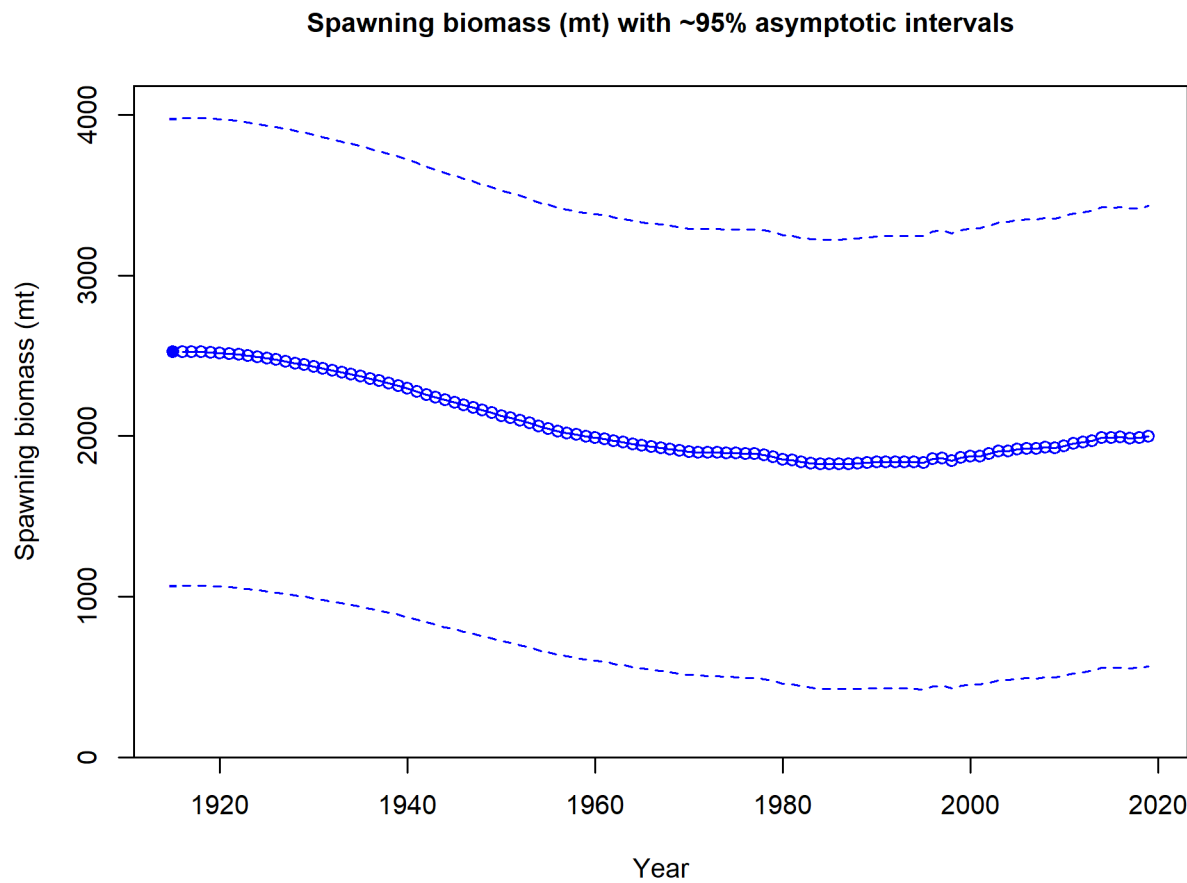


Figure c: Time series of spawning biomass trajectory (circles and line: median; light broken lines: 95% credibility intervals) for the base case assessment model.

Recruitment

Recruitment was assumed to follow the Beverton-Holt stock recruit curve with the steepness parameter fixed at $h = 0.4$, so uncertainty in estimated recruitment is due to uncertainty in the estimated unfished equilibrium recruitment R_0 as well as uncertainty in growth and mortality (Figure d and Table c).

Table c: Recent recruitment for the model.

Year	Estimated Recruitment (1,000s)	~ 95% confidence interval
2010	6617	(3044 - 14385)
2011	6637	(3059 - 14402)
2012	6649	(3068 - 14411)
2013	6662	(3077 - 14420)
2014	6694	(3102 - 14448)
2015	6693	(3102 - 14443)
2016	6697	(3105 - 14442)
2017	6685	(3098 - 14426)
2018	6689	(3102 - 14426)
2019	6706	(3115 - 14438)

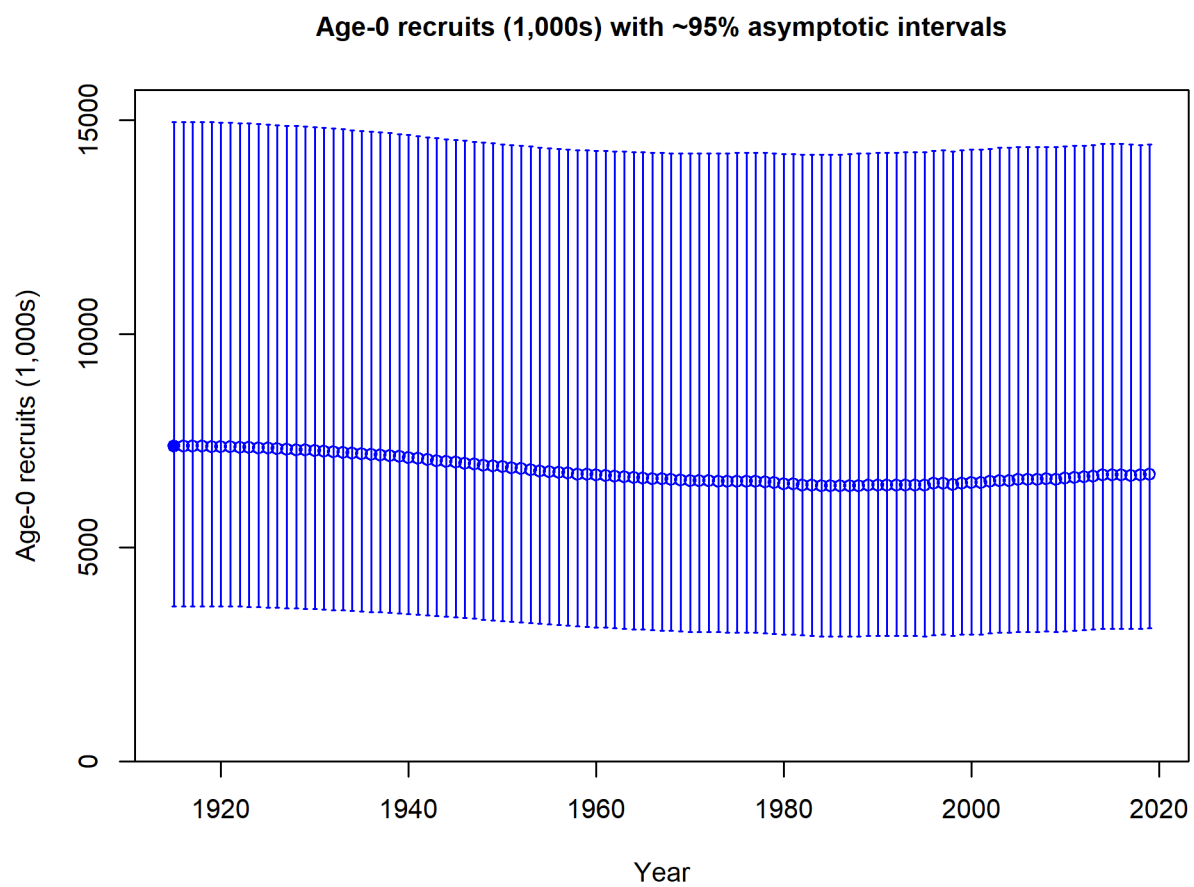


Figure d: Time series of estimated Big Skate recruitments for the base-case model with 95% confidence or credibility intervals.

Exploitation Status

Harvest rates estimated by the base model indicate catch levels have been below the 100% relative fishing intensity upper limit defined as $(1 - SPR)/(1 - SPR_{target})$ (Table d and Figures e and f). SPR is calculated as the lifetime spawning potential per recruit at a given fishing level relative to the lifetime spawning potential per recruit with no fishing. The annual exploitation rate of age 2+ fish has been below 2% over the recent 10-year period.

Table d: Recent trend in spawning potential ratio and exploitation for Big Skate in the model. Relative fishing intensity is $(1-SPR)$ divided by 50% (the SPR target) and exploitation is catch divided by age 2+ biomass.

Year	Relative fishing intensity	~ 95% confidence interval	Exploitation rate	~ 95% confidence interval
2009	0.174	(0.059-0.289)	0.010	(0.003-0.016)
2010	0.165	(0.057-0.273)	0.009	(0.003-0.015)
2011	0.220	(0.079-0.362)	0.012	(0.004-0.02)
2012	0.220	(0.079-0.361)	0.012	(0.004-0.02)
2013	0.115	(0.04-0.191)	0.006	(0.002-0.01)
2014	0.300	(0.114-0.486)	0.017	(0.006-0.028)
2015	0.269	(0.1-0.437)	0.015	(0.005-0.025)
2016	0.332	(0.128-0.537)	0.019	(0.007-0.031)
2017	0.231	(0.084-0.379)	0.013	(0.004-0.021)
2018	0.147	(0.052-0.243)	0.008	(0.003-0.013)

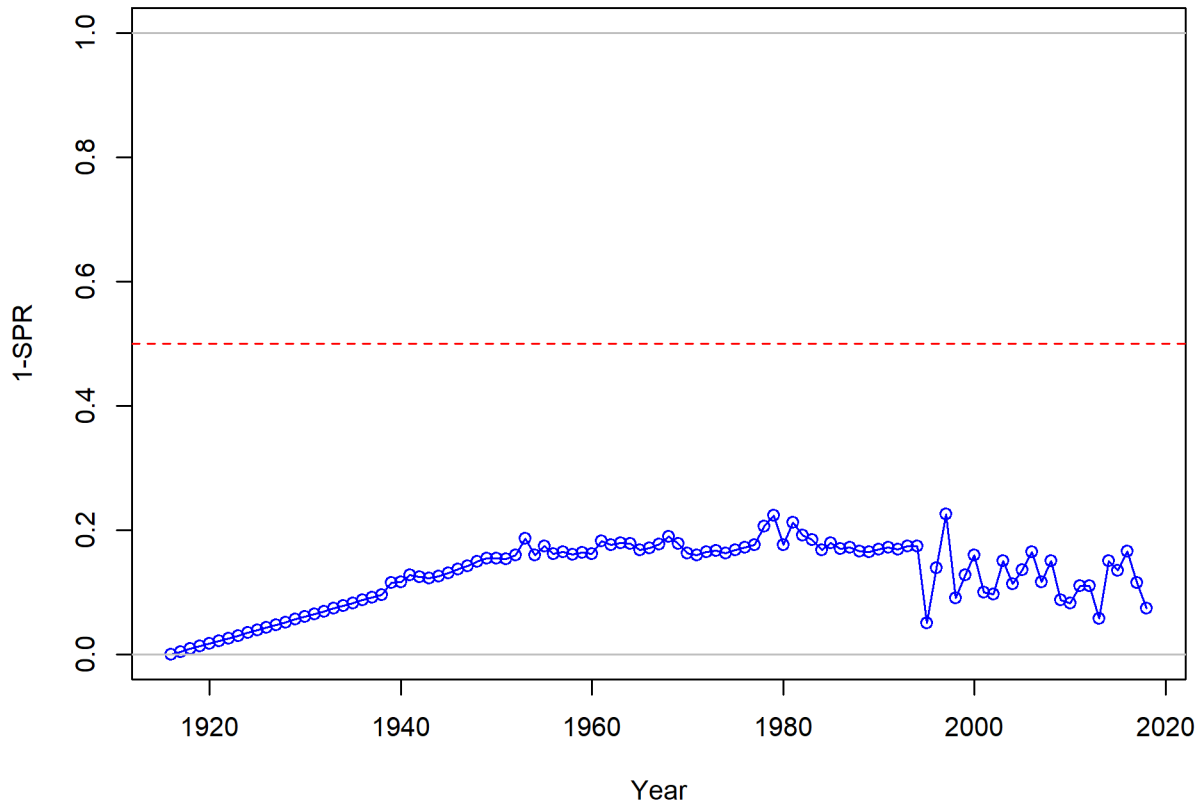


Figure e: Estimated Spawning Potential Ratio (SPR) for the base-case model. One minus SPR is plotted so that higher exploitation rates occur on the upper portion of the y-axis. The management target is plotted as a red horizontal line and values above this reflect harvests in excess of the overfishing proxy based on the SPR_{50%} harvest rate. The last year in the time series is 2018.

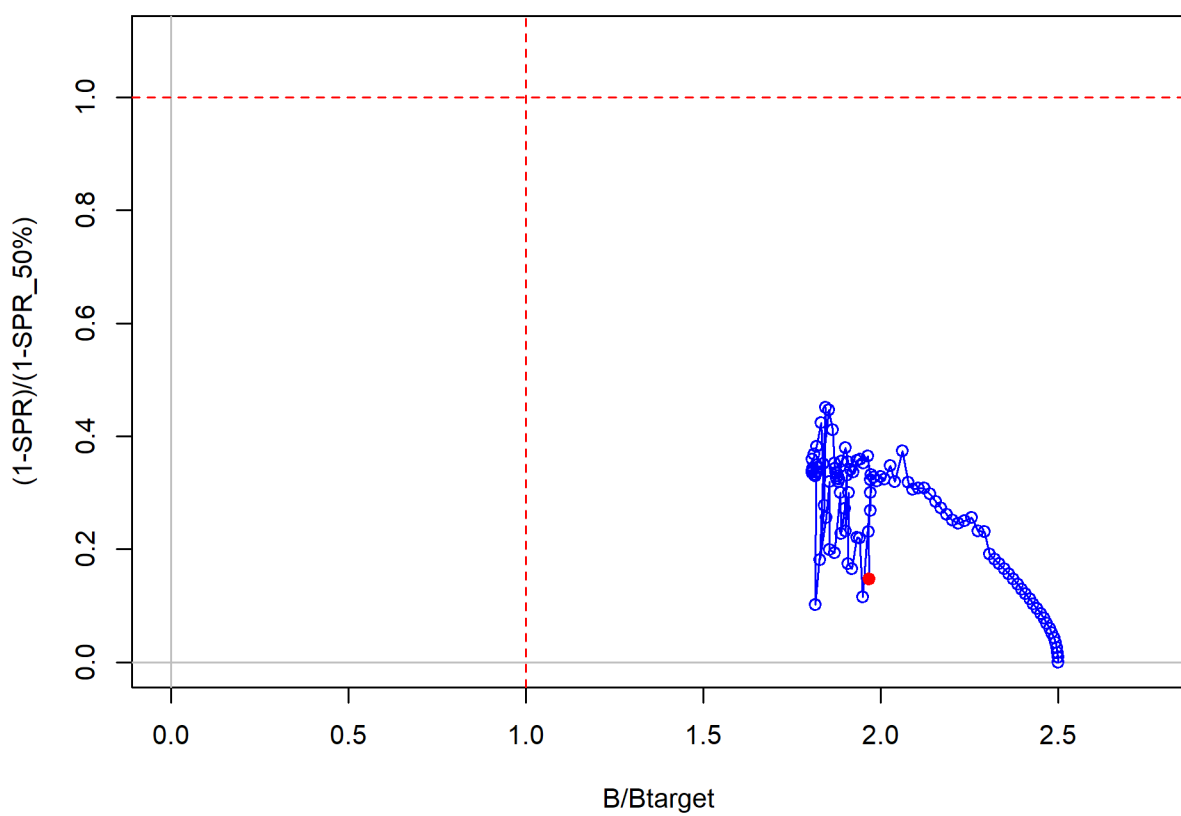


Figure f: Phase plot of biomass vs. fishing intensity.

xi

Reference Points

This stock assessment estimates that Big Skate is above the biomass target ($B_{40\%}$), and well above the minimum stock size threshold ($B_{25\%}$). The estimated fraction unfished level for the base model in 2019 is 79.2% (95% asymptotic interval: $\pm 65.5\%-92.9\%$, relative to an unfished spawning biomass of 2,525 mt (95% asymptotic interval: 1,068-3,981 mt) (Table e). Unfished age 2+ biomass was estimated to be 27,268 mt in the base case model. The target spawning biomass ($B_{40\%}$) is 1,010 mt, which corresponds with an equilibrium yield of 701 mt. Equilibrium yield at the proxy F_{MSY} harvest rate corresponding to $SPR = 50\%$ is 590 mt (Figure g).

Table e: Summary of reference points and management quantities for the base case model.

Quantity	Estimate	Low 2.5% limit	High 2.5% limit
Unfished spawning biomass (mt)	2,525	1,068	3,981
Unfished age 2+ biomass (mt)	27,268	12,854	41,683
Unfished recruitment (R_0 , thousands)	7,366	1,974	12,759
Spawning biomass (2019 mt)	1,999	566	3,433
Fraction unfished (2019)	0.792	0.655	0.929
Reference points based on $B_{40\%}$			
Spawning biomass ($B_{40\%}$)	1,010	427	1,592
SPR resulting in $B_{40\%}$ ($SPR_{B40\%}$)	0.625	0.625	0.625
Exploitation rate resulting in $B_{40\%}$	0.048	0.042	0.055
Yield with $SPR_{B40\%}$ at $B_{40\%}$ (mt)	701	316	1,086
Reference points based on $SPR = 50\%$ proxy for MSY			
Spawning biomass (mt)	505	214	796
SPR_{proxy}	0.5		
Exploitation rate corresponding to $SPR = 50\%$	0.071	0.061	0.08
Yield with $SPR = 50\%$ at $B_{SPR=50\%}$ (mt)	590	266	915
Reference points based on estimated MSY values			
Spawning biomass at MSY (B_{MSY})	944	393	1,496
SPR_{MSY}	0.609	0.604	0.614
Exploitation rate at MSY	0.051	0.045	0.057
Dead Catch MSY (mt)	703	316	1,089
Retained Catch MSY (mt)	650	294	1,005

Ecosystem Considerations

Big Skate have broad thermal tolerances and are broadly distributed, occurring from the southeastern Bering Sea to southern Baja California and the Gulf of California. They have been reported at depths of 2-501 m but are most common on the inner continental shelf (< 100 m). Big Skates are opportunistic predators with highly variable spatio-temporal trophic roles.

In this assessment, neither environmental nor ecosystem considerations were explicitly included in the analysis. This is primarily due to a lack of relevant data or results of analyses that could contribute ecosystem-related quantitative information for the assessment.

Management Performance

Annual Catch Limits have only been in place for Big Skate in recent years and total catch, including discards has remained below these limits with the exception of 2014, where in retrospect the catch was above the ACL although still below the Overfishing Limit (Table f).

Table f: Recent trend in total catch (mt) relative to the management guidelines. Big skate was managed in the Other Species complex in 2013 and 2014, designated an Ecosystem Component species in 2015 and 2016, and managed with stock-specific harvest specifications since 2017. Estimated total mortality includes dead discards estimated in the model (assuming a discard mortality rate of 50%).

Year	OFL (mt; ABC prior to 2011)	ABC (mt)	ACL (mt; OY prior to 2011)	Landings (mt)	Estimated total mortality (mt)
2009				205.7	217.2
2010				196.2	206.6
2011				268.4	282.0
2012				269.6	282.4
2013	458	317.9	317.9	135.0	144.3
2014	458	317.9	317.9	372.5	396.9
2015				331.6	350.6
2016				411.5	440.7
2017	541	494.0	494.0	277.6	297.2
2018	541	494.0	494.0	172.6	185.4
2019	541	494.0	494.0		
2020	541	494.0	494.0		

Unresolved Problems and Major Uncertainties

The data provide little information about the scale of the population, necessitating the use of a prior on catchability to maintain stable model results. During the review panel the prior was updated from the one developed in the 2007 Longnose Skate stock assessment to better account for Big Skate occurrences in shallower water than the surveyed region, but further refinement of this prior could be considered in the future.

There is little evidence that the population is overfished or experiencing overfishing, but forecasts of overfishing limits vary considerably among the sensitivity analyses explored (though all remain well above the recent average catch).

The fit to the length data was significantly improved by estimating a difference between female and male selectivity, with females having a lower maximum selectivity than males, but the behavioral processes that might contribute to this difference are not understood.

Scientific uncertainty

The Sigma values associated with the 2019 spawning biomass (calculated from the normal approximation and converted to the log-standard deviation of a lognormal distribution) was 0.35, well below the minimum 1.0 value associated with Category 2, the most likely classification for this assessment.

Decision Table

The catchability of the WCGBT Survey was chosen as the axis of uncertainty during the STAR panel given the importance of this value in determining the scale of the population and the influence of the prior distribution on this quantity. The high state of nature had $\log(q) = -0.766$, $q = 0.465$ and was chosen based on 1.15 units of standard deviation in the estimated $\log(q)$ parameter from the base model. The 2019 spawning biomass for the high state of nature was close to the 87.5% quantile of the base model. The low state of nature had $\log(q) = 0.223$, $q = 1.250$ and was chosen to approximate the 12.5% quantile of the 2019 spawning biomass in the base model as the method of using 1.15 units of standard deviation was closer to the 25% quantile.

Based on input from the Groundfish Management Team representative to the STAR panel, the catch streams chosen for the decision table were a constant catch of 250 mt per year (based on recent low catch values), a constant catch of 494 mt per year (based on the status quo harvest limits), and the ACL = ABC from the base model assuming a Category 2 sigma and $P^* = 0.45$.

Projected Landings, OFLs and Time-varying ACLs

Potential OFLs projected by the model are shown in Table g. These values are based on an SPR target of 50%, a P* of 0.45, and a time-varying Category 2 Sigma which creates the buffer shown in the right-hand column. The OFL and ACL values for 2019 and 2020 are the current harvest specifications (also shown in Table f) while the landings for 2019 and 2020 represent the average landings over the most recent 5 years (2014–2018).

Table g: Projections of landings, total mortality, OFL, and ACL values. For 2019 and 2020, mortality estimates were provided by the Groundfish Management Team based on recent trends in catch. For 2021 and beyond, estimated total mortality is assumed equal to the ACL in each year.

Year	Landings (mt)	Estimated total mortality (mt)	OFL (mt)	ACL (mt)	Buffer
2019	225.2	241.3	541.0	494.0	
2020	225.3	241.3	541.0	494.0	
2021	1374.8	1476.8	1689.6	1476.8	0.874
2022	1290.6	1389.0	1605.8	1389.0	0.865
2023	1224.8	1320.5	1540.8	1320.5	0.857
2024	1174.0	1267.1	1492.4	1267.1	0.849
2025	1134.3	1224.4	1455.9	1224.4	0.841
2026	1100.3	1187.7	1425.8	1187.7	0.833
2027	1070.2	1155.0	1398.3	1155.0	0.826
2028	1039.9	1122.0	1371.6	1122.0	0.818
2029	1010.1	1089.7	1345.3	1089.7	0.810
2030	982.0	1059.3	1319.2	1059.3	0.803

Table h: Summary of 12-year projections beginning in 2019 for alternate states of nature based on the axis of uncertainty for the model. Columns range over low, mid, and high states of nature associated with WCGBT Survey catchability values of 0.960 for the low state, 0.668 for the base state, and 0.465 for the high state (where higher catchability is associated with lower stock size). Rows range over different assumptions of catch levels.

		States of nature						
		Low State (q=0.960)			Base State (q=0.668)		High State (q=0.465)	
	Year	Catch	Spawning Biomass	Fraction Unfished	Spawning Biomass	Fraction Unfished	Spawning Biomass	Fraction Unfished
Low catch, 250 mt	2019	241.3	1130	0.629	1999	0.792	2829	0.854
	2020	241.3	1137	0.633	2005	0.794	2834	0.855
	2021	250.0	1145	0.638	2012	0.797	2840	0.857
	2022	250.0	1154	0.643	2019	0.800	2847	0.859
	2023	250.0	1165	0.649	2028	0.803	2856	0.862
	2024	250.0	1177	0.655	2039	0.808	2865	0.865
	2025	250.0	1189	0.662	2049	0.812	2875	0.868
	2026	250.0	1200	0.668	2057	0.815	2882	0.870
	2027	250.0	1208	0.673	2063	0.817	2888	0.872
	2028	250.0	1214	0.676	2067	0.819	2891	0.873
	2029	250.0	1218	0.678	2070	0.820	2894	0.873
	2030	250.0	1223	0.681	2074	0.821	2896	0.874
Middle catch, 494 mt	2019	241.3	1130	0.629	1999	0.792	2829	0.854
	2020	241.3	1137	0.633	2005	0.794	2834	0.855
	2021	494.0	1145	0.638	2012	0.797	2840	0.857
	2022	494.0	1131	0.630	1997	0.791	2825	0.853
	2023	494.0	1119	0.623	1984	0.786	2812	0.849
	2024	494.0	1107	0.617	1971	0.781	2799	0.845
	2025	494.0	1095	0.610	1958	0.776	2786	0.841
	2026	494.0	1082	0.602	1944	0.770	2772	0.836
	2027	494.0	1066	0.594	1929	0.764	2756	0.832
	2028	494.0	1051	0.585	1914	0.758	2740	0.827
	2029	494.0	1038	0.578	1900	0.753	2727	0.823
	2030	494.0	1027	0.572	1890	0.749	2717	0.820
Default harvest, for base state	2019	241.3	1130	0.629	1999	0.792	2829	0.854
	2020	241.3	1137	0.633	2005	0.794	2834	0.855
	2021	1476.8	1145	0.638	2012	0.797	2840	0.857
	2022	1389.0	1040	0.579	1908	0.756	2737	0.826
	2023	1320.5	943	0.525	1812	0.718	2642	0.797
	2024	1267.1	852	0.475	1724	0.683	2554	0.771
	2025	1224.5	768	0.428	1641	0.650	2471	0.746
	2026	1187.7	690	0.384	1563	0.619	2394	0.722
	2027	1155.0	620	0.345	1492	0.591	2323	0.701
	2028	1122.0	560	0.312	1432	0.567	2263	0.683
	2029	1089.6	512	0.285	1385	0.549	2218	0.669
	2030	1059.3	473	0.263	1353	0.536	2187	0.660

Table i: Base case results summary.

Quantity	2010	2011	2012	2013	2014	2015	2016	2017	2018	2019
Landings (mt)	225.2	225.3	1374.8	1290.6	1224.8	1174.0	1134.3	1100.3	1070.2	1039.9
Total Est. Catch (mt)	241.3	241.3	1476.8	1389.0	1320.5	1267.1	1224.4	1187.7	1155.0	1122.0
OFL (mt)	541.0	541.0	1689.6	1605.8	1540.8	1492.4	1455.9	1425.8	1398.3	1371.6
ACL (mt)	494.0	494.0	1476.8	1389.0	1320.5	1267.1	1224.4	1187.7	1155.0	1122.0
(1-SPR)(1-SPR _{50%})	0.16	0.22	0.22	0.12	0.30	0.27	0.33	0.23	0.15	
Exploitation rate	0.01	0.01	0.01	0.01	0.02	0.02	0.02	0.01	0.01	
Age 2+ biomass (mt)	22838.5	22993.9	23136.9	23191.8	23240.0	23409.4	23327.4	23308.8	23217.2	23278.8
Spawning Biomass	1938.7	1952.3	1960.1	1969.0	1991.1	1990.4	1992.8	1984.9	1987.9	1999.3
95% CI	(507.5-3369.9)	(519.8-3384.9)	(527.3-3393)	(535.8-3402.1)	(556-3426.2)	(556.3-3424.5)	(559.1-3426.6)	(552.5-3417.3)	(555.4-3420.4)	(565.7-3433)
Fraction Unfished	0.8	0.8	0.8	0.8	0.8	0.8	0.8	0.8	0.8	0.8
95% CI	(0.616-0.92)	(0.624-0.922)	(0.628-0.924)	(0.634-0.926)	(0.648-0.93)	(0.647-0.929)	(0.649-0.929)	(0.645-0.927)	(0.647-0.927)	(0.655-0.929)
Recruits	6617	6637	6649	6662	6694	6693	6697	6685	6689	6706
95% CI	(3044 - 14385)	(3059 - 14402)	(3068 - 14411)	(3077 - 14420)	(3102 - 14448)	(3102 - 14443)	(3105 - 14442)	(3098 - 14426)	(3102 - 14426)	(3115 - 14438)

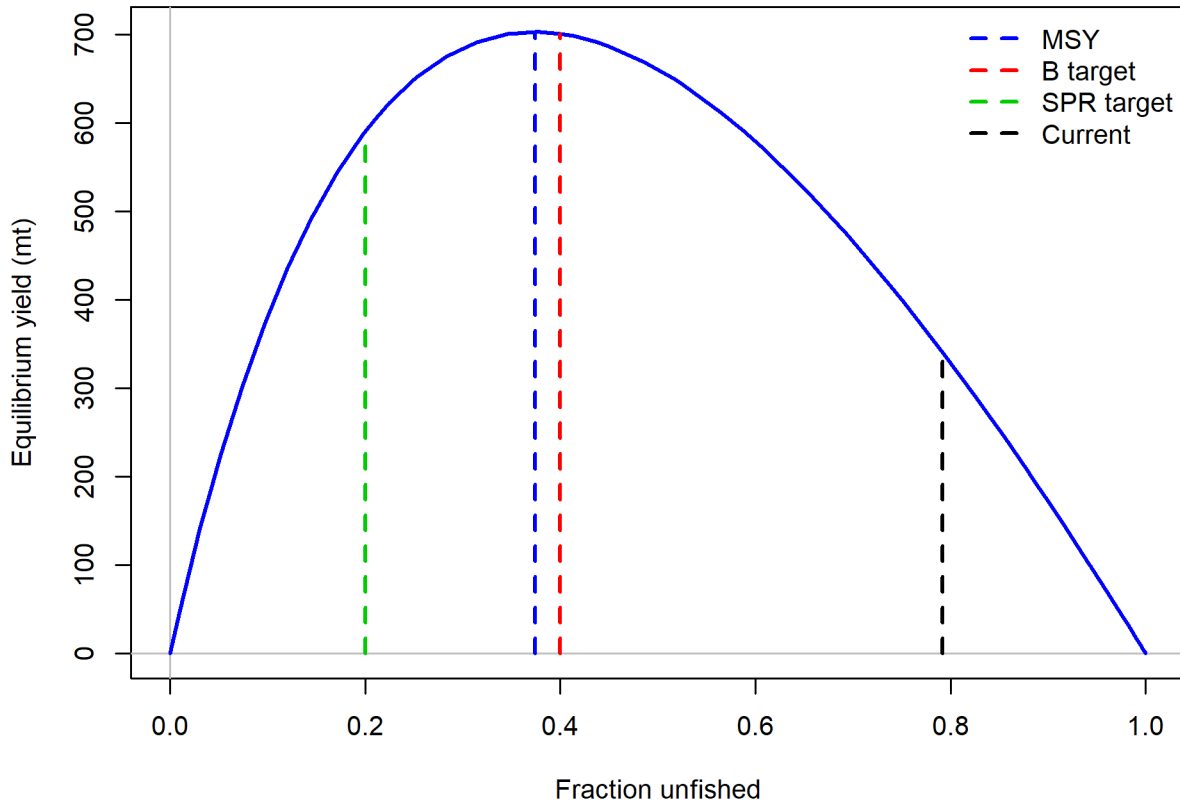


Figure g: Equilibrium yield curve for the base case model. Values are based on the 2018 fishery selectivity and retention with steepness fixed at 0.4.

Research and Data Needs

We recommend the following research be conducted before the next assessment.

1. **Extend all ongoing data streams used in this assessment.** A longer fishery-independent index from a continued WCGBT Survey with associated compositions of length and age-at-length will improve understanding of dynamics of the stock. Continued sampling of lengths and ages from the landed catch and lengths, mean body weights, and discard rates from the fishery will be even more valuable for the years ahead now that Big Skate are landed as a separate market category and the estimates will be more precise.
2. **Investigate factors contributing to estimated lower selectivity for females than males.** Sex-specific differences in selectivity were included in the base model to better fit differences in sex ratios in the length composition data but the behavioral processes that might contribute to this pattern are not understood and other explanations for the sex ratios are possible.
3. **Pursue additional approaches for estimating historical discards.** The approaches used here were based on averages applied over a period of decades. The catch reconstructions conducted for each state were much more sophisticated, but were applied only to the subset of the catch that was landed. Reconstructed spatial patterns of fishing effort could be used to estimate changes in total mortality over time.
4. **Improve understanding of links between Big Skate on the U.S. West Coast and other areas.** Tagging studies in Alaska indicated that Big Skate are capable of long distance movements. A better understanding of links through tagging in other areas and genetic studies could highlight strengths or weaknesses of the status quo approach.
5. **Conduct studies of mortality of discarded skates in commercial fisheries.** Estimates of discard mortality for skates in general could be improved.
6. **Improve understanding of catch history and population dynamics of California Skate.** California Skate is the third most commonly occurring Skate in California waters after Longnose Skate and Big Skate and the catch reconstruction indicated that the center of abundance for California Skate is centered around San Francisco, where the fishery was strongest in the early years. If California Skate is found to be at a low biomass compared to historical levels it would have implications for the catch reconstruction of the other two species, as well as suggesting that management of California Skate should be a higher priority.

1 Introduction

Skates are the largest and most widely distributed group of batoid fish with approximately 245 species ascribed to two families (Ebert et al. (2007), McEachran et al. (1990)). Skates are benthic fish that are found in all coastal waters but are most common in cold temperatures and polar waters (Ebert et al. 2007).

There are eleven species of skates in three genera (*Amblyraja*, *Bathyraja*, and *Raja*) present in the Northeast Pacific Ocean off California, Oregon and Washington (Ebert 2003). Of that number, just three species (Longnose Skate, *Beringraja rhina*; Big Skate, *Beringraja binoculata*; and Sandpaper Skate, *Bathyraja interrupta*) make up over 95 percent of West Coast Groundfish Bottom Trawl Survey (WCGBTS) catches in terms of biomass and numbers, with the Longnose Skate leading in both categories (with 62 percent of biomass and 56 percent of numbers).

Big Skate (*Beringraja binoculata*) is the largest of the skate species in North America with a documented maximum length of 244 cm total length and a maximum weight of 91 kg (Eschmeyer et al. 1983). The species name “binoculata” (two-eyed) refers to the prominent ocellus at the base of each pectoral fin. Big Skates are usually seen buried in sediment with only their eyes showing.

1.1 Biology

Big Skate is oviparous, and is one of two skate species that have multiple embryos per egg case (Ebert et al. 2008). From 1–8 embryos can be contained in a single, large egg capsule, but most have 3–4 (DeLacy et al. 1935, Hitz 1964, Ford 1971). Eggs are deposited year-round on sand or mud substrates at depths of ~50–150 m (Hitz 1964, Ebert et al. 2007). Embryos hatch from eggs after 6–20 months, with shorter developmental periods associated with warmer temperatures (Hoff, GR 2009). In captivity, Big Skate females may produce > 350 eggs/year (average of 2 embryos/egg case; Chiquillo et al. (2014)) from long-term sperm storage . Size at birth is 18–23 cm TL (Ebert 2003). Maximum size is 244 cm TL (Eschmeyer et al. 1983), with females growing to larger sizes.

Size at maturity has been variably estimated for Big Skate populations off California, British Columbia, and Alaska. Off central California, Zeiner and Wolf (1993) reported sizes at first maturity of ~129 cm TL (females) and ~100 cm TL (males). A similar size at maturity was estimated for females from the Gulf of Alaska (first = 126 cm TL, 50% = 149 cm TL), but male estimates were considerably greater (first = 124 cm TL, 50% = 119 cm TL; Ebert et al. (2008)). Much smaller sizes at first (female = 60 cm TL, male = 50 cm TL) and 50% (female = 90 cm TL, male = 72 cm TL) maturity were generated for the Longnose Skate populations off British Columbia (GA et al. 2006); however, maturity evaluation criteria were flawed (subadults were considered to be mature), and these results are therefore not considered valid.

Age and growth parameters have been established from California, British Columbia, and the Gulf of Alaska. Maximum ages off central California (females = 12, males = 11; Zeiner, S.J. and P. Wolf. (1993)) and in the Gulf of Alaska (females = 14, males = 15; Gburski et al. 2007) were similar, but estimates off British Columbia were much greater (females = 26, males = 25; McFarlane and King 2006). It is important to note that age estimates are based on an unvalidated method and geographic differences in size or age may reflect differences in sampling or ageing criteria. In the Gulf of Alaska, Big Skates reach 50% maturity at 10 years and 7 years for females and males, respectively (Gburski et al. (2007), Ebert et al. (2008)). Generation length estimates range from 11.5 (Zeiner, S.J. and P. Wolf. 1993) to 17 years (GA et al. 2006).

Table 1: Regional comparison of life history parameter estimates.

	California		British Columbia		Gulf of Alaska	
	Female	Male	Female	Male	Female	Male
1st Maturity (TL cm)	129	100	60	50	126	124
50% Maturity (TL cm)			90	72	149	119
Max Age (year)	12	11	26	25	14	15
1st Maturity (year)	12	10	6	5	7	9
50% Maturity (year)			8	10	10	7

1.2 Distribution and Life History

The Big Skate is most common in soft-sediment habitats in coastal waters of the continental shelf (Bizzarro et al. (2014), Farrugia et al. (2016)). Use of mixed substrate (e.g., mud with boulders) increases with ontogeny but hard substrates are largely avoided (Bizzarro (2015)). In the GOA, the Big Skate is the most commonly encountered skate species in continental shelf waters at 100–200 m depth, and is most abundant in the central and western areas of the GOA (Stevenson et al. (2008); Bizzarro et al. (2014)). Off the U.S. Pacific Coast, the Big Skate is most densely distributed on the inner continental shelf (< 100 m; Bizzarro et al. (2014)). Eggs are mainly deposited between 70–90 m on sand or mud substrates (Hitz (1964); NMFS-NWFSC-FRAM, unpub. data). Juveniles typically occur in shallower waters than adults (Bizzarro (2015)). Core habitat regions of Big Skate off the U.S. Pacific Coast and in the Gulf of Alaska are spatially segregated from those of other species (Bizzarro et al. (2014)).

Big Skates are highly mobile and capable of long range (> 2000 km) movements (King, JR and McFarlane, GA (2010); Farrugia et al. (2016)). For example, in British Columbia, a study revealed that ~75% of tagged individuals were recaptured within 21 km of the tagging locations, but 15 of the tagged individuals (0.1%) moved over 1,000 km (max = 2340 km; King, JR and McFarlane, GA (2010)). In the Gulf of Alaska, a year of satellite tag data showed that six of twelve tagged individuals moved over 100 km, with one skate moving >

2,000 km (Farrugia et al. 2016). Although primarily benthic, Big Skates utilize the entire water column including surface waters (Farrugia et al. (2016)). They have broad thermal tolerances 2–19° C that enable their occurrence from boreal to subtropical latitudes (Love, Milton S (2011); Farrugia et al. (2016)).

The Big Skate is broadly distributed, occurring from the southeastern Bering Sea (Mecklenburg et al. 2002) to southern Baja California (22.90° N, 110.03° W; (Castro-Aguirre et al. 1993)) and the Gulf of California (Castro-Aguirre et al. 1996). It has been reported at depths of 2–501 m (min: Miller et al. (1980); max: Farrugia et al. (2016)) but is most common on the inner continental shelf (< 100 m; (Love, Milton S 2011); (Bizzarro 2015)). Big Skates are highly mobile and capable of long range (> 2000 km) movements ((King et al. 2009); (Farrugia et al. 2016)).

In 2012, the Big Skate was moved from genus *Raja* to the new genus *Beringraja* together with the Mottled Skate (*B. pulchra*) (Ishihara et al. 2012). These are the only two skates with multiple embryos per egg case, and they are very similar morphologically and genetically (Bizzarro, J. 2019). More recently, Longnose Skate has also moved to *Beringraja* (Last et al. 2016).

1.3 Ecosystem Considerations

Big Skates are opportunistic, generalist mesopredators with highly variable spatio-temporal trophic roles (Ebert et al. (2007); Bizzarro (2015)). Off central California, diet of Big Skates is composed mainly of fishes, shrimps, and crabs (in descending order), with larger skates incorporating more fishes (Bizzarro et al. (2007)); however, in the Gulf of Alaska, Big Skate diet consists mainly of crabs (esp. Tanner Crabs) throughout ontogeny, with relatively small portions of fishes and shrimps (Bizzarro (2015)). Correspondingly, trophic level and general diet composition estimates differ significantly between California and Gulf of Alaska Big Skate populations (Bizzarro (2015)).

Big Skates and their egg cases are preyed upon by a variety of vertebrates and invertebrates. Snails and other molluscs bore holes in egg cases to feed on developing embryos and especially their protein rich yolk-sacs (Bizzarro, pers. obs; Hoff, GR (2009)). Sevengill Sharks, Brown Rockfish, and Stellar Sea Lions are known predators of juvenile and adult Big Skates (Ebert (2003), Love, Milton S (2011)). Northern Sea Lions consume free-living Big Skates and their egg cases (Ebert (2003), Love, Milton S (2011)).

In this assessment, neither environmental nor ecosystem considerations were explicitly included in the analysis. This is primarily due to a lack of relevant data or results of analyses that could contribute ecosystem-related quantitative information for the assessment.

1.4 Fishery Information

Big Skate are caught in commercial and recreational fisheries on the West Coast using line and trawl gears. There is a limited market for pectoral fins (skate wings).

The history of Big Skate is not well documented. They were used as a food source by the native Coastal and Salish Tribes (Batdorf, C [1990](#)) long before Europeans settled in the Pacific Northwest and then as fertilizer by the settlers (Bowers, G. M. [1909](#)). No directed fishery for Big Skate has been documented; rather, they were taken along with other skates and rays as “scrap fish” and used for fertilizer, fish meal and oil ([Lippert 2019](#)).

Skates have been regarded as a predator on desirable market species such as Dungeness crab, and were thought of as nuisance fish with no appeal as a food item save for small local markets. They had been discarded or harvested at a minimal level until their livers became valued along with those of other cartilaginous fishes for the extraction of vitamin A in the 1940s. Chapman ([1944](#)) recorded that “At present they are being fished heavily, in common with the other elasmobranchs of the coast, for the vitamins in their livers. The carcasses are either thrown away at sea or made into fish meal. Little use is made of the excellent meat of the wings”.

Little information is available about the historic Washington fishery for Big Skate. In records before 2000, they are lumped together with other skates or in market categories that include non-skate species ([Lippert 2019](#)); this necessitates considerable attention to reconstructing the fishery by observing the composition of skate catches in the modern fishery and applying those to the recently reconstructed historical records.

Very little information is known about the Big Skate historical fishery in Oregon. The information we do have is mainly from historical landing data and species composition samples starting in the mid-nineties. The bulk of the catch is from the bottom trawl and longline fisheries, with smaller amounts as by-catch in mid-water trawl and the shrimp trawl fishery. Big Skate was lumped into the nominal “Skate” category until 2015 when it was separated into its own market category. Species composition data have been vitally important in reconstructing the pre-2015 historical catch ([Calavan 2019](#)).

1.5 Stock Status and Management History

The history of Big Skate management is documented in Pacific Fishery Management Council ([2018](#)), reproduced with minor edits for clarity and brevity in the following two paragraphs.

Big Skate were managed in the “Other Fish” complex until 2015 when they were designated an Ecosystem Component (EC) species. Catches of Big Skate are estimated to have averaged 95 mt from 2007–2011, along with large landings of “Unspecified Skate”. Analysis of Oregon port-sampling data indicates that about 98 percent of the recent Unspecified Skate landings

in Oregon were comprised of Big Skate. Such large landings indicates targeting of Big Skate has occurred and an EC designation was not warranted. Based on this evidence, Big Skate was redesignated as an actively-managed species in the fishery. Big Skate has been managed with stock-specific harvest specifications since 2017 (Pacific Fishery Management Council 2018).

The recent OFL of 541 mt was calculated by applying approximate MSY harvest rates to estimates of stock biomass from the Northwest Fisheries Science Center (NWFSC) West Coast Groundfish Bottom Trawl Survey. This survey-based biomass estimate is likely underestimated since Big Skate are distributed all the way to the shoreline and no West Coast trawl surveys have been conducted in water shallower than 55 meters. This introduces an extra source of uncertainty to management and suggests that increased precaution is needed to reduce the risk of overfishing the stock (Pacific Fishery Management Council 2018).

There has been consideration for managing Big Skate in a complex with Longnose Skate, the other actively-managed West Coast skate species, but the two species have disparate distributions and fishery interactions (Longnose Skate is much more deeply distributed than Big Skate) and that option was not endorsed. The Pacific Fishery Management Council has chosen to set the Annual Catch Limit (ACL) equal to the Allowable Biological Catch (ABC) with a buffer for management uncertainty (P^*) of 0.45 (Pacific Fishery Management Council 2018).

1.6 Fisheries Off Alaska, Canada and Mexico

1.6.1 Alaska

In Alaska, skates were primarily taken as bycatch in both longline and trawl fisheries until 2003, when a directed skate fishery developed in the Gulf of Alaska, where Longnose and Big Skate comprise the majority of the skate biomass.

The Gulf of Alaska (GOA) skate complex is managed as three units. Big skates and Longnose Skates each have separate harvest specifications, with acceptable biological catches (ABCs) specified for each GOA regulatory area (western, central, and eastern). A single gulfwide overfishing level (OFL) is specified for each stock. All remaining skate species are managed as an “Other Skates” group with gulfwide harvest specifications. All GOA skates are managed as Tier 5 stocks, where OFL and ABC are based on survey biomass estimates and natural mortality rate (Alaska Fisheries Science Center 2018).

In the Bering Sea and Aleutian Islands, skates are assessed as a group rather than as separate species.

Stock Assessment models for Big Skate and Longnose Skate in the Gulf of Alaska were developed by Farrugia (2017) but have not yet been used for management. For both species

there was an increasing trend in the Gulf of Alaska bottom trawl survey spanning the years 1984-2013 that could not be well fit by the models and catchability was set to 1.0 to provide information about population scale in the absence of adequate information in the data.

1.6.2 Canada

In Canada historic information regarding skate catches goes back to the 1950's. Prior to 1990's skates were taken mostly as bycatch and landings were reported as part of a skate complex (not by species). As with the U.S. West Coast, the trawl fishery is responsible for the largest amount of bycatch. Skate catches off British Columbia accelerated in the early 1990's, partly due to emerging Asian markets. Since 1996, Longnose Skate has been targeted by the B.C. trawl fishery and as a result, catches have been more accurately reported.

Assessments of Longnose Skate and Big Skate were conducted by Canada's Division of Fisheries and Oceans in 2015 (King et al. 2015). For Big Skate, a Bayesian surplus production model failed to provide plausible results, and two data-limited approaches were investigated: Depletion-Corrected Average Catch Analysis (DCAC), and a Catch-MSY (maximum sustainable yield) Approach.

DCAC produced a range of potential yield estimates that were above the long-term average catch, with an upper bound that was three orders of magnitude larger than the long-term average catch. The Catch-MSY approach was found to be quite sensitive to assumptions and was not recommended as the sole basis of advice to managers.

The recommendation for management for both skate species was that they should be managed with harvest yields based on mean historic catch, with consideration given to survey trends and to the ranges of maximum sustainable yield estimates identified by the Catch-MSY approach. However, the analysis found no significant trends in abundance indices for Big Skate, and mean historical catches were below the maximum MSY estimate from the catch-MSY results.

1.6.3 Mexico

No information is available on any fishery for Big Skate in Mexican waters, where they rarely occur, however they may be taken in the artisanal fishery.

2 Fishery Data

2.1 Data

Data used in the Big Skate assessment are summarized in Figure 1. Descriptions of the data sources are in the following sections.

2.2 Fishery Landings and Discards

Catch information for Big Skate is very limited, in part because the requirement to sort landings of Big Skate in the shore-based Individual Fishing Quota fishery from landings in the “Unidentified Skate” category was not implemented until June 2015. The historical catch of Big Skate therefore relies on the historical reconstruction of the landings of all skates as well as an analysis of discards of Longnose Skate. The estimated landings for each state and the tribal fishery are provided in Table 3 and shown in Figure 4. Landings for the years 1935 onward were assumed to be the sum of the catch reconstructions described below for each of the three coastal states as well as tribal fisheries.

2.2.1 Washington Commercial Skate Landings Reconstruction

New estimates of landings in Washington were developed in collaboration between NWFSC and Washington Department of Fish and Wildlife (WDFW). Landings from 1940–2003 were estimated as a fraction of the total skate landings based on ratios of species compositions by depth as described in more detail in (Gertseva, V. 2019). The approach relied on trawl survey estimates of the ratios among all skates by depth bin combined with logbook estimates of fishing depths in each year.

The WCGBT Survey data was used to estimate proportions of Longnose and Big Skates by depth (aggregated into 100m bins) and year for the period of the survey (between 2003 and 2018). Big Skate were primarily found in the 0–100m and 100–200m bins. Trawl logbook data include information on the amount of retained catch of skate (all species combined) within each haul as well depth of catch. The proportion of Big Skate for each depth bin was assigned to the skate catch for each haul within those depth bins and summed to get a total for each year. When survey skate information was available (2003–2018), survey skate proportions were applied by depth and year to account for inter-annual variability in those proportions. For the period prior to 2003, average proportions from 2003–2007 within each depth bin were applied.

These estimated annual proportions of Big Skate relative to all skates from the logbook analysis was then applied to total Washington skate landings by year (provided by WDFW)

to account for landings that weren't included in the available logbook data. For the period prior to 1987 (when no logbook data were available), the average proportion of Big Skate within the combined skate category, calculated from 1987-1992 logbook data, was applied to total skate landings in Washington. Estimated Big Skate landings provided by WDFW were used for the period from 2004 forward. This later period had adequate species composition sampling to divide the unspecified skate category by species with reasonable accuracy.

2.2.2 Oregon Commercial Skate Landings Reconstruction

Oregon Department of Fish and Wildlife (ODFW) provided newly reconstructed commercial landings for all observed skate species for the 2019 assessment cycle (1978 – 2018). In addition, the methods were reviewed at a pre-assessment workshop (with report available at <https://www.pcouncil.org/groundfish/stock-assessments/by-year/gf-2019/>). Historically, skates were landed as a single skate complex in Oregon. In 2009, Longnose Skate was separated into its own single-species landing category, and Big Skate was separated in 2014. The reconstruction methodology differed by these three time blocks in which species composition collections diverged (1978 – 2008; 2009 – 2014; 2015 – 2018).

Species compositions of skate complexes from commercial port sampling are available throughout this time period but are generally limited, which precluded the use of all strata for reconstructing landings. Quarter and port were excluded, retaining gear type, PMFC area, and market category for stratifying reconstructed landings within the three time blocks. Bottom trawl gear types include multiple bottom trawl gears, and account for greater than 98% of skate landings . Minor gear types include primarily bottom longline gear, but also include mid-water trawl, hook and line, shrimp trawl, pot gear and scallop dredge.

For bottom trawl gears, trawl logbook areas and adjusted skate catches were matched with stratum-specific species compositions. In Time Block 1 (1978 – 2008), all bottom trawl gear types were aggregated due to a lack of specificity in the gear recorded on the fish tickets. However, in Time Blocks 2 and 3, individual bottom trawl gear types were retained. Some borrowing of species compositions was required (31% of strata) and when necessary, borrowed from the closest area or from the most similar gear type . Longline gear landings were reconstructed in a similar fashion as to bottom trawl and required some borrowing among strata as well (25%).

Due to insufficient species compositions, mid-water trawl landings were reconstructed using a novel depth-based approach. Available compositions indicate that the proportion by weight of Big Skate within a composition drops to zero at approximately 100 fathoms, and an inverse relationship is observed for Longnose Skate, where the proportion by weight is consistently one beyond 100 – 150 fathoms . Complex-level landings were assigned a depth from logbook entries and these species specific depth associations were used to parse out landings by species. The approach differed somewhat by time block . Landings from shrimp trawls were

handled using a similar methodology. Finally, very minor landings from hook and line, pot gear and scallop dredges were assigned a single aggregated species composition, as they lack any gear-specific composition samples. Landings from within a time block were apportioned by year using the proportion of the annual ticket landings.

Results indicate that the species-specific landings from this reconstruction are very similar to those from Oregon's commercial catch reconstruction (Karnowski et al. 2014) during the overlapping years but cover a greater time period with methodology more applicable to skates in particular. ODFW intends to incorporate reconstructed skate landings into PacFIN in the future (Whitman 2019).

2.2.3 California Catch Reconstruction

A reconstruction of historical skate landings from California waters was developed for the 1916–2017 time period using a combination of commercial catch data (spatially explicit block summary catches and port sample data from 2009–2017) and fishery-independent survey data (Bizzarro, J. 2019). Virtually all landings in California were of “unspecified skate” until species-composition sampling of skate market categories began in 2009.

From 2009 through 2017, catch estimates were based on these market category species-composition samples, and the average of those species-compositions was hindcast to 2002, based on the assumption that those data were representative of the era of large area closures in the post-2000 period.

For the period from 1936-1980, spatially explicit landings data (the California Department of Fisheries and Wildlife (CDFW) block summary data) were merged with survey data to provide species-specific estimates.

For years 1981-2001, a “blended” product of these two approaches was taken, in which a linear weighting scheme blended the two sets of catch estimates through that period. Landings estimates were also scaled upwards by an expansion factor for skates landed as “dressed” based on fish ticket data. Prior to 1981 these data had not been reported and skate landings were scaled by the “average” percentage landed as dressed in the 1981-1985 time period, but by the late 1980s nearly all skates were landed round.

As no spatial information on catch is available from 1916-1930, and the block summary data were very sparse in the first few years of the CDFW fish ticket program (1931–1934), spatial information from the late 1930's was used to hindcast to the 1916–1935 time period. However, since Washington and Oregon did not have catch estimates for this year period, the California estimates of catch prior to 1939 were not used in the model as they were subsumed into an estimate of the total catch across all states increasing linearly from 1916 to 1950.

2.2.4 Tribal Catch in Washington

Tribal catch of Big Skate was provided by WDFW as all landings took place in Washington State. The landings were estimated from limited state sampling of species compositions in combined skate category. Anecdotal evidence suggests that most of the catch in tribal fishery is retained, and discard is minimal.

2.2.5 Fishery Discards

Fishery discards of Big Skate are highly uncertain. The method used to estimate discards for Longnose Skate was based on a strong correlation ($R^2 = 95.7\%$) between total mortality of that species, and total mortality of Dover Sole for the years 2009–2017 during which Longnose were landed separately from other skates. In contrast, the sorting requirement for Big Skate occurred too recently to provide an adequate range of years for this type of correlation. Furthermore, there is greater uncertainty in the total mortality for the shallow-water species with which Big Skate most often co-occurs, such as Sand Sole and Starry Flounder, than there is for Dover Sole, which has been the subject of recurring stock assessments.

The minimal discard rate information that is available for Big Skate, together with anecdotal information from those involved in the fishery for both skate species indicate that discarding for Big Skate and Longnose Skate in the years prior to 1995 was driven by the same market forces, and the discard rates were similar. Therefore, the discard rate for Longnose Skate was used as a proxy for the discards of Big Skate in order to estimate Big Skate discards as described in more detail below.

The reconstructed landings of Big Skate for the period 1950–1994 had a mean of 63.1 t with no significant trend (a linear model fit to the data increased from 62.8 t in 1950 to 63.5 in 1995). The estimated tribal catch prior to 1995 averaged less than 1 t and was not included in this analysis of Big Skate discards for the years prior to 1995.

The mean discard rate for Longnose Skate in this period was 92.46%, also with no significant linear trend (the linear fit decreased from 92.8% in 1950 to 92.1% in 1995). An estimate of the mean annual discard amount can therefore be calculated as from the mean discard rate and the mean landings as $\bar{L}/(1 - \bar{d})$ where \bar{L} is the mean landings across that time period and \bar{d} is the mean discards (Figure 5).

Two alternative methods were explored to estimate the mean annual discard amount: applying the annual Longnose Skate discard rates to the annual Big Skate landings (as reconstructed for each of the three states), and applying 3-year moving averages of these two quantities. The use of the annual values resulted in an implausibly high degree of annual variability among the estimates, with the most extreme being a spike of 2146.4 in 1979 compared to 1032.7 t the year before and 654.0 the year after. The use of the 3-year moving

average damped this variability and these estimates were retained for a sensitivity analysis (Figure 5).

A discard mortality rate of 50 percent was assumed for all discards, following the assumption used for the Longnose Skate assessment conducted for the U.S. West Coast in 2007 (Gertseva et al. 2007) The same rate has been used for skates in the trawl fishery in British Columbia, based on an approximate average of these reported rates. In 2015, PFMC’s Groundfish Management Team (GMT) conducted a comprehensive literature review of skate discard mortality, and concluded that the current assumption regarding Big Skate discard mortality is consistent with existing reported rates for other similar species.

Estimation of discard rates (discard amount relative to total catch) during the period of the West Coast Groundfish Observer Program (WCGOP), which began in 2002, was hindered by the landings of Big Skate primarily occurring in the “unspecified skate” category prior to 2015. Therefore, a discard rate was computed for this period using the combination of Big Skate and unspecified skate, under the assumption that the vast majority of the unspecified skates were Big Skate. A coefficient of variation was calculated for this rate by bootstrapping vessels within ports, because the observer program randomly chooses vessels within ports to be observed. For the years after the catch share program was implemented in 2011, the trawl fishery was subject to 100% observer coverage and discarding is assumed to be known with minimal error (CV = 0.01).

The mean body weight of discarded Big Skates, calculated from the weight and count of baskets of discarded Big Skate, was available for the years 2002–2017.

3 Fishery-Independent Data Sources

3.1 Indices of abundance

Description of two indices used in the model and one that was not included are below. Index values, diagnostics, and maps are provided in Table 4 and Figures 7 through 15.

3.1.1 Alaska Fisheries Science Center (AFSC) Triennial Shelf Survey

Research surveys have been used since the 1970s to provide fishery-independent information about the abundance, distribution, and biological characteristics of Big Skate. A coast-wide survey was conducted in 1977 (Gunderson, DR and Sample, TM 1980) by the Alaska Fisheries Science Center, and repeated every three years through 2001. The final year of this survey, 2004, was conducted by the NWFSC according to the AFSC protocol. We refer to this as the **Triennial Survey**.

The survey design used equally-spaced transects from which searches for tows in a specific depth range were initiated. The depth range and latitudinal range was not consistent across years, but all years in the period 1980-2004 included the area from 40° 10'N north to the Canadian border and a depth range that included 55-366 meters, which spans the range where the vast majority of Big Skate are encountered in all trawl surveys. Therefore the index was based on this depth range. The survey as conducted in 1977 had incomplete coverage and is not believed to be comparable to the later years, and is not used in the index.

3.1.2 Northwest Fisheries Science Center West Coast Groundfish Bottom Trawl Survey

In 2003, the NWFSC took over an ongoing slope survey that the AFSC had been conducting, and expanded it spatially to include the continental shelf. This survey, referred to in this document as the “WCGBT Survey” or “WCGBTS”, is conducted annually. It uses a random-grid design covering the coastal waters from a depth of 55 m to 1,280 m from late-May to early-October (Bradburn, M.J. and Keller, A.A and Horness, B.H. 2011 , Keller, A.A. and Wallace, J.R. and Methot, R.D. 2017). Four chartered industry vessels are used in most years. The location of Big Skate catches relative to all survey stations in WCGBT Survey are shown in Figure 2.

3.1.3 Index Standardization

The index standardization methods for the two bottom trawl surveys matched that used for Longnose Skate, and additional detail is provided in (Gertseva, V. 2019). The data from both surveys was analyzed using a spatio-temporal delta-model (Thorson, J. T. and Shelton, A. O. and Ward, E. J. and Skaug, H. J. 2015), implemented as the VAST R package (Thorson, James T. and Barnett, Lewis A. K. 2017), and publicly available online (<https://github.com/James-Thorson/VAST>). Spatial and spatio-temporal variation is specifically included in both encounter probability and positive catch rates, using a logit-link for encounter probability, and a log-link for positive catch rates. Vessel-year effects were included for each unique combination of vessel and year in the database for the WCGBT Survey, but not for the Triennial survey. Further details regarding model structure are available in the user manual (https://github.com/James-Thorson-NOAA/VAST/blob/master/manual/VAST_model_structure.pdf). Gamma and lognormal error structures were considered for the positive catch rates, and the gamma model was chosen based on the patterns in the quantile-quantile (Q-Q) diagnostic plots (Figure 7).

The VAST geostatistical estimates were compared to a simpler design-based index estimate to ground-truth the geostatistical methods. The design-based estimates were based on the mean catch per swept area within each of four strata, scaled to the area of the strata and combined. The strata were divided at 42 degrees North latitude and at 183 m depth, where the depth boundary is associated with a change in the sampling density of the survey. The

two deeper strata were extended to 549 m, the next depth at which sampling density changes in the survey, and beyond the 459 m at which the deepest observation of Big Skate occurred.

The VAST estimates with Gamma error are very similar to the designed-based estimates, while the VAST models with Lognormal error are higher, with greater inter-annual variability (Figures 8 and 9). The unweighted mean biomass across all years in the WCGBT Survey was 12,143 mt for the design-based estimate and 12,184 mt for the VAST estimate with Gamma error. This difference of less than 1% suggests that interpretation of catchability of the index is not significantly influenced by the use of VAST for standardization, at least for the Gamma error that was chosen.

Spatial patterns in the standardized survey density estimates show Big Skate widely distributed along the coast, with higher densities in the central and more northerly areas and closer to shore (Figures 11 and 12). Examination of spatial patterns of the residuals for the encounter probability and catch rate for each of the indices (shown only for the WCGBT Survey in Figures 13 and 14) showed no obvious pattern of misfit to spatial patterns in the observed data

3.1.4 International Pacific Halibut Commission Longline Survey

The IPHC has conducted an annual longline survey for Pacific Halibut off the coast of Oregon and Washington since 1997 (no surveys were performed in 1998 or 2000). This survey was considered for inclusion in the assessment model but the encounters of Big Skate are relatively infrequent compared to Longnose Skate and including the survey in early model explorations was found to make little difference in the model results. A description of the survey methods and analysis are included below for consideration in future Big Skate assessments.

Beginning in 1999, this has been a fixed station design, with 84 locations (station locations differed in 1997, and are therefore not comparable with subsequent surveys). 400 to 800 hooks have been deployed at each station in 100-hook groups (typically called “skates” although that term will be avoided here to avoid confusion). The gear used to conduct the survey was designed to efficiently sample Pacific Halibut and used 16/0 (#3) circle hooks baited with Chum Salmon.

In some years from 2011 onward, additional stations were added to the survey to sample Yelloweye Rockfish. These stations were excluded from the analysis, as were additional stations added in 2013, 2014, and 2017, off the coast of California (south of 42 degrees latitude). Some variability in exact sampling location is practically unavoidable, and leeway is given in the IPHC methods to center the set on the target coordinates, while allowing wind and currents to dictate the actual direction in which the gear is deployed. This can result in different habitats being accessed at each fixed deployment location across years. One station that was very close to the U.S. Canada border had the mid-point of the set in Canada in 2 out of the 19 years of the survey. For consistency among years, all samples from this station were included in the analysis, including those in Canada.

In most years, bycatch of non-halibut species has been recorded during this survey on the first 20 hooks of each 100-hook group, although in 2003 only 10% of the hooks were observed for bycatch, and starting in 2012, some stations had 100% of the hooks observed for bycatch. Combining these observation pattern with the number of hooks deployed each year resulted in most stations having 80, 100, 120, 140, or 160 hooks observed, with a mean of 144 hooks and a maximum of 800 hooks observed. The depth range of the 84 stations considered was 42–530 m, thus extending beyond the range of Big Skate, but 74% of the stations were shallower than 200 m. Big Skate have been observed at 51 of the 84 standard stations that were retained for this analysis, but no station had Big Skates observed in more than 12 out of the 19 years of survey data, and only 10% of the station/year combinations had at least one observed Big Skate (Figure 15). Of those station/year combinations with at least one Big Skate observed, the Big Skates were observed on an average of 1.3% of the hooks observed. The highest proportion was 10 Big Skates out of 81 hooks observed at one station.

The IPHC longline survey catch data were standardized using a Generalized Linear Model (GLM) with binomial error structure. Catch-per-hook was modeled, rather than catch per station due to the variability in the number of hooks deployed and observed each year. The binomial error structure was considered logical, given the binary nature of capturing (or not) a Longnose Skate on each longline hook. The modeling approach is identical to that which has been applied in the past for Yelloweye Rockfish (Stewart et al. 2009), and Spiny Dogfish (Gertseva et al. 2011). MCMC sampling of the GLM parameters was used to estimate the variability around each index estimate. The median index estimates themselves were approximately equal to the observed mean catch rate in each year (Figure 10). In recent years, the IPHC standardization of the index of halibut abundance has included an adjustment to account for missing baits on hooks returned empty, in an effort to account for reduced catchability of the gear that may result from the lost bait. This adjustment was not included in the analysis for Big Skate although it could be considered in future years.

4 Biological Parameters and Data

4.1 Measurement Details and Conversion Factors

Size measurements of skates are not always total-length measurements, requiring conversion factors. Some size measurements in the data are recorded as either disc width or inter-spiracle width. A conversion factor from disc width to total-length was estimated as $L = 1.3399 * W$, based on 95 samples from the WCGBT Survey, where both measurements were collected ($R^2 = 0.9983$). Little sex difference is observed, so the data were converted using a single relationship for both sexes (Figure 22). This estimate is similar to the conversion estimated by Ebert (2008) for Big Skate in Alaska. The inter-spiracle width to total length conversion was based on estimates from Downs & Cheng (2013), and does differ by sex:

$$L = 12.111 + 9.761 * ISW \text{ (females)},$$

$$L = 3.824 + 10.927 * ISW \text{ (males)}.$$

4.2 Fishery dependent length and age composition data

Fishery length composition data from PacFIN were available for the years 1995–2018 (with the exception of 2000) as shown in Table 5. Ages were available only from 2004, 2008–2012, and 2018. These were all represented in the model as conditioned on length, in order to provide more detailed information about the relationship between age and length. Treating the data this way also reduces any influence of size-based selectivity on the age composition, and ensures independence from the length samples. Furthermore, samples recorded in data from Washington in 2009 were sampled using a length-stratified system, and therefore should only be treated as conditioned on length.

Length compositions of Big Skate discarded in commercial fisheries and measured by the West Coast Groundfish Observer program were available for the years 2010–2017.

The input sample sizes for the length compositions were calculated via the Stewart Method (Stewart 2019):

$$\text{Input } N = N_{\text{hauls}} + 0.138 * N_{\text{fish}} \text{ if } N_{\text{fish}}/N_{\text{hauls}} \text{ is } < 44,$$

$$\text{Input } N = 7.06 * N_{\text{hauls}} \text{ if } N_{\text{fish}}/N_{\text{hauls}} \text{ is } \geq 44.$$

However, no haul had more than 44 Big Skate sampled, so only the first formula was used.

4.3 Survey length and age composition data

Lengths of Big Skate were only collected from the Triennial survey in 1998, 2001, and 2004, but in 1998 only 3 Big Skate were sampled, so those lengths were excluded from this analysis. Length compositions were available for all years of the WCGBT Survey. Sample sizes for both surveys are provided in Table 6. The WCGBT Survey measured disc width for the years 2006 and 2007, and total length in all other years. Those samples for which only disc width was measured were converted to total length using the formula above.

The length compositions from the fishery and each of the two surveys aggregated across all years is shown in Figure 16.

Ages were available from the WCGBT Survey in the years 2009, 2010, 2016, 2017, and 2018. No ages were available from the Triennial Survey.

Ageing Precision and Bias

Ages of Big Skate were all estimated based on growth band counts of sectioned vertebrae. Ageing precision and bias were estimated using double-reads of 518 Big Skate vertebrae using the approach of Punt et al. (2008). The results showed strong agreement among readers (Figure 20), with a standard deviation of the ageing error increasing from about 0.4 at age 0 to 1.6 years at age 15 (Figure 21).

Weight-Length

The mean weight as a function of length was estimated from 1159 samples from the WCGBT Survey using a linear regression on a log-log scale. Sex was not found to be a significant predictor, so a single relationship was estimated: $Weight = 0.00000749 * Length^{2.9925}$ (Figure 22).

Sex Ratio, Maturity, and Fecundity

The female maturity relationship was based on visual maturity estimates from port samplers ($n = 278$, of which 241 were from Oregon and 37 from Washington, with 24 mature specimens) as well as 55 samples from the WCGBT Survey (of which 4 were mature). The resulting relationship was $L_{50\%} = 148.245$ with a slope parameter of $Beta = -0.13155$ in the relationship $M = (1 + Beta(L - L_{50\%}))^{-1}$ (Figure 23). This result is consistent with the estimated maturity of Big Skate in Alaska (Table 1).

Fecundity was assumed to be proportional to body weight for mature females, as no relationship has been estimated between body weight and the annual number of egg cases produced (and/or embryos per egg case).

4.4 Environmental or Ecosystem Data Included in the Assessment

In this assessment, neither environmental nor ecosystem considerations were explicitly included in the analysis. This is primarily due to a lack of relevant data or results of analyses that could contribute ecosystem-related quantitative information for the assessment.

5 Assessment

5.1 Previous Assessments

This analysis represents the first stock assessment that has been conducted for Big Skate. The current management of the stock is based on an OFL estimate calculated from a proxy for F_{MSY} and average survey biomass from the WCGBT Survey during the years 2010–2012 (Taylor IG and Cope, J and Hamel O and Thorson, J [2013](#)). The F_{MSY} estimate was based on the product of an assumed F_{MSY}/M ratio and an M estimate of 0.162 based on the maximum age of 26 reported by McFarlane and King (GA et al. [2006](#)). Values were sampled from an assumed distribution around all these quantities to develop a measure of uncertainty around the OFL estimate.

5.2 Model Description

5.2.1 Modeling Software

The STAT team used Stock Synthesis version 3.30.13 (Methot, Richard D. and Wetzel, Chantell R. ([2013](#)), Methot et al. ([2019](#))). The r4ss package version 1.35.1 (Taylor et al. [2019](#)) was used to post-process the output data from Stock Synthesis.

5.2.2 Summary of Data for Fleets and Areas

Catch is divided among 4 fleets in the base model:

- Fishery (current) combines all non-tribal sources of catch for the years 1995 onward,
- Discard (historical) is the estimated discard amount calculated from the estimated Longnose Skate discard rate as described above. The input catch for this fleet was 50% of the total estimate, to account for the assumed 50% discard mortality rate. This data covers the period 1916–1994.
- Fishery (historical) includes the reconstructed landings estimates from each of the three states for 1916–1994.
- Tribal includes the estimates of catch of Big Skate by treaty tribes.

The use of a separate fleet for historical discards allowed greater flexibility in choosing how to model discards outside the model, but also prevented uncertainty in those estimates to be

propagated through to the estimated uncertainty in the model results. All four fleets were assumed to have the same selectivity.

A retention function was estimated for the current fishery, and discards were estimated within the model based on the fit to discard rates and mean body weight of the discarded fish (along with all other data in the integrated analysis). The choice to model retention explicitly only for the current fishery implies that the historical landings and historical discards represented the same subset of the population. During the historical period, the landed catch is likely to have contained fewer small fish than the discards, but the estimated discard rate is greater than 90%, so it necessarily includes fish of all sizes. During the historical period, skates were used for animal food and reduction to fish meal or fertilizer, markets which may have accepted skate of all sizes.

5.2.3 Other Specifications

This assessment covers the U.S. West Coast stock of Big Skate in off the coasts of Washington, Oregon and California, the area bounded by the U.S.-Canada border to the north, and the U.S.-Mexico border to the south. The population is treated as a single coastwide stock with no net movement in or out of the area. Females and males are modeled separately as there is evidence for differences in growth based on both the age and length data, as well as patterns in the sex ratios associated with the length composition data. Natural mortality is estimated within the model using a natural mortality prior developed by Hamel (2015). A Beverton-Holt stock-recruit function is assumed. No deviations from the spawner-recruit curve are estimated.

The length composition data are stratified into 37 5-cm bins, ranging between 20 and 200 cm. The age data are stratified into ages 0–15+, conditioned on the same length bin structure. The population dynamics are computed over a larger range of lengths-at-age, with the 5-cm length bins extending up to 250 cm and the numbers-at-age computed up to age 20.

5.2.4 Data Weighting

The Francis data weighting method “TA1.8” (Francis, R.I.C.C. 2011), as implemented in the r4ss package was used for all length and age composition data. This method is based on adjusting the input sample sizes to make the variability in mean length or age around the model expectation match the variability expected based on the adjusted input sample size. Sensitivity analyses to both the McAllister-Ianelli tuning method (McAllister, M K and Ianelli, J N 1997) and a Dirichlet-Multinomial approach (Thorson et al. 2017) were also explored.

The weight given to the indices of abundance was adjusted automatically through the estimation of an additional standard deviation parameter for each index, which was added to the standard deviation values estimated within the index standardization process.

No data-weighting algorithm was applied to the discard rate or mean body weight observations.

5.2.5 Priors

Natural Mortality A log-normal prior for natural mortality was based on the Hamel (2015) meta-analysis. The Hamel prior for M is lognormal($\ln(5.4/\text{max age})$, .438). For Big Skate, the maximum age is based on the single 15-year-old fish observed out of 1034 ages from the WCGBT Survey. This results in a lognormal($\log(0.36) = -1.021651$, 0.438) prior.

Survey Catchability The lack of contrast in the data resulted in unstable model results under a variety of configurations. In order to keep biomass estimates within a plausible range, the assessment uses a revised prior on the WCGBT Survey catchability parameter (q) that is based on one that was originally developed for the 2007 Longnose Skate assessment (Gertseva et al. (2007), Dorn et al. (2007)), and is being used for the concurrent Longnose Skate assessment (Gertseva, V. 2019). The description that follows first addresses the method used to develop the original prior, followed by a description of the additional work used to tailor it for Big Skate.

The original prior is based on consideration of the availability of Longnose Skate to the survey gear and the probability that a skate in the path of the gear would be caught and retained by the gear. The methodology for developing the prior involves identifying factors that contribute to Longnose Skate catch in trawl gear, specifying the potential range in the proportion of fish that are available to the gear according to each factor, and the potential range in the vulnerability to the gear. These are “best guesses” for the individual probabilities associated with each factor. These values are translated into a lognormal prior where the median of the lognormal is the “best guess” and the range of plausible values covers 99% of the lognormal distribution.

Four factors inform catchability in the survey. The WCGBT Survey covers the full latitudinal range of Longnose Skate modeled in the assessment, and thus, the latitudinal availability factor was assumed to be one (complete latitudinal coverage). The survey coverage exceeds the maximum depth distribution of Longnose Skates but doesn’t fully cover the shallow end of the skate distribution. A range of 95 to 100 percent was assumed for the depth availability in the 2007 Longnose Skate prior, but this was revised for Big Skate as noted below. A range of 75 to 95 percent was assumed for vertical availability on the basis that skates are known to bury in the mud, and therefore some may be unavailable to the bottom trawl gear.

The largest bounds were placed on the probability of capture, given that a fish is in the net path. It is known that flatfish can be herded by the wire running between the trawl doors and the trawl footrope, and it is possible that this could also occur for skates. However, it is also possible that skate could avoid the trawl nets. For the capture probability, a range

of 75 to 150 percent was assumed. The best estimates for each of these factors were set at the midpoint of the range for individual factors, except for the probability of capture, which was given a value of one. The overall estimate in the Longnose Skate prior for the survey catchability was the product of the best estimates, 0.83. The bounds on catchability are the products of the low and high values for factor ranges, respectively, which are 0.53 and 1.43. The overall estimate was equated to the median of a lognormal distribution, and the bounds to 99% of that distribution. This gave a normal prior on $\log(q)$, with mean -0.188 and a standard deviation of 0.187.

Two additional factors were developed for revising the WCGBTS prior for the present (2019) Big Skate assessment. These focused on the assumptions about depth availability, and on accounting for untrawlable habitat.

Big Skate have a shallower depth distribution than Longnose Skate, and encounters in the WCGBT Survey are most frequent in the shallowest depths (Figure 3). The area of the coastal waters within the 55–200 m depth range where Big Skate are most often found was estimated at 4.17 million hectares (Whitmire 2019). The area shallower than 55 m which is not included in the survey is estimated at 1.61 million ha, or 38.5% of the area within 55–200 m.

An analysis of trawl fishery data (involving both discarded and retained fish) provided insight into the changes in Big Skate density by depth. An ODFW Flatfish survey conducted in the 1970s (Mirick 2019) was also considered as a source of information, however we found that there were very few hauls in that study with Big Skate (in 42 of 350 hauls), relative to the fishery data (where Big Skate were present in 14,896 of 160,168 hauls), so that data was ultimately not used in the analysis.

The following steps were used to estimate the fraction of Big Skate biomass unavailable to the WCGBT Survey due to occurring shallower than the 55 m limit of the survey design (Figure B-1).

- Catch data provided by the WCGOP program comprising both retained and discard catch was utilized after filtering for bottom trawl gear and the years 2015-2017 during which Big Skate were landed in a separate market category.
- The ratio of hauls containing Big Skate to all hauls was calculated in each of four depth bins: (0-25], (25-55], (55-75], and (75-100] meters.
- The analysis was stratified by the following regions: Washington (46-49 degrees N latitude), Oregon (42-46 degrees N), Northern California (36-42 degrees), and Southern California (32-36 degrees). However, during the range of years chosen, sufficient data were only available for trips that had landings in Northern California and Oregon, so the estimates for Oregon were assumed representative of Washington and the estimates of Northern California were assumed representative of Southern California.

- The median biomass of Big Skate in hauls in those same depth bins was calculated.
- The median biomass was combined with the fraction of hauls containing Big Skate to get a relative biomass among these depth bins within each region.
- The ratios among the 0-25, 25-55, and 55-75 meter bins were applied to the catch rates in the survey for the 55-75 bin within each region to extrapolate the survey catch rates into the shallower water.
- The extrapolated catch rates in each depth bin within each region were expanded by the spatial area of that bin to get an absolute estimate of biomass in each case.

The resulting estimates showed the largest amount of unsurveyed biomass occurred in Northern California where the commercial catch rate was highest in the 25-55 m depth bin (Figure B-1). This was consistent with patterns in the survey data which showed this region was the only one where the survey biomass estimate was highest in the shallowest surveyed depth bin. Commercial fishery catch rates in Oregon declined almost linearly from the 55-75 m bin to the two shallower bins. The survey data for Washington and Oregon had similar catch rates in the 55-75 m bin so the assumption of applying the same ratio from the commercial data to the shallower bins seems reasonable. Southern California had the lowest catch rates in the WCGBT Survey so the assumption of using the Northern California fishery catch rates for this area was unlikely to have much influence on the total extrapolation regardless of how representative the commercial catch rates from Northern California are for this area.

The extrapolated biomass shallower than 55 m, combined across all regions, represented 25.8% of the total biomass (extrapolated plus surveyed area). This value was used as the basis for reducing the best guess for the “Depth availability” component of the catchability prior from 0.975 used in the 2007 Longnose Skate assessment to 0.75 with minimum and maximum values changed from 0.95 and 1.0 to 0.6 and 0.9, respectively (Table 2).

Table 2: Factors used in the analysis of the catchability prior (q).

Factor	Minimum	Best Guess	Maximum
Depth availability	0.600	0.750	0.900
Latitudinal availability	1.000	1.000	1.000
Vertical availability	0.750	0.850	0.950
Probability of capture given in net path	0.750	1.000	1.500
Habitat availability	1.000	1.100	1.200
Product of all factors	0.338	0.701	1.539

A further change to the prior was made to add a “Habitat availability” component to account for the possibility raised during the STAR panel that Big Skate density was likely to be lower in untrawlable habitat—the areas where survey operations have not taken place because the bottom is too rugged or too steep. Big Skate are unlikely to occur in these rugose bottom

types, so the extrapolation of the survey density is likely to overestimate the biomass of Big Skate for these areas. There is no quantitative estimate of untrawlable habitat for the survey region, so an approximation was made based on the fraction of survey cells that had failed searches for trawlable habitat, which was 625 cells out of 7098 cells visited up through 2017, or 8.8% (Whitmire 2019). This is likely an underestimate because some cells which have had successful tows include untrawlable area as well. Thus, a best guess value of 1.1 was used to account for the overestimation of Big Skate biomass due to untrawlable habitat, with a range of 1.0-1.2.

The product of the 5 factors resulted in a value of 0.701 for the combined best guess survey catchability, reduced from 0.83 in the Longnose Skate prior. The bounds were also broader at 0.338 for the minimum and 1.539 for the maximum, compared to 0.53 and 1.43 for the Longnose Skate prior.

A lognormal prior based on the three values was calculated following the basic approach used for the 2007 Longnose Skate prior. The minimum and maximum values were first shifted slightly to be equidistant from the best guess value on a log scale. The log of the min, best guess, and max values were -1.086 , -0.355 , and 0.431 , with an average difference of 0.759. Equidistant min and max values were calculated as $\min = \exp(-0.355 - 0.759) = 0.328$ and $\max = \exp(-0.355 + 0.759) = 1.497$. A lognormal distribution with median 0.701 and log-standard deviation 0.326 has 1% and 99% quantiles at the equally proportioned min and max values. This was represented in the Stock Synthesis model as a normal prior on $\log(q)$ with mean $= \log(0.701) = -0.355$ and standard deviation $= 0.326$.

During the STAR panel, a revised version of the new prior was explored, where the “minimum” and “maximum” values were assigned to the 10% and 90% quantiles, but this was found to be too uninformative (the 95% interval on spawning biomass encompassed 0) and insufficiently representative of the prior belief about catchability, so the final model retained the 1% and 99% quantile assumption used in development of the Longnose Skate catchability prior as described above.

5.2.6 Estimated Parameters

A full list of all estimated and fixed parameters is provided in Tables 8.

The base model has a total of 44 estimated parameters in the following categories:

- 1 stock-recruit parameter ($\log(R_0)$) controlling equilibrium recruitment)
- 1 natural mortality parameter applied to both sexes,
- 6 parameters related to female growth and the variability in length at age
- 2 parameters relating male growth to female growth,

- 3 catchability parameters (1 for the WCGBT Survey and 1 each for the early and late periods of the Triennial Survey)
- 2 extra standard deviation parameters (1 for each survey)
- 29 selectivity parameters, including 16 related to time-varying retention rate

The estimated parameters are described in greater detail below and a full list of all estimated and fixed parameters is provided in Table 8.

Recruitment. The parameter $\log(R_0)$ is the log of the equilibrium recruitment (in thousands). Other aspects of the stock-recruit relationship are described below under Fixed Parameters.

Natural Mortality. Male natural mortality was assumed equal to the value estimated for females. Sensitivity analyses were used to test the impact of both the prior on natural mortality and the assumption of equal natural mortality for both sexes.

Growth. Examination of patterns of age-at-length and length-at-age indicated unusual patterns of growth for Big Skate. The youngest fish show near-linear growth, and average size for both sexes is similar. However, older fish show considerable sex-based differences in size. This led to the choice to model growth using the “growth cessation model” recently developed by Maunder et al. (2018). The estimated growth curves are shown in Figure 24. This growth model assumes linear growth initially and then uses a logistic function to model how the growth rate falls to zero at greater ages. As implemented in Stock Synthesis, the four parameters associated with the mean length at age are the length at an initial reference age (set to age 0 for Big Skate), the length where growth ceases (L_∞), the age at the midpoint of the transition between linear growth and no growth, and the slope of the logistic function that provides that transition. All four parameters were estimated for females, and male offsets were estimated for L_∞ and the transition age. Two parameters controlling variability in length at age at young and old ages were also estimated and assumed to apply equally to females and males.

The growth cessation model provided two key advantages over the more common von Bertalanffy growth model in the case of Big Skate: it allowed essentially linear growth for the early years and it allowed growth for the earlier ages to be similar between females and males while diverging at older ages. The growth cessation model also improve the negative log-likelihood by 45 units relative to the von Bertalanffy growth model.

Selectivity.

A double-normal selectivity function was used for all fleets to allow consideration of both asymptotic and dome-shaped patterns. No length composition data was available for the historical fishery, the historical discards, or the tribal fishery, so selectivity was assumed equal for all fisheries in all time periods, and will be referenced simply as “the fishery” in many areas below. For the fishery and the Triennial survey, the difference in likelihood between dome-shaped and asymptotic patterns was very small and in the case of the Triennial

survey, the dome-shape occurred at a length beyond almost all observations, indicating that this shape was likely driven by the fit to other data sources, such as the index, rather than the length composition data. The WCGBT Survey was allowed to remain dome-shaped, as the model estimated the selectivity peak at a smaller length than the other fleets, and the likelihood was improved by the dome-shape. The WCGBT Survey also has the shortest hauls, with 15 minutes or less of bottom contact, so larger skates may be better able to escape the net.

In order to fit a strong skew in the sex ratios toward males for the length bins in which the majority of the samples were found, it was necessary to estimate a sex-specific offset of selectivity. Two offset parameters were estimated for all fleets, one for the difference in length at peak selectivity, and another for the maximum selectivity at that peak. This allows one sex to have a maximum of 1.0 at the peak and the other to have a maximum less than 1.0. The ascending slope was assumed equal in all cases, as was the descending slope for the WCGBT Survey.

Fishery retention was estimated as a logistic function applied to the selected catch from 1995 onward, to estimate discards within the model. Discards prior to 1995 were estimated outside the model and input as the historical discard fleet as discussed above. Three retention parameters were estimated, the length at 50% retention, a slope parameter, and the asymptotic retention rate. The asymptotic retention rate was estimated as time-varying, with separate parameters covering 1995–2004, individual years from 2005 to 2016, and 2017–onward. The choice of these time blocks was made to allow the model to fit the discard rates during the 2005–2016 period well. This is the period with the most information about discard rates. The first three years with data on discard rates and mean body weight of the discarded fish (2002–2004) were included in the same 1995–2004 block and thus used as the basis for the estimate applied to the 1995–2001 period without discard data. Fitting this early period to the estimate from 2002 only provided less plausible discard estimates although the overall impact on the model was small.

5.2.7 Fixed Parameters

The steepness of the Beverton-Holt stock-recruit curve was fixed at 0.4. The same value was used in the 2007 Longnose Skate assessment (Gertseva et al. 2007) and is being considered for the ongoing 2019 Longnose Skate assessment. This value reflects a K-type reproductive strategy associated with elasmobranchs in general. The influence of the assumption of $h = 0.4$ on model output was explored via a likelihood profile analysis. No deviations around the stock-recruit curve were estimated, and the stock was assumed to be at an unfished equilibrium in the first year (1916).

Parameters controlling the weight-length relationship and maturity-at-length were fixed at the externally estimated values.

As noted above, the descending limb of the double-normal selectivity function was fixed at a high value resulting in asymptotic selectivity for both the fishery and the Triennial Survey.

5.3 Model Selection and Evaluation

5.3.1 Key Assumptions and Structural Choices

The modeled stock was assumed to be a single closed population within the EEZ of the U.S. West Coast, with fishing mortality the only driver of changes in abundance. Neither variability in recruitment nor any other biological or ecological process that would contribute to changes in abundance were included in the final model. Recruitment variability was explored but found to be insufficiently supported by information in the data.

Some modeling choices were made based on similar choices for the concurrent Longnose Skate stock assessment, such as the division of the historical fishery into separate fleets for landed and discarded fish with the same selectivity, and the choice to model the tribal fishery separately in the recent period. In all these cases, alternative approaches would likely have yielded similar results, so the exploration of alternative models focused on the issues that seemed to have the biggest impact on the estimated dynamics.

5.3.2 Alternate Models Considered

Numerous alternative configurations were explored for growth, selectivity, mortality, and historical discards. A selection of these alternative approaches were retained as sensitivity analyses, described below.

5.3.3 Convergence

One hundred sets of jittered starting values were generated using the jitter function built into Stock Synthesis, using jitter input = 0.1. The same likelihood as the base model was returned by 48 out of the 100 runs, while the others all had worse outcomes (Table 13). No analysis was conducted for the starting values associated with those jitter runs which failed to return to the same likelihood as the base model, but throughout the model selection process, models which started with a low $\log(R_0)$ parameter or other initial values that led to a crashed population had convergence problems. This was straightforward to resolve during the model selection process, but may have been the cause of many of the jittered models failing to reach the best observed likelihood. The 52% failure rate also suggests that the 0.1 jitter input value was high enough to produce a broad range of starting values to test the model, where a very high success rate might suggest too low a jitter value.

5.4 Response to the Current STAR Panel Requests

Figures illustrating responses to these requests are in Appendix B.

Request 1: Explore possible changes to the prior distribution on survey q for the West Coast Bottom Trawl Survey.

Rationale: The scale of the population is determined by the assumed prior of the survey q for the West Coast Bottom Trawl Survey, which was based on the 2007 longnose skate assessment. Longnose skate have a very different depth distribution than big skate which occur in shallower depths than longnose skate or the West Coast Bottom Trawl Survey.

STAT Response: An estimate of the fraction of Big Skate biomass unavailable to the survey due to occurrence shallower than 55 m was estimated at 25.8

Replacing the Longnose Skate catchability prior with the new Big Skate catchability prior resulted in a lower catchability estimate and a higher biomass (Figure [B-2](#)).

The revised catchability prior was considered by the STAT to be a better choice for Big Skate and was used in all subsequent analyses with the exception of the responses to Requests 2 and 3 below which were conducted concurrently with the revision to the prior.

Request 2: Explore changes to the model to provide better fits to the trawl surveys.

Rationale: The models explored to date do not fit the survey trends well.

STAT Response: The stock assessment team acknowledges that the increasing trends in both the Triennial and WCGBT Surveys is not well fit by the model as discussed at length elsewhere in this report. Models were developed with a start year of 1980 to allow more flexibility in the population size at the start of the survey time series with the hope that this would improve the fit to the survey indices. In one case, the initial conditions were based on an estimated equilibrium fishing mortality with the associated fished equilibrium age structure. In the other case the initial age structure was allowed to be more flexible by estimating recruitment deviations for the years 1965-1980 to allow out-of-equilibrium age structure in 1980.

The model with flexible initial conditions had very similar estimates of unfished equilibrium and current biomass to the pre-STAR base model (Figure [B-3](#)) while the model with less flexible initial conditions had implausibly low biomass in 1980 and an oscillating pattern of biomass as the population rebuilt from initial conditions associated with the change from a fished equilibrium associated with initial fishing mortality about 10 times higher than the estimated mortality for the years 1980-1984. The oscillations

in model with less flexible equilibrium conditions fit the both indices of abundance slightly better (by a total of 2.1 units of negative log-likelihood) but the equilibrium catch was implausibly high while the model with more flexible initial conditions had a very similar fit to the indices (Figures B-4 and B-5).

Request 3: Explore a time-varying M model.

Rationale: To explore this as a mechanism to better fit survey trends.

STAT Response:

Time-varying natural mortality (M) was implemented using a wide range of settings related to overall variability and autocorrelation among years in the setup of time-varying natural mortality. In some cases, the resulting time series of M was implausibly variable, while other estimates were more reasonable.. However, the associated time series of biomass and recruitment showed implausible patterns for all but the least flexible setups (Figures B-8 and B-9). The improvement in the fit to the indices was biggest for the least plausible scenarios and relatively small for the least flexible one (Figures B-10 and B-11).

This exploration indicated that even a small amount of time-varying natural mortality could explain some of the observed variability in the indices, but the STAT felt that Big Skate did not have sufficient data to reliably estimate time-varying M .

Request 4: Provide a run with the new prior from request #1 with diagnostics, fits, and likelihood profiles, if possible.

Rationale: The scale of the population is determined by the assumed prior of the survey q for the West Coast Bottom Trawl Survey, which was based on the 2007 longnose skate assessment. Longnose skate have a very different depth distribution than big skate which occur in shallower depths than longnose skate or the West Coast Bottom Trawl Survey. The new prior has more information specific to big skate distribution.

STAT Response:

A full set of r4ss outputs for this new candidate base model were provided to the STAR panel through the FTP site. Likelihood profiles on catchability and steepness were also provided. The profile with no prior is the same as was provided for the pre-STAR base model (Figure 59), while the profile including the prior (Figure 60) showed that the change in negative log-likelihood over the range of $q = 0.5$ to 2.0 was smaller than before, with a change of about 5 units compared to over 10 units for the Longnose Skate catchability prior (not shown).

The steepness profile (Figure 62) showed that the change in likelihood over the range $h = 0.3$ to 0.9 was even smaller than in the pre-STAR base model, with a total change of about 0.5 units of negative log-likelihood compared to about 0.7 previously.

Request 5: Provide the diagnostics, fits, and the likelihood profiles associated with the model from run #4 with Dirichlet weighting.

For the likelihood profiles:

- (1) do not allow the Dirichlet weights to change from the maximum likelihood values
- (2) allow full implementation of the Dirichlet weighting

For both treatments, do not let the estimated SDs for the surveys change from their maximum likelihood estimates.

Rationale: To confirm the model with Dirichlet weights better estimates scale without relying as heavily on the survey q prior. There is a need to understand what is driving this counter-intuitive result. This may provide the basis for a new base model.

STAT Response:

A full set of r4ss outputs for this alternative model were provided to the STAR panel through the FTP site. A likelihood profile was conducted over survey catchability of the survey but there was a problem with convergence requiring further investigation (Figure B-12). As the Dirichlet-Multinomial model was not chosen for the based model, further investigations in the profiles were not attempted.

Request 6: Repeat run #4 with no survey q prior and a run with the mean of the survey q prior of at half the mean of the prior from run #4.

Rationale: To ensure the model is capable of estimating scale.

STAT Response:

The q prior from request #4 had mean 0.701 corresponding to $\log(q) = -0.355$. A model with the prior at half this value, $q = 0.3505$, $\log(q) = -1.048$ had a maximum likelihood estimate of $q = 0.343$, $\log(q) = -1.070$, indicating that the estimated values is closely following the prior. This is expected given the likelihood profile indicated that the best total likelihood occurred at the minimum q values among those considered. A model with no prior on survey catchability has the q estimated at the lower bound of $\log(q) = -2$ (Figure B-13).

Request 7: Catch streams for the decision table should be as follows:

- (a) Assume the 2017-2018 average total catch for 2019 and 2020 catches
- (b) Low catch stream: 250 mt/year
- (c) The default harvest control rule: 494 mt/year

- (d) High catch stream: ACL = ABC ($P^* = 0.45$)
- (e) Use the category 2 sigma schedule recommended by the SSC (see Table 3 of the March SSC Report)

Rationale: To define the removal assumptions in the decision table.

STAT Response:

Based on the discussion in the review, the following steps were taken to develop the states of nature and the decision table. Catchability of the WCGBT Survey was used as the axis of uncertainty. The new base model estimate has $q = 0.668$, $\log(q) = -0.403$, with the standard deviation of 0.315 for the estimated $\log(q)$ parameter. Using the formula of 1.15 units of standard deviation (provided in the terms of reference) to get low and high values leads to $\log(q) = -0.766$ and $\log(q) = -0.041$, corresponding to catchability values of $q = 0.465$, and $q = 0.960$. The high q value was associated with a low state of nature which was near the 25

The time series of spawning biomass and distribution of estimated 2019 spawning biomass were provided to the panel (Figures B-14 and B-15).

5.5 Base Case Model Results

The base model parameter estimates and their approximate asymptotic standard errors are shown in Table 8. Estimates of derived reference points and approximate 95% asymptotic confidence intervals are shown in Table 17. Time-series of estimated stock size over time are shown in Table 7.

5.5.1 Parameter Estimates

Values of all estimated parameters are provided in Table 8. A few key parameters of note include natural mortality estimated at 0.449, slightly above the 0.36 median of the prior and with much narrower uncertainty than the prior (Figure 25). L_∞ was estimated at 175.66 for females and 120.96 for males (based on an exponential offset of -0.373). The $\log(R_0)$ parameter was estimated at 8.905, corresponding to an unfished equilibrium recruitment of 7.37 million.

Catchability from the WCGBT Survey was estimated at 0.67, close the median of the prior applied to this parameter, with uncertainty estimated as very similar to the uncertainty in the prior (Figure 25).

Selectivity was estimated to be asymptotic for the WCGBT Survey (the only fleet for which it was allowed to be dome-shaped), with the peak selectivity occurring at 76 cm, below the

peak of the fishery selectivity at 94 cm (Figure 26). These two fleets had a similar estimate for the lower maximum selectivity for females than males, at 0.698 for the survey and 0.744 for the fishery. Selectivity for the Triennial survey was substantially different from the other two, with an additional parameter estimated for the initial selectivity of the smallest sizes necessary to fit the very flat length compositions from the two years of data available, and with a peak occurring at 188 cm, far higher than the other two curves. When converted to age, the selectivity peaked at about age-4 for the WCGBT Survey, age-5 for the fishery, and ages 7 and 12 for males and females in the Triennial Survey, respectively (Figure 27).

The length at 50% retention was estimated to be 66 cm, which is similar to the length at 50% selectivity, but the slope of the retention function was steeper. Thus, the fish that were discarded were primarily those sizes that were not fully selected (Figure 28). The asymptotic retention rate increased from 2004 to 2008 with a peak at close to 100%, followed by a decreasing trend from 2012 onward (Figure 29).

5.5.2 Fits to the Data

Indices. The observed indices show much more variability than the model expectation, with the fit to the WCGBT Survey essentially a flat line (Figure 30). The fit to the Triennial Survey shows a noticeable change over time due to the separate catchability parameters estimated for the early and late periods (Figure 31).

Length Data. The fits to the length data were reasonably good (Figures 32–33 and A-1–A-4). The observed length compositions for males in both the fishery and the WCGBT Survey is bimodal, with modes in the 80 cm and 115 cm length bins for the fishery, and in the 60 cm and 115 cm bins for the survey. The model expectation has modes in similar locations in both cases, where the first mode is close to the estimated peak selectivity value and the second is close to the estimated male L-infinity parameter. However, the second mode in the model expectation is less pronounced than in the observed data (Figure 32). The residual patterns in the fit to the length compositions don't show strong patterns, with the WCGBT Survey data especially well fit. There are a few large residuals over a range of lengths in the early years as well as a few years where there were observations of small (under 50 cm) fish in the retained fishery catch which the model expected would have been discarded (Figure 33). The fit to the length data in alternative models that lacked either the growth cessation model or the sex-specific offsets to selectivity were less good (results not shown).

Conditional Age-at-Length. The conditional age-at-length data is likewise fit reasonably well, with some patterns in residuals showing variability among years, but no clear pattern that is consistent across years (Figures 34 and 35).

Sex Ratios. Sex ratio data is not included in the likelihood as such, but as a part of the length composition likelihood. The proportions of females and males are compiled into a single vector that is compared to the model expectations in the multinomial likelihood. The

patterns in sex ratio by length bin show fewer females than males for the middle range of sizes (70–120 cm), with a shift to almost 100% females for the largest size bins (over 130 cm). These patterns are shown in Figures 36 and 37. The approximate uncertainty associated with the observed ratios is represented by a Jeffreys interval (Brown et al. 2001) based on the combination of the proportion of the lengths with each length bin and the adjusted input sample size. The use of sex-specific growth curves was adequate to fit the ratios for the largest bins, but the ratio skews toward males at lengths where the mean ages are similar for females and males. The fit to this part of the sex ratio pattern required an offset in selectivity.

Discards Rates and Mean Weight of the Discards. Fit to the discard fraction estimates (Figure 38) and the mean weight of the discards (Figure 39) show reasonably good fits. The model expectation is able to match the trend of decreasing discard fractions and decreasing mean weights over the years 2002–2010 by estimating an increasing trend in the asymptotic retention rate from 2004 to 2008 with a peak at close to 100%, followed by a decreasing trend from 2012 onward (Figures 28 and 29). The years 2008–2012 with the highest asymptotic retention rates have little retention of large fish leading to lower discard rates and smaller mean weight of the discarded fish. The period from 2011 onward had observer coverage increased to 100% for the catch-shares trawl fishery, leading to more precise data and consistent patterns in the two data types. The first few years (which form the basis for the estimates going back to 1995), are more uncertain and less well fit, with the discard rates over 30%. This is inconsistent with the mean weight under 1.5 kg in 2003 and 2004.

5.5.3 Uncertainty and Sensitivity Analyses

A number of sensitivity analyses were conducted, including:

- Sensitivities to assumptions about selectivity and catchability
 - Allowing all selectivity curves to be dome-shaped
 - Removing the sex-specific offset on the selectivity curves
 - Using the prior on catchability for Longnose Skate (this is the pre-STAR base model)
 - Removing the prior on catchability for the WCGBT Survey
 - Estimating a single catchability for all years in the Triennial Survey
- Sensitivities to assumptions about biology
 - Estimating separate natural mortality parameters for males and females
 - Removing the prior on natural mortality
 - Using the von Bertalanffy growth model

- Using the Richards growth model
- Sensitivities to data weighting and recruitment
 - Tuning the sample sizes using the McAllister-Ianelli method
 - Tuning the sample sizes using the Dirichlet-Multinomial likelihood
 - Removing the extra standard deviation parameter added to the index uncertainty
 - Estimating recruitment deviations around the stock-recruit curve
 - Estimating recruitment deviations around the stock-recruit curve without the prior on WCGBT Survey catchability (q)
- Sensitivities to historical catch and discards
 - Estimating historical discards based on 3yr average of discard rates and landings
 - Changing discard mortality from 0.5 to 0.4
 - Changing discard mortality from 0.5 to 0.6
 - Adjusting historical catch by estimating multipliers on discards over blocks of time
 - Adjusting historical catch to match a time series of fishing mortality for Petrale Sole

Results of these sensitivity analyses are shown in Figures 45 to 50, and Tables 9 to 55. More detailed descriptions of each group of sensitivities is provided below.

Additional sensitivity analyses were conducted during the STAR panel review, the results of which are discussed in the “Response to the Current STAR Panel Requests” section above.

Selectivity and catchability (Figure 45 and Table 9)

Allowing the selectivity for all fleets to be dome-shaped resulted in domed selectivity for all fleets, but only improved the total negative log-likelihood by 0.9 units, mostly through a slightly improved fit to the length compositions, although the fit to the surveys was slightly worse (Table 9). Removing the offset between female and male selectivity caused the negative log-likelihood to be worse by 18.1 units, mostly through a worse fit to the length compositions but also a worse fit to the conditional age-at-length compositions. The conditional age data was represented independently for each sex, so no sex-ratio information was present in the data, but the growth curves were changed slightly to compensate for the change in fit to the length data, resulting in a poorer fit to the age data as well. The scale of the population remained somewhat similar to the base model under both of these sensitivities (Figure 45).

The model with the Longnose Skate catchability prior was the base model prior to the STAR review panel where the catchability prior was updated. The spawning biomass was lower

in this model to allow a higher catchability value consistent with the Longnose Skate prior, but as explored in detail during the review, the fit to data and other aspects of this model are very similar to the new base model with the updated catchability prior which is more consistent with the depth distribution of Big Skate relative to the survey area.

Removing the prior on catchability for the WCGBT Survey had a large change in the estimated scale of the population, with the unfished equilibrium biomass increasing from the 2,224 mt estimated in the base model to 9,932 mt (“No q prior on WCGBTS” in Figure 45 and Table 9). This population scale is constrained by an arbitrary lower limit of 0.2 on the catchability parameter. However, the change in likelihood was relatively small, with the total improving by 0.4 units, of which 0.04 was associated with the prior itself.

Removing the offset on the catchability between the early and late periods of the Triennial had negligible impact on the model results and the fit to the Triennial survey was essentially a straight line through the middle (not shown).

Biology (Figure 46 and Table 10)

The sensitivity analyses related to biology and data weighting included assumptions about natural mortality (M), growth, and data weighting (Figure 46 and Table 10). Allowing separate estimates of female and male natural mortality led to estimates of 0.48 for females and 0.40 for males, which are nearly symmetric around the 0.449 estimate of the shared mortality parameter in the base model. This difference allows more males to be present in the population and therefore better matches the skewed sex ratios in the length composition data. The scale of the unfished equilibrium spawning biomass dropped to 58% of the base model estimate due to the smaller fraction of females living to maturity with the higher M , but the estimate of total biomass in the age 2+ biomass remained at 89% of the base model (Table 10). The improvement in likelihood is 2.2 units, which is modest given the extra parameter estimated. Additional explorations (not shown) indicated that a model with differential M and no sex-specific offsets on the selectivity had much poorer fit to the data than either the base model or this sensitivity analysis. Therefore, given that the differential selectivity provided a greater improvement in model fit than the sex-specific M , only the more influential factor was included in the base model.

Removing the prior on M had little impact on the model with M increasing from 0.449 in the base model to 0.451 without the prior.

The use of either von Bertalanffy (1938) or Richards (1959) growth models provided poorer fits to both the conditional age-at-length and length data, and higher estimated variability in length-at-age (Figure 47). The increase in variability in length-at-age suggests that the model is using this variability to compensate for lack of fit to the mean length-at-age. The Richards model is a generalization of the von Bertalanffy growth model with an additional parameter allowing a more sigmoidal shape. The model with Richards growth had estimated growth curves that were closer to the base model, but still had a total negative log-likelihood that was 22 units worse than the base model, with most of that difference occurring in the

length composition likelihood component where the lack of the cessation in male growth prevented the Richards model from fitting the bimodal patterns in both the survey and fishery data.

Data weighting and recruitment (Figure 48, Figure 49, and Table 11)

The base model sample size adjustments from the Francis (2011) method for the length composition data were 0.240 for the fishery lengths, 0.067 for the WCGBT Survey lengths, and 1.0 for the Triennial Survey lengths (constrained to avoid upweighting as the input sample size was already the number of fish for this one source). The sample size adjustments for the age data were 0.084 for the fishery and 0.054 for the WCGBT Survey. Tuning the sample sizes using the McAllister-Ianelli (1997) method had a relatively small impact on the model results (Figure 48 and Table 11), with a lower weight given to the fishery lengths (0.107) than the status quo Francis tuning method, and a higher weight given to the WCGBT Survey lengths (0.637). The lengths from the Triennial Survey were given similar weight. Ages from both the fishery and the WCGBT Survey were increased to 0.410 and 0.404, respectively. The likelihoods could not be compared due to these changes in the adjusted sample sizes, but the estimated parameters were all relatively similar to those in the base model. Tuning the sample sizes using the Dirichlet-Multinomial likelihood (2017) resulted in higher weights for all length and age data, with sample size adjustments between 0.97 and 1.0 for all of the input length and age data. The scale of the spawning biomass increased with the Dirichlet-Multinomial likelihood (Figure 48 and Table 11). Given the relatively good fit of the base model to the length and age data compared to the other inputs, especially the indices, the alternative data-weighting methods, which in general increased the weight on these composition data, did not seem justified.

When recruitment deviations were estimated, the model was better able to fit the higher values in the most recent 5 years of the WCGBT Survey as well as the lower values for the preceding 5 years (Figure 49). This more flexible model no longer required the catchability prior to keep the scale of the population from blowing up to implausibly high values as demonstrated by an additional sensitivity analysis with recruitment deviations and no catchability prior (Figure 48, Figure 49, and Table 11). However, the recruitment deviation estimates in both models were highly uncertain as expected given the limited age data available, with the 95% uncertainty intervals overlapping 0 in almost all years with the exception of the years 2010–2012 where the above average recruitment supported the increasing trend in the available survey biomass a few years later rather. The limited age data showed little improvement from the recruitment deviations, with a change of less than one unit of log-likelihood in spite of the extra 135 estimated parameters. Although recruitment variability is likely to be present in the population and excluding this process from the base model likely contributes to the lack of fit to the indices, the data available for Big Skate don't seem to support the additional model complexity required to add these parameters.

Catch and discards (Figure 50 and Table 12)

The sensitivity analyses related to discard mortality resulted in little change in the scale of the population for any scenario (Figure 50 and Table 12). Increasing or decreasing the

discard mortality from 0.5 to 0.4 or 0.6 had the least impact, while the two alternative time series of discards caused the population to fall to a lower level around 1990 and increase faster in the recent period. The discards based on 3-yr average analysis simply used the alternative time series of historical discards described above and shown in Figure 5.

The sensitivity analysis in which historical catch was adjusted by estimating multipliers on discards over blocks of time made use of the relatively new “catch multiplier” option in Stock Synthesis. Multiplier parameters controlling the ratio of the discards removed from the model relative to the input values were estimated for blocks of time covering the periods 1916–1949, 1950–1959, 1960–1969, 1970–1979, 1980–1989, and 1990–1994. These multiplier parameters were bounded to keep the input catch relative to the estimated total within the range 0.5–1.5 and a weak Beta prior distribution spanning this range was applied to the parameters to keep them from hitting the bounds and cause them to remain at 1.0 in the absence of information in the data.

The resulting pattern of historical discards shows a steadily increasing catch, with higher catch relative to the input values in all the blocks up to a peak in the 1980s, followed by a decrease in the estimated catch for the 1990–1994 period (Figures 54 and 52). These changes provide a greater contrast in the catch history, causing the estimated time series of spawning biomass to fall to a lower level and then increase faster from the 1990s onward, thus fitting the WCGBT Survey slightly better (Figures 50 and {fig:Sensitivity_catch2}). However, the improvement in likelihood for the survey was only 0.3 units (Table 12).

The sensitivity analysis in which historical catch was adjusted to match a time series of fishing mortality for Petrale Sole for the period 1950–1994 was based on the premise that fishing mortality for Petrale Sole is correlated with that for Big Skate. Petrale Sole frequently co-occur with Big Skate in both the fishery and survey (Wallace 2019). Whereas the Dover Sole population used in the estimation of Longnose Skate discards has been very stable with the fraction unfished never estimated as having fallen below 63% of B_0 , Petrale Sole was overfished for decades and the most recent stock assessment (Stawitz et al. 2015) estimated that the spawning biomass fell to 5% of the unfished level by 1993 before subsequently rebuilding to about 30% of unfished biomass. Therefore, total catch of Petrale Sole is reflective of both the fishing mortality and the change in biomass over time. An additional complexity is that while the summer fishing grounds for Petrale are in relatively shallow water, there is also a winter fishery on Petrale Sole spawning aggregations in deeper water where Big Skate are likely less common.

In the Petrale Sole stock assessment, the fishery was divided into separate Summer and Winter components and further divided between northern and southern areas, with the dividing line at 42 degrees N latitude (the boundary between Oregon and California). To develop an index of fishing mortality, a weighted average of the estimated F time series for each of the two Summer fisheries was calculated by applying weights of 0.424 to the F from the southern area and 0.576 for the northern area. These weights were based on the average ratio of estimated Big Skate biomass in the WCGBT Survey north and south of 42 degrees as estimated in the VAST index standardization. The resulting time series of Petrale Sole F was

then input to the Big Skate model as an index of F for the historical fishery. As this index applied to the combination of both discarded and retained catch, those two components of the historical fishery were combined. The input catch values were treated as uncertain and the likelihood weight given to the index of F was set high enough to ensure that the F time series was matched exactly. The F time series was fit for the years 1950–1994. Attempts to include the years prior to 1950 in the fit led to models that did not converge.

The resulting estimates of F and catch for Big Skate from this sensitivity analysis were somewhat similar to those derived from the catch multiplier sensitivity analysis described above, with higher mortality and catch in the 1970s and 1980s than in the 1950s (Figures 53 and 54). The resulting time series of spawning biomass started slightly above the base model and ended in a very similar place. The estimates of uncertainty in spawning biomass associated with the catch multiplier and Petrale F sensitivity analyses were very similar to the base model (the Sigma associated with 2019 spawning biomass was within 0.34–0.37 for the three models), but the uncertainty in the fraction unfished was much larger for the catch multiplier model, reflecting the broader range of catch histories and associated population trajectories that could be associated with the additional flexibility (Figure 55).

5.5.4 Retrospective Analysis

Retrospective analyses, in which the final 5 years of data are successively removed from the model, showed relatively little change in the scale of the estimated population, but the uncertainty about the population size increased (Figure 56). The WCGBT Survey observations were underfit for the final 5 years, so removing these points, combined with a prior on catchability lowers the status of the stock, and led to a slightly reduced estimated spawning biomass.

5.5.5 Likelihood Profiles

Likelihood profiles were conducted over the parameter controlling unfished equilibrium recruitment $\log(R_0)$, catchability of the WCGBT Survey (q), stock-recruit steepness (h) and natural mortality (M). Results of these profiles are shown in Figures 57 to 65. The contribution of different data sources to the changes in likelihood within the profiles were considered in the context of a change of less than 1.92 units of negative log-likelihood, sometimes considered small, based on half of the 95% quantile of a Chi-squared distribution with 1 degree of freedom.

The profile over $\log(R_0)$ shows that the change in likelihood over a broad range of values is relatively small compared to models with more contrast in the data, with a total change in likelihood of less than 4 units over a range of 8.2 to 9.6, corresponding to a range in equilibrium recruitment of 3.6 million to 14.8 million (the $\log(R_0)$ parameter is the log of R_0 in thousands). Models with $\log(R_0) < 8.2$ did not converge. The age data and discard data

are best fit at the highest R_0 considered while the index and mean body weight data are best fit at the lowest R_0 . Only the priors and the length data are best fit at intermediate values. The length data was best fit at $\log(R_0) = 8.9$, while prior likelihood (mostly the prior on catchability as the prior on M was less informative) were best fit at $\log(R_0) = 8.8$. The base model estimate balancing all these components was $\log(R_0) = 8.905$. The spawning biomass estimates from the models in the profile were all relatively similar as a result of the models with higher R_0 also having a higher M estimate, leading to a similar number of fish surviving to maturity (the range was $M = 0.489$ at $\log(R_0) = 9.6$ to $M = 0.403$ at $\log(R_0) = 8.2$).

The profile over catchability of the WCGBT Survey (q) provides a better illustration of the information in the data about the scale of the population, because the prior on q is no longer influencing the estimates of all other parameters. The range considered for the parameter $\log(q)$ corresponded to $q = 0.5$ to $q = 2.0$, where $q = 0.5$ has the observed survey biomass equal to half of the true population after accounting for selectivity of the survey, and $q = 2.0$ corresponds to the survey observations being double the true population. The likelihood contributions are represented here both without and with the prior likelihood (Figures 59 and 60). The prior has a much stronger influence on the changes in likelihood over the range considered, with a total change of greater than 10 units of negative log-likelihood. The length data is the most influential of the other components, with a change of 2.6 units over the range of q considered, with the best fit occurring at the smallest q values. All three sources of length data were best fit at the lowest q values with the fishery contributing 71% of the change, the WCGBT Survey 27% and the remaining %1 from the Triennial survey. The mean body weight data is also better fit at low q while the indices and discard data are best fit at $q = 1.75$. The age data and the prior on natural mortality show very little change in likelihood over the range of q considered (less than 0.1 unit of negative log-likelihood).

The spawning biomass estimated for the models included in the q profile (Figure 61) show similar trajectories, with the scale of the population negatively correlated with the q values as expected.

The profile over steepness of the stock-recruit curve shows less than 0.5 units of likelihood over the range $h = 0.3$ to $h = 0.9$. The best fit occurred at $h = 0.5$, indicating that a model with steepness estimated would have been relatively similar to the base model where h was fixed at 0.4. However, earlier explorations indicated that models with h estimated sometimes produced unstable results, where small changes in model configuration could cause the parameter to be estimated at either the upper or lower bound of the 0.2–1.0 range on which it's defined for the Beverton-Holt stock-recruit curve.

The profile over natural mortality (M) shows that most of the information in the likelihood about M was from the length and age data, with additional information in the discard rates and the mean body weight data. The prior on M provided relatively little contribution to the total likelihood. The length data had the largest change in likelihood over the 0.25–0.55 range of M considered, and was best fit at 0.45, close to the base model estimate of 0.449.

5.5.6 Reference Points

Reference points were calculated using the estimated selectivities and catch distribution among fleets in the most recent year of the model, (2018). Sustainable total yield (landings plus discards) were 590 mt when using an $SPR_{50\%}$ reference harvest rate and with a 95% confidence interval of 266 mt based on estimates of uncertainty. The spawning biomass equivalent to 40% of the unfished level ($SB_{40\%}$) was 1,010 mt.

The 2019 spawning biomass relative to unfished equilibrium spawning biomass is above the target of 40% of unfished levels (Figure 41). The relative fishing intensity, $(1 - SPR)/(1 - SPR_{50\%})$, has been below the management target for the entire time series of the model (Table 7).

Table 17 shows the full suite of estimated reference points for the base model and Figure 66 shows the equilibrium curve based on a steepness value of 0.4.

6 Harvest Projections and Decision Tables

The forecasts of stock abundance and yield were developed using the final base model, with the forecasted calculations of the OFL and ACL presented in Table 15. For 2019 and 2020, mortality estimates were provided by the Groundfish Management Team based on recent trends in catch. For 2021 and beyond, estimated total mortality is assumed equal to the ACL in each year.

The decision table including alternative catch streams for the alternative states of anture is presented in Table 16.

7 Regional Management Considerations

Big Skate is not managed to regional specifications.

8 Research and Data Needs

We recommend the following research be conducted before the next assessment.

1. **Extend all ongoing data streams used in this assessment.** A longer fishery-independent index from a continued WCGBT Survey with associated compositions of length and age-at-length will improve understanding of dynamics of the stock. Continued sampling of lengths and ages from the landed catch and lengths, mean body weights, and discard rates from the fishery will be even more valuable for the years ahead now that Big Skate are landed as a separate market category and the estimates will be more precise.
2. **Investigate factors contributing to estimated lower selectivity for females than males.** Sex-specific differences in selectivity were included in the base model to better fit differences in sex ratios in the length composition data but the behavioral processes that might contribute to this pattern are not understood and other explanations for the sex ratios are possible.
3. **Pursue additional approaches for estimating historical discards.** The approaches used here were based on averages applied over a period of decades. The catch reconstructions conducted for each state were much more sophisticated, but were applied only to the subset of the catch that was landed. Reconstructed spatial patterns of fishing effort could be used to estimate changes in total mortality over time.
4. **Improve understanding of links between Big Skate on the U.S. West Coast and other areas.** Tagging studies in Alaska indicated that Big Skate are capable of long distance movements. A better understanding of links through tagging in other areas and genetic studies could highlight strengths or weaknesses of the status quo approach.
5. **Conduct studies of mortality of discarded skates in commercial fisheries.** Estimates of discard mortality for skates in general could be improved.
6. **Improve understanding of catch history and population dynamics of California Skate.** California Skate is the third most commonly occurring Skate in California waters after Longnose Skate and Big Skate and the catch reconstruction indicated that the center of abundance for California Skate is centered around San Francisco, where the fishery was strongest in the early years. If California Skate is found to be at a low biomass compared to historical levels it would have implications for the catch reconstruction of the other two species, as well as suggesting that management of California Skate should be a higher priority.

9 Acknowledgments

The authors gratefully acknowledge the time and effort Stacey Miller, John DeVore, Owen Hamel, and Jim Hastie put into making this a more polished document.

We thank the STAR panel Chair, David Sampson, and reviewers Robin Cook, Henrik Sparholt, and Cody Szulwalski.

The Reconstructions of historical catch were critical to this assessment, and there are many people who contributed, among them

our colleagues at WDFW: Theresa Tsou, Jessi Doerpinghaus, and Greg Lippert,

our colleagues at ODFW: Ali Whitman, Patrick Mirick, and Ted Calavan,

our colleagues at the SWFSC: John Field and Rebecca Miller,

and others whose knowledge of the fishery provided context: Gerry Richter and Todd Phillips.

Our colleagues at NFWFC, including Chantel Wetzel, Kelli Johnson, and John Wallace all provided valuable contributions to the extraction and processing of the survey and fishery data.

Curt Whitmire's input was critical to the development of the new catchability prior for the WCGBTS.

Finally, we are deeply grateful to Melissa Monk of the SWFSC, for creating the RMarkdown template which was used to produce this assessment report.

10 References

- Alaska Fisheries Science Center. 2018. Assessment of the skate stock complex in the Gulf of Alaska. Available from <https://www.afsc.noaa.gov/REFM/Docs/2018/GOA/GOAskate.pdf>.
- Batdorf, C. 1990. Northwest Native Harvest. Hancock House Publishers Ltd.; Surrey, B.C., Canada.
- Bizzarro, J. 2015. Comparative resource utilization of eastern north pacific skates (rajiformes: Rajidae) with applications for ecosystem-based fisheries management. WA: University of Washington.
- Bizzarro, J. 2019. Manuscript in preparation.
- Bizzarro, J., Broms, K., Logsdon, M., Ebert, D., Yoklavich, M., Kuhnz, L., and Summers, A. 2014. Spatial segregation in eastern north Pacific skate assemblages. *PloS one* **9**(10).
- Bizzarro, J., Robinson, H., Rinewalt, C., and Ebert, D. 2007. Comparative feeding ecology of four sympatric skate species off central California, USA. *In Biology of skates*. Springer. pp. 91–114.
- Bowers, G. M. 1909. Report of The Commissioner For the Year Ending June 30, 1909. Part XXVIII. Washington Printing Office.
- Bradburn, M.J. and Keller, A.A and Horness, B.H. 2011. The 2003 to 2008 US West Coast bottom trawl surveys of groundfish resources off Washington, Oregon, and California: estimates of distribution, abundance, length, and age composition. NOAA Technical Memorandum NMFS NOAA-TM-NMFS-NWFSC-114: 323 pp.
- Brown, L.D., Cai, T.T., and DasGupta, A. 2001. Interval estimation for a binomial proportion. *Statistical science*: 101–117. JSTOR.
- Calavan, T. 2019. Oregon Department of Fisheries; Wildlife; Personal Communication, Newport, OR, USA.
- Castro-Aguirre, J.L., and Pérez, H.E. 1996. Catálogo sistemático de las rayas y especies afines de méxico: Chondrichthyes: Elasmobranchii: Rajiformes: Batoideiomorpha. Unam.
- Castro-Aguirre, J., Schmitter, J., Balart, E., and Torres-Orozco, R. 1993. Sobre la distribución geográfica de algunos peces bentónicos de la costa oeste de baja california sur, méxico, con consideraciones ecológicas y evolutivas. *In Anales de la escuela nacional de ciencias biológicas*, méxico. pp. 75–102.

Chapman, W.M. 1944. The Latent Fisheries of Washington and Alaska. Washington State Department of Fisheries.

Chiquillo, K.L., Ebert, D.A., Slager, C.J., and Crow, K.D. 2014. The secret of the mermaid's purse: Phylogenetic affinities within the Rajidae and the evolution of a novel reproductive strategy in skates. *Molecular Phylogenetics and Evolution* **75**: 245–251. Elsevier.

DeLacy, A.C., and Chapman, W.M. 1935. Notes on some elasmobranchs of puget sound, with descriptions of their egg cases. *Copeia* **1935**(2): 63–67. JSTOR.

Dorn, M., Cordue, P., and Haist, V. 2007. Pacific Fishery Management Council, Portland, OR. Available from https://www.pcouncil.org/wp-content/uploads/STARReport_Skate.pdf.

Downs, D.E., and Cheng, Y.W. 2013. Length-length and width-length conversion of long-nose skate and big skate off the pacific coast: Implications for the choice of alternative measurement units in fisheries stock assessment. *North American journal of fisheries management* **33**(5): 887–893. Taylor & Francis.

Ebert, D. 2003. Sharks, rays, and chimaeras of california. Univ of California Press.

Ebert, D.A., and Compagno, L.J. 2007. Biodiversity and systematics of skates (chondrichthyes: Rajiformes: Rajoidei). In *Biology of skates*. Springer. pp. 5–18.

Ebert, D.A., Smith, W.D., and Cailliet, G.M. 2008. Reproductive biology of two commercially exploited skates, *raja binoculata* and *r. Rhina*, in the western gulf of alaska. *Fisheries Research* **94**(1): 48–57. Elsevier.

Eschmeyer, W.N., and Herald, E.S. 1983. A field guide to pacific coast fishes: North america. Houghton Mifflin Harcourt.

Farrugia, Thomas J. 2017. Interdisciplinary Assessment of the Skate Fishery in the Gulf of Alaska. PhD Dissertation, University of Alaska Fairbanks.

Farrugia, T.J., Goldman, K.J., Tribuzio, C., and Seitz, A.C. 2016. First use of satellite tags to examine movement and habitat use of big skates *beringraja binoculata* in the gulf of alaska. *Marine Ecology Progress Series* **556**: 209–221.

Ford, P. 1971. Differential growth rate in the tail of the pacific big skate, (*Raja binoculata*). *Journal of the Fisheries Board of Canada* **28**(1): 95–98. NRC Research Press.

Francis, R.I.C.C. 2011. Data weighting in statistical fisheries stock assessment models. *Canadian Journal of Fisheries and Aquatic Sciences* **68**: 1124–1138.

GA, M., and JR, K. 2006. Age and growth of big skate (*Raja binoculata*) and longnose skate (*Raja rhina*) in British Columbia waters. *Fisheries Research* **May 1 (2-3)**: 169–78.

Gburski, C., Gaichas, S., and Kimura, D. 2007. Age and growth of big skate (*Raja binoculata*) and longnose skate (*Raja rhina*) in the Gulf of Alaska. In Biology of Skates. Springer, Dordrecht.

Gertseva, V. 2019. Manuscript in preparation.

Gertseva, V., and Schirippa, M. 2007. Status of the Longnose Skate (*Raja rhina*) off the continental US Pacific Coast in 2007. Pacific Fishery Management Council, Portland, OR. Available from <http://www.pcouncil.org/groundfish/stock-assessments/>.

Gertseva, V., and Taylor, I. 2011. Status of spiny dogfish shark resource off the continental us pacific coast in 2011. PFMC. 2011. Pacific Fishery Management Council, Portland, OR. Available from <http://www.pcouncil.org/groundfish/stock-assessments/>.

Gunderson, DR and Sample, TM. 1980. Distribution and abundance of rockfish off Washington, Oregon and California during 1977. Northwest and Alaska Fisheries Center, National Marine Fisheries Service. Available from <http://spo.nmfs.noaa.gov/mfr423-4/mfr423-42.pdf>.

Hamel, Owen S. 2015. A method for calculating a meta-analytical prior for the natural mortality rate using multiple life history correlates. ICES Journal of Marine Science: Journal du Conseil **72**(1): 62–69. doi: [10.1093/icesjms/fsu131](https://doi.org/10.1093/icesjms/fsu131).

Hitz, C.R. 1964. Observations on egg cases of the big skate (*raja binoculata girard*) found in oregon coastal waters. Journal of the Fisheries Board of Canada **21**(4): 851–854. NRC Research Press.

Hoff, GR. 2009. Skate *Bathyraja* spp. egg predation in the eastern Bering Sea. J. Fish. Biol. **74**: 250–269.

Ishihara, H., Treloar, M., Bor, P., Senou, H., and Jeong, C. 2012. The comparative morphology of skate egg capsules (Chondrichthyes: Elasmobranchii: Rajiformes). Bulletin of the Kanagawa Prefectural Museum (Natural Science) **41**: 9–25.

Keller, A.A. and Wallace, J.R. and Methot, R.D. 2017. The Northwest Fisheries Science Center's West Coast Groundfish Bottom Trawl Survey: History, Design, and Description. NOAA Technical Memorandum NMFS NOAA-TM-NMFS-NWFSC-136: 38 pp.

King, J., and McFarlane, G. 2009. Biological results of the strait of georgia spiny dogfish (*squalus acanthias*) longline survey, october 10-22, 2008. Fisheries; Oceans Canada, Science Branch, Pacific Region.

King, JR and McFarlane, GA. 2010. Movement patterns and growth estimates of big skate (*Raja binoculata*) based on tag-recapture data. Fish. Res. **101**: 50–59.

King, S., J.R., and Starr, P. 2015. Big skate (*Raja binoculata*) and longnose skate (*R. rhina*) stock assessments for British Columbia. Ottawa : Canadian Science Advisory Secretariat.

Last, P., White, W., Carvalho, M. de, Séret, B., Stehmann, M., and Naylor GJP (eds.). 2016. *Rays of the World*. CSIRO Publishing, Comstock Publishing Associates.

Lippert, G. 2019. Washington Department of Fisheries; Wildlife; Personal Communication, Olympia, Washington, USA.

Love, Milton S. 2011. Certainly more than you want to know about the fishes of the Pacific Coast: a postmodern experience. Really Big Press.

Maunder, M.N., Deriso, R.B., Schaefer, K.M., Fuller, D.W., Aires-da-Silva, A.M., Minte-Vera, C.V., and Campana, S.E. 2018. The growth cessation model: A growth model for species showing a near cessation in growth with application to bigeye tuna (*thunnus obesus*). *Marine biology* **165**(4): 76. Springer.

McAllister, M K and Ianelli, J N. 1997. Bayesian stock assessment using catch-age data and the sampling - importance resampling algorithm. *Canadian Journal of Fisheries and Aquatic Sciences* **54**(2): 284–300.

McEachran, J., and Miyake, T. 1990. 1990. Zoogeography and bathymetry of skates (chondrichthyes, rajidae). Elasmobranchs as living resources. *Advances in biology, Ecology, Systematics and the status of the fisheries*: 305–326.

Mecklenburg, C., Mecklenburg, T., and Thorsteinson, L. 2002. *Fishes of Alaska*. American Fisheries Society, Bethesda, Maryland.

Methot, Richard D. and Wetzel, Chantell R. 2013. Stock synthesis: A biological and statistical framework for fish stock assessment and fishery management. *Fisheries Research* **142**: 86–99.

Methot, R.J., Wetzel, C., and Taylor, I. 2019. Stock Synthesis User Manual Version 3.30.13. NOAA Fisheries. Seattle, WA. Available from <https://vlab.ncep.noaa.gov/web/stock-synthesis>.

Miller, B.S., Cross, J.N., Steinfort, S.N., Fresh, K.L., and Simenstad, C.A. 1980. Nearshore fish and macroinvertebrate assemblages along the strait of juan de fuca including food habits of the common nearshore fish.

Mirick, P. 2019. Oregon Department of Fish; Wildlife; Personal Communication, Newport, Oregon, USA.

Pacific Fishery Management Council. 2018. Status of the Pacific Coast Groundfish Fishery. Available from http://www.pcouncil.org/wp-content/uploads/2017/02/SAFE_Dec2016_02_28_2017.pdf.

Punt AE and Smith DC and KrusicGolub K and Robertson S. 2008. Quantifying age-reading error for use in fisheries stock assessments, with application to species in Australia's southern and eastern scalefish and shark fishery. Canadian Journal of Fisheries and Aquatic Sciences.

Richards, F. 1959. A flexible growth function for empirical use. *Journal of experimental Botany* **10**(2): 290–301. Oxford University Press.

Stawitz, C., Hurtado-Ferro, F., Kuriyama, P., Trochta, J., Johnson, K., Haltuch, M., and Hamel, O. 2015. Stock assessment update: Status of the us petrale sole resource in 2014. Pacific Fishery Management Council, Portland, OR, USA.

Stevenson, D., Orr, J., Hoff, G., and McEachran, J. 2008. Emerging patterns of species richness, diversity, population density, and distribution in the skates (Rajidae) of Alaska. *Fish Bull* **106**: 24–39.

Stewart, I. 2019. International Pacific Halibut Commission; Personal Communication, Seattle, Washington, USA.

Stewart, I.J., Wallace, J.R., and McGilliard, C. 2009. Status of the us yelloweye rockfish resource in 2009. *In* Pacific Fishery Management Council, Portland, OR. Available from <http://www.pcouncil.org/groundfish/stock-assessments/>.

Taylor, I.G., Stewart, I.J., Hicks, A.C., Garrison, T.M., Punt, A.E., Wallace, J.R., Wetzel, C.R., Thorson, J.T., Takeuchi, Y., Ono, K., Monnahan, C.C., Stawitz, C.C., A'mar, Z.T., Whitten, A.R., Johnson, K.F., Emmet, R.L., Anderson, S.C., Lambert, G.I., Stachura, M.M., Cooper, A.B., Stephens, A., Klaer, N.L., McGilliard, C.R., Iwasaki, W.M., Doering, K., and Havron, A.M. 2019. R4ss: R code for stock synthesis. Available from <https://github.com/r4ss>.

Taylor IG and Cope, J and Hamel O and Thorson, J. 2013. Deriving estimates of OFL for species in the “Other Fish” complex or potential alternative complexes. Pacific Fishery Management Council, Portland, OR. Available from <http://www.pcouncil.org/groundfish/stock-assessments/>.

Thorson, James T. and Barnett, Lewis A. K. 2017. Comparing estimates of abundance trends and distribution shifts using single- and multispecies models of fishes and biogenic habitat. *ICES Journal of Marine Science: Journal du Conseil*: fsw193. doi: [10.1093/icesjms/fsw193](https://doi.org/10.1093/icesjms/fsw193).

Thorson, J., Johnson, K., Methot, R., and Taylor, I. 2017. Model-based estimates of effective sample size in stock assessment models using the dirichlet-multinomial distribution. *Fisheries Research* **192**: 84–93. Elsevier.

Thorson, J. T. and Shelton, A. O. and Ward, E. J. and Skaug, H. J. 2015. Geostatistical delta-generalized linear mixed models improve precision for estimated abundance indices for West Coast groundfishes. *ICES Journal of Marine Science* **72**(5): 1297–1310. doi: [10.1093/icesjms/fsu243](https://doi.org/10.1093/icesjms/fsu243).

von Bertalanffy, L. 1938. A quantitative theory of organic growth. *Human Biology* **10**: 181–213.

Wallace, J. 2019. Northwest Fisheries Science Center; Personal Communication, Seattle, Washington, USA.

Whitman, A. 2019. Oregon Department of Fisheries; Wildlife; Personal Communication, Newport, Oregon, USA.

Whitmire, C. 2019. Northwest Fisheries Science Center; Personal Communication, Seattle, Washington, USA.

Zeiner, S.J. and P. Wolf. 1993. Growth characteristics and estimates of age at maturity of two species of skates (*Raja binoculata*) and (*Raja rhina*) from Monterey Bay, California.

11 Tables

11.1 Data Tables

Table 3: Landings by source. For detail on the source of the different estimates, see 'Fishery Landings and Discards' above. Values prior to 1939 were not included in the final model and augmented by an estimated linear increase in total catch including discards from 1916 to 1950. Estimated discards are not included in this table.

Year	CA (mt)	OR (mt)	WA (mt)	Tribal (mt)	Total (mt)
1916	78.30	0.00	0.00	0.00	78.30
1917	80.10	0.00	0.00	0.00	80.10
1918	101.20	0.00	0.00	0.00	101.20
1919	75.20	0.00	0.00	0.00	75.20
1920	122.00	0.00	0.00	0.00	122.00
1921	17.80	0.00	0.00	0.00	17.80
1922	30.80	0.00	0.00	0.00	30.80
1923	34.20	0.00	0.00	0.00	34.20
1924	33.40	0.00	0.00	0.00	33.40
1925	46.70	0.00	0.00	0.00	46.70
1926	59.30	0.00	0.00	0.00	59.30
1927	67.10	0.00	0.00	0.00	67.10
1928	116.70	0.00	0.00	0.00	116.70
1929	107.50	0.00	0.00	0.00	107.50
1930	70.80	0.00	0.00	0.00	70.80
1931	43.60	0.00	0.00	0.00	43.60
1932	73.30	0.00	0.00	0.00	73.30
1933	46.50	0.00	0.00	0.00	46.50
1934	57.40	0.00	0.00	0.00	57.40
1935	70.60	0.00	0.00	0.00	70.60
1936	87.70	0.00	0.00	0.00	87.70
1937	115.40	0.00	0.00	0.00	115.40
1938	99.40	0.00	0.00	0.00	99.40
1939	90.90	0.00	0.00	0.00	90.90
1940	60.30	5.30	0.00	0.00	65.70
1941	53.10	56.40	0.00	0.00	109.40
1942	27.00	34.40	0.00	0.00	61.40
1943	20.40	0.90	0.00	0.00	21.30
1944	7.80	1.60	0.00	0.00	9.50
1945	13.30	0.30	0.00	0.00	13.50
1946	17.10	1.80	0.00	0.00	18.90
1947	24.10	0.00	0.00	0.00	24.10
1948	30.70	5.70	0.00	0.00	36.30

Continued on next page

Table 3: Landings by source. For detail on the source of the different estimates, see 'Fishery Landings and Discards' above. Values prior to 1939 were not included in the final model and augmented by an estimated linear increase in total catch including discards from 1916 to 1950. Estimated discards are not included in this table.

Year	CA (mt)	OR (mt)	WA (mt)	Tribal (mt)	Total (mt)
1949	31.90	0.00	7.20	0.00	39.10
1950	32.20	2.10	2.10	0.00	36.40
1951	21.70	4.70	3.90	0.00	30.30
1952	39.10	0.10	7.80	0.00	46.90
1953	124.90	1.20	1.60	0.00	127.60
1954	38.80	2.30	1.20	0.00	42.40
1955	45.70	35.60	1.60	0.00	82.90
1956	40.40	2.60	3.10	0.00	46.10
1957	49.50	0.00	2.50	0.00	52.00
1958	38.80	0.00	0.20	0.00	38.90
1959	46.50	0.00	0.80	0.00	47.30
1960	39.20	0.00	0.70	0.00	39.80
1961	54.40	40.90	4.60	0.00	99.80
1962	44.40	27.90	5.20	0.00	77.60
1963	53.20	30.40	2.10	0.00	85.70
1964	49.90	28.30	2.70	0.00	80.90
1965	34.30	12.80	3.50	0.00	50.60
1966	36.40	20.10	0.60	0.00	57.00
1967	53.30	15.60	6.60	0.00	75.50
1968	55.30	45.40	8.80	0.00	109.50
1969	32.50	33.80	6.60	0.00	72.90
1970	16.30	11.90	0.10	0.00	28.20
1971	18.50	3.10	0.00	0.00	21.60
1972	33.50	2.00	0.10	0.00	35.60
1973	40.70	0.90	0.00	0.00	41.70
1974	21.90	5.90	0.10	0.00	27.80
1975	39.80	2.00	0.00	0.00	41.80
1976	20.70	31.30	0.20	0.00	52.20
1977	32.80	31.50	0.60	0.00	64.90
1978	67.70	77.30	4.00	0.00	149.10
1979	90.50	75.50	30.40	0.00	196.40
1980	17.60	34.10	5.20	0.00	56.90
1981	138.00	14.80	6.50	0.00	159.30
1982	78.30	5.20	14.60	0.00	98.10
1983	55.30	14.20	8.90	0.00	78.40
1984	26.20	4.90	1.60	0.00	32.70
1985	60.30	0.40	4.90	0.00	65.60
1986	27.20	1.60	8.90	0.00	37.80

Continued on next page

Table 3: Landings by source. For detail on the source of the different estimates, see 'Fishery Landings and Discards' above. Values prior to 1939 were not included in the final model and augmented by an estimated linear increase in total catch including discards from 1916 to 1950. Estimated discards are not included in this table.

Year	CA (mt)	OR (mt)	WA (mt)	Tribal (mt)	Total (mt)
1987	22.60	1.90	18.40	1.00	43.90
1988	15.30	0.30	10.90	1.20	27.60
1989	18.90	0.20	6.20	0.00	25.30
1990	25.10	0.00	9.60	0.10	34.90
1991	22.80	0.20	21.50	0.10	44.60
1992	24.60	0.30	11.20	0.00	36.10
1993	29.00	0.20	21.00	0.60	50.70
1994	27.70	2.50	20.50	0.10	50.70
1995	43.00	41.20	21.80	0.10	106.00
1996	146.70	138.50	22.80	0.10	308.10
1997	228.40	215.40	84.00	0.20	528.00
1998	120.50	51.40	22.70	0.20	194.90
1999	109.50	131.30	41.40	0.40	282.60
2000	69.40	193.60	97.70	0.30	361.00
2001	75.30	115.10	26.70	0.40	217.50
2002	34.70	102.80	70.80	4.80	213.10
2003	48.80	223.00	65.70	5.40	342.80
2004	45.20	105.90	98.00	4.60	253.80
2005	33.40	151.30	113.10	15.70	313.40
2006	102.40	206.60	66.20	24.90	400.00
2007	35.50	190.40	29.10	19.90	274.90
2008	46.00	280.10	36.80	3.20	366.00
2009	9.60	162.00	16.50	17.50	205.70
2010	1.20	157.50	25.00	12.50	196.20
2011	0.50	231.50	10.00	26.40	268.40
2012	6.80	216.30	5.00	41.60	269.60
2013	20.90	92.30	13.00	8.80	135.00
2014	41.00	286.00	16.80	28.60	372.40
2015	35.20	218.80	1.00	76.60	331.50
2016	15.00	317.50	1.20	77.80	411.50
2017	28.00	188.00	1.40	60.20	277.60
2018	23.80	115.80	2.40	30.60	172.60

Table 4: Modeled and design-based indices for the assessment model. The WCGBT and Triennial Surveys were standardized using the VAST geostatistical software and are in units of metric tons.

Year	Triennial				WCGBTs			
	VAST		Design		VAST		Design	
	Obs	se_log	Obs	se_log	Obs	se_log	Obs	se_log
1980	468	0.53	747	0.53				
1983	912	0.30	1339	0.35				
1986	997	0.29	1914	0.47				
1989	1432	0.22	1767	0.21				
1992	2426	0.20	2722	0.19				
1995	497	0.26	807	0.26				
1998	2438	0.20	3324	0.20				
2001	1670	0.23	2671	0.22				
2003					8171	0.20	8049	0.15
2004	3674	0.19	5404	0.17	14349	0.18	15035	0.18
2005					12123	0.16	11576	0.14
2006					9274	0.18	8559	0.16
2007					8137	0.18	7747	0.16
2008					5495	0.21	5534	0.20
2009					10721	0.17	10025	0.15
2010					11475	0.14	12097	0.13
2011					8030	0.16	8646	0.15
2012					11594	0.16	11512	0.16
2013					11522	0.17	12100	0.16
2014					19856	0.13	18998	0.11
2015					19251	0.13	19056	0.12
2016					17142	0.15	16733	0.19
2017					13237	0.14	13779	0.13
2018					14569	0.14	14836	0.12

Table 5: PacFIN length and age sample sizes by year and state with the number of unique tows from which Big Skate were sampled as well as the number of individual Big Skates that were measured. Samples from all landings were combined for the fishery length and age compositions, while samples from discards provided separate annual compositions.

Year	CA		OR		WA		All Landings		Discards	
	Ntows	Nfish	Ntows	Nfish	Ntows	Nfish	Ntows	Nfish	Ntows	Nfish
Lengths										
1995			6	55			6	55		
1996			3	8			3	8		
1997			1	14			1	14		
1998			1	2			1	2		
1999			1	8			1	8		
2000										
2001			3	43			3	43		
2002			6	199			6	199		
2003			9	202			9	202		
2004			2	27	2	12	4	39		
2005			7	123	6	87	13	210		
2006			13	310	15	191	28	501		
2007	1	1	10	128	9	172	20	301		
2008			10	94	8	94	18	188		
2009	8	32	17	234	1	18	26	284		
2010	2	8	15	186			17	194	149	349
2011	2	2	29	418	4	9	35	429	554	1518
2012	3	43	24	477	3	38	30	558	544	1405
2013	11	201	11	252	8	168	30	621	443	987
2014	15	217	11	237	5	249	31	703	676	1625
2015	25	237	21	411	2	5	48	653	688	1557
2016	14	181	34	444	7	98	55	723	652	1456
2017	14	239	50	668	12	47	76	954	508	1248
2018	15	133	46	552	14	98	75	783		
Ages										
2004					2	11	2	11		
2008			8	80			8	80		
2009			10	87	8	65	18	152		
2010			10	102			10	102		
2011			21	202			21	202		
2012			12	120			12	120		
2018			6	39	13	93	19	132		

Table 6: Survey length and age sample sizes by year with the number of unique tows or sets from which Big Skate were sampled as well as the number of individual Big Skates that were measured.

Year	Triennial		WCGBTS		IPHC	
	Ntows	Nfish	Ntows	Nfish	Nsets	Nfish
Lengths						
2001	41	81				
2003			60	197		
2004	39	100	81	262		
2005			99	328		
2006			67	154		
2007			76	192		
2008			53	159		
2009			82	305		
2010			130	466		
2011			99	360		
2012			104	395		
2013			84	316		
2014			149	552	14	54
2015			134	546		
2016			105	422		
2017			125	496		
2018			123	331		
Ages						
2009			77	230		
2010			124	333		
2016			100	138		
2017			110	164		
2018			118	169		

11.2 Model Results Tables

Table 7: Time-series of population estimates from the base-case model. Relative exploitation rate is $(1 - SPR)/(1 - SPR_{50\%})$.

Year	Total biomass (mt)	Spawning biomass (mt)	Fraction unfished	Age-0 recruits	Total catch (mt)	Relative exploitation rate	SPR
1916	29359	2525	1.000	7367	0	0.00	1.00
1917	29359	2525	1.000	7367	12	0.00	1.00
1918	29348	2523	1.000	7365	25	0.00	0.99
1919	29326	2521	0.999	7363	37	0.00	0.99
1920	29296	2518	0.997	7359	49	0.00	0.98
1921	29258	2513	0.995	7354	62	0.00	0.98
1922	29214	2507	0.993	7348	74	0.00	0.97
1923	29164	2501	0.991	7340	86	0.00	0.97
1924	29108	2493	0.987	7332	99	0.00	0.97
1925	29047	2484	0.984	7322	111	0.00	0.96
1926	28982	2475	0.980	7312	123	0.00	0.96
1927	28911	2465	0.976	7300	136	0.01	0.95
1928	28836	2455	0.972	7289	148	0.01	0.95
1929	28756	2444	0.968	7277	160	0.01	0.94
1930	28673	2433	0.964	7264	172	0.01	0.94
1931	28585	2421	0.959	7251	185	0.01	0.94
1932	28495	2409	0.954	7237	197	0.01	0.93
1933	28401	2397	0.949	7222	210	0.01	0.93
1934	28305	2384	0.944	7207	222	0.01	0.92
1935	28205	2371	0.939	7192	234	0.01	0.92
1936	28103	2357	0.934	7176	246	0.01	0.91
1937	27999	2344	0.928	7159	259	0.01	0.91
1938	27892	2329	0.923	7142	271	0.01	0.90
1939	27783	2315	0.917	7125	329	0.01	0.88
1940	27630	2296	0.910	7102	329	0.01	0.88
1941	27490	2278	0.903	7080	363	0.01	0.87
1942	27332	2258	0.895	7055	351	0.01	0.88
1943	27199	2240	0.887	7032	343	0.01	0.88
1944	27085	2224	0.881	7011	350	0.01	0.87
1945	26973	2208	0.875	6991	364	0.01	0.87
1946	26854	2192	0.868	6970	379	0.02	0.86
1947	26729	2176	0.862	6949	394	0.02	0.86
1948	26598	2160	0.856	6928	412	0.02	0.85
1949	26459	2144	0.849	6907	426	0.02	0.85
1950	26318	2127	0.843	6885	424	0.02	0.85

Continued on next page

Table 7: Time-series of population estimates from the base-case model. Relative exploitation rate is $(1 - SPR)/(1 - SPR_{50\%})$.

Year	Total biomass (mt)	Spawning biomass (mt)	Fraction unfished	Age-0 recruits	Total catch (mt)	Relative exploitation rate	SPR
1951	26191	2112	0.837	6864	418	0.02	0.85
1952	26079	2097	0.831	6844	434	0.02	0.84
1953	25959	2082	0.825	6823	515	0.02	0.81
1954	25772	2060	0.816	6792	430	0.02	0.84
1955	25680	2047	0.811	6774	470	0.02	0.83
1956	25555	2031	0.804	6751	434	0.02	0.84
1957	25472	2019	0.800	6735	439	0.02	0.84
1958	25387	2008	0.795	6719	426	0.02	0.84
1959	25317	1999	0.792	6706	435	0.02	0.84
1960	25241	1990	0.788	6693	427	0.02	0.84
1961	25174	1983	0.786	6682	487	0.02	0.82
1962	25053	1971	0.781	6665	465	0.02	0.82
1963	24963	1962	0.777	6651	473	0.02	0.82
1964	24873	1952	0.773	6636	468	0.02	0.82
1965	24794	1942	0.769	6622	438	0.02	0.83
1966	24750	1935	0.766	6611	444	0.02	0.83
1967	24700	1927	0.763	6600	463	0.02	0.82
1968	24635	1919	0.760	6587	497	0.02	0.81
1969	24540	1908	0.756	6571	460	0.02	0.82
1970	24485	1902	0.753	6561	416	0.02	0.84
1971	24475	1899	0.752	6557	409	0.02	0.84
1972	24468	1898	0.752	6556	423	0.02	0.83
1973	24446	1897	0.751	6553	429	0.02	0.83
1974	24417	1894	0.750	6549	415	0.02	0.84
1975	24402	1893	0.750	6548	429	0.02	0.83
1976	24374	1891	0.749	6545	440	0.02	0.83
1977	24339	1888	0.748	6540	452	0.02	0.82
1978	24295	1884	0.746	6534	536	0.02	0.79
1979	24178	1872	0.742	6515	584	0.03	0.78
1980	24028	1856	0.735	6489	444	0.02	0.82
1981	24025	1851	0.733	6482	547	0.02	0.79
1982	23924	1838	0.728	6461	486	0.02	0.81
1983	23888	1830	0.725	6449	466	0.02	0.82
1984	23870	1826	0.723	6442	420	0.02	0.83
1985	23890	1826	0.723	6442	453	0.02	0.82
1986	23871	1824	0.723	6440	425	0.02	0.83
1987	23875	1827	0.724	6444	431	0.02	0.83

Continued on next page

Table 7: Time-series of population estimates from the base-case model. Relative exploitation rate is $(1 - SPR)/(1 - SPR_{50\%})$.

Year	Total biomass (mt)	Spawning biomass (mt)	Fraction unfished	Age-0 recruits	Total catch (mt)	Relative exploitation rate	SPR
1988	23870	1829	0.725	6448	415	0.02	0.83
1989	23879	1834	0.726	6454	413	0.02	0.83
1990	23891	1837	0.728	6460	422	0.02	0.83
1991	23894	1839	0.728	6463	432	0.02	0.83
1992	23889	1839	0.728	6463	424	0.02	0.83
1993	23895	1838	0.728	6462	438	0.02	0.83
1994	23888	1836	0.727	6459	438	0.02	0.83
1995	23883	1834	0.727	6456	120	0.01	0.95
1996	24179	1859	0.736	6495	348	0.02	0.86
1997	24231	1864	0.738	6502	596	0.03	0.77
1998	24047	1847	0.732	6476	220	0.01	0.91
1999	24238	1864	0.738	6503	319	0.01	0.87
2000	24318	1873	0.742	6517	407	0.02	0.84
2001	24309	1874	0.742	6518	245	0.01	0.90
2002	24454	1889	0.748	6542	240	0.01	0.90
2003	24590	1905	0.754	6565	386	0.02	0.85
2004	24574	1907	0.755	6569	286	0.01	0.89
2005	24657	1918	0.760	6585	347	0.02	0.86
2006	24678	1923	0.762	6593	429	0.02	0.83
2007	24627	1920	0.761	6589	292	0.01	0.88
2008	24716	1928	0.764	6601	387	0.02	0.85
2009	24711	1926	0.763	6598	217	0.01	0.91
2010	24868	1939	0.768	6617	207	0.01	0.92
2011	25017	1952	0.773	6637	282	0.01	0.89
2012	25077	1960	0.776	6649	282	0.01	0.89
2013	25128	1969	0.780	6662	144	0.01	0.94
2014	25303	1991	0.789	6694	397	0.02	0.85
2015	25227	1990	0.788	6693	351	0.02	0.87
2016	25208	1993	0.789	6697	441	0.02	0.83
2017	25116	1985	0.786	6685	297	0.01	0.88
2018	25176	1988	0.787	6689	185	0.01	0.93
2019	0	1999	0.792	6706			

Table 8: List of parameters used in the base model, including estimated values and standard deviations (SD), bounds (minimum and maximum), estimation phase (negative values indicate not estimated), status (indicates if parameters are near bounds, and prior type information (mean, SD)).

No.	Parameter	Value	Phase	Bounds	Status	SD	Prior (Exp.Val, SD)
1	NatM_p_1_Fem_GP_1	0.449	3	(0.1, 0.6)	OK	0.031	Log_Norm (-1.02165, 0.438)
2	L_at_Amin_Fem_GP_1	20.082	2	(10, 40)	OK	1.031	None
3	Linf_Fem_GP_1	175.663	2	(100, 300)	OK	4.004	None
4	Cessation_age_Fem_GP_1	12.141	1	(0.005, 30)	OK	0.358	None
5	Cessation_slope_Fem_GP_1	5.610	3	(0.1, 10)	OK	11.851	None
6	SD_young_Fem_GP_1	5.703	5	(1, 20)	OK	0.901	None
7	SD_old_Fem_GP_1	7.084	5	(1, 20)	OK	0.920	None
8	Wtlen_1_Fem_GP_1	0.000	-3	(0, 3)			None
9	Wtlen_2_Fem_GP_1	2.993	-3	(2, 4)			None
10	Mat50%_Fem_GP_1	148.245	-3	(10, 140)			None
11	Mat_slope_Fem_GP_1	-0.132	-3	(-0.09, -0.05)			None
12	Eggs/kg_inter_Fem_GP_1	1.000	-3	(-3, 3)			None
13	Eggs/kg_slope_wt_Fem_GP_1	0.000	-3	(-3, 3)			None
14	NatM_p_1_Mal_GP_1	0.000	-2	(-3, 3)			None
15	L_at_Amin_Mal_GP_1	0.000	-2	(-1, 1)			None
16	Linf_Mal_GP_1	-0.373	2	(-1, 1)	OK	0.025	None
17	Cessation_age_Mal_GP_1	0.101	3	(-10, 20)	OK	0.034	None
18	Cessation_slope_Mal_GP_1	0.200	-3	(-3, 3)			None
19	SD_young_Mal_GP_1	0.000	-5	(-1, 1)			None
20	SD_old_Mal_GP_1	0.000	-5	(-1, 1)			None
21	Wtlen_1_Mal_GP_1	0.000	-3	(0, 3)			None
22	Wtlen_2_Mal_GP_1	2.993	-3	(2, 4)			None
23	CohortGrowDev	1.000	-5	(0, 2)			None
24	FracFemale_GP_1	0.500	-99	(0.001, 0.999)			None
25	SR_LN(R0)	8.905	3	(5, 15)	OK	0.373	None
26	SR_BH_stEEP	0.400	-3	(0.2, 1)			None

Continued on next page

Table 8: List of parameters used in the base model, including estimated values and standard deviations (SD), bounds (minimum and maximum), estimation phase (negative values indicate not estimated), status (indicates if parameters are near bounds, and prior type information (mean, SD)).

No.	Parameter	Value	Phase	Bounds	Status	SD	Prior (Exp.Val, SD)
27	SR_sigmaR	0.300	-2	(0, 0.4)			None
28	SR_regime	0.000	-1	(-2, 2)			None
29	SR_autocorr	0.000	-99	(0, 0)			None
78	LnQ_base_WCGBT5(5)	-0.403	1	(-2, 2)	OK	0.315	Normal (-0.355, 0.326)
79	Q_extraSD_WCGBT5(5)	0.163	1	(0, 2)	OK	0.057	None
80	LnQ_base_Triennial(6)	-1.252	1	(-10, 2)	OK	0.743	None
81	Q_extraSD_Triennial(6)	0.366	1	(0, 2)	OK	0.146	None
82	LnQ_base_Triennial(6)_1995	-0.935	1	(-7, 0)	OK	0.741	None
83	Size_DblN_peak_(1)	94.111	4	(80, 150)	OK	4.899	None
84	Size_DblN_top_logit_(1)	-15.000	-5	(-15, 4)			None
85	Size_DblN_ascend_se_(1)	7.153	4	(-1, 9)	OK	0.118	None
86	Size_DblN_descend_se_(1)	20.000	-5	(-1, 20)			None
87	Size_DblN_start_logit_(1)	-999.000	-4	(-999, 9)			None
88	Size_DblN_end_logit_(1)	-999.000	-5	(-999, 9)			None
89	Retain_L_infl_(1)	66.214	2	(15, 150)	OK	0.671	None
90	Retain_L_width_(1)	4.876	2	(0.1, 10)	OK	0.354	None
91	Retain_L_asymptote_logit_(1)	2.052	3	(-10, 20)	OK	0.359	None
92	Retain_L_maleoffset_(1)	0.000	-3	(0, 0)			None
93	DiscMort_L_infl_(1)	5.000	-4	(5, 15)			None
94	DiscMort_L_width_(1)	0.000	-4	(0.001, 10)			None
95	DiscMort_L_level_old_(1)	0.500	-5	(0, 1)			None
96	DiscMort_L_male_offset_(1)	0.000	-5	(0, 0)			None
97	SzSel_Fem_Peak_(1)	-5.522	4	(-50, 50)	OK	2.162	None
98	SzSel_Fem_Ascend_(1)	0.000	-4	(-5, 5)			None
99	SzSel_Fem_Descend_(1)	0.000	-4	(-5, 5)			None
100	SzSel_Fem_Final_(1)	0.000	-4	(-5, 5)			None
101	SzSel_Fem_Scale_(1)	0.744	4	(0.5, 1.5)	OK	0.095	None

Continued on next page

Table 8: List of parameters used in the base model, including estimated values and standard deviations (SD), bounds (minimum and maximum), estimation phase (negative values indicate not estimated), status (indicates if parameters are near bounds, and prior type information (mean, SD)).

No.	Parameter	Value	Phase	Bounds	Status	SD	Prior	(Exp.Val, SD)
102	Size_DblN_peak_WCGBT5(5)	76.147	4	(50, 150)	OK	6.638	None	
103	Size_DblN_top_logit_WCGBT5(5)	-15.000	-5	(-15, 4)			None	
104	Size_DblN_ascend_se_WCGBT5(5)	6.498	4	(-1, 9)	OK	0.369	None	
105	Size_DblN_descend_se_WCGBT5(5)	16.548	5	(-1, 20)	OK	55.858	None	
106	Size_DblN_start_logit_WCGBT5(5)	-5.000	-4	(-999, 9)			None	
107	Size_DblN_end_logit_WCGBT5(5)	-999.000	-5	(-999, 9)			None	
108	SzSel_Fem_Peak_WCGBT5(5)	-7.975	4	(-50, 50)	OK	4.143	None	
109	SzSel_Fem_Ascend_WCGBT5(5)	0.000	-4	(-5, 5)			None	
110	SzSel_Fem_Descend_WCGBT5(5)	0.000	-4	(-5, 5)			None	
111	SzSel_Fem_Final_WCGBT5(5)	0.000	-4	(-5, 5)			None	
112	SzSel_Fem_Scale_WCGBT5(5)	0.698	4	(0.5, 1.5)	OK	0.126	None	
113	Size_DblN_peak_Triennial(6)	187.543	4	(50, 200)	OK	34.611	None	
114	Size_DblN_top_logit_Triennial(6)	-15.000	-5	(-15, 4)			None	
115	Size_DblN_ascend_se_Triennial(6)	8.472	4	(-1, 9)	OK	0.420	None	
116	Size_DblN_descend_se_Triennial(6)	20.000	-5	(-1, 20)			None	
117	Size_DblN_start_logit_Triennial(6)	-4.794	4	(-15, 9)	OK	0.784	None	
118	Size_DblN_end_logit_Triennial(6)	-999.000	-5	(-999, 9)			None	
119	SzSel_Fem_Peak_Triennial(6)	0.000	-4	(-50, 50)			None	
120	SzSel_Fem_Ascend_Triennial(6)	0.000	-4	(-5, 5)			None	
121	SzSel_Fem_Descend_Triennial(6)	0.000	-4	(-5, 5)			None	
122	SzSel_Fem_Final_Triennial(6)	0.000	-4	(-5, 5)			None	
123	SzSel_Fem_Scale_Triennial(6)	0.607	4	(0.5, 1.5)	OK	0.130	None	
124	Retain_L_asymptote_logit_2005	2.300	4	(-10, 20)	OK	0.565	None	
125	Retain_L_asymptote_logit_2006	3.304	4	(-10, 20)	OK	1.302	None	
126	Retain_L_asymptote_logit_2007	3.963	4	(-10, 20)	OK	1.978	None	
127	Retain_L_asymptote_logit_2008	11.079	4	(-10, 20)	OK	112.035	None	

Continued on next page

Table 8: List of parameters used in the base model, including estimated values and standard deviations (SD), bounds (minimum and maximum), estimation phase (negative values indicate not estimated), status (indicates if parameters are near bounds, and prior type information (mean, SD)).

No.	Parameter	Value	Phase	Bounds	Status	SD	Prior (Exp.Val, SD)
128	Retain_L_asymptote_logit_2009	4.912	4	(-10, 20)	OK	3.712	None
129	Retain_L_asymptote_logit_2010	13.242	4	(-10, 20)	OK	88.134	None
130	Retain_L_asymptote_logit_2011	14.640	4	(-10, 20)	OK	74.028	None
131	Retain_L_asymptote_logit_2012	13.892	4	(-10, 20)	OK	81.517	None
132	Retain_L_asymptote_logit_2013	3.456	4	(-10, 20)	OK	0.333	None
133	Retain_L_asymptote_logit_2014	3.620	4	(-10, 20)	OK	0.277	None
134	Retain_L_asymptote_logit_2015	3.405	4	(-10, 20)	OK	0.261	None
135	Retain_L_asymptote_logit_2016	2.885	4	(-10, 20)	OK	0.192	None
136	Retain_L_asymptote_logit_2017	2.817	4	(-10, 20)	OK	0.193	None

Table 9: Sensitivity of the base model to assumptions about selectivity and catchability. Likelihood values are negative log-likelihood where smaller values indicate a better fit.

Label	Base	All selectivity domed	No sex-specific selectivity	Longnose Skate catchabil- ity prior	Remove catchabil- ity prior	No catcha- bility change in Triennial
TOTAL likelihood	402.02	400.45	420.16	402.12	401.67	402.31
Survey likelihood	-9.63	-9.63	-9.75	-9.72	-9.31	-9.34
Length comp likelihood	341.21	339.27	356.43	341.44	340.46	341.22
Age comp likelihood	97.13	97.56	100.60	97.14	97.08	97.13
Discard likelihood	-22.38	-22.73	-22.75	-22.45	-22.14	-22.37
Mean body wt likelihood	-4.46	-4.09	-4.49	-4.42	-4.60	-4.47
Parm priors likelihood	0.14	0.05	0.11	0.12	0.17	0.14
Recr Virgin millions	7.37	5.74	6.32	6.18	34.78	7.35
log(R0)	8.90	8.66	8.75	8.73	10.46	8.90
M Female	0.45	0.41	0.44	0.45	0.46	0.45
M Male	0.45	0.41	0.44	0.45	0.46	0.45
Linf Female	175.66	178.33	177.03	175.67	175.61	175.66
Linf Male	120.96	120.78	120.73	120.97	120.95	120.96
WCGBTS catchability	0.67	0.67	0.68	0.81	0.14	0.67
SSB Virgin 1000 mt	2.52	3.39	2.12	2.22	9.93	2.52
SSB 2019 1000 mt	2.00	2.75	1.50	1.67	9.50	2.00
Fraction unfished 2019	0.79	0.81	0.71	0.75	0.96	0.79
Fishing intensity 2018	0.15	0.13	0.21	0.18	0.03	0.15
Retained Catch MSY mt	649.59	693.46	503.92	558.67	2793.89	648.35
Dead Catch MSY mt	702.69	750.92	544.02	603.92	3030.18	701.35
Virgin age 2+ bio 1000 mt	27.27	27.86	24.58	23.47	116.82	27.21
OFL mt 2021	1677.05	1846.69	1183.05	1390.54	8154.10	1673.22

Table 10: Sensitivity of the base model to assumptions about biology. Likelihood values are negative log-likelihood where smaller values indicate a better fit.

Label	Base	Sex-specific M	No prior on M	von B growth	Richards growth
TOTAL likelihood	402.02	399.83	401.89	445.23	424.90
Survey likelihood	-9.63	-9.79	-9.63	-9.50	-9.70
Length comp likelihood	341.21	338.54	341.25	387.51	361.38
Age comp likelihood	97.13	97.55	97.08	94.07	99.86
Discard likelihood	-22.38	-22.75	-22.40	-22.35	-22.43
Mean body wt likelihood	-4.46	-3.96	-4.44	-5.07	-4.27
Parm priors likelihood	0.14	0.23	0.01	0.54	0.04
Recr Virgin millions	7.37	5.99	7.52	20.51	4.94
log(R0)	8.90	8.70	8.93	9.93	8.51
M Female	0.45	0.48	0.45	0.57	0.40
M Male	0.45	0.40	0.45	0.57	0.40
Linf Female	175.66	175.55	175.64	584.73	240.49
Linf Male	120.96	120.13	120.99	235.51	137.22
WCGBTS catchability	0.67	0.67	0.66	0.72	0.68
SSB Virgin 1000 mt	2.52	1.47	2.50	1.40	2.43
SSB 2019 1000 mt	2.00	1.01	1.99	1.19	1.80
Fraction unfished 2019	0.79	0.69	0.79	0.84	0.74
Fishing intensity 2018	0.15	0.22	0.15	0.11	0.18
Retained Catch MSY mt	649.59	481.25	654.34	856.12	556.17
Dead Catch MSY mt	702.69	519.12	707.84	925.97	601.07
Virgin age 2+ bio 1000 mt	27.27	24.20	27.42	38.74	25.82
OFL mt 2021	1677.05	1103.90	1690.92	2270.94	1377.42

Table 11: Sensitivity of the base model to assumptions about data weighting and recruitment. Likelihood values are negative log-likelihood where smaller values indicate a better fit.

Label	Base	McAllister-Ianelli tuning	Dirichlet-Multinomial tuning	No extra SD on indices	Estimate rec. devs.	Estimate rec. devs., no q prior
TOTAL likelihood	402.02	1116.43	3053.30	415.53	342.66	342.33
Survey likelihood	-9.63	-9.56	-9.42	3.73	-11.72	-12.04
Length comp likelihood	341.21	563.83	1630.45	341.25	284.23	284.63
Age comp likelihood	97.13	591.28	1449.60	97.25	96.44	96.42
Discard likelihood	-22.38	-22.26	-20.92	-22.52	-14.79	-15.00
Mean body wt likelihood	-4.46	-7.18	2.52	-4.33	-11.14	-11.21
Parm priors likelihood	0.14	0.31	1.04	0.16	0.06	0.02
Recr Virgin millions	7.37	9.26	12.22	6.48	5.50	3.02
log(R0)	8.90	9.13	9.41	8.78	8.61	8.01
M Female	0.45	0.46	0.47	0.44	0.41	0.39
M Male	0.45	0.46	0.47	0.44	0.41	0.39
Linf Female	175.66	176.94	177.66	175.73	175.60	175.56
Linf Male	120.96	120.50	120.43	120.93	121.28	121.31
WCGBTS catchability	0.67	0.59	0.46	0.77	0.74	1.54
SSB Virgin 1000 mt	2.52	2.85	3.53	2.35	2.98	2.14
SSB 2019 1000 mt	2.00	2.35	3.07	1.80	2.03	1.04
Fraction unfished 2019	0.79	0.82	0.87	0.76	0.68	0.49
Fishing intensity 2018	0.15	0.13	0.09	0.17	0.14	0.28
Retained Catch MSY mt	649.59	746.50	966.78	586.90	604.61	382.71
Dead Catch MSY mt	702.69	807.57	1048.31	634.59	654.50	412.78
Virgin age 2+ bio 1000 mt	27.27	30.97	39.40	24.78	25.79	16.47
OFL mt 2021	1677.05	1974.58	2658.38	1479.99	1510.61	752.32

Table 12: Sensitivity of the base model to assumptions about catches and discards. Likelihood values are negative log-likelihood where smaller values indicate a better fit..

Label	Base	Discards based on 3yr-avg.	Discard mortality = 0.4	Discard mortality = 0.6	Multipliers on historic discards	Fit time series of F from Petrale
TOTAL likelihood	402.02	401.60	401.80	402.21	401.87	-116.08
Survey likelihood	-9.63	-9.80	-9.85	-9.44	-9.83	-528.22
Length comp likelihood	341.21	340.99	341.37	341.08	341.14	341.71
Age comp likelihood	97.13	97.21	97.14	97.12	97.18	97.12
Discard likelihood	-22.38	-22.45	-22.56	-22.23	-22.52	-22.89
Mean body wt likelihood	-4.46	-4.48	-4.43	-4.48	-4.46	-4.37
Parm priors likelihood	0.14	0.12	0.12	0.16	0.35	0.12
Recr Virgin millions	7.37	6.95	7.24	7.49	7.05	7.20
log(R0)	8.90	8.85	8.89	8.92	8.86	8.88
M Female	0.45	0.45	0.45	0.45	0.45	0.44
M Male	0.45	0.45	0.45	0.45	0.45	0.44
Linf Female	175.66	175.74	175.67	175.65	175.69	175.64
Linf Male	120.96	120.95	120.96	120.97	120.96	120.95
WCGBTS catchability	0.67	0.71	0.69	0.65	0.70	0.70
SSB Virgin 1000 mt	2.52	2.46	2.55	2.51	2.49	2.62
SSB 2019 1000 mt	2.00	1.89	1.97	2.03	1.91	1.95
Fraction unfished 2019	0.79	0.77	0.77	0.81	0.77	0.74
Fishing intensity 2018	0.15	0.16	0.15	0.14	0.15	0.15
Retained Catch MSY mt	649.59	621.45	646.34	653.55	630.64	654.54
Dead Catch MSY mt	702.69	671.99	698.98	707.14	681.93	707.54
Virgin age 2+ bio 1000 mt	27.27	26.21	27.16	27.40	26.56	27.50
OFL mt 2021	1677.05	1572.97	1644.55	1707.59	1596.57	1628.14

Table 13: Results from 100 jitters from the base case model.

Description	Value
Returned to base case	48
Found local minimum	52
Found better solution	0
Error in likelihood	0
Total	100

Table 14: Projection of potential OFL, spawning biomass, and depletion for the base case model.

Yr	OFL contribution (mt)	ACL landings (mt)	Age 2+ biomass (mt)	Spawning Biomass (mt)	Depletion
2019	1676.940	313.160	0.000	1999.350	0.792
2020	1677.230	313.160	0.000	1996.660	0.791
2021	1677.050	1370.714	0.000	1994.570	0.790
2022	1595.590	1288.638	0.000	1890.960	0.749
2023	1532.450	1224.512	0.000	1795.530	0.711
2024	1485.240	1174.926	0.000	1707.150	0.676
2025	1449.200	1135.692	0.000	1624.780	0.644
2026	1419.050	1101.938	0.000	1548.240	0.613
2027	1391.410	1071.888	0.000	1479.220	0.586
2028	1364.510	1041.508	0.000	1420.800	0.563
2029	1337.960	1011.727	0.000	1375.850	0.545
2030	1311.740	983.655	0.000	1344.390	0.533

Table 15: Projections of landings, total mortality, OFL, and ACL values.

Year	Landings (mt)	Estimated total mortality (mt)	OFL (mt)	ACL (mt)	Buffer
2019	225.2	241.3	541.0	494.0	
2020	225.3	241.3	541.0	494.0	
2021	1374.8	1476.8	1689.6	1476.8	0.874
2022	1290.6	1389.0	1605.8	1389.0	0.865
2023	1224.8	1320.5	1540.8	1320.5	0.857
2024	1174.0	1267.1	1492.4	1267.1	0.849
2025	1134.3	1224.4	1455.9	1224.4	0.841
2026	1100.3	1187.7	1425.8	1187.7	0.833
2027	1070.2	1155.0	1398.3	1155.0	0.826
2028	1039.9	1122.0	1371.6	1122.0	0.818
2029	1010.1	1089.7	1345.3	1089.7	0.810
2030	982.0	1059.3	1319.2	1059.3	0.803

Table 16: Summary of 12-year projections beginning in 2019 for alternate states of nature based on the axis of uncertainty for the model. Columns range over low, mid, and high states of nature, and rows range over different assumptions of catch levels.

		States of nature						
		Low State (q=0.960)		Base State (q=0.668)	High State (q=0.465)			
	Year	Catch	Spawning Biomass	Frac. Unfished	Spawning Biomass	Frac. Unfished	Spawning Biomass	Frac. Unfished
Low catch, 250 mt	2019	241.3	1130	0.629	1999	0.792	2829	0.854
	2020	241.3	1137	0.633	2005	0.794	2834	0.855
	2021	250.0	1145	0.638	2012	0.797	2840	0.857
	2022	250.0	1154	0.643	2019	0.800	2847	0.859
	2023	250.0	1165	0.649	2028	0.803	2856	0.862
	2024	250.0	1177	0.655	2039	0.808	2865	0.865
	2025	250.0	1189	0.662	2049	0.812	2875	0.868
	2026	250.0	1200	0.668	2057	0.815	2882	0.870
	2027	250.0	1208	0.673	2063	0.817	2888	0.872
	2028	250.0	1214	0.676	2067	0.819	2891	0.873
	2029	250.0	1218	0.678	2070	0.820	2894	0.873
	2030	250.0	1223	0.681	2074	0.821	2896	0.874
Middle catch, 494 mt	2019	241.3	1130	0.629	1999	0.792	2829	0.854
	2020	241.3	1137	0.633	2005	0.794	2834	0.855
	2021	494.0	1145	0.638	2012	0.797	2840	0.857
	2022	494.0	1131	0.630	1997	0.791	2825	0.853
	2023	494.0	1119	0.623	1984	0.786	2812	0.849
	2024	494.0	1107	0.617	1971	0.781	2799	0.845
	2025	494.0	1095	0.610	1958	0.776	2786	0.841
	2026	494.0	1082	0.602	1944	0.770	2772	0.836
	2027	494.0	1066	0.594	1929	0.764	2756	0.832
	2028	494.0	1051	0.585	1914	0.758	2740	0.827
	2029	494.0	1038	0.578	1900	0.753	2727	0.823
	2030	494.0	1027	0.572	1890	0.749	2717	0.820
Default harvest, for base state	2019	241.3	1130	0.629	1999	0.792	2829	0.854
	2020	241.3	1137	0.633	2005	0.794	2834	0.855
	2021	1476.8	1145	0.638	2012	0.797	2840	0.857
	2022	1389.0	1040	0.579	1908	0.756	2737	0.826
	2023	1320.5	943	0.525	1812	0.718	2642	0.797
	2024	1267.1	852	0.475	1724	0.683	2554	0.771
	2025	1224.5	768	0.428	1641	0.650	2471	0.746
	2026	1187.7	690	0.384	1563	0.619	2394	0.722
	2027	1155.0	620	0.345	1492	0.591	2323	0.701
	2028	1122.0	560	0.312	1432	0.567	2263	0.683
	2029	1089.6	512	0.285	1385	0.549	2218	0.669
	2030	1059.3	473	0.263	1353	0.536	2187	0.660

Table 17: Summary of reference points and management quantities for the base case model.

Quantity	Estimate	Low 2.5% limit	High 2.5% limit
Unfished spawning biomass (mt)	2,525	1,068	3,981
Unfished age 2+ biomass (mt)	27,268	12,854	41,683
Unfished recruitment (R_0 , thousands)	7,366	1,974	12,759
Spawning biomass (2019 mt)	1,999	566	3,433
Fraction unfished (2019)	0.792	0.655	0.929
Reference points based on $B_{40\%}$			
Spawning biomass ($B_{40\%}$)	1,010	427	1,592
SPR resulting in $B_{40\%}$ ($SPR_{B_{40\%}}$)	0.625	0.625	0.625
Exploitation rate resulting in $B_{40\%}$	0.048	0.042	0.055
Yield with $SPR_{B_{40\%}}$ at $B_{40\%}$ (mt)	701	316	1,086
Reference points based on $SPR = 50\%$ proxy for MSY			
Spawning biomass (mt)	505	214	796
SPR_{proxy}	0.5		
Exploitation rate corresponding to $SPR = 50\%$	0.071	0.061	0.08
Yield with $SPR = 50\%$ at $B_{SPR=50\%}$ (mt)	590	266	915
Reference points based on estimated MSY values			
Spawning biomass at MSY (B_{MSY})	944	393	1,496
SPR_{MSY}	0.609	0.604	0.614
Exploitation rate at MSY	0.051	0.045	0.057
Dead Catch MSY (mt)	703	316	1,089
Retained Catch MSY (mt)	650	294	1,005

12 Figures

12.1 Data Figures

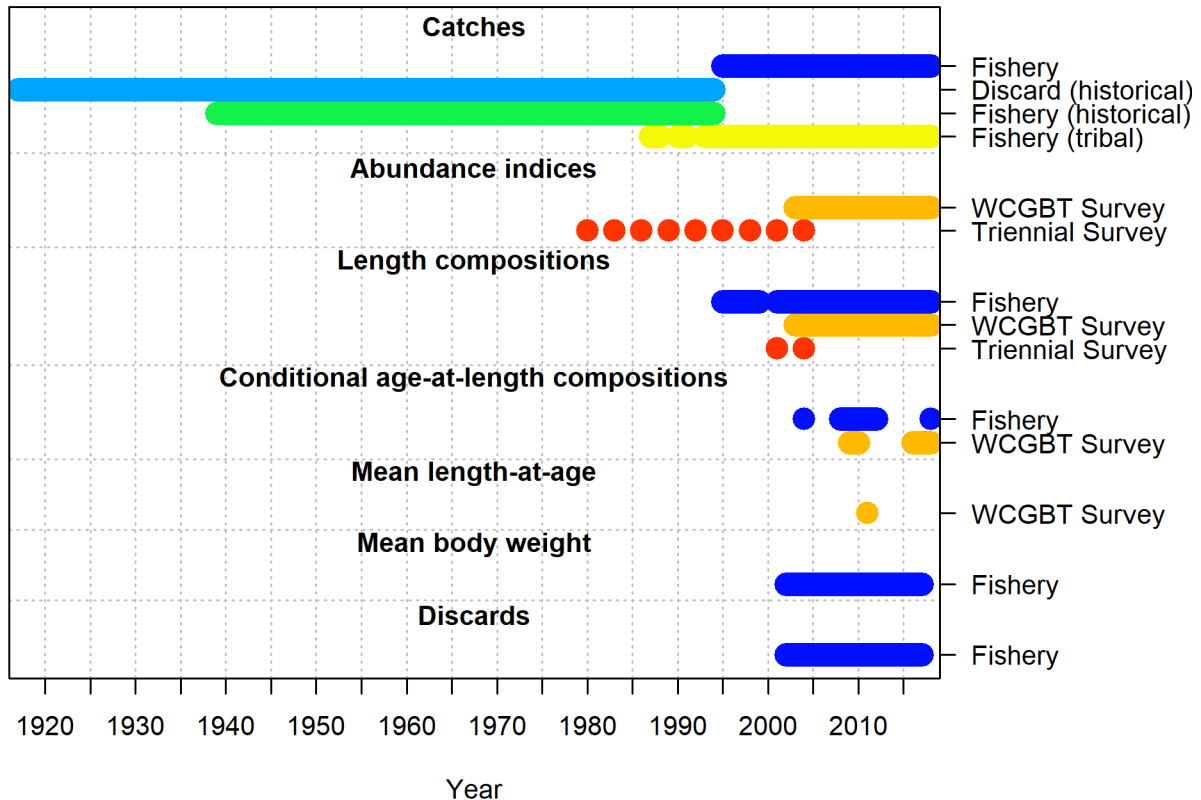


Figure 1: Summary of data sources used in the model.

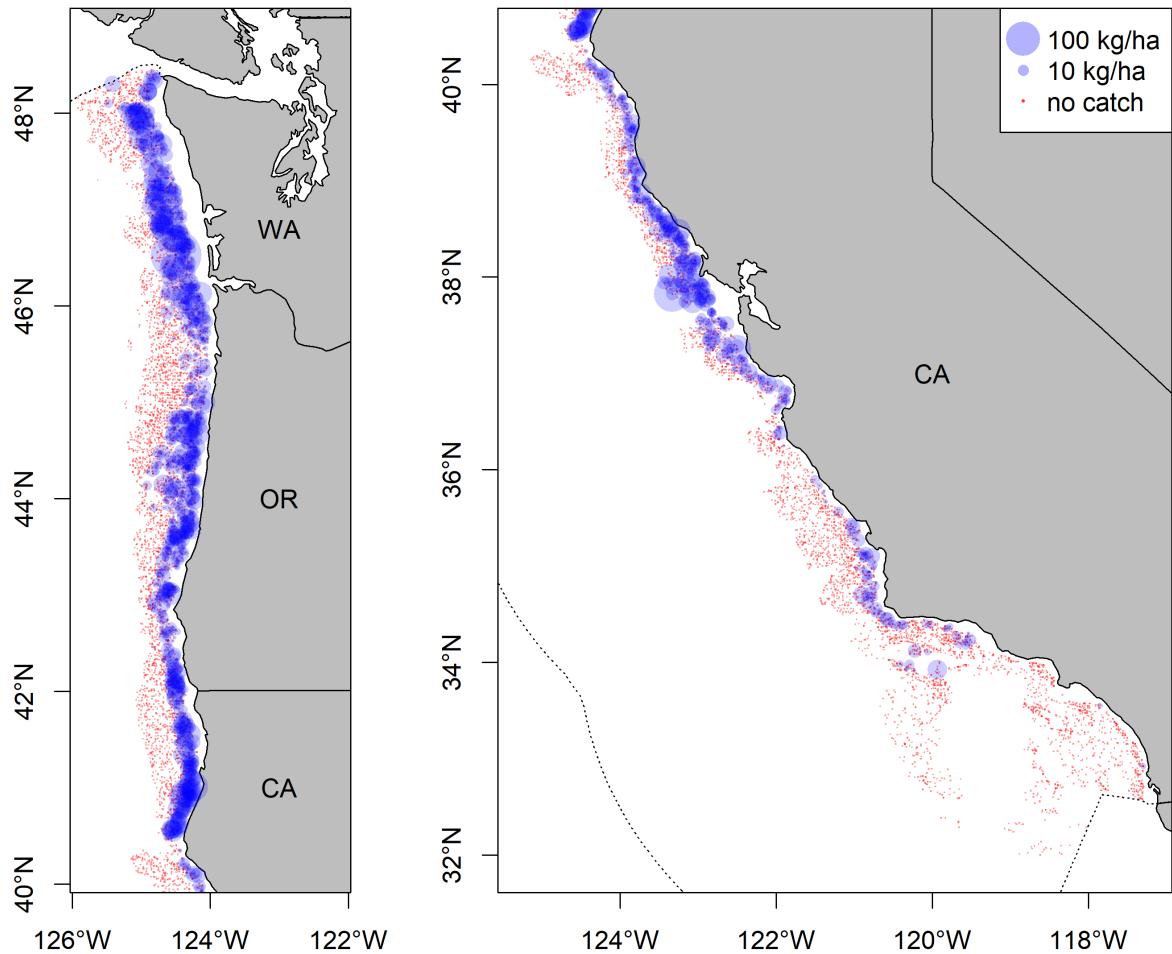


Figure 2: Map showing the distribution of Big Skate within the area covered by the West Coast Groundfish Bottom Trawl Survey aggregated over the years 2003–2018.

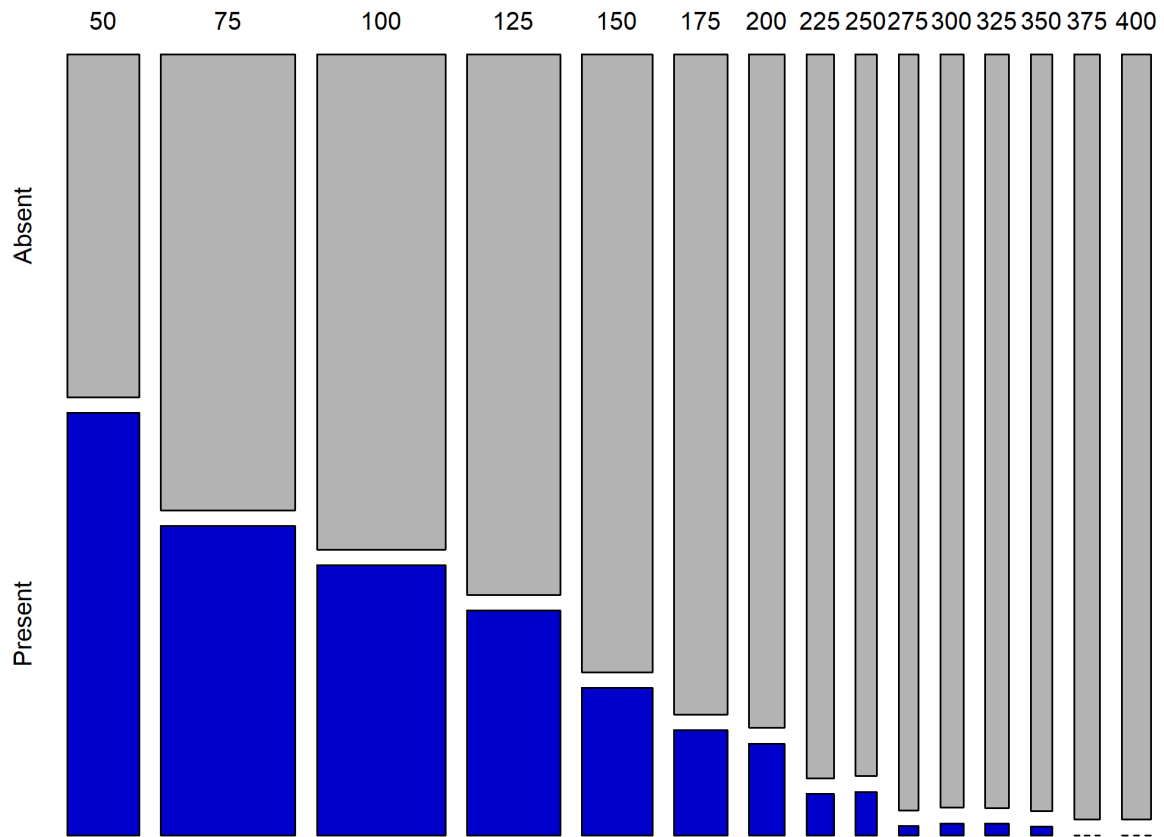


Figure 3: Presence or absence of Big Skate in the WCGBT Survey by 25 m depth bin for all 6,382 hauls with depth less than 425 m over the years 2003–2018. The height and width of each block are proportional to the number of hauls within that bin. For 50–75 m, there were 324 hauls with Big Skate present and 263 with no Big Skate.

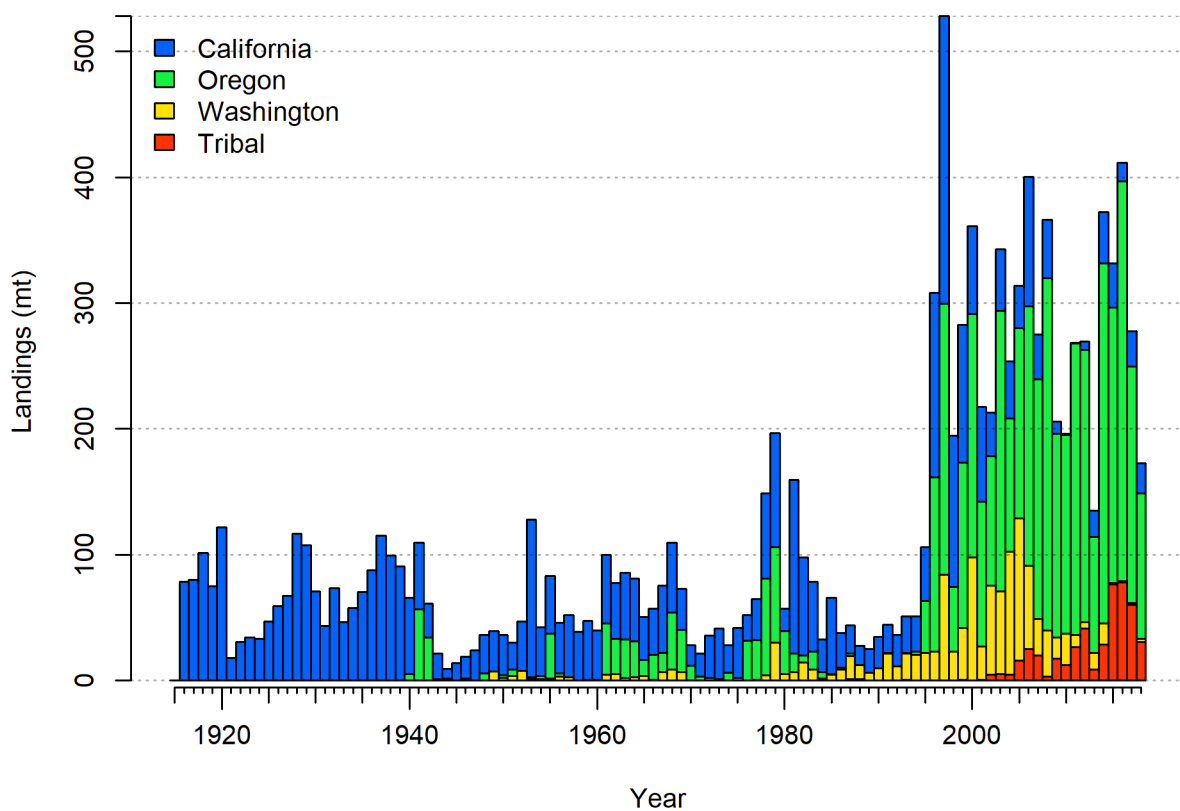


Figure 4: Reconstructed landings by area. Tribal catch was all landed in Washington.

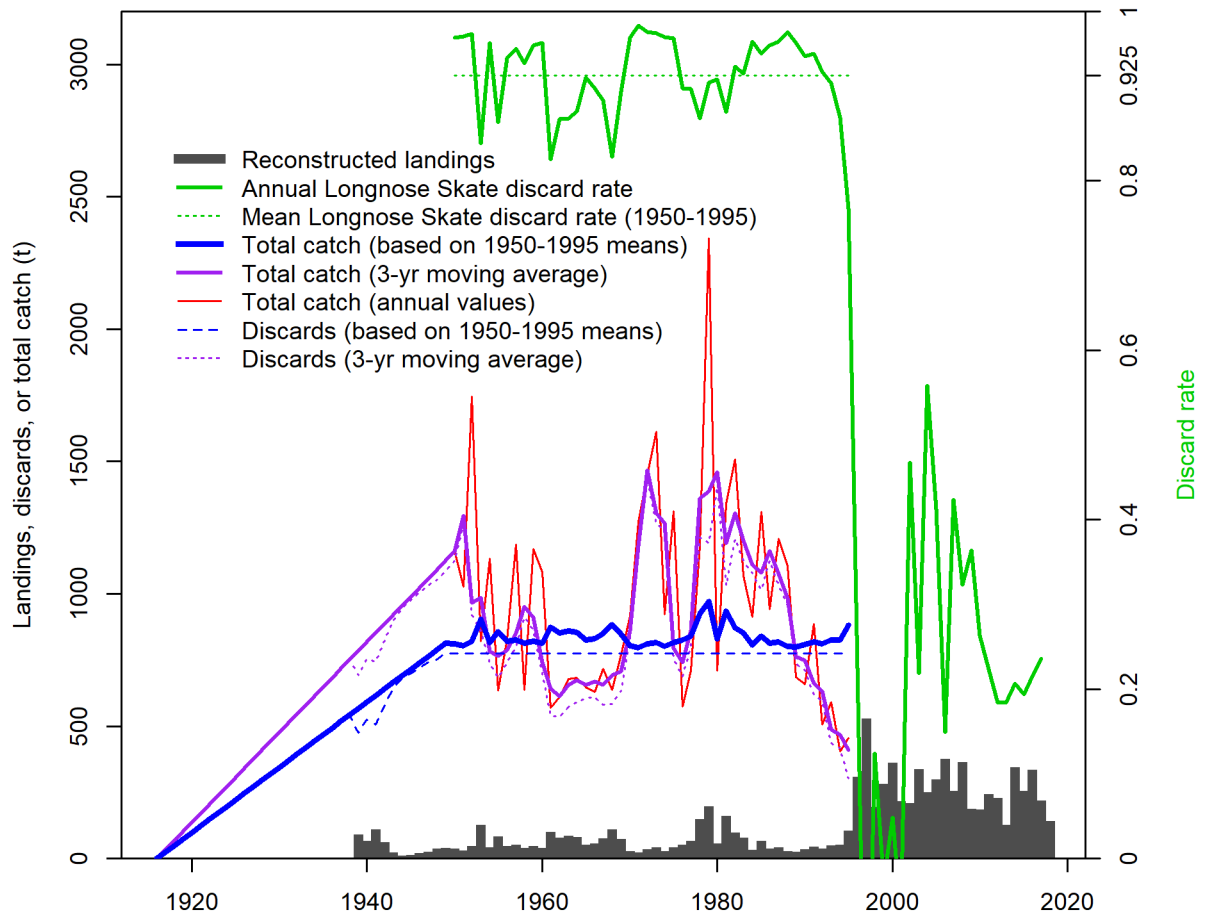


Figure 5: Estimated total catch using different assumptions for discards. The discard rates shown in green lines are relative to the right-hand axis while all other values are relative to the left-hand axis.

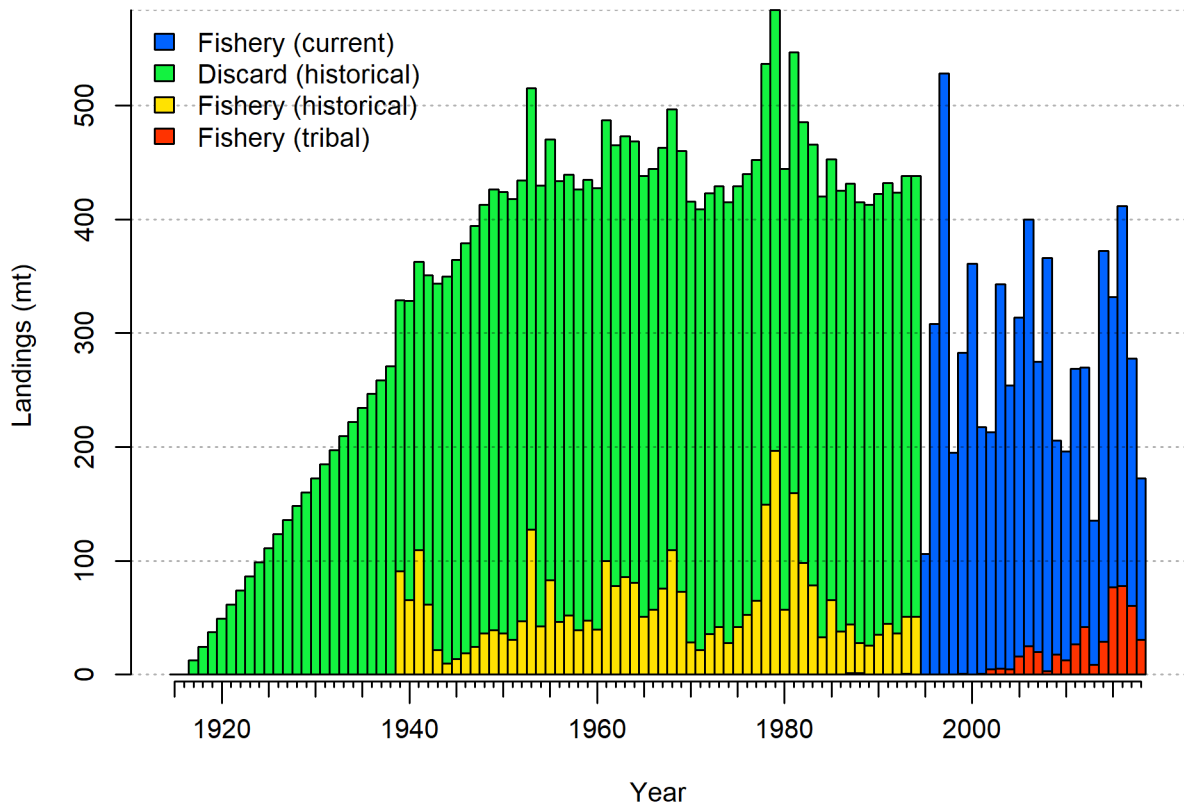


Figure 6: Catch data input to the model under assumed fleet structure. The historical discards shown in green have been scaled to account for an assumed 50% discard mortality. Discards during the period from 1995 onward are not represented here as they are estimated within the model.

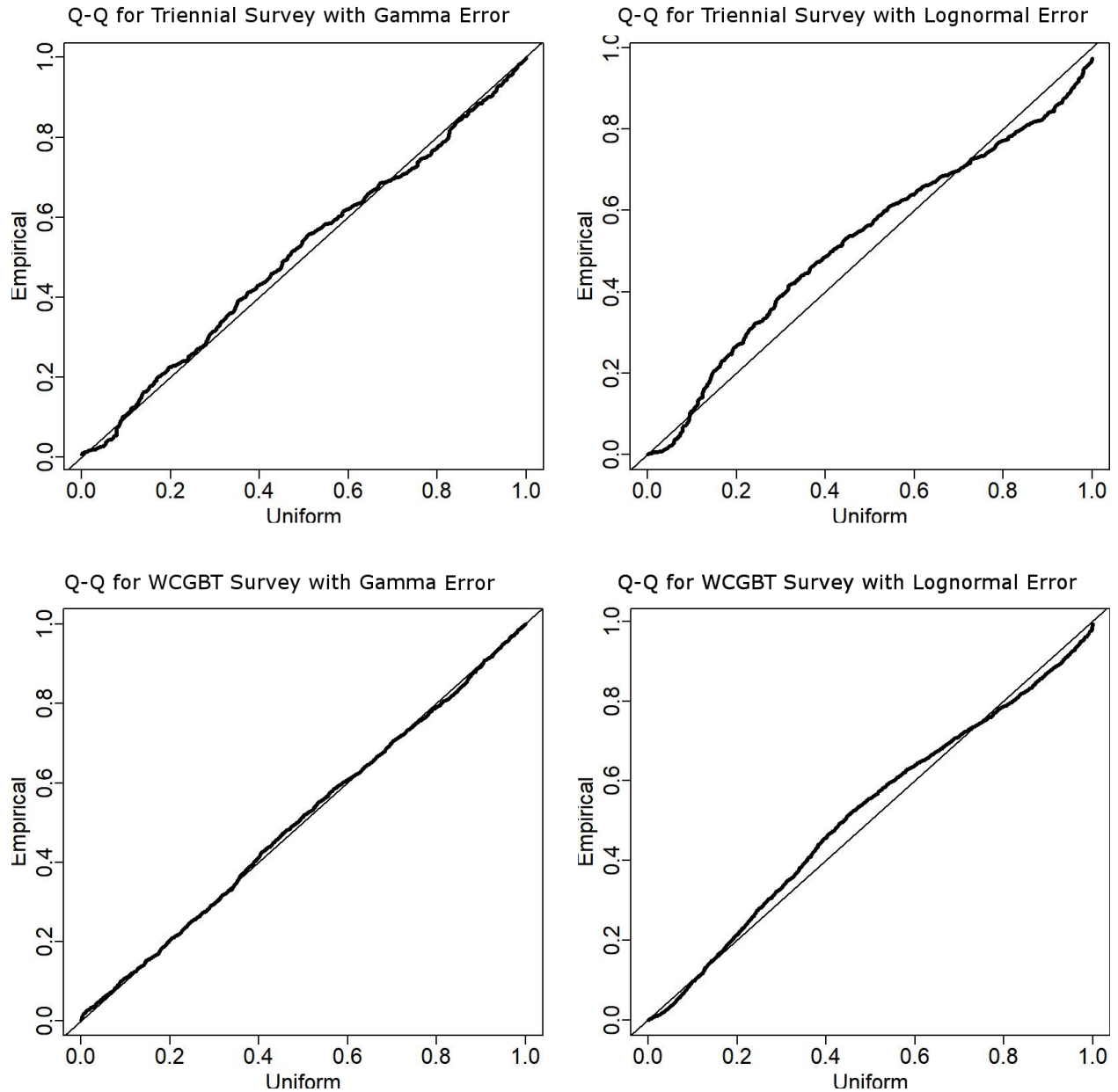


Figure 7: Quantile-quantile (Q-Q) plot showing empirical quantiles of the positive catch rate relative to their expected theoretical quantiles within the VAST geostatistical standardization for the two surveys with both Gamma and Lognormal error structures.

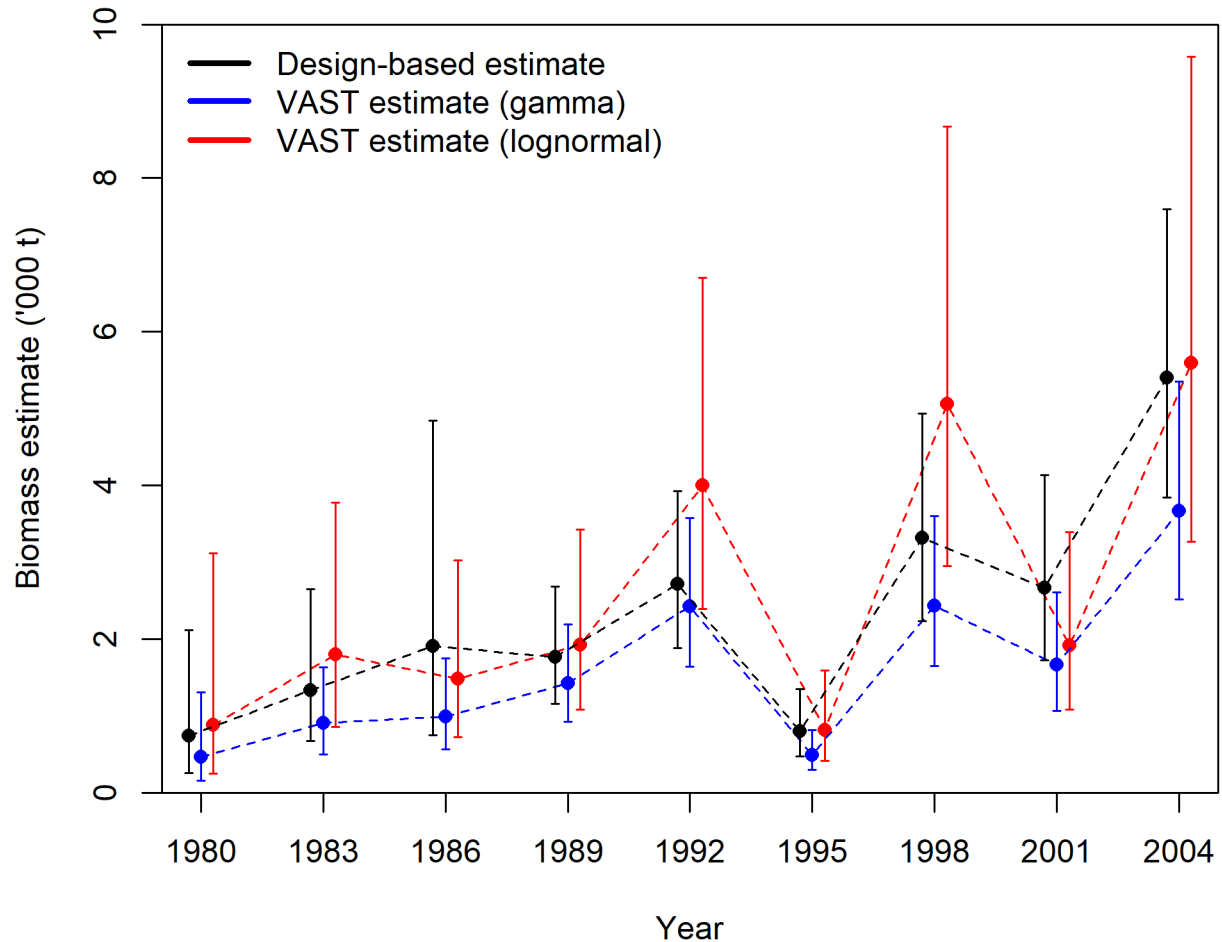


Figure 8: Index of abundance from the Triennial Survey calculated three ways.

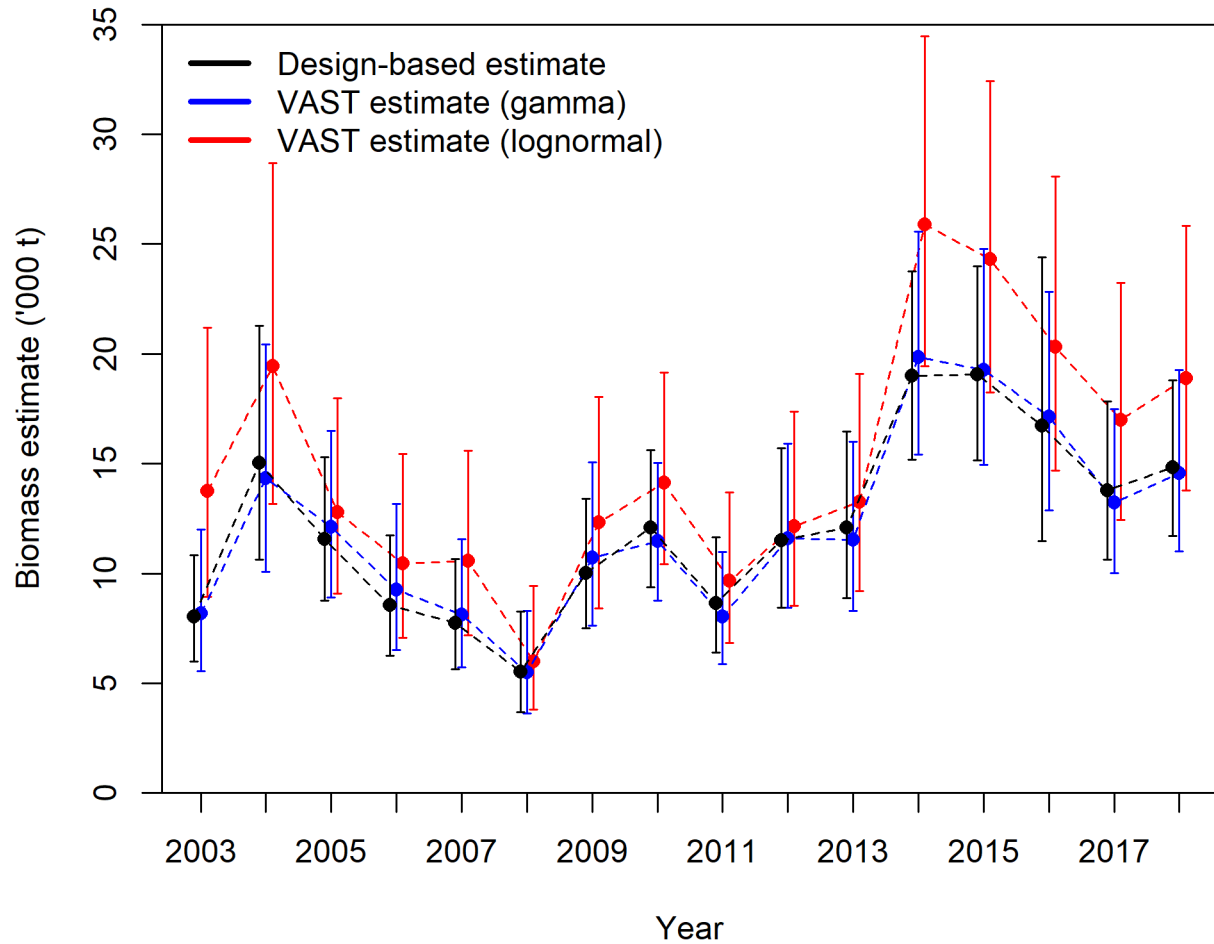


Figure 9: Index of abundance from the WCGBT Survey calculated three ways.

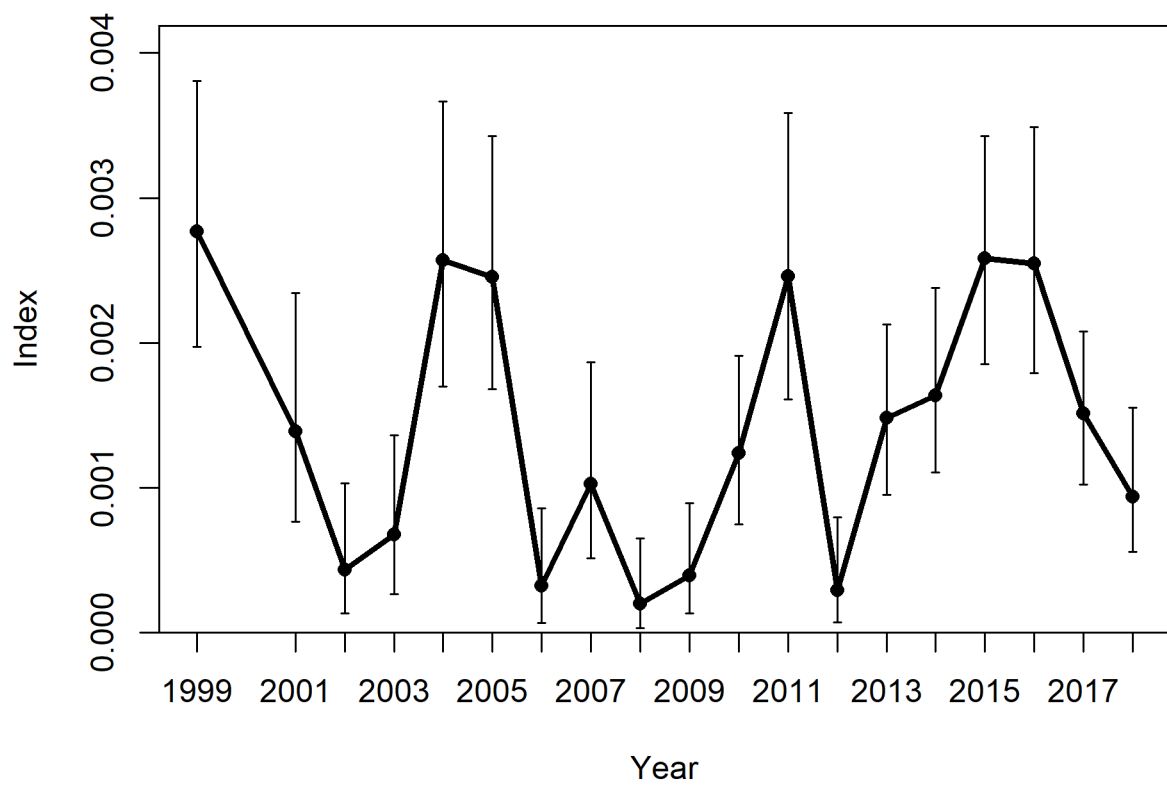


Figure 10: Index of abundance from the International Pacific Halibut Commission longline survey (not used in the assessment model).

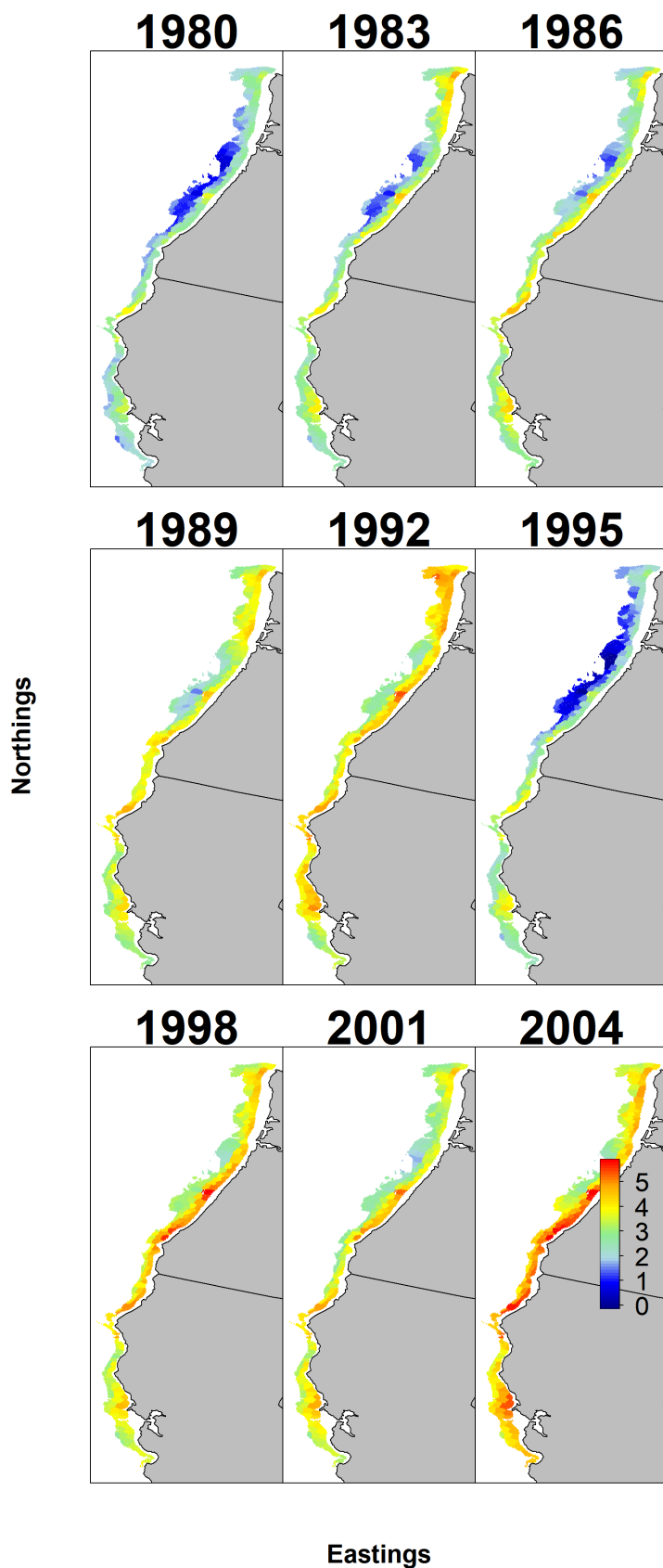


Figure 11: Map of estimated density by year for Big Skate in the Triennial survey calculated using VAST with a Gamma error structure. 82

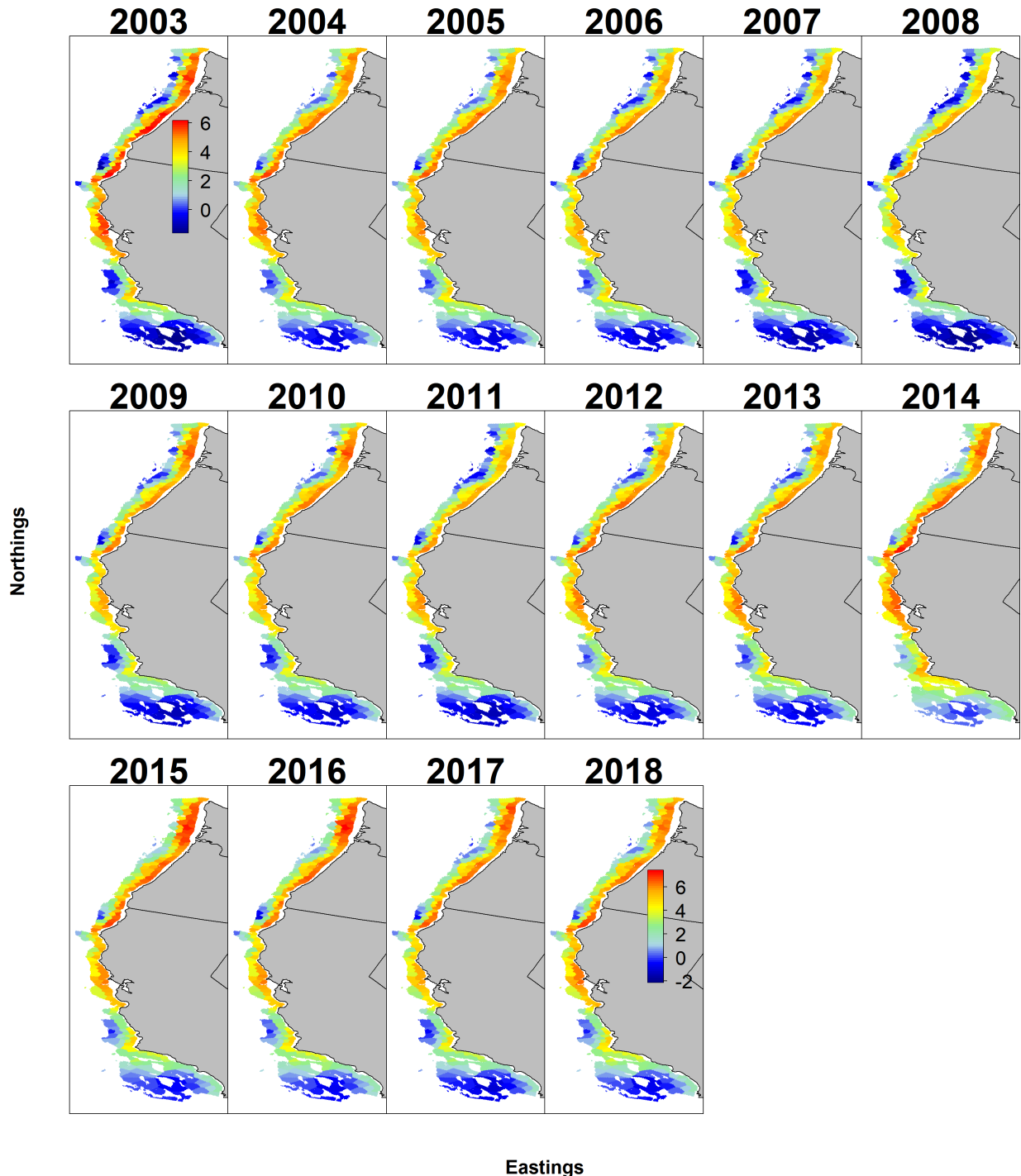


Figure 12: Map of estimated density by year for Big Skate in the WCGBT Survey calculated using VAST with a Gamma error structure.

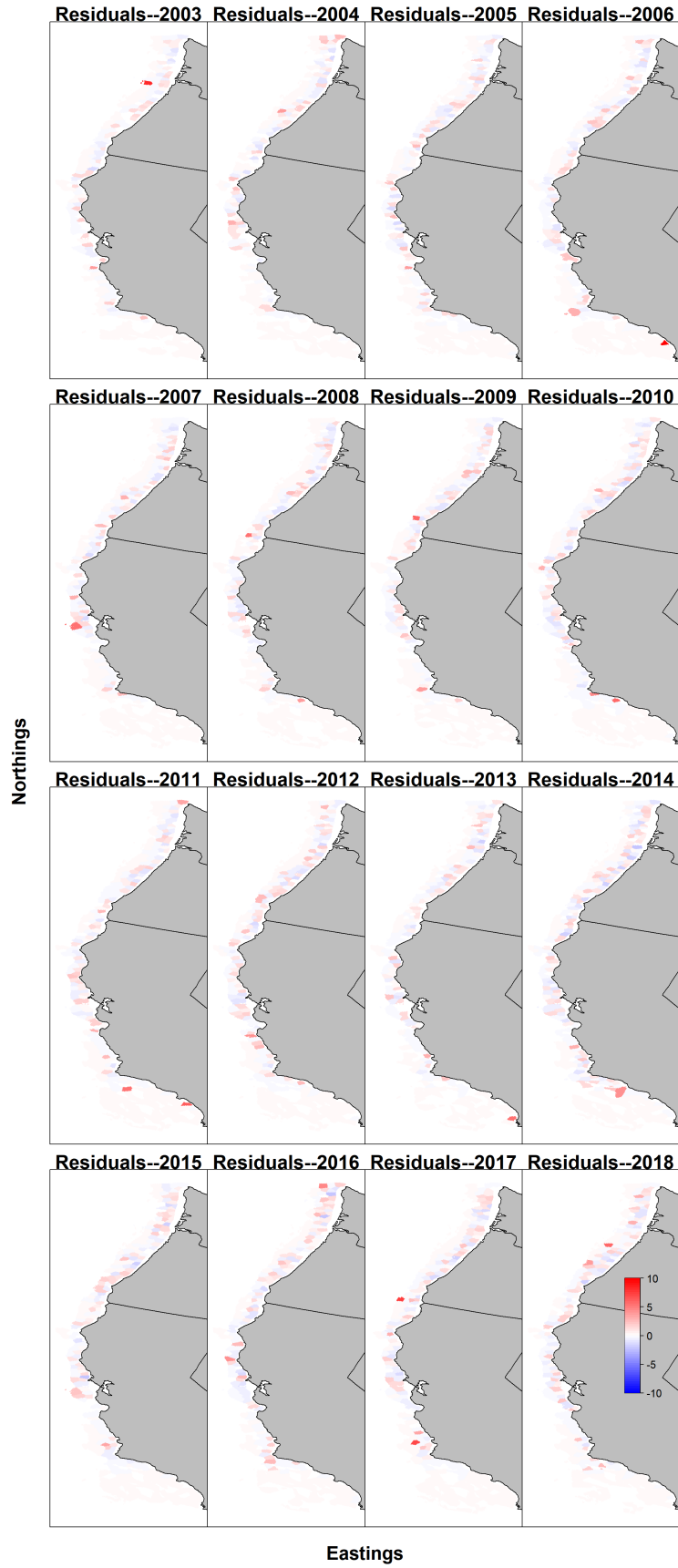


Figure 13: Map of Pearson residuals for the encounter probability in the WCGBT Survey
associated with each knot in the VAST standardization.

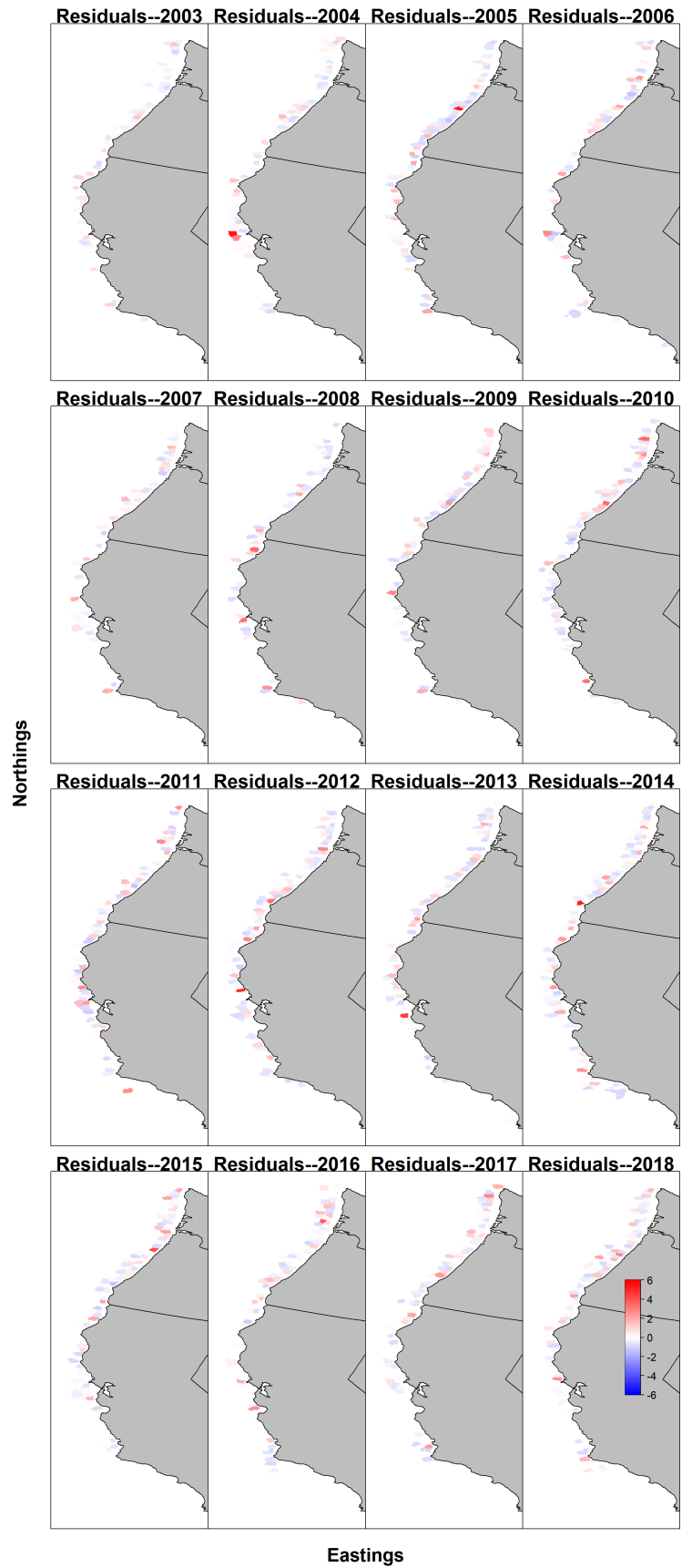


Figure 14: Map of Pearson residuals for the catch rate in the WCGBT Survey associated with each knot in the VAST standardization.⁸⁵

Big Skate per 100 observed hooks in IPHC longline survey

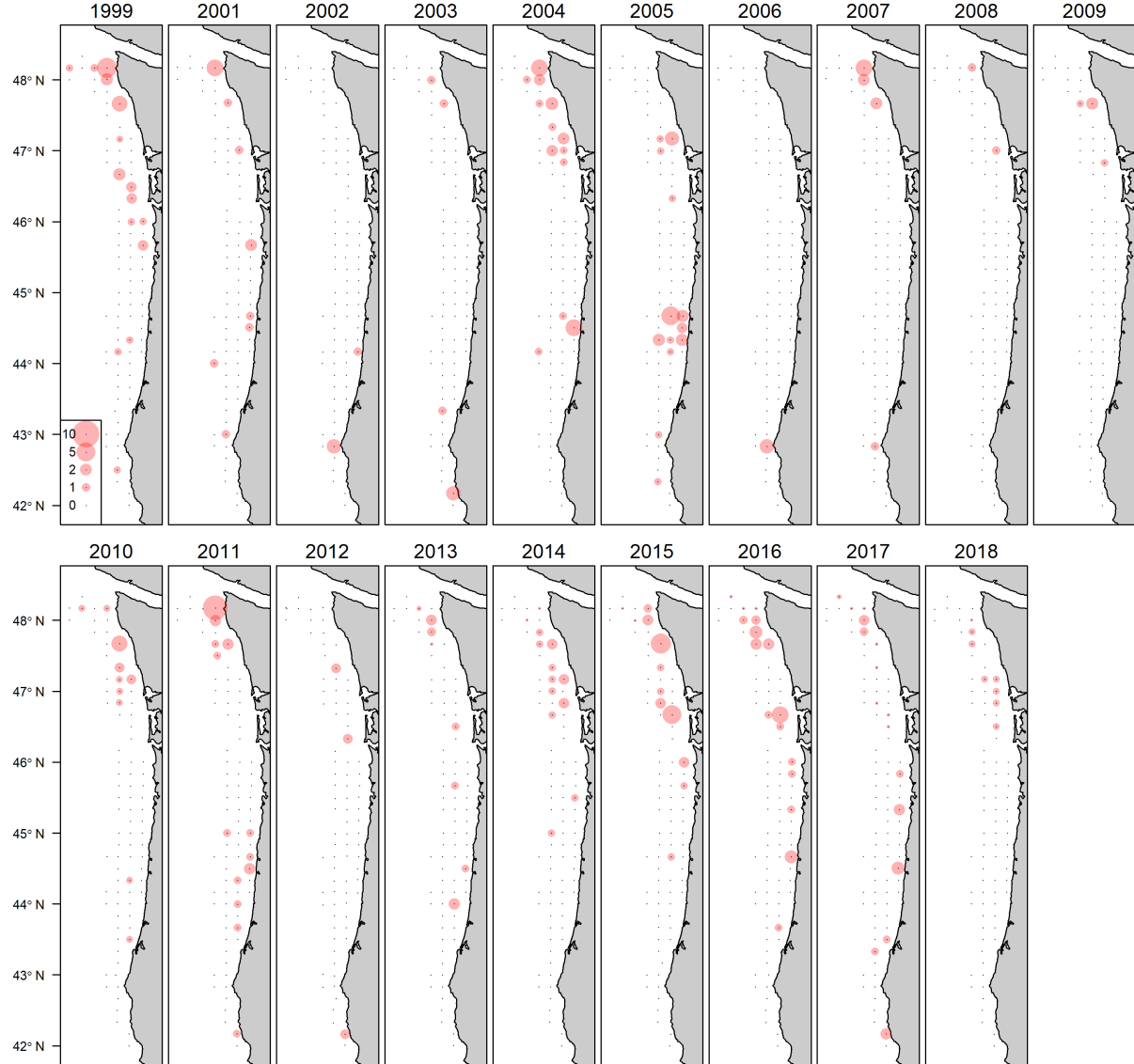


Figure 15: Map of catch rates by year for Big Skate in the International Pacific Halibut Commission longline survey.

12.2 Biology Figures

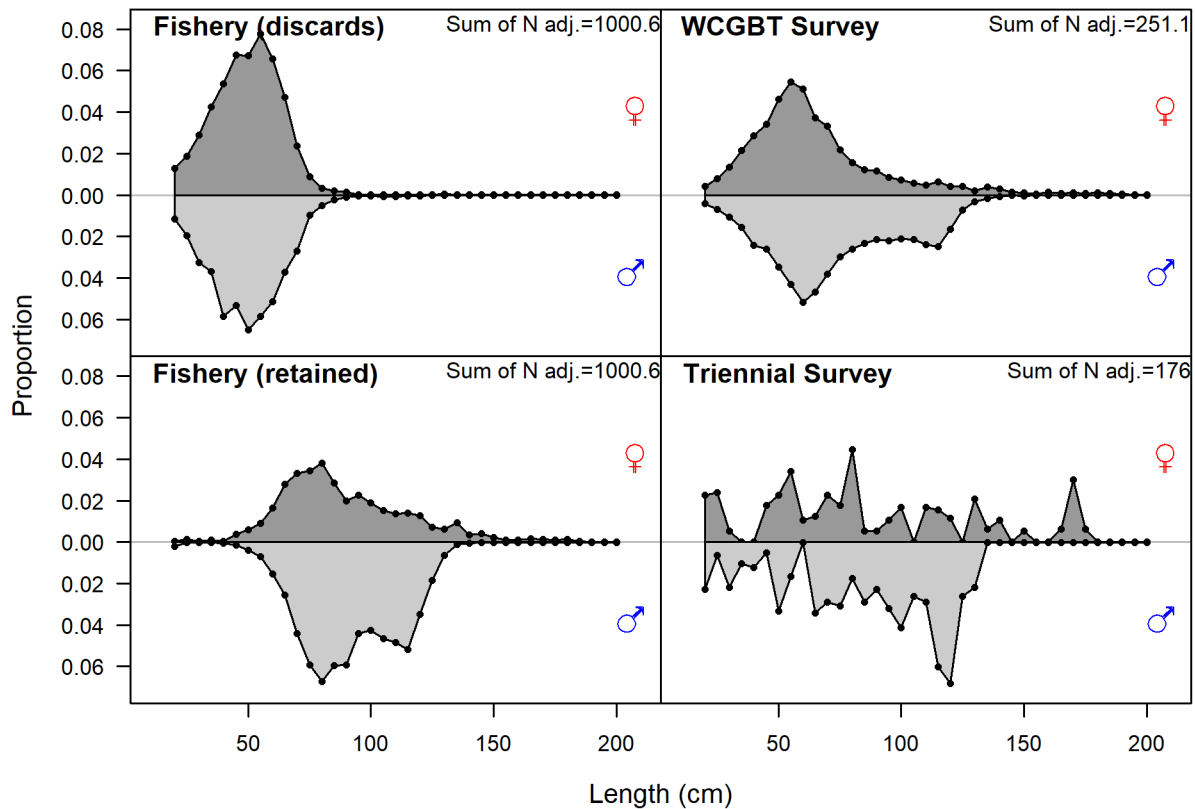


Figure 16: Length comp data, aggregated across time by fleet.

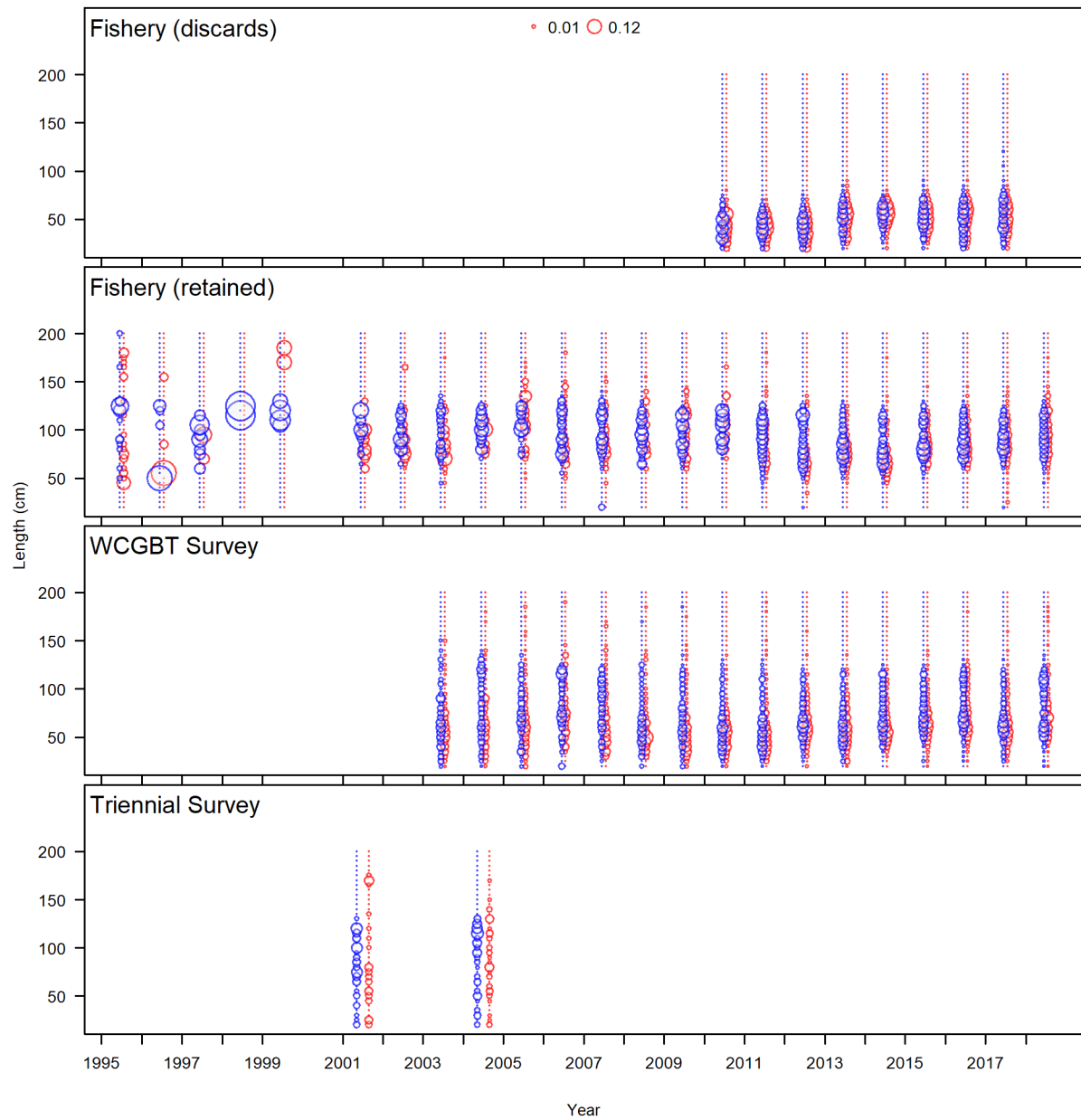


Figure 17: Length comp data for all years and fleets. Bubble size indicates the observed proportions, with females in red and males in blue.

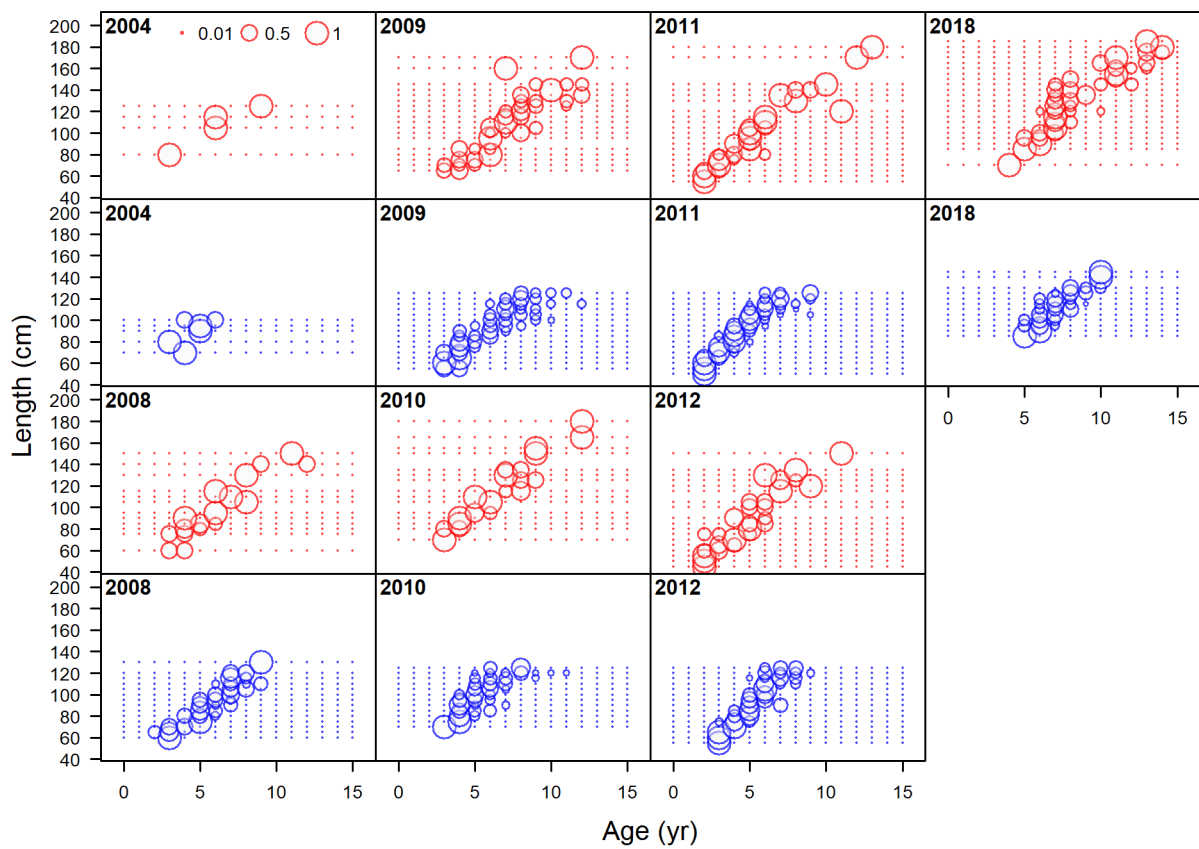


Figure 18: Conditional age-at-length data from the current fishery.

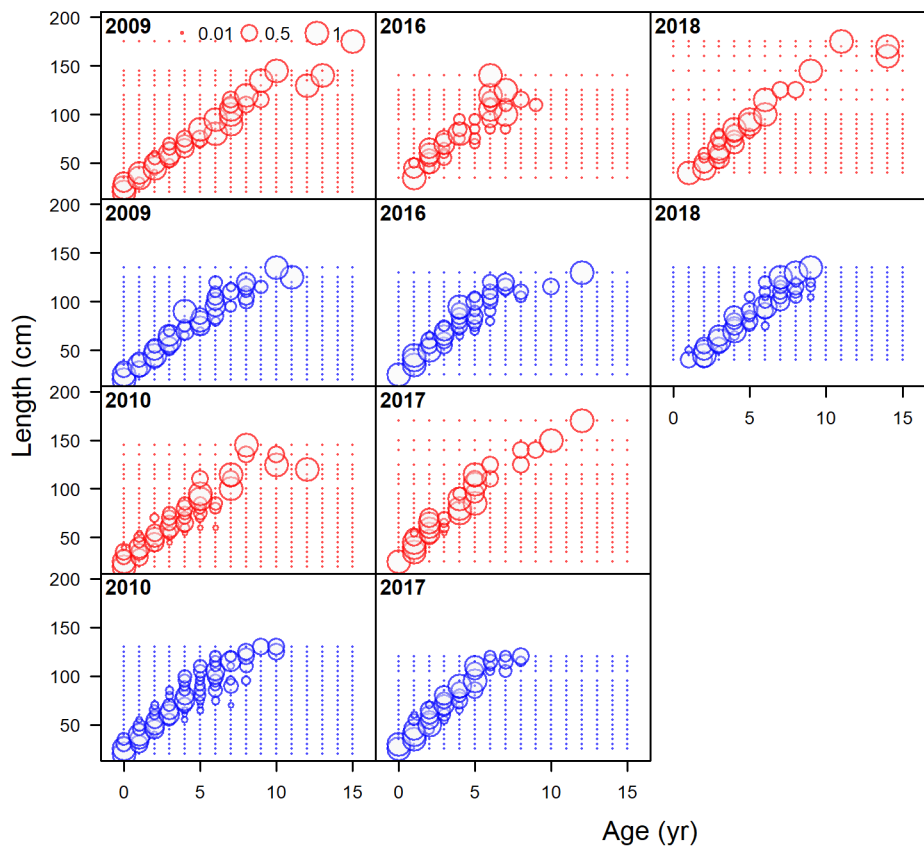


Figure 19: Conditional age-at-length data from the WCGBT Survey.

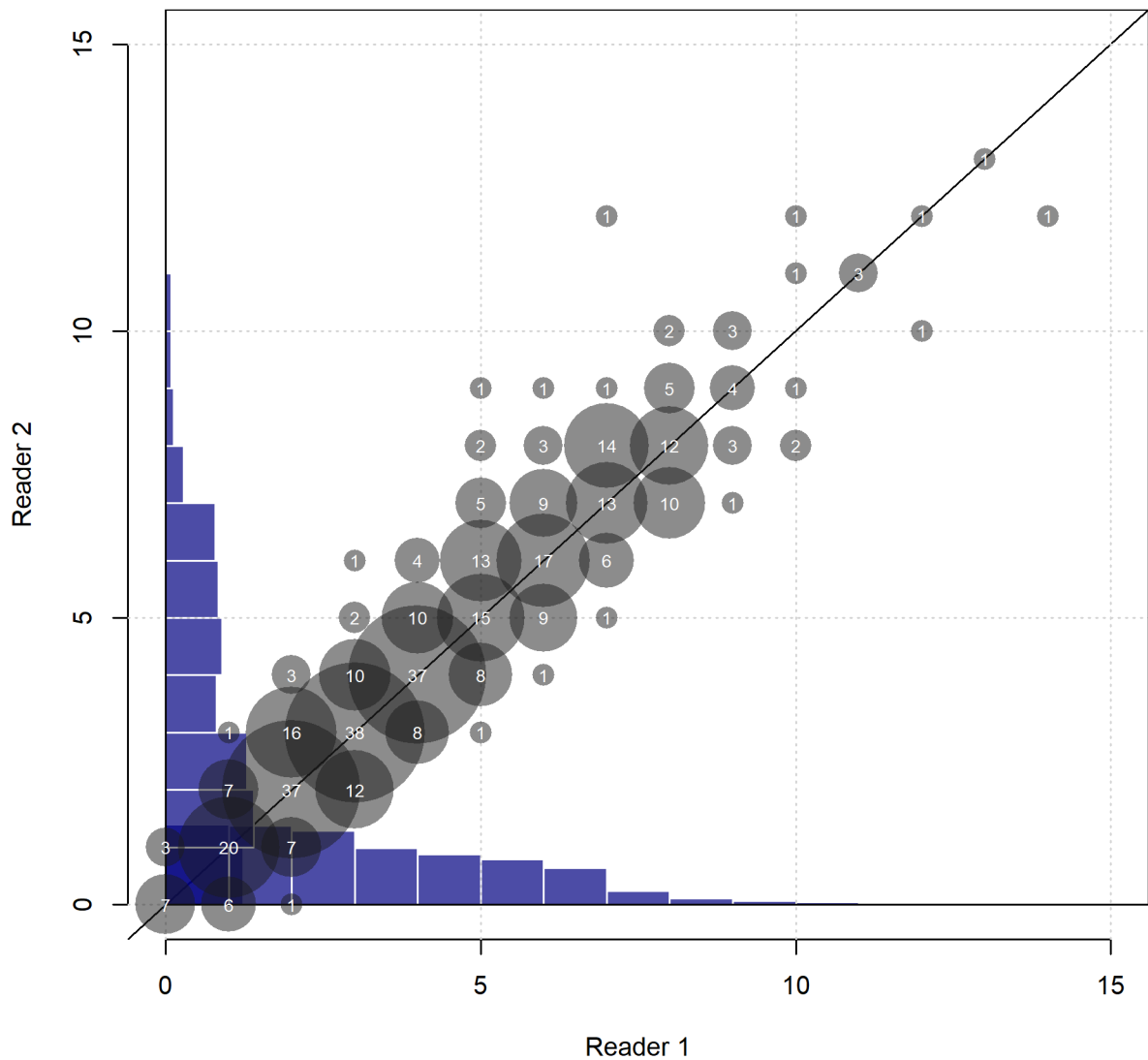


Figure 20: Comparison of reads from each of two age readers for Big Skate. Sample sizes associated with each combination of ages are shown by the size circles and the numbers within them. The blue histograms show the distribution of ages estimated by each reader.

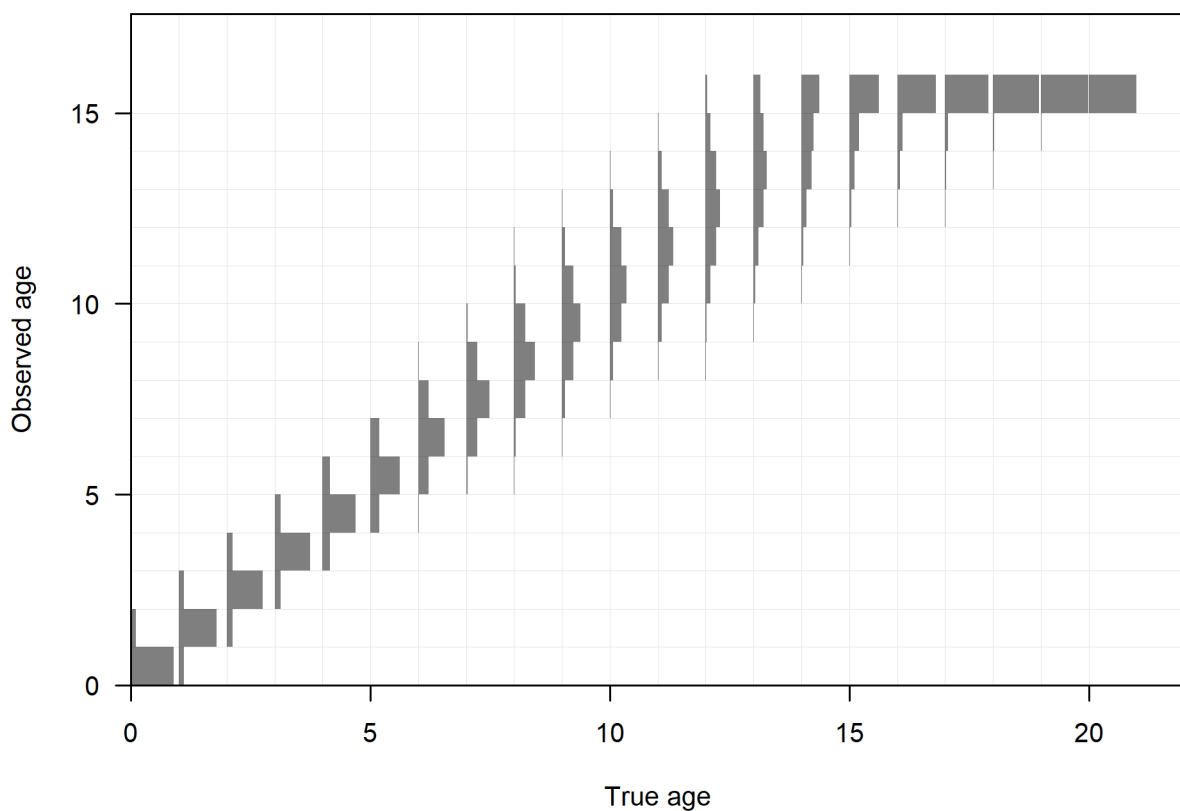


Figure 21: Estimated ageing imprecision.

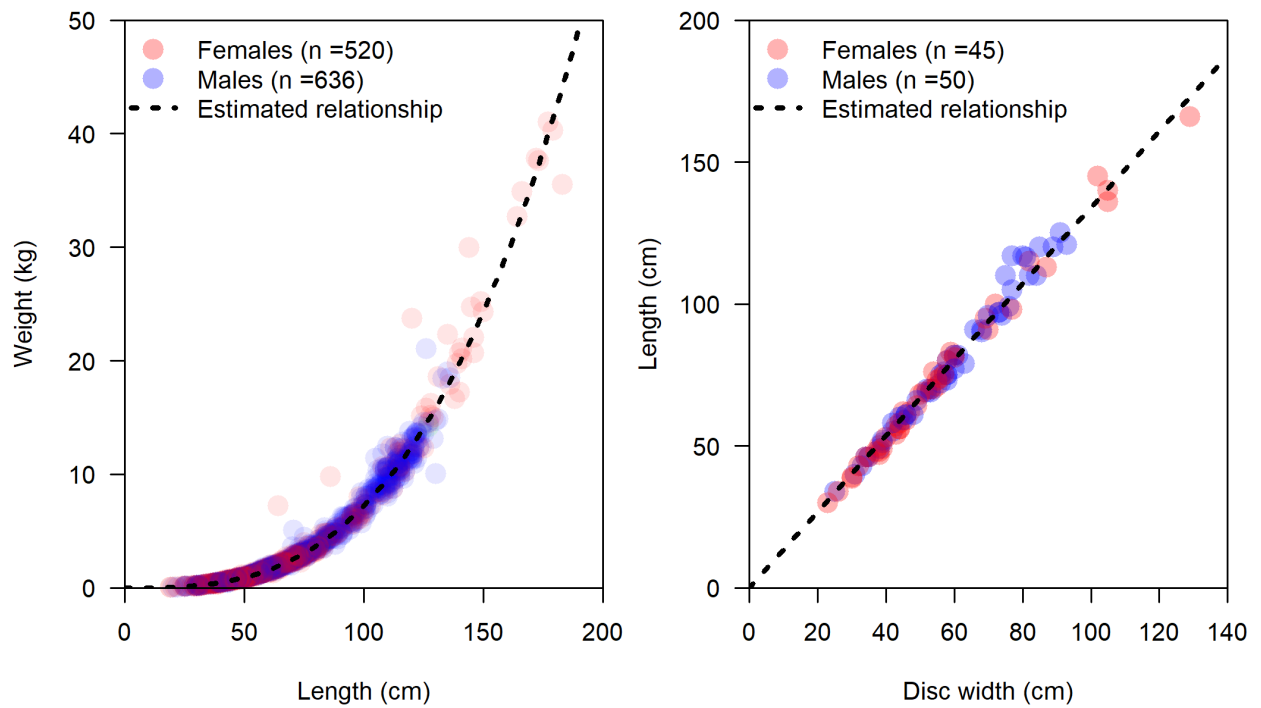


Figure 22: Estimated relationship between length and weight (left) and disc-width and length (right) for Big Skate. Colored points show observed values and the black line indicates the estimated relationship $W = 0.0000074924L^{2.9925}$.

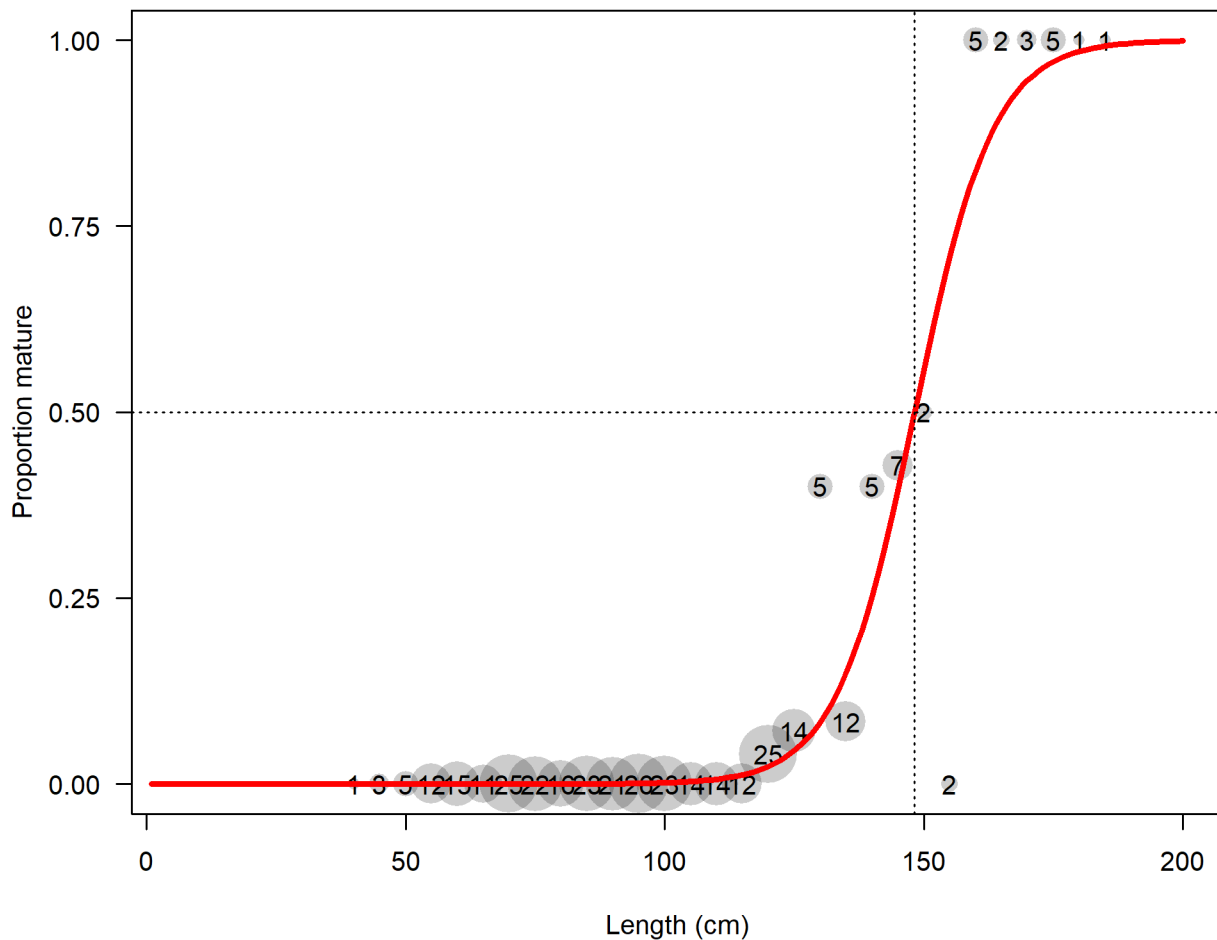


Figure 23: Estimated maturity relationship for female Big Skate. Gray points indicate average observed functional maturity within each length bin with point size proportional to the number of samples (indicated by text within each point).

12.3 Model Results Figures

12.3.1 Growth and Selectivity

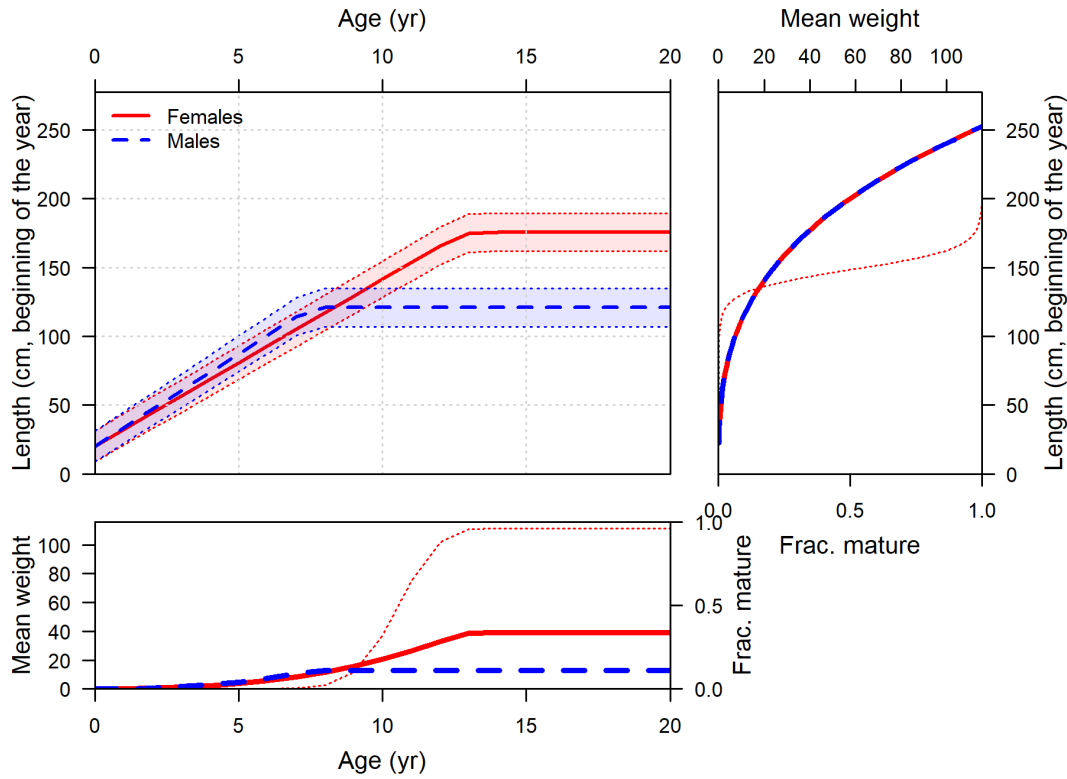


Figure 24: Estimated length-at-age for female and male Big Skate (top left panel). Shaded areas indicate 95% intervals for distribution of lengths at each age. Values represent beginning-of-year growth. Weight (thick line) and maturity (thin line) are shown in the top-right and lower-left panels as a function of length and age, respectively, where the values-at-age are calculated by mapping the length-based relationships through the estimated distribution of length at each age.

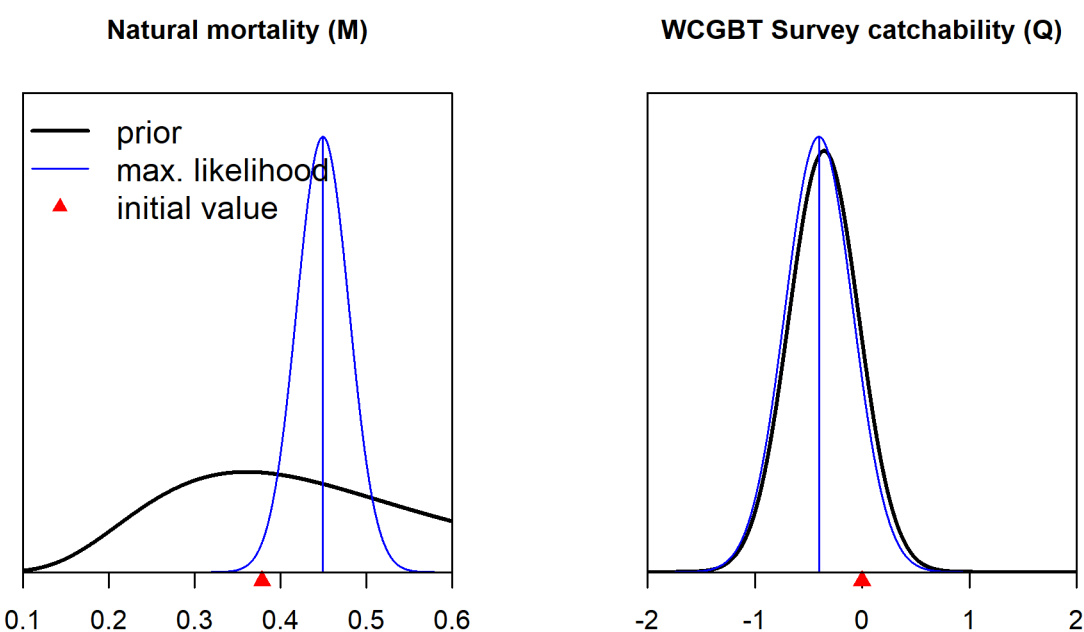


Figure 25: Estimates of natural morality and catchability of the WCGBT Survey with normal approximations to their uncertainty compared to their prior distributions.

Length-based selectivity by fleet in 2018

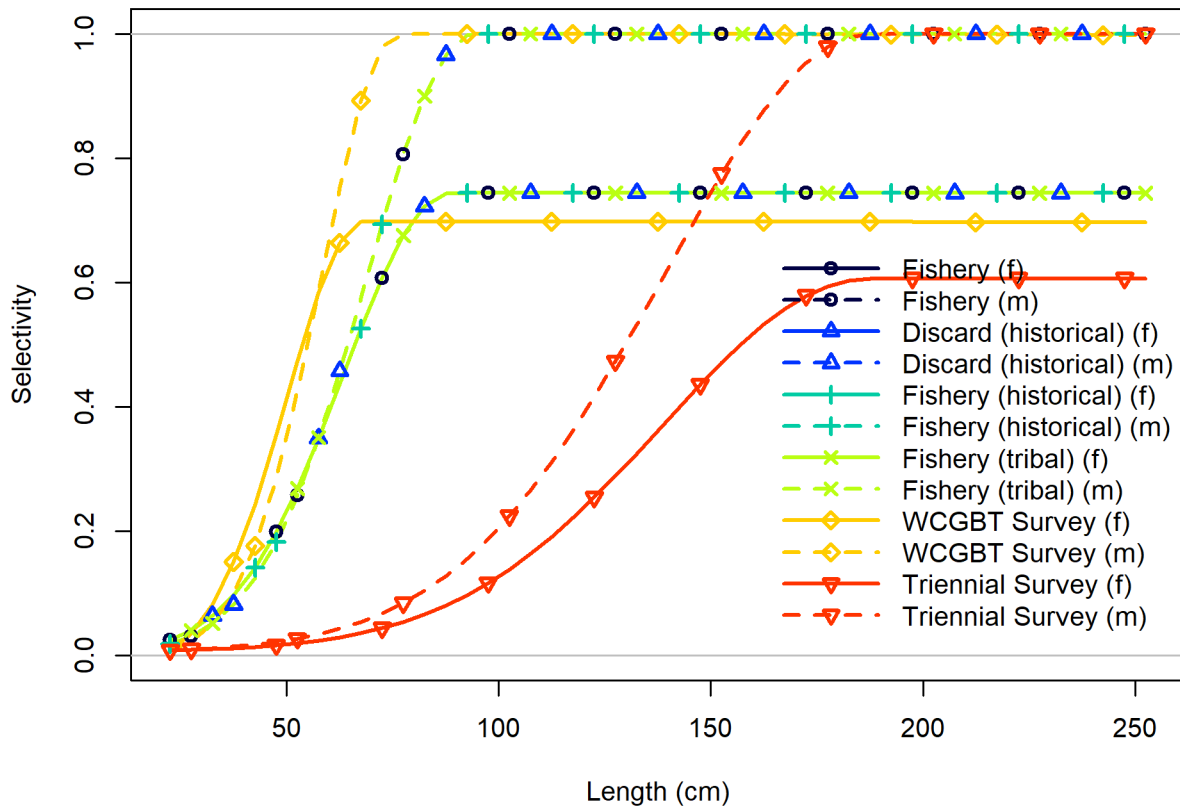


Figure 26: Selectivity at length for all of the fleets in the base model. Female selectivity is shown in the solid lines and males in the dashed lines.

Derived age-based from length-based selectivity by fleet in 2018

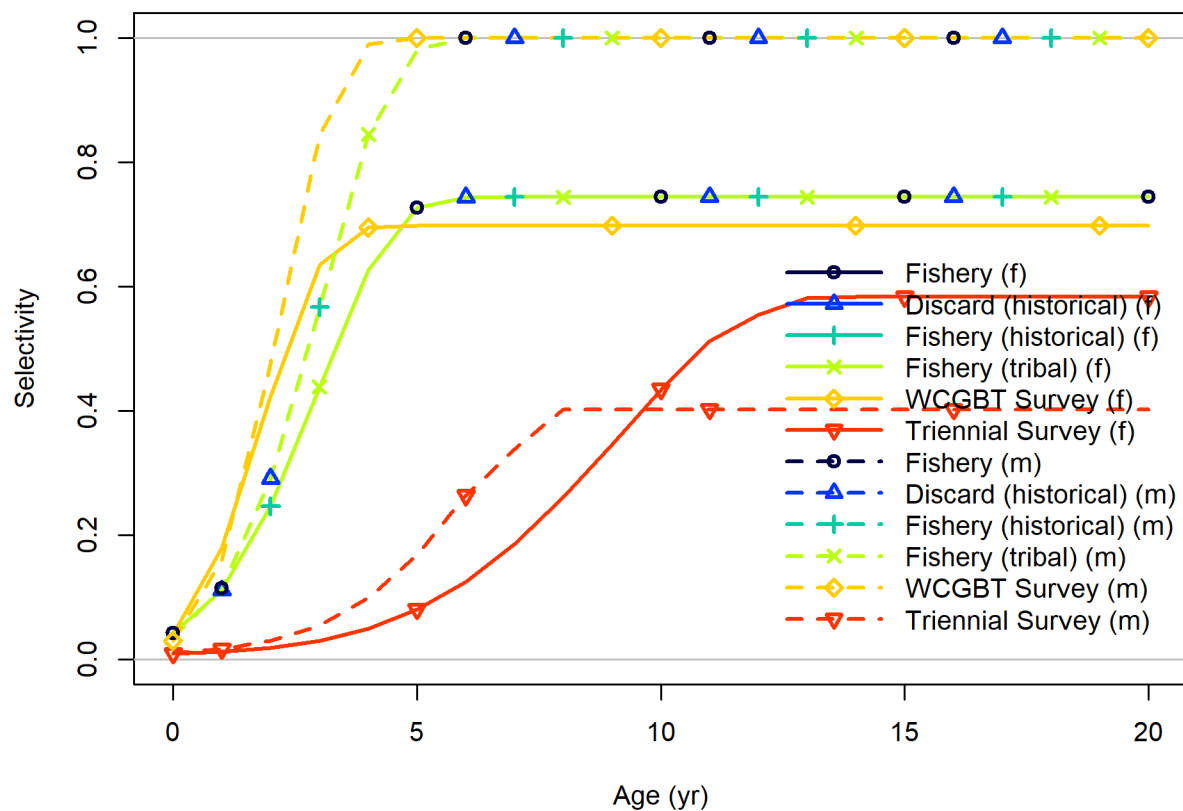


Figure 27: Selectivity at age derived from the combination of selectivity-at-length (shown above) and the estimated distribution of length at each age for all of the fleets in the base model. Female selectivity is shown in the solid lines and males in the dashed lines.

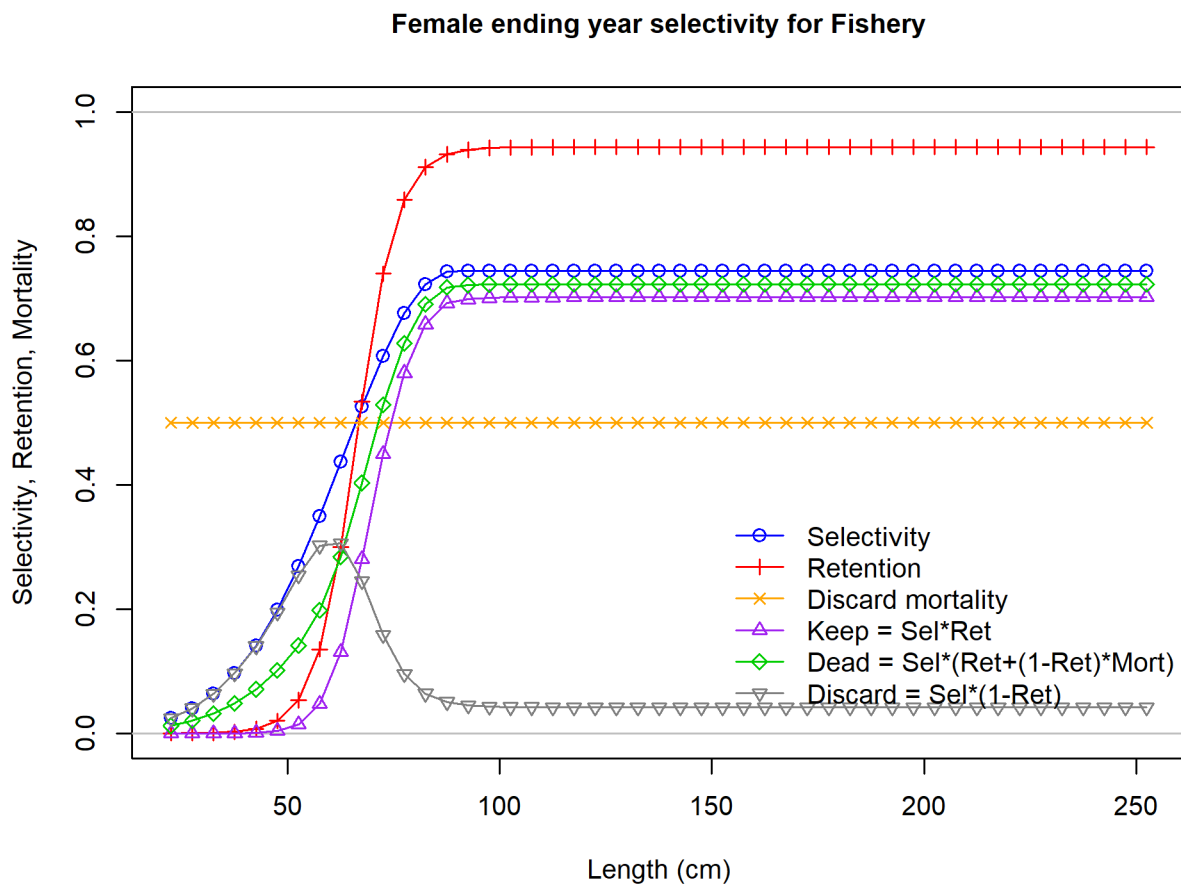


Figure 28: Female fishery selectivity and retention in 2018 with associated derived quantities.

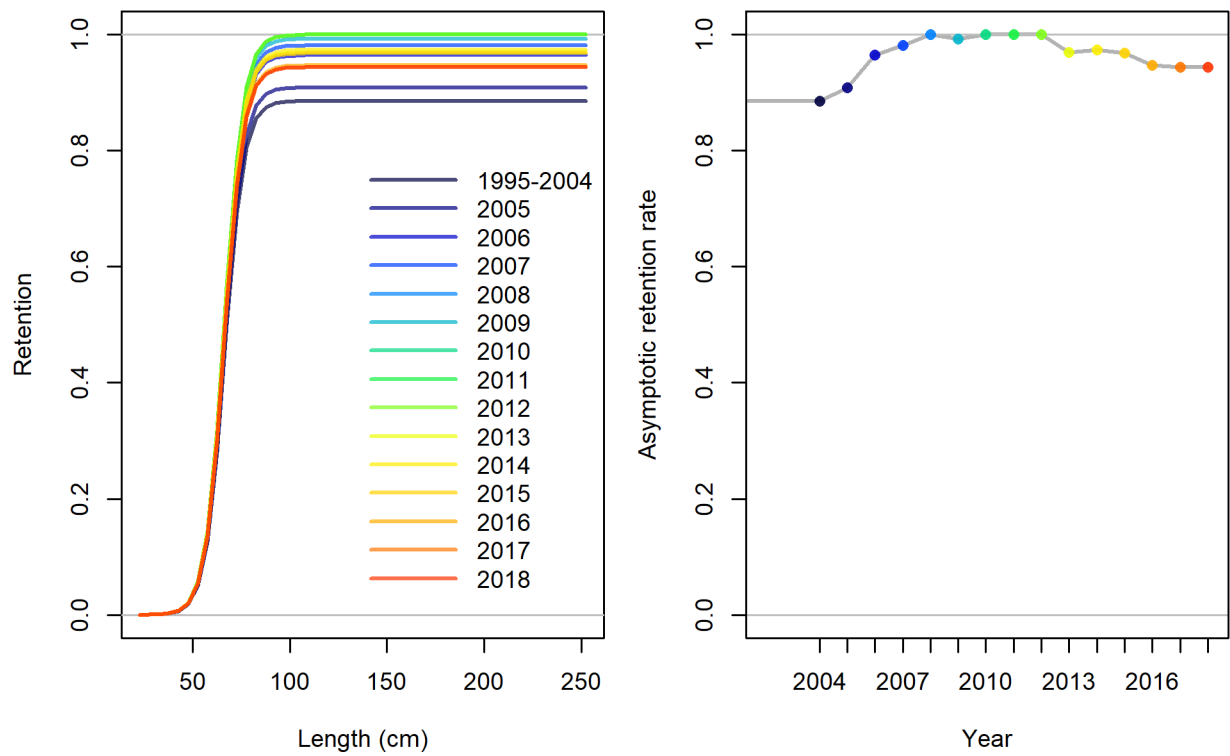


Figure 29: Time-varying retention for the fishery (left) with the time-series of asymptotic retention rates (right).

12.3.2 Fits to the Data

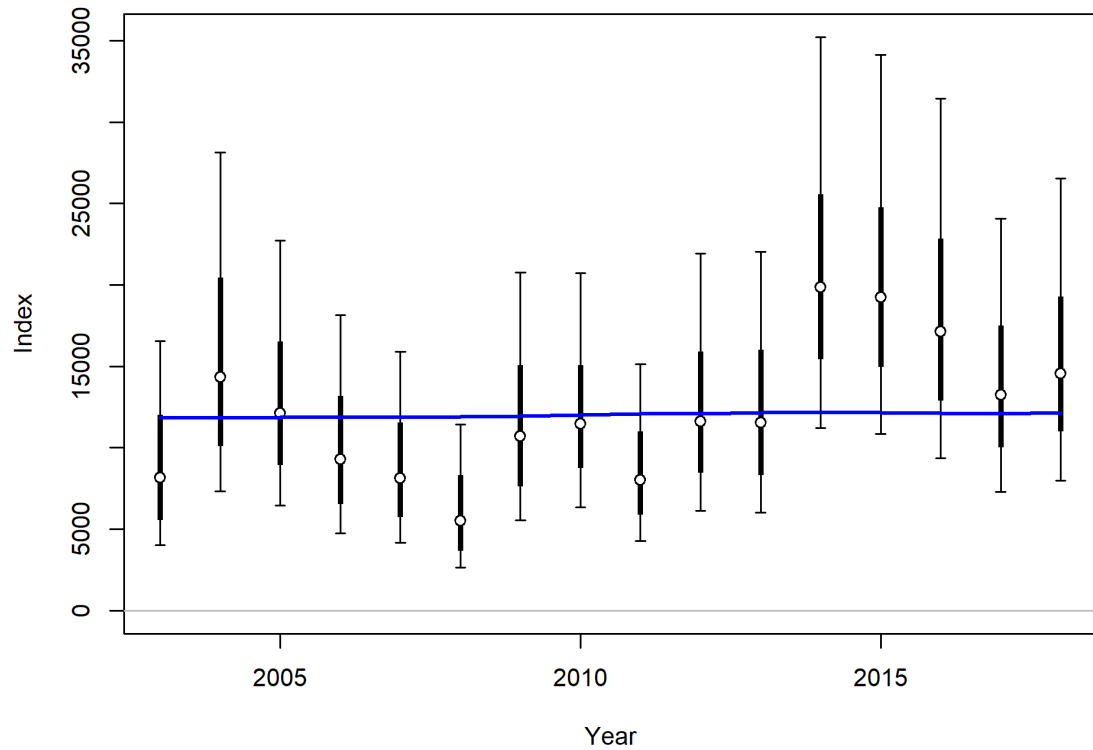


Figure 30: Fit to index data for WCGBT Survey.

Lines indicate 95% uncertainty interval around index values. Thicker lines indicate input uncertainty before addition of estimated additional uncertainty parameter. The blue line indicates the model estimate.

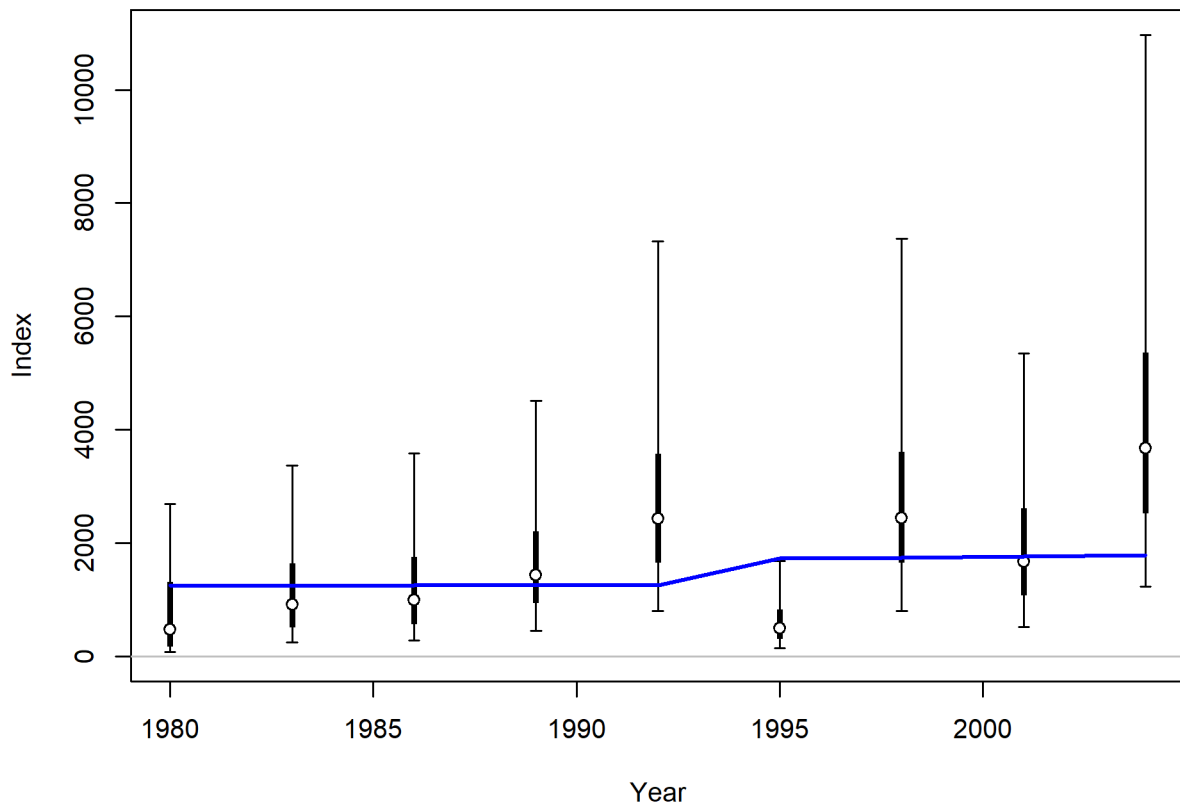


Figure 31: Fit to index data for Triennial Survey. Lines indicate 95% uncertainty interval around index values. Thicker lines indicate input uncertainty before addition of estimated additional uncertainty parameter. The blue line indicates the model estimate with a change between 1992 and 1995 associated with the estimated change in catchability.

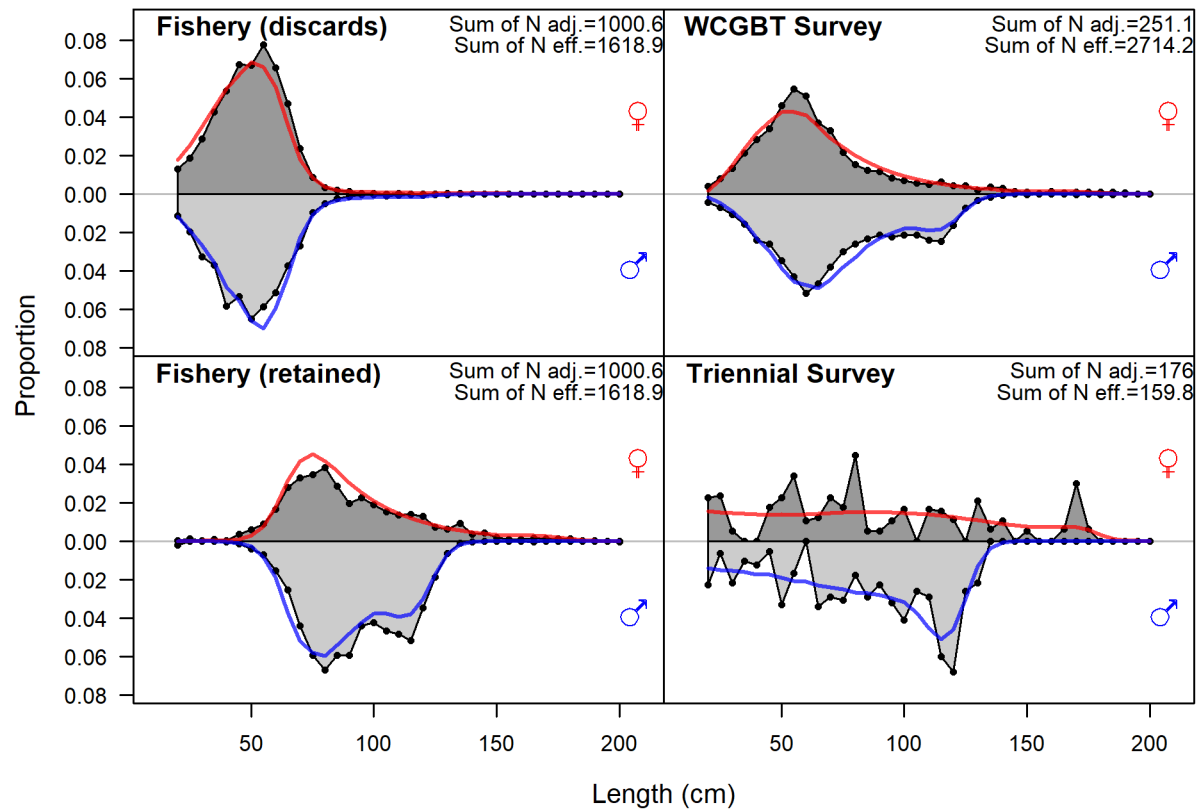


Figure 32: Fits to length comp data, aggregated across time by fleet.

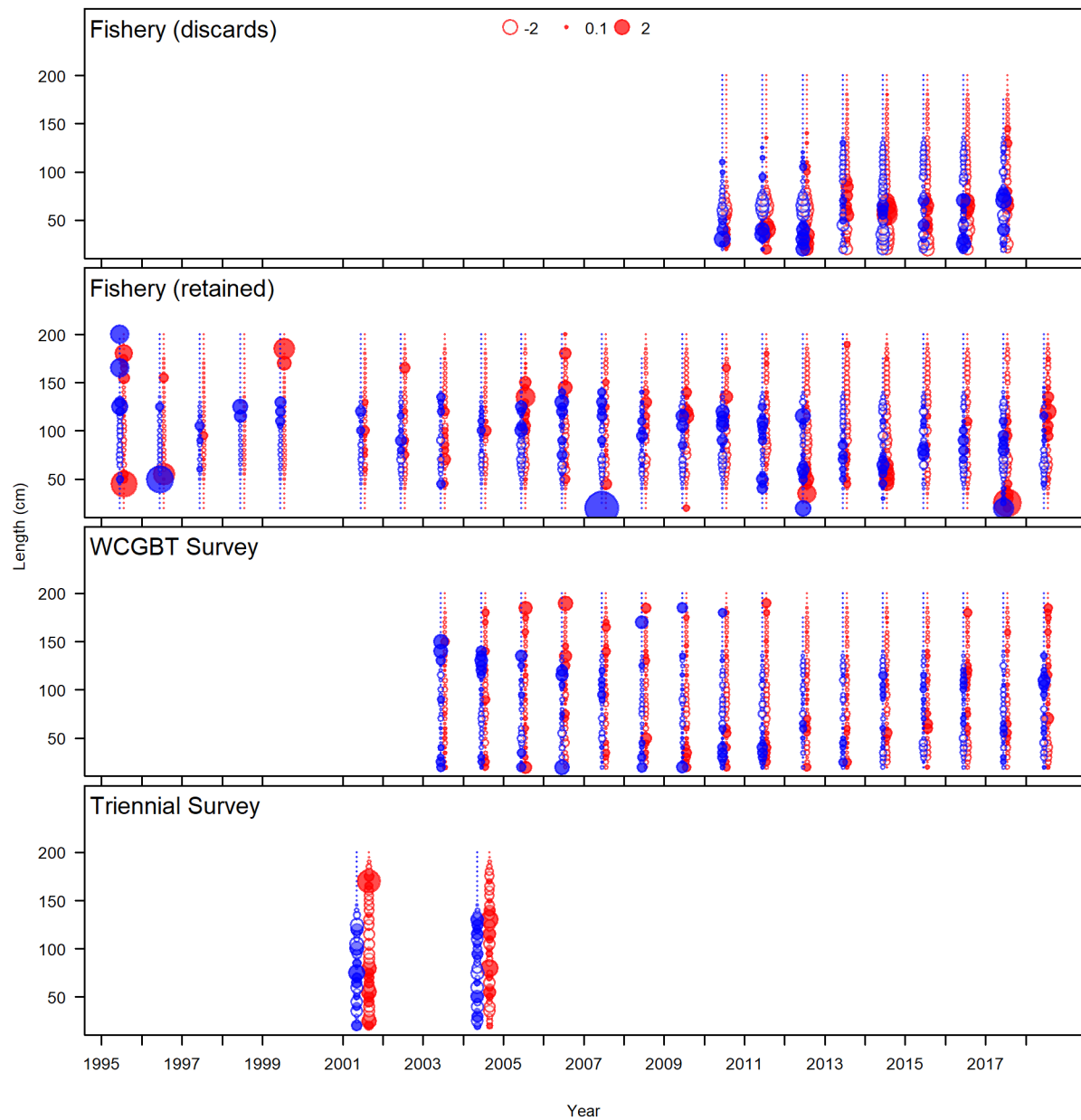


Figure 33: Pearson residuals for length composition data for all years and fleets, with females in red and males in blue. Closed bubbles are positive residuals ($\text{observed} > \text{expected}$) and open bubbles are negative residuals ($\text{observed} < \text{expected}$).

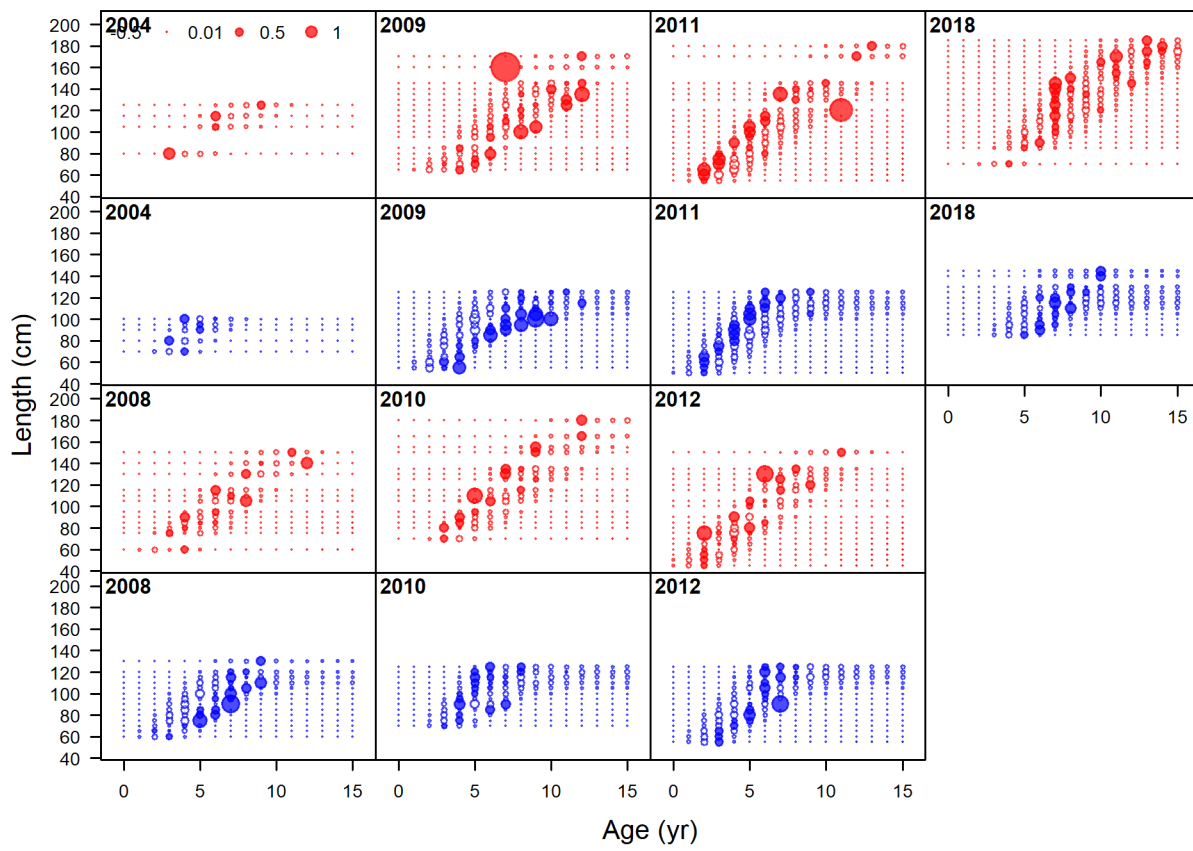


Figure 34: Pearson residuals for the fit to conditional age-at-length data from the fishery. Closed bubbles are positive residuals (observed > expected) and open bubbles are negative residuals (observed < expected).

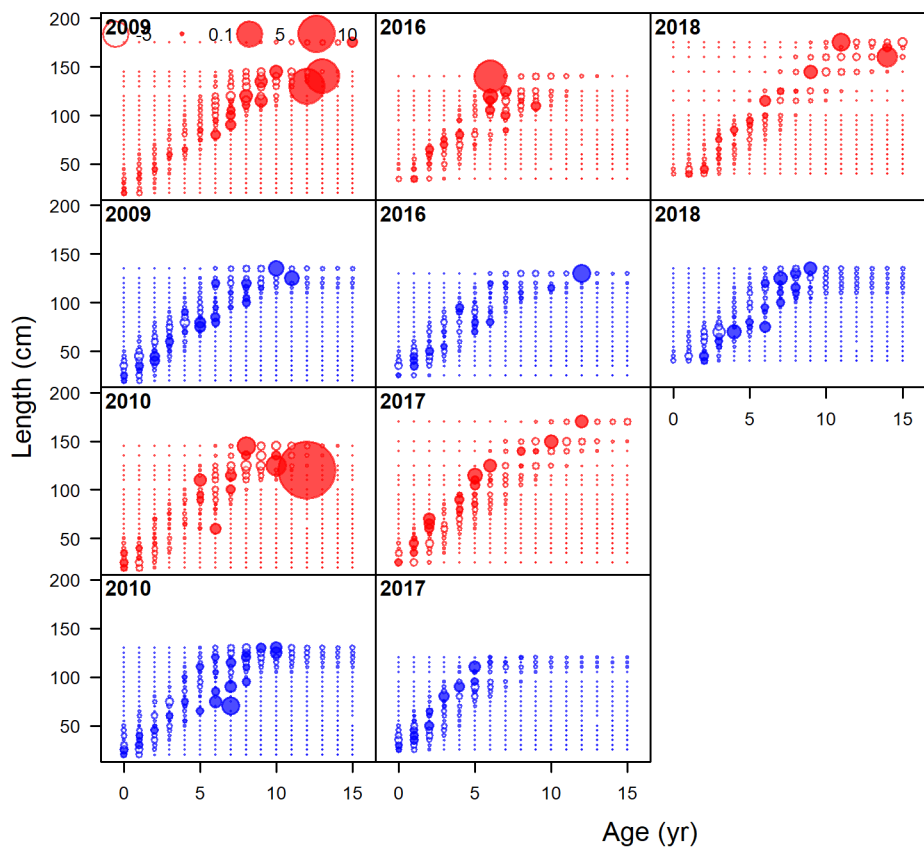


Figure 35: Pearson residuals for the fit to conditional age-at-length data from the WCGBT Survey. Closed bubbles are positive residuals (observed $>$ expected) and open bubbles are negative residuals (observed $<$ expected).

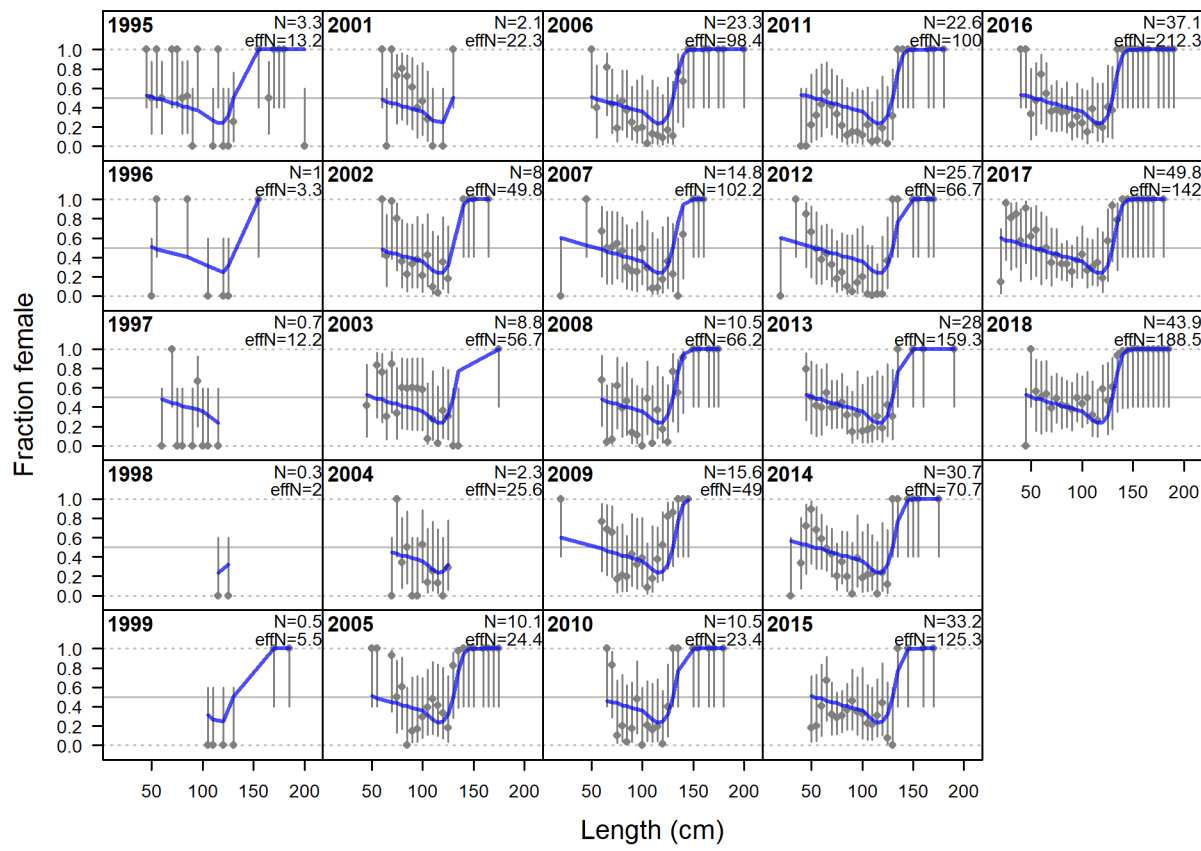


Figure 36: Observed sex ratios (points) from the fishery length comp data with 75% intervals (vertical lines) calculated as a Jeffreys interval based on the adjusted input sample size. The model expectation is shown in the blue line.

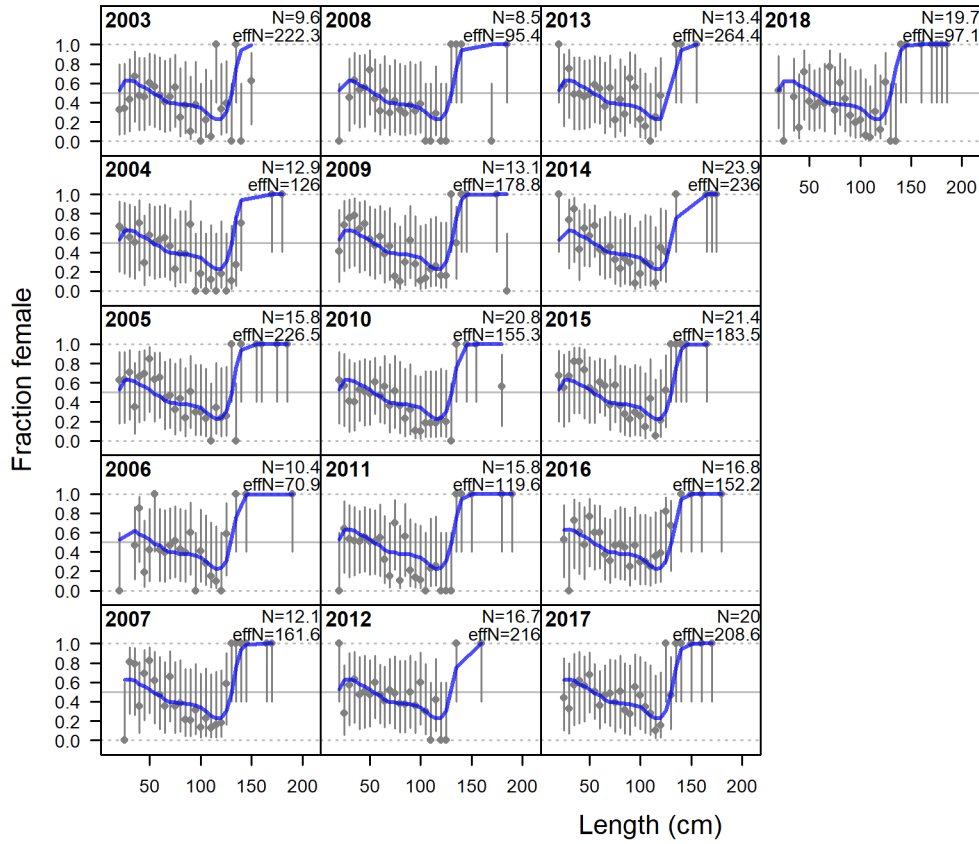


Figure 37: Observed sex ratios (points) from the WCGBT Survey length comp data with 75% intervals (vertical lines) calculated as a Jeffreys interval based on the adjusted input sample size. The model expectation is shown in the blue line.

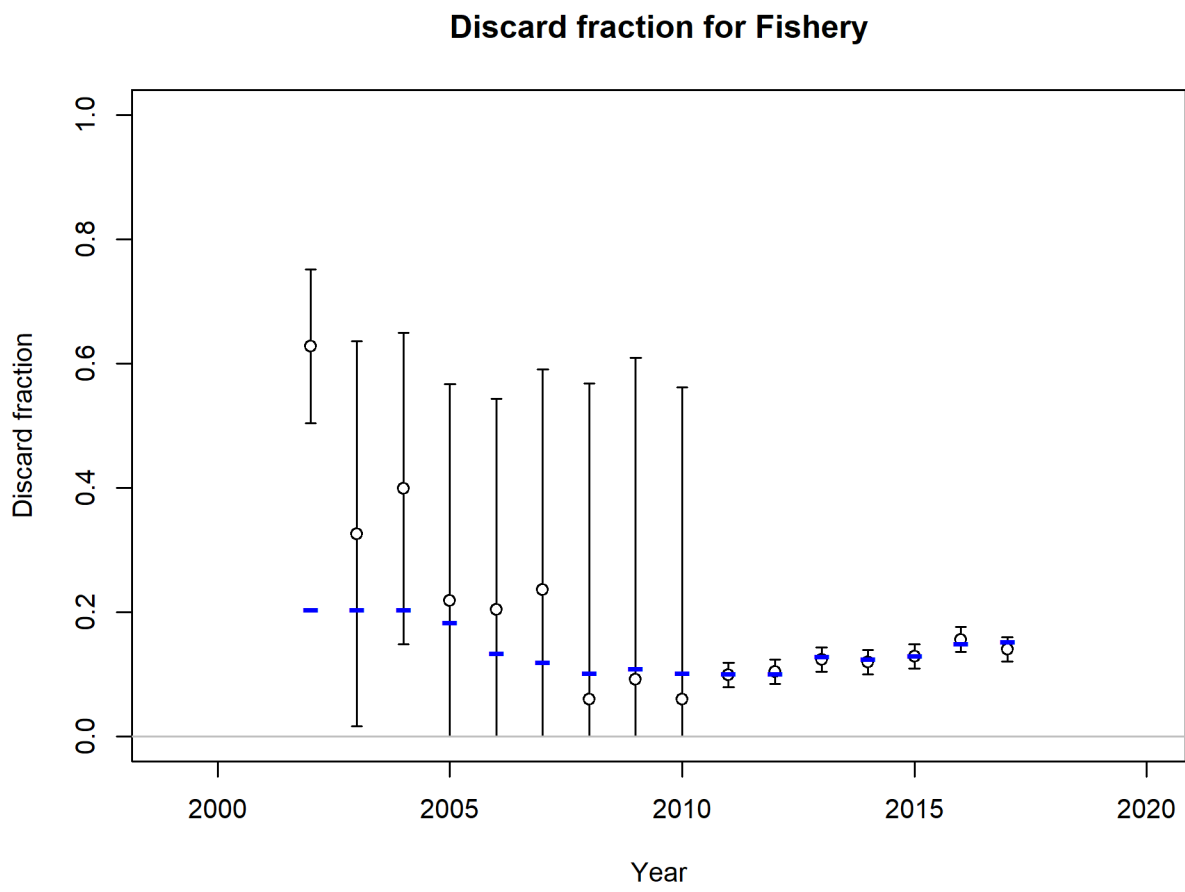


Figure 38: Fit to the discard fraction estimates. Points are model estimates with 95% uncertainty intervals. The model estimate is shown in the blue lines.

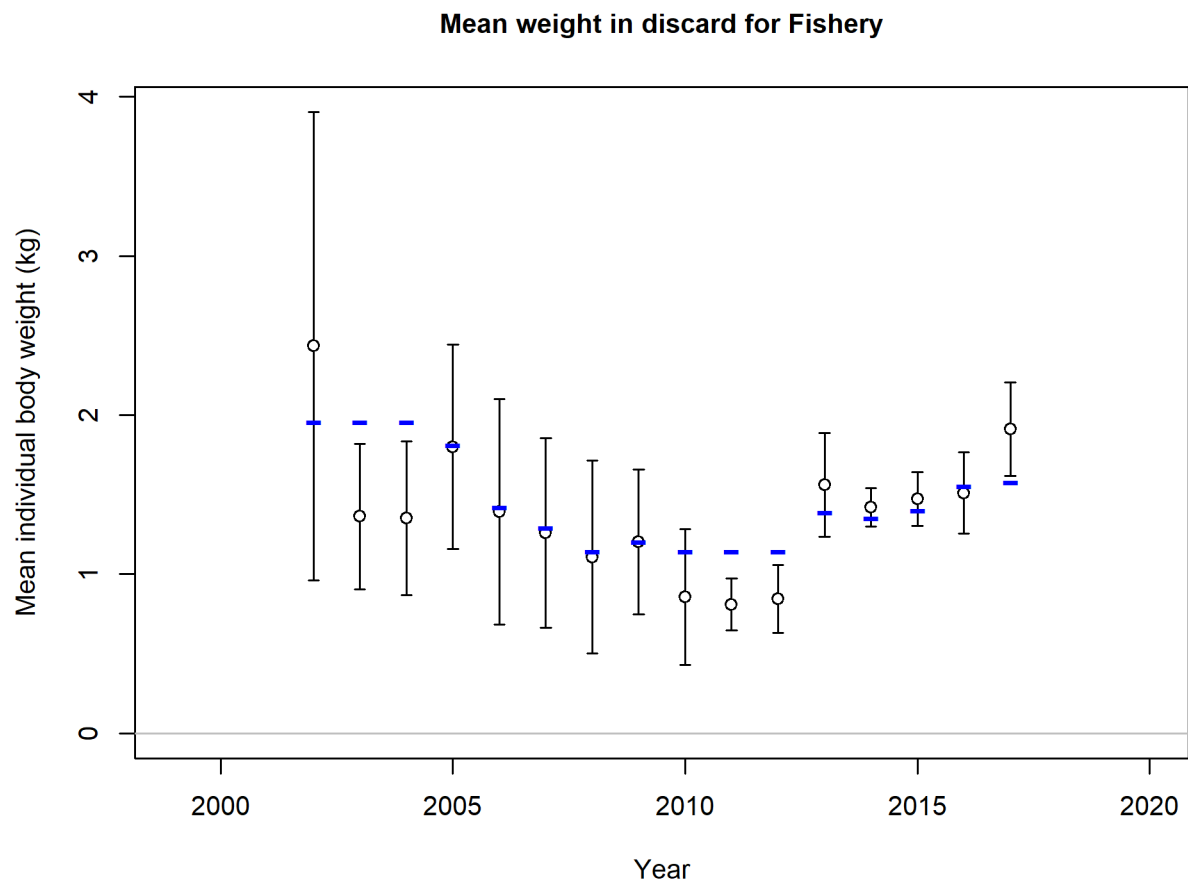


Figure 39: Fit to the mean weight of the discards. Points are model estimates with 95% uncertainty intervals. The model estimate is shown in the blue lines.

12.3.3 Time Series Figures

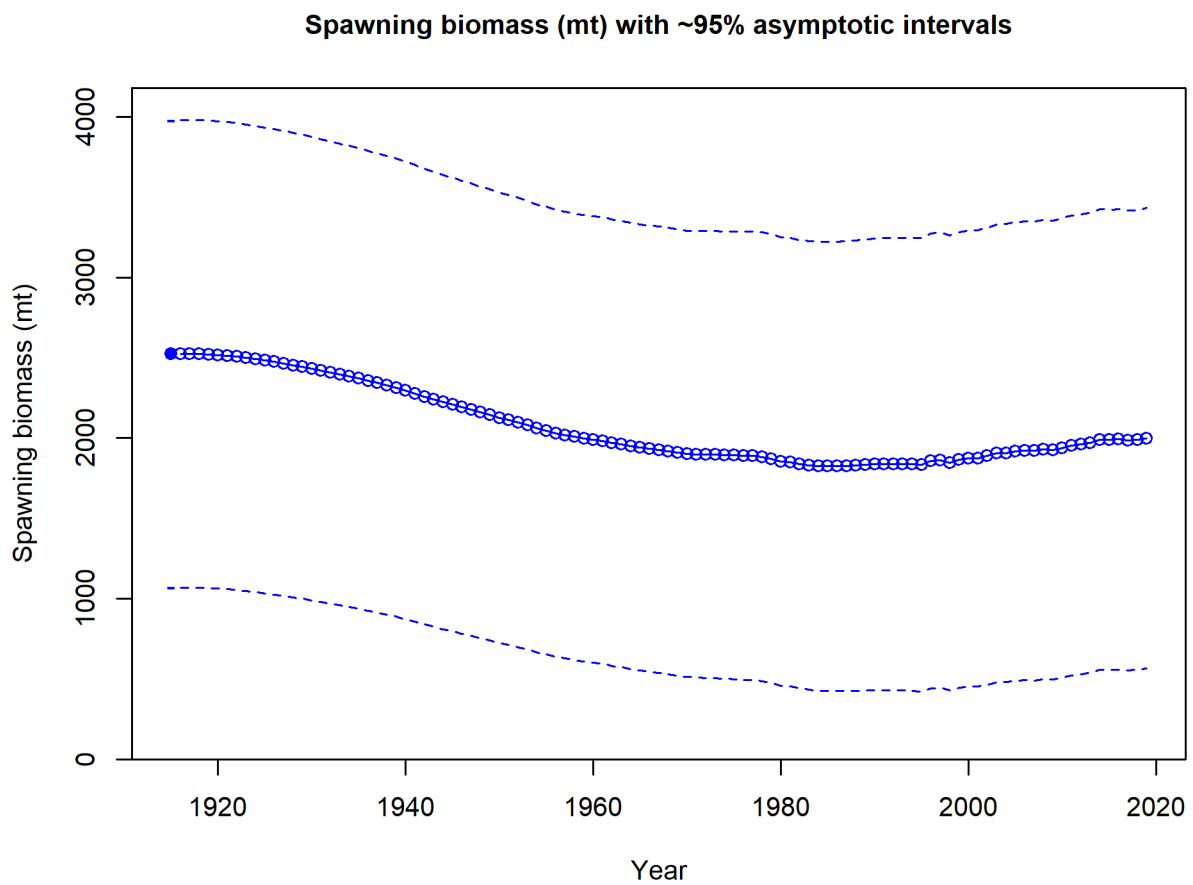


Figure 40: Estimated spawning biomass (mt) with approximate 95% asymptotic intervals.

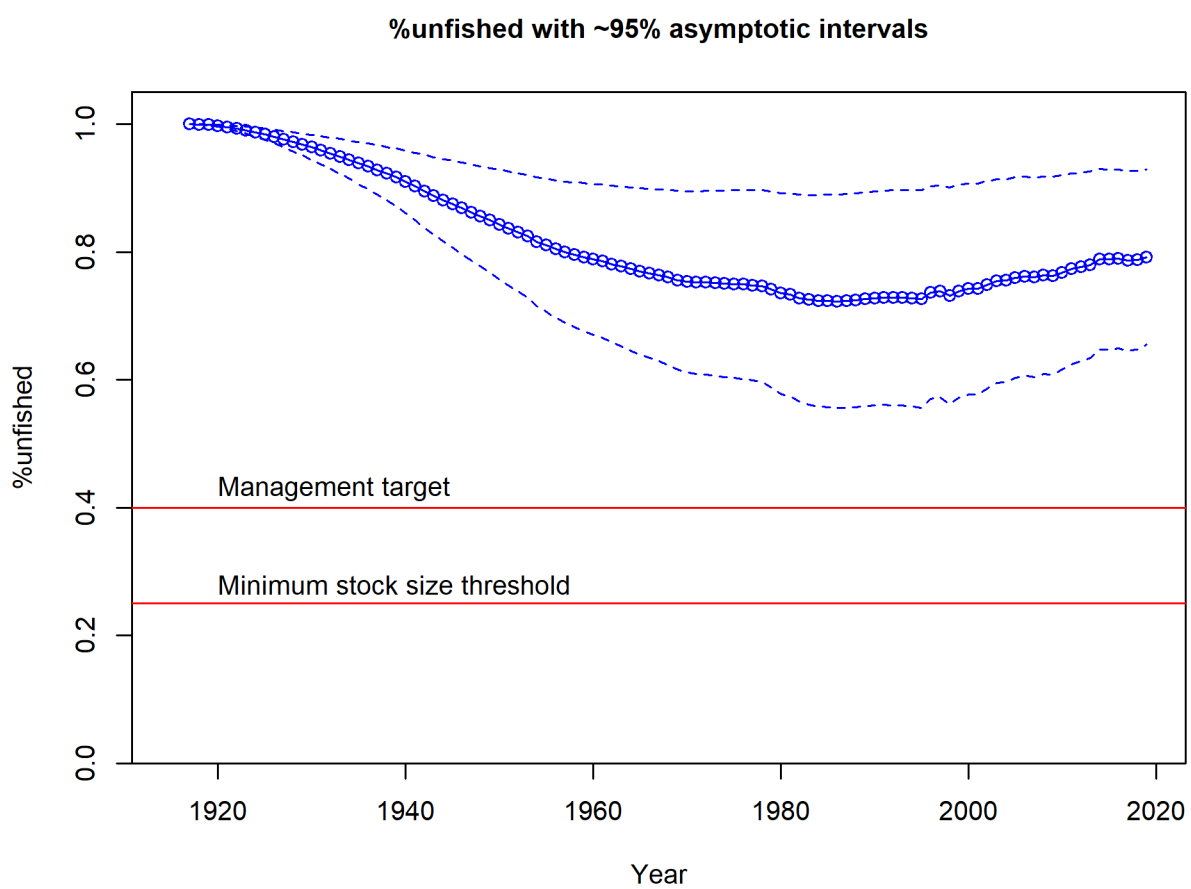


Figure 41: Estimated %unfished with approximate 95% asymptotic intervals.

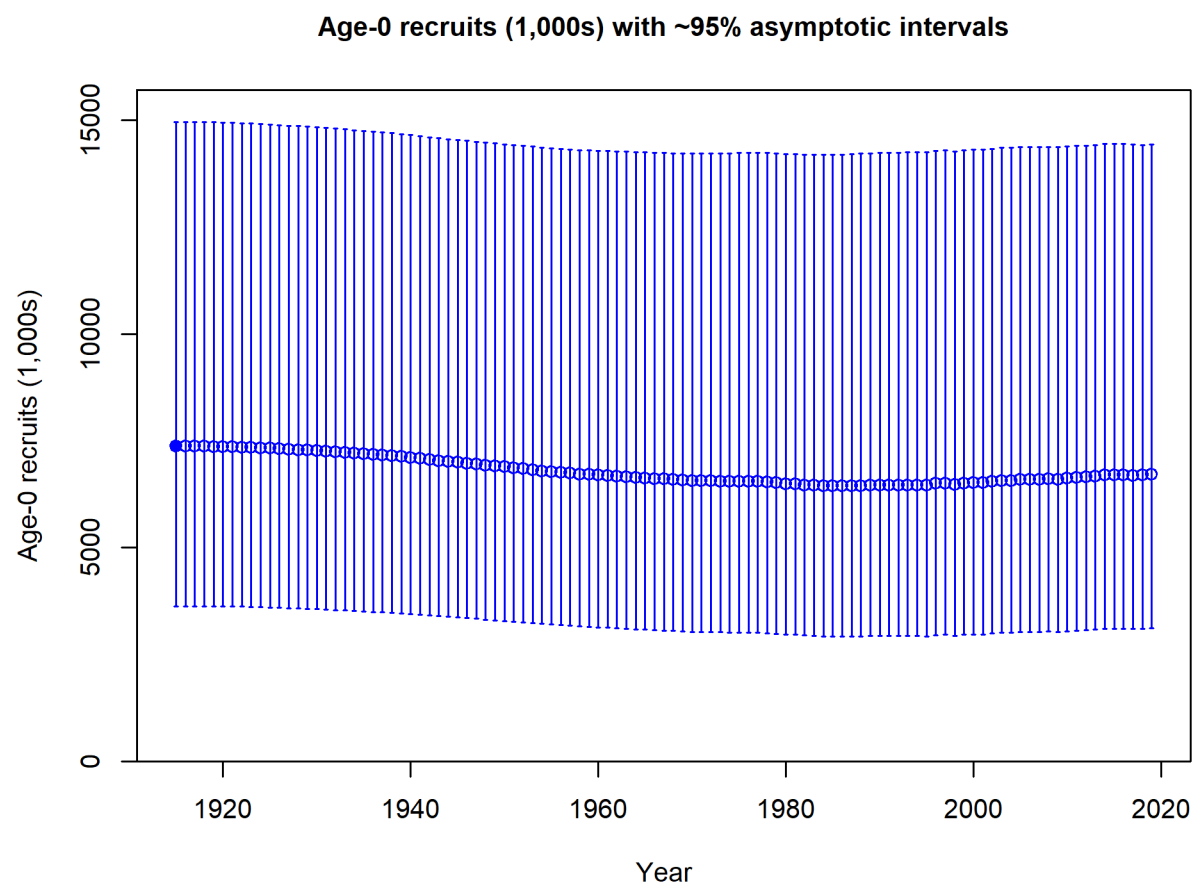


Figure 42: Estimated time-series of recruitment for Big Skate.

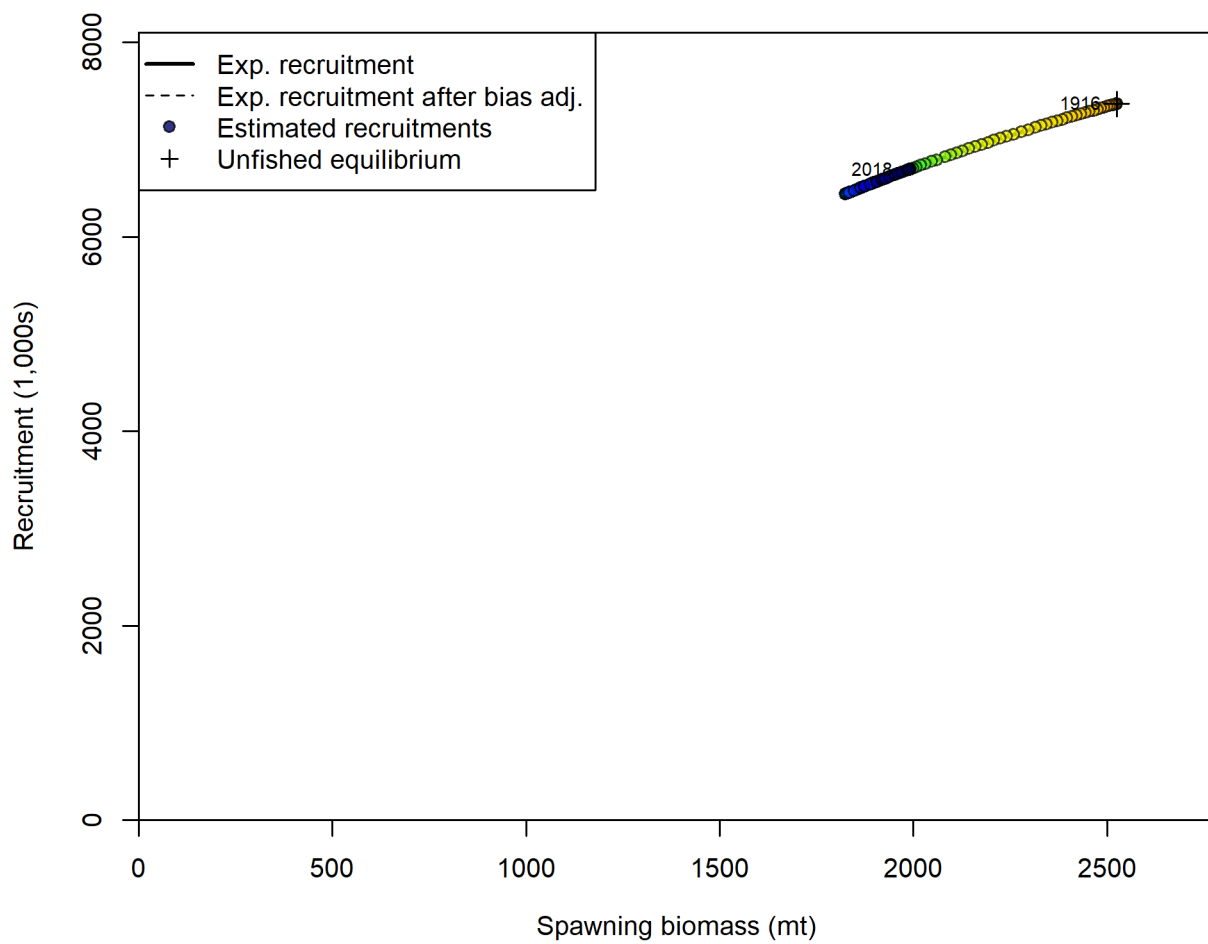


Figure 43: Estimated recruitment and the assumed stock-recruit relationship.

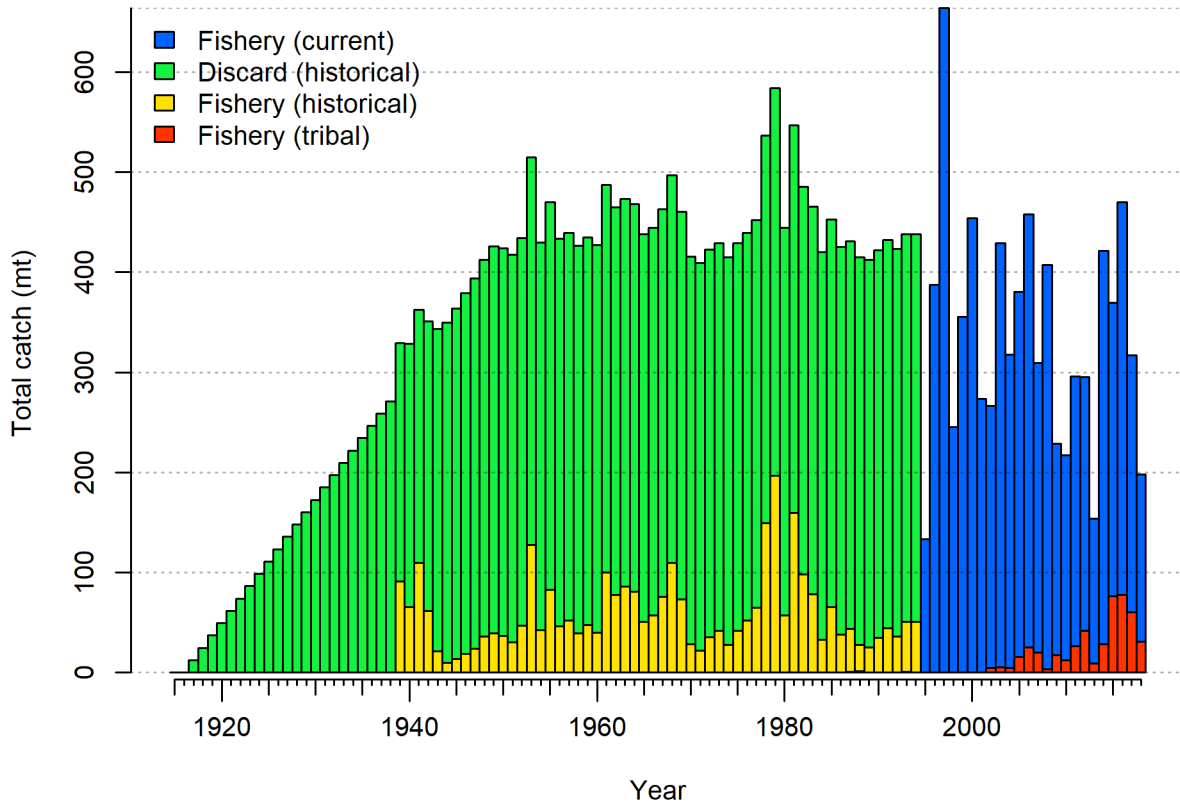


Figure 44: Estimated total catch including discards estimated within the model. The historical discards shown in green have been scaled to account for an assumed 50% discard mortality but the discards in the recent period show both live and dead discards.

12.3.4 Sensitivity Analyses and Retrospectives

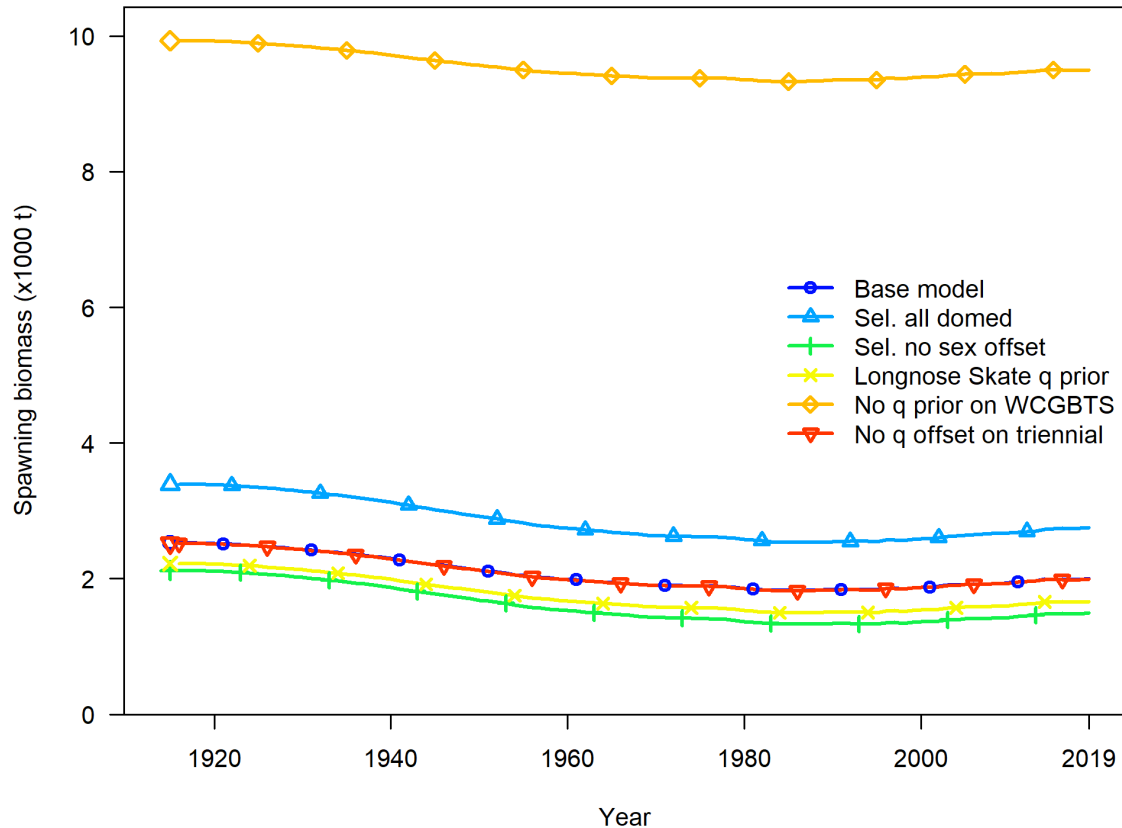


Figure 45: Time series of spawning biomass (mt) estimated in sensitivity analyses related to selectivity and catchability.

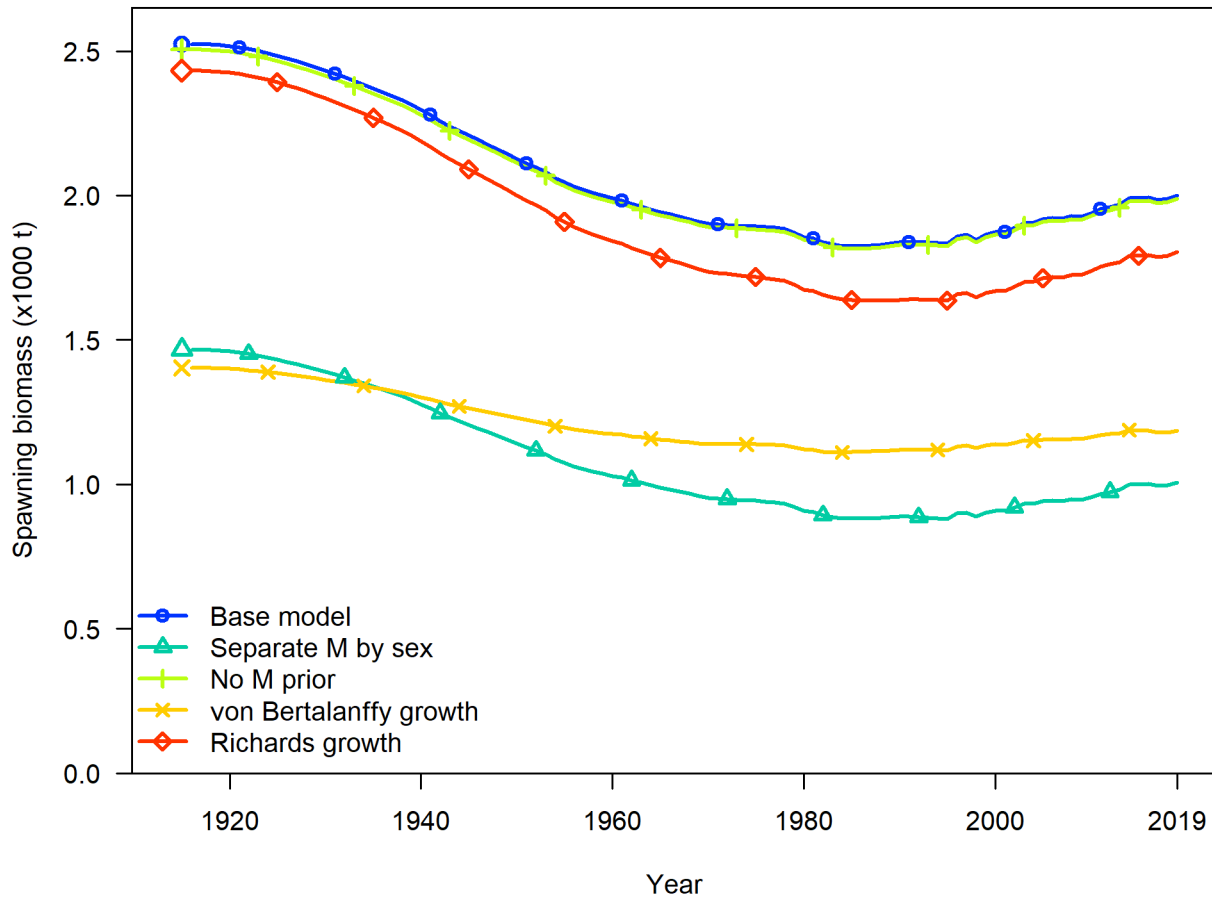


Figure 46: Time series of spawning biomass (mt) estimated in sensitivity analyses related to biology.

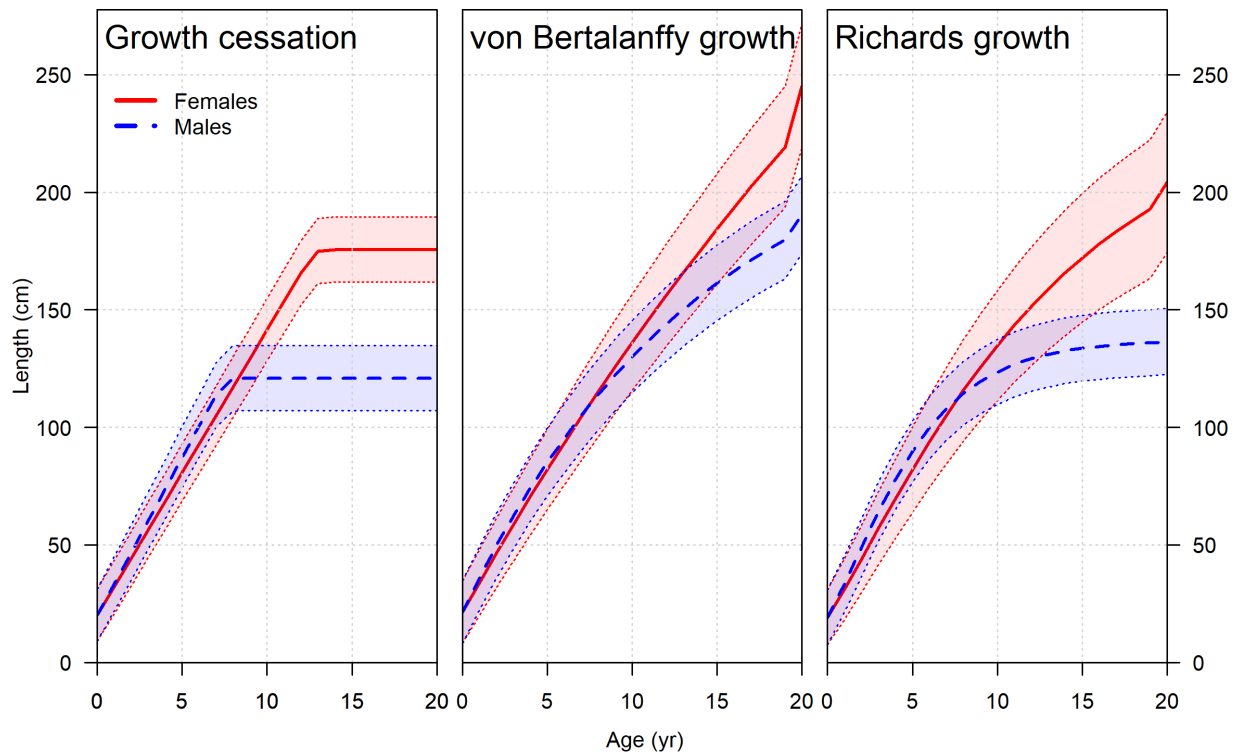


Figure 47: Comparison of the estimated growth curves from the sensitivities analyses. The increase at age 20 in the von Bertalanffy and Richards growth models is an adjustment to account for average size in the plus group based on an assumed exponential decay of the numbers at age beyond age 20.

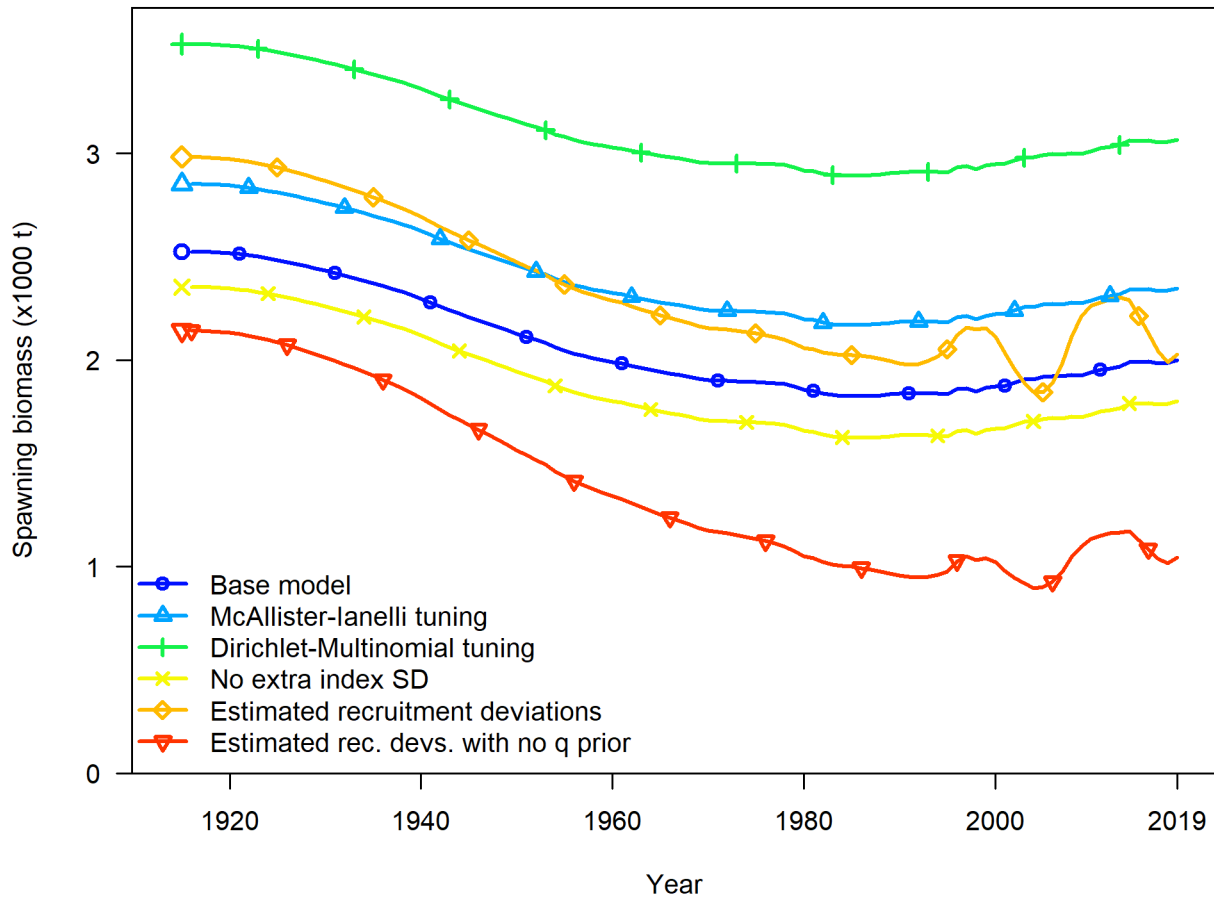


Figure 48: Time series of spawning biomass (mt) estimated in sensitivity analyses related to data weighting and recruitment.

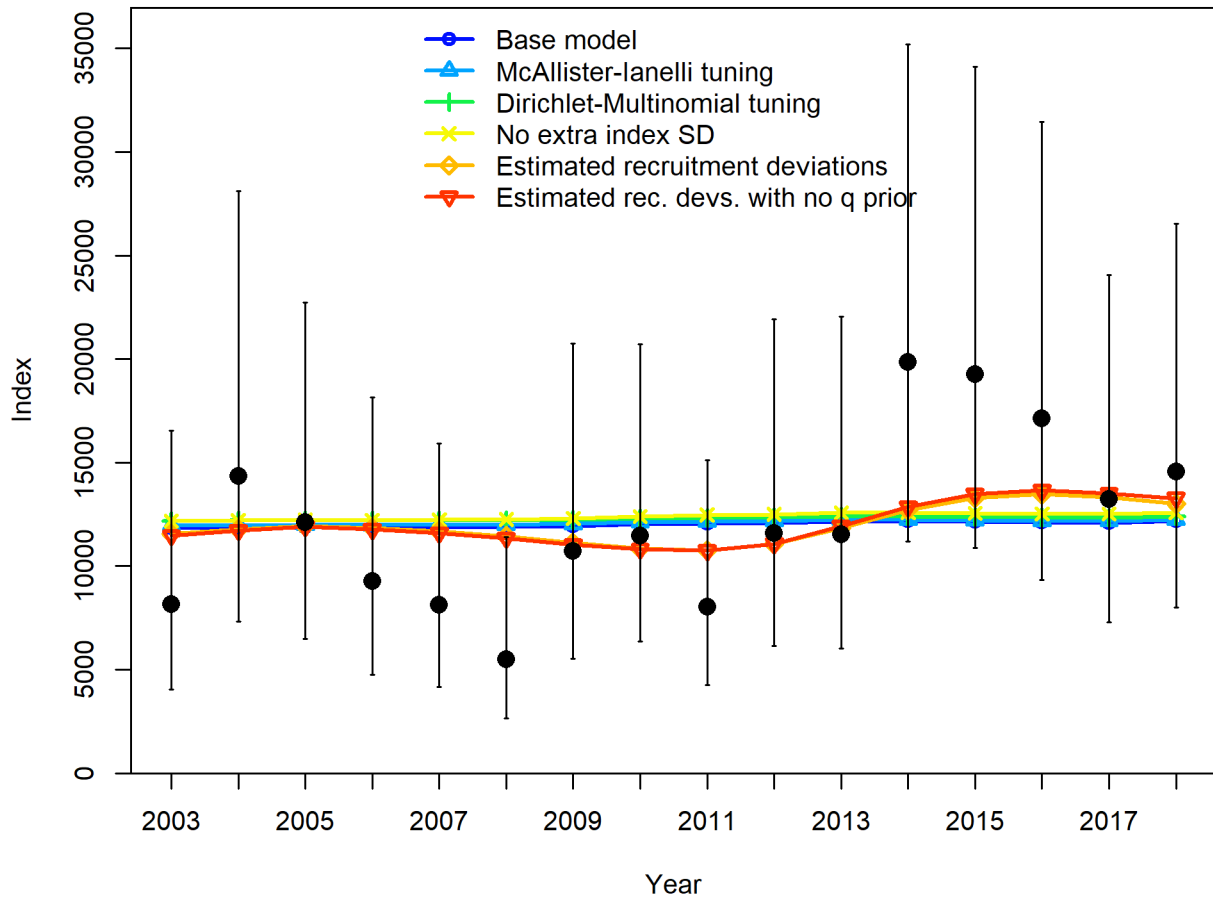


Figure 49: Fit to the WCGBT Survey estimated in the sensitivity analyses related to data weighting and recruitment.

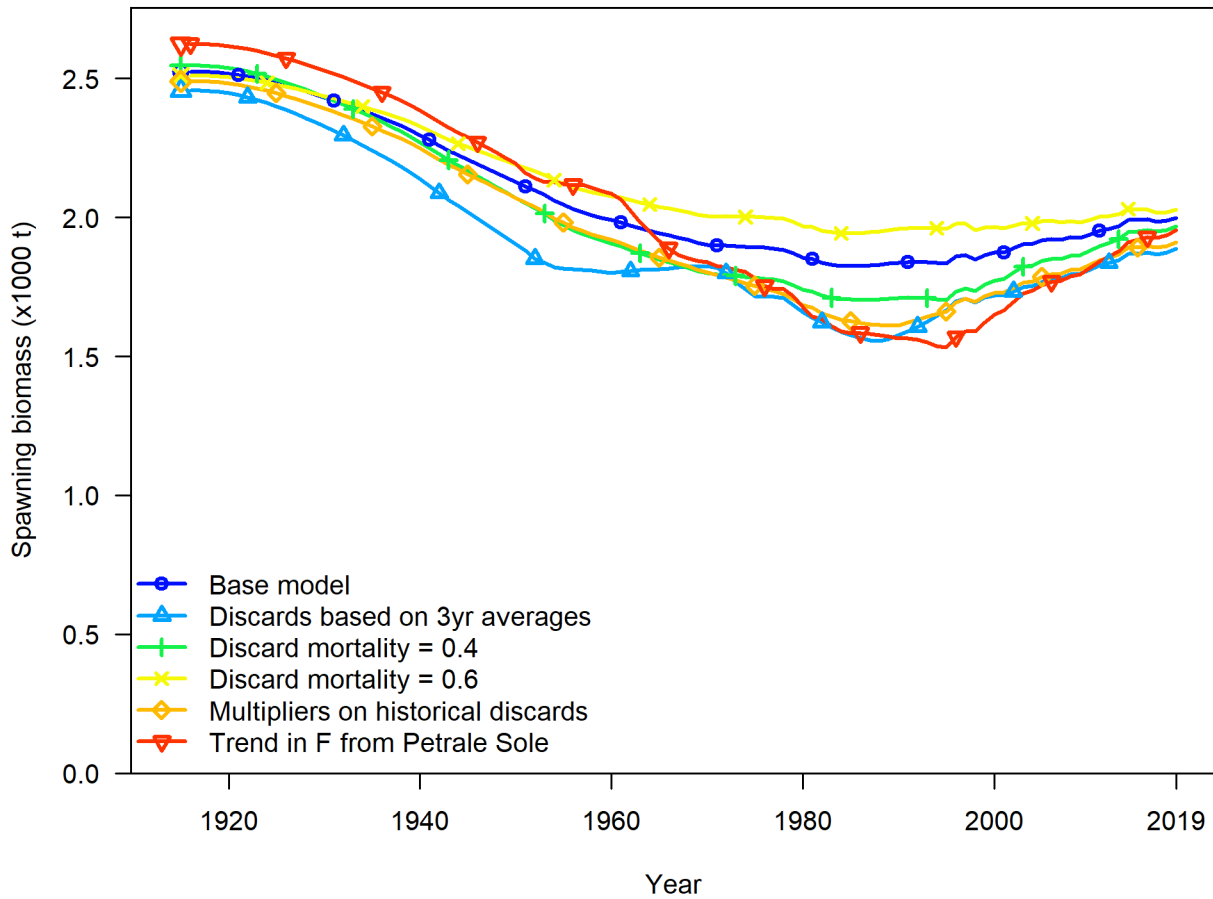


Figure 50: Time series of spawning biomass (mt) estimated in sensitivity analyses related to historic catch and discards.

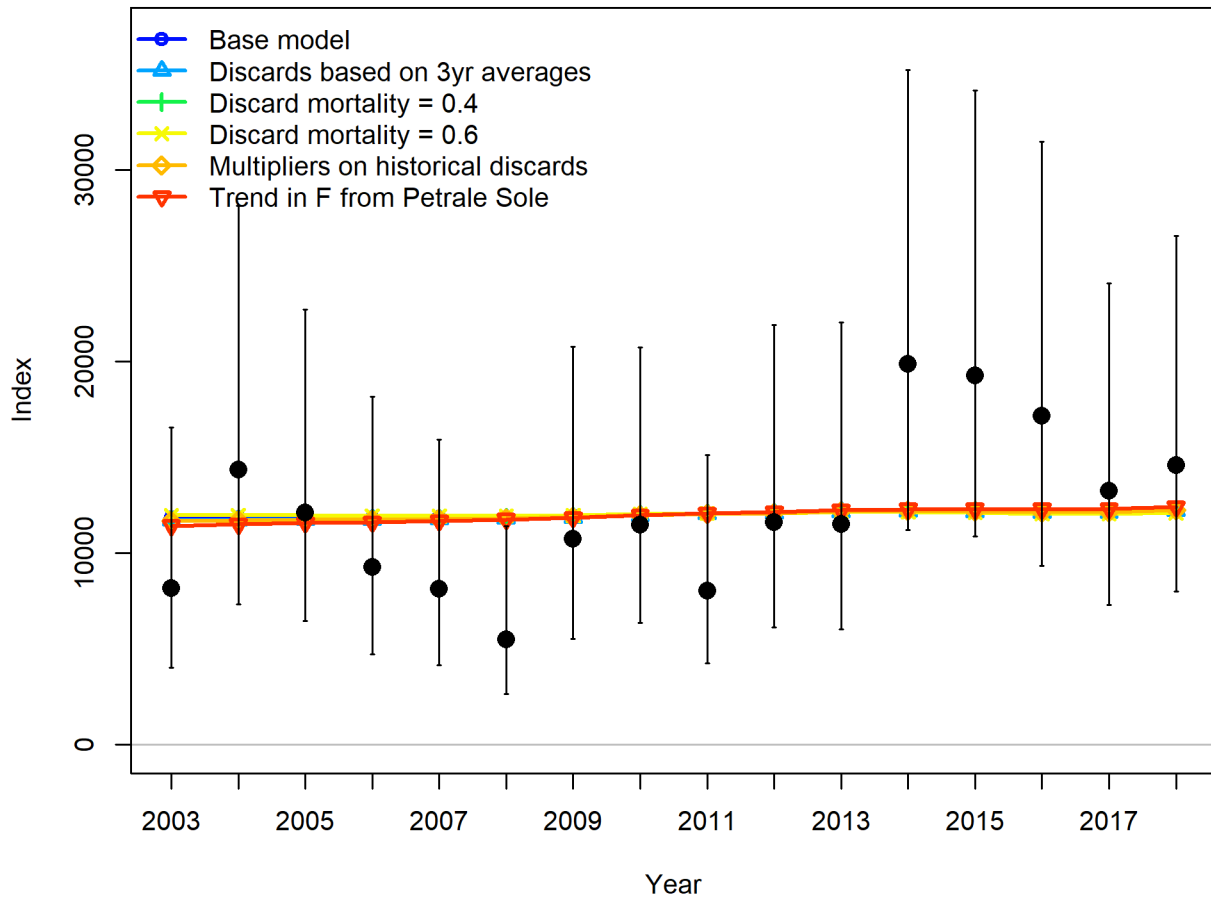


Figure 51: Fit to the WCGBT Survey estimated in the sensitivity analyses related to historic catch and discards.

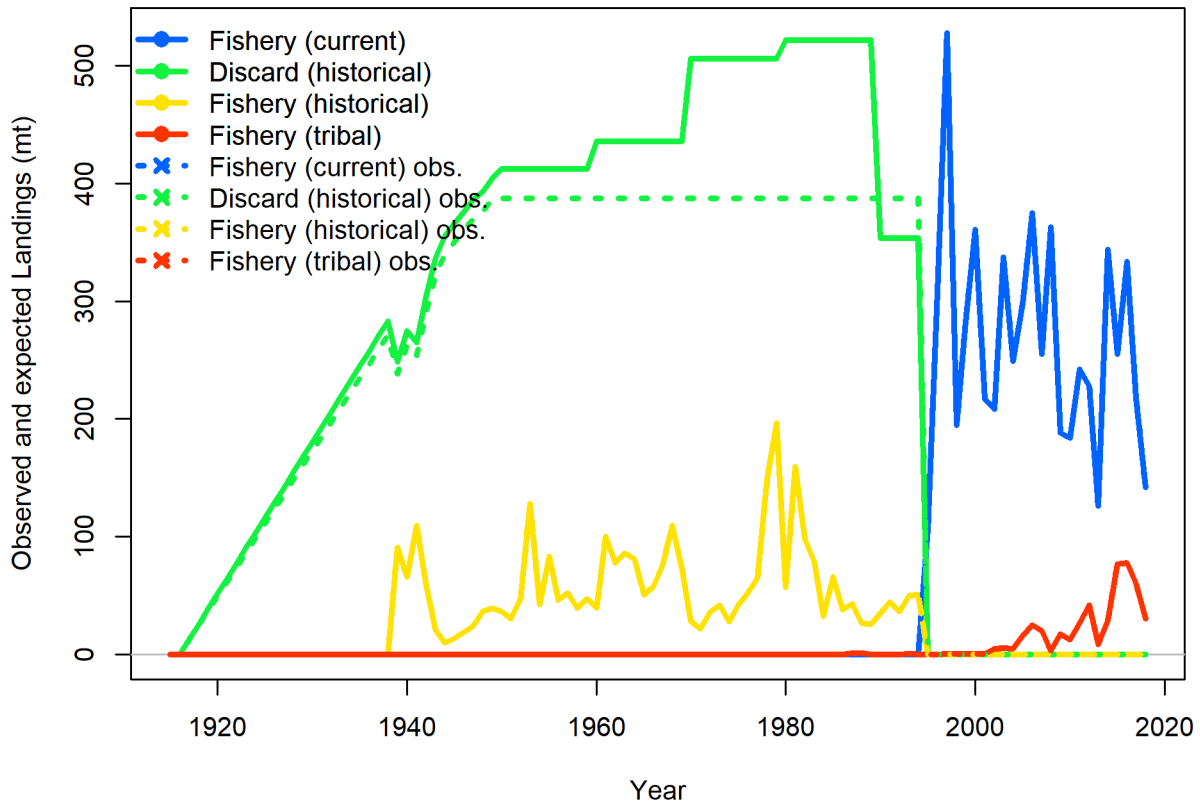


Figure 52: Catch by category for the sensitivity analysis where multipliers on historical discards were estimated. The estimated time series including the multipliers is shown in the solid green line and the input values in the base model are shown in the dashed green line.

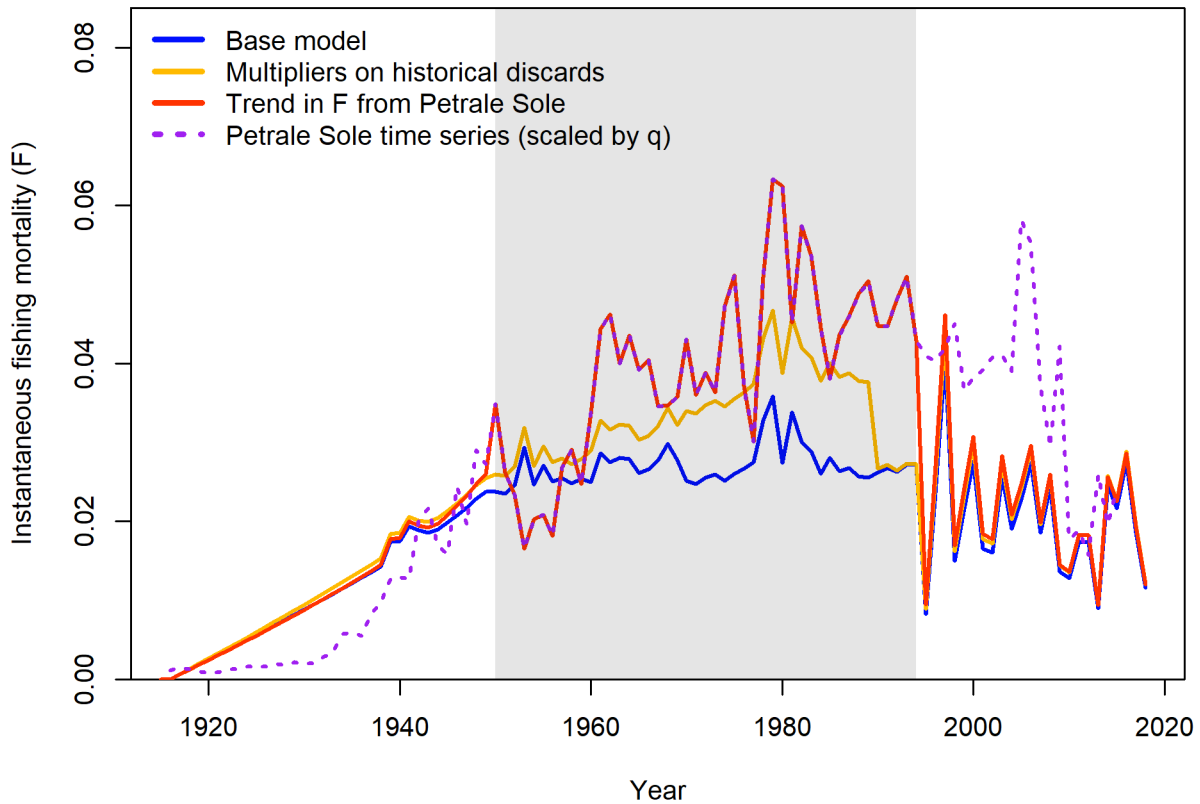


Figure 53: Comparison of the instantaneous rate of fishing mortality for fully selected ages for the base model and the sensitivity analyses where historic catch was adjusted either by the estimated multipliers or to match the time series of F for Petrale Sole. The Petrale Sole time series is shown for comparison, where the F for Petrale divided by 2.54 to match the estimated Big Skate F . The 1950–1994 period in which the Big Skate F was fit to the Petrale F is shaded in gray.

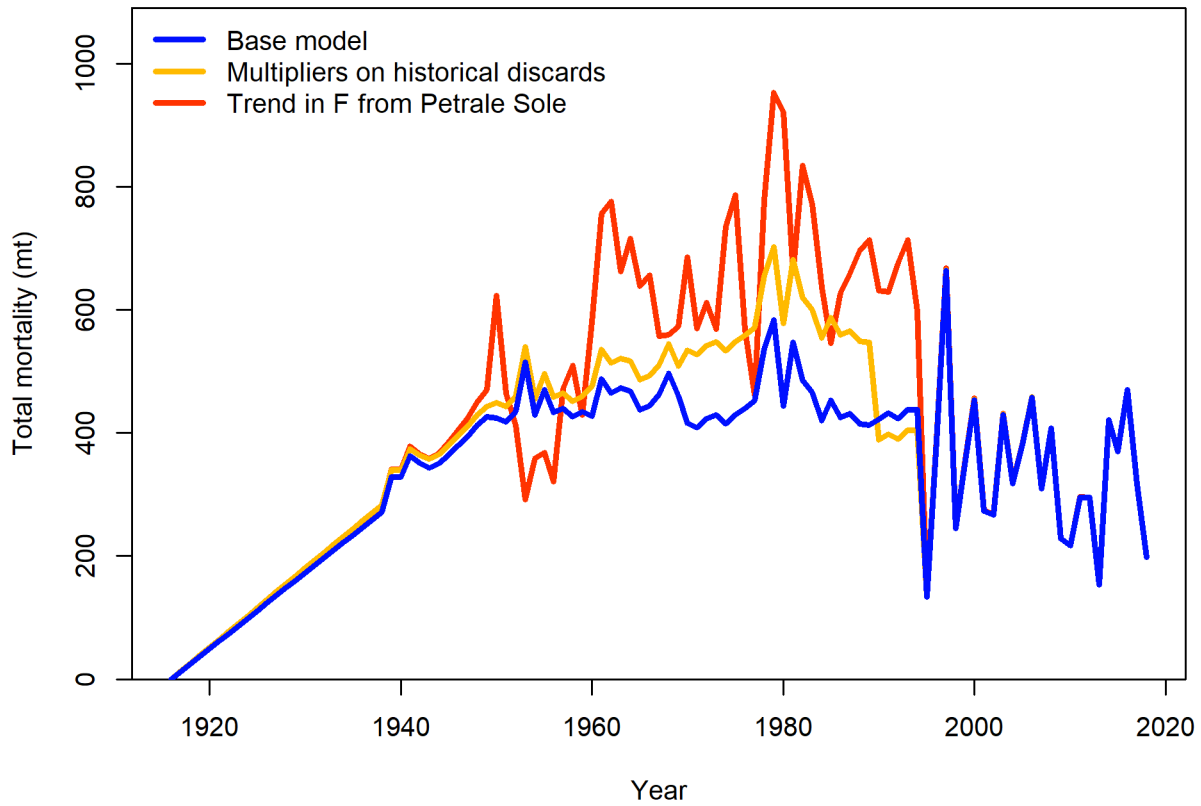


Figure 54: Comparison of total mortality for the base model and the sensitivity analyses where historic catch was adjusted either by the estimated multipliers or to match the time series of F for Petrale Sole. Total mortality shown here includes discards with the discard rate applied.

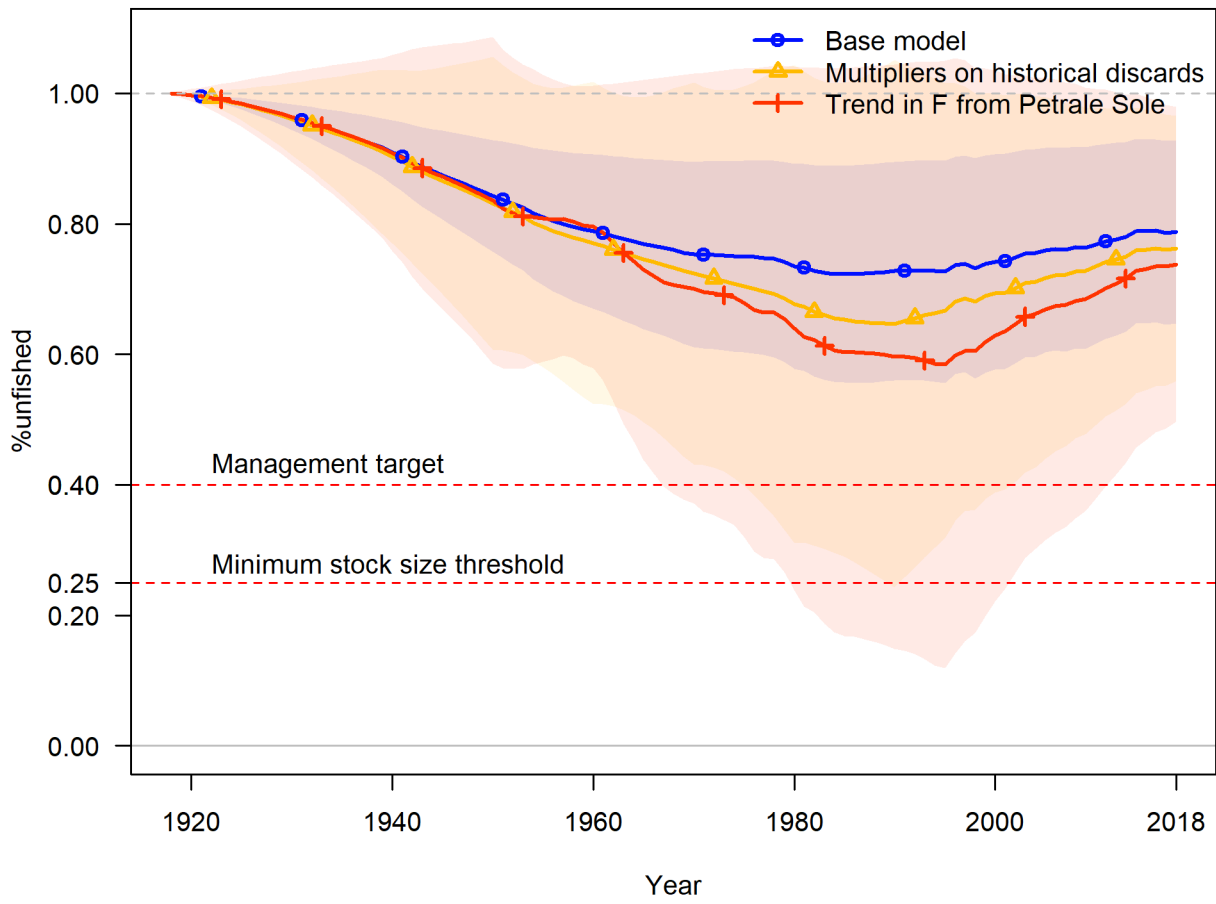


Figure 55: Time series of fraction unfished with approximate 95% asymptotic intervals estimated for the base model and the sensitivity analyses where historic catch was adjusted either by the estimated multipliers or to match the time series of F for Petrale Sole.

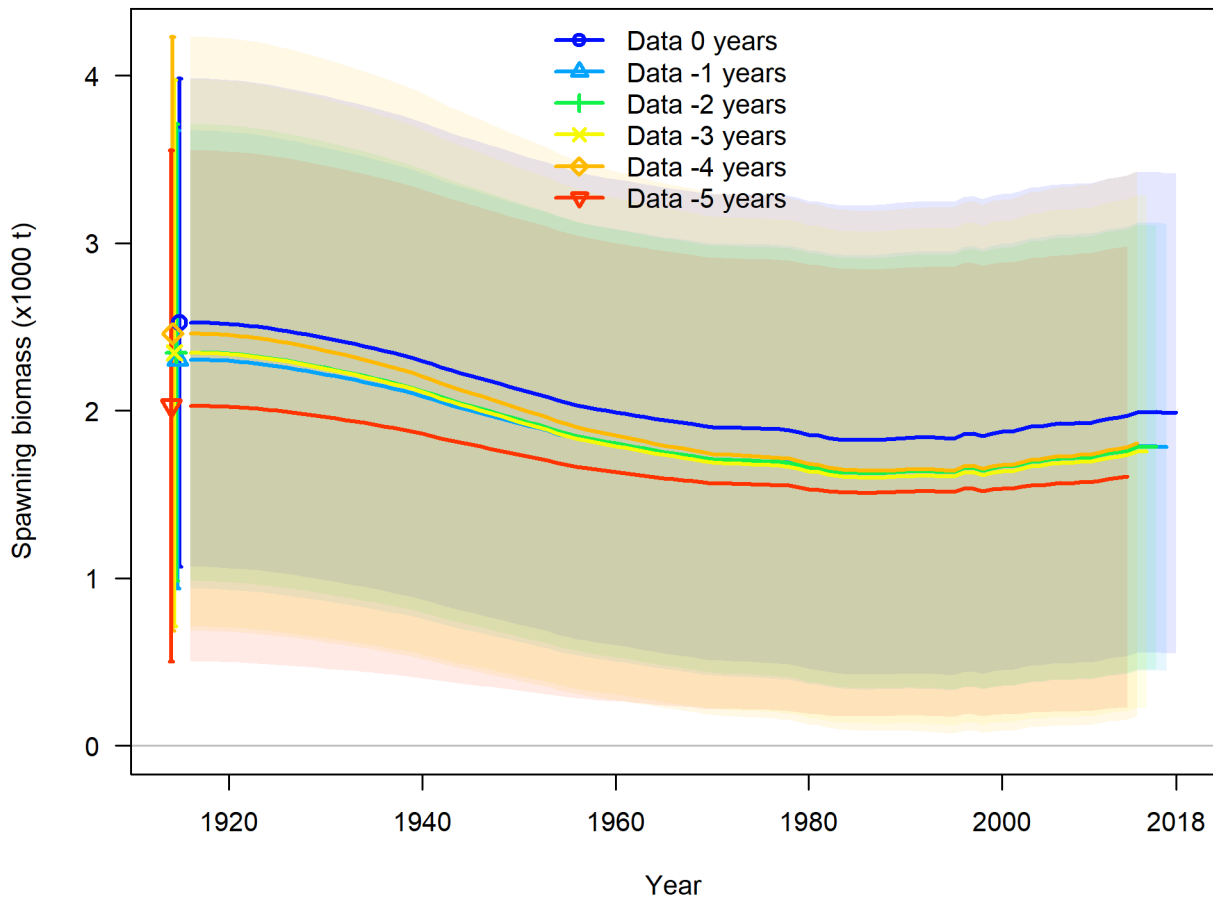


Figure 56: Time series of spawning biomass (mt) with approximate 95% asymptotic intervals estimated in retrospective analyses in which the final 5 years of data are successively removed from the model.

12.3.5 Likelihood Profiles

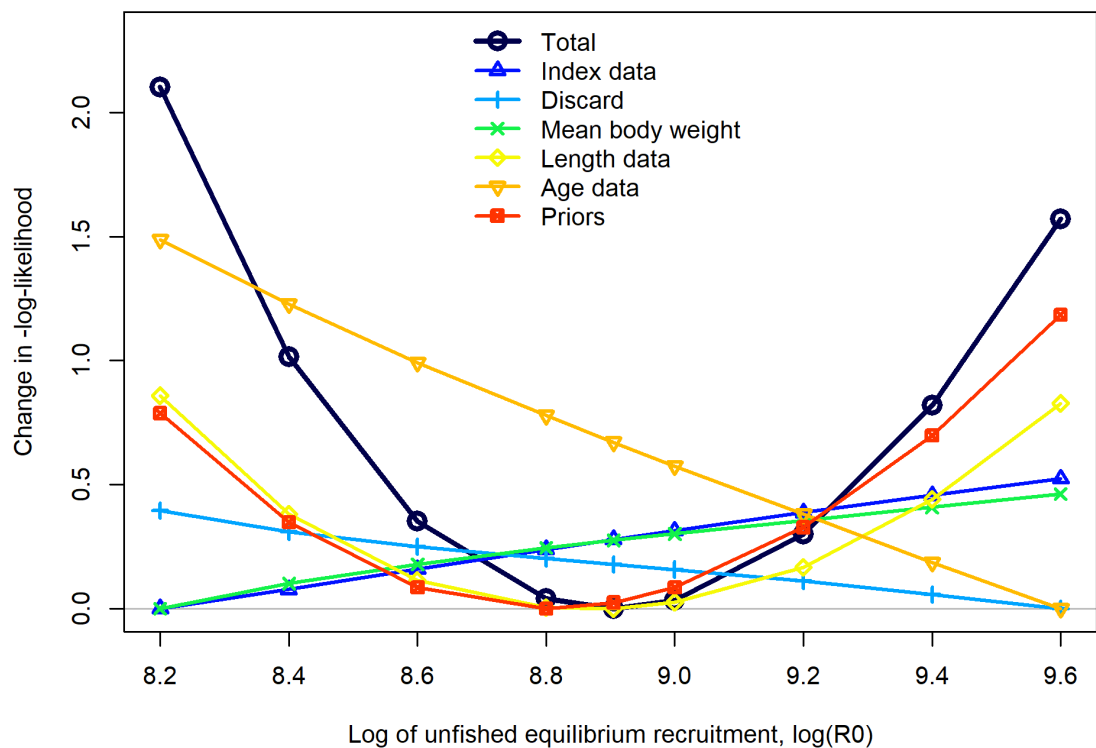


Figure 57: Likelihood profile over the log of equilibrium recruitment (R_0).

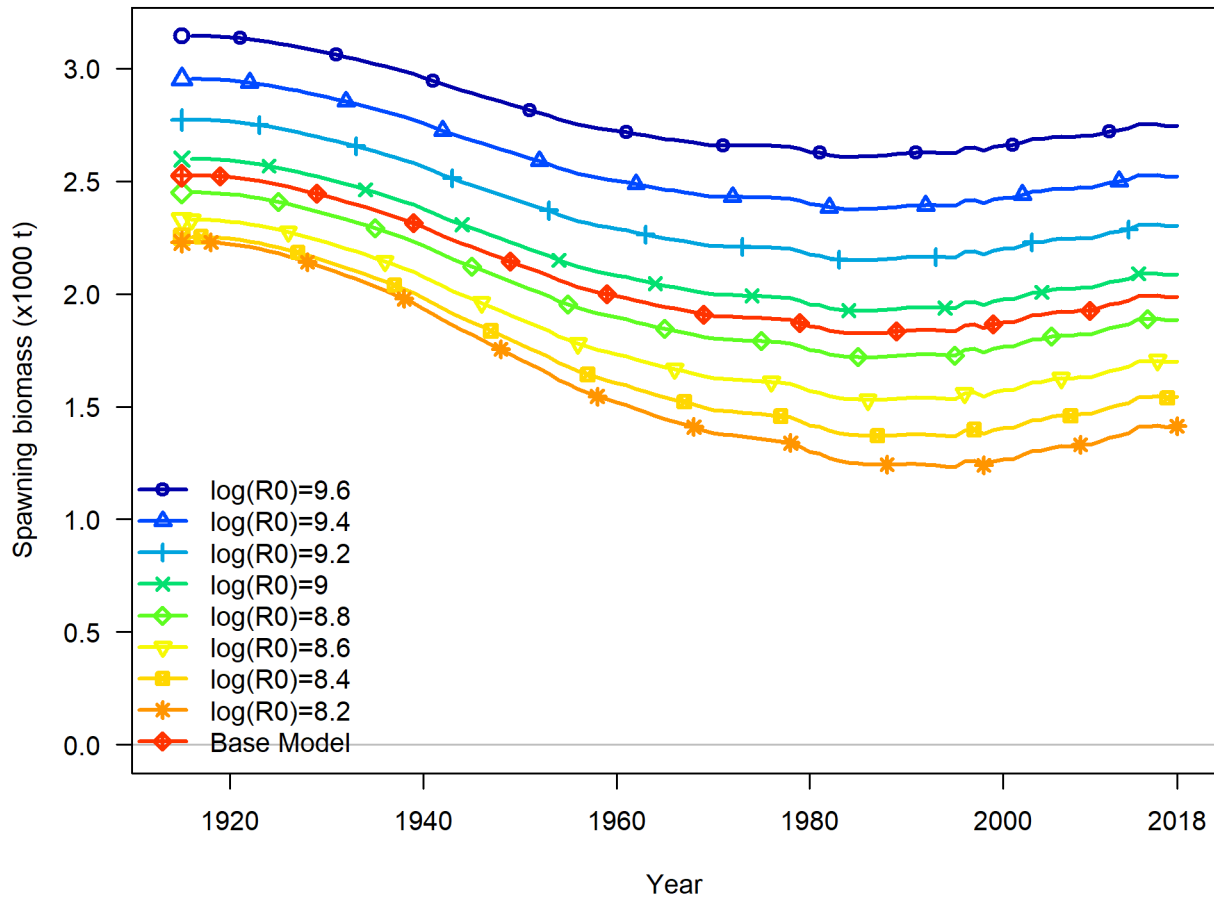


Figure 58: Time series of spawning biomass (mt) estimated for the models included in the profile over the log of equilibrium recruitment (R_0).

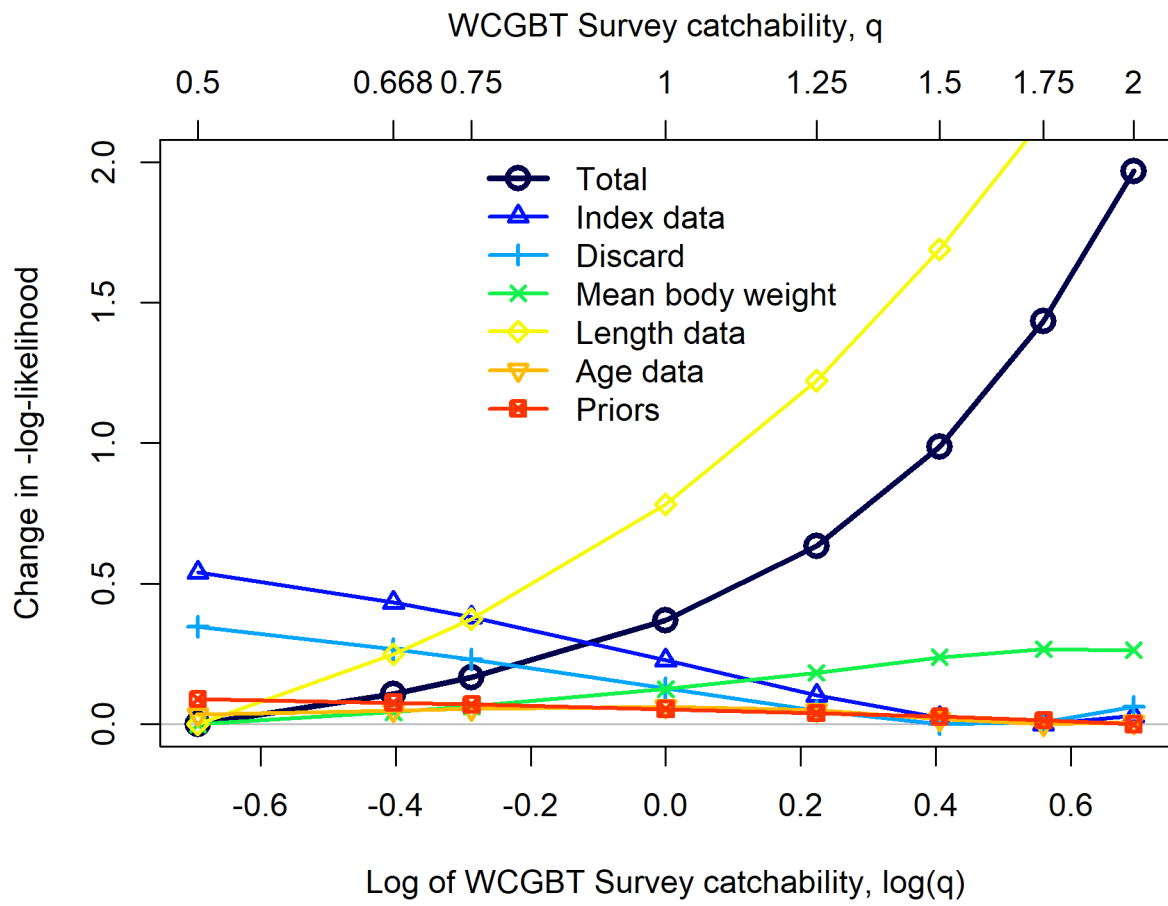


Figure 59: Likelihood profile over the catchability of the WCGBT survey (q) without the addition of the prior likelihood for q (the prior on natural mortality remains).

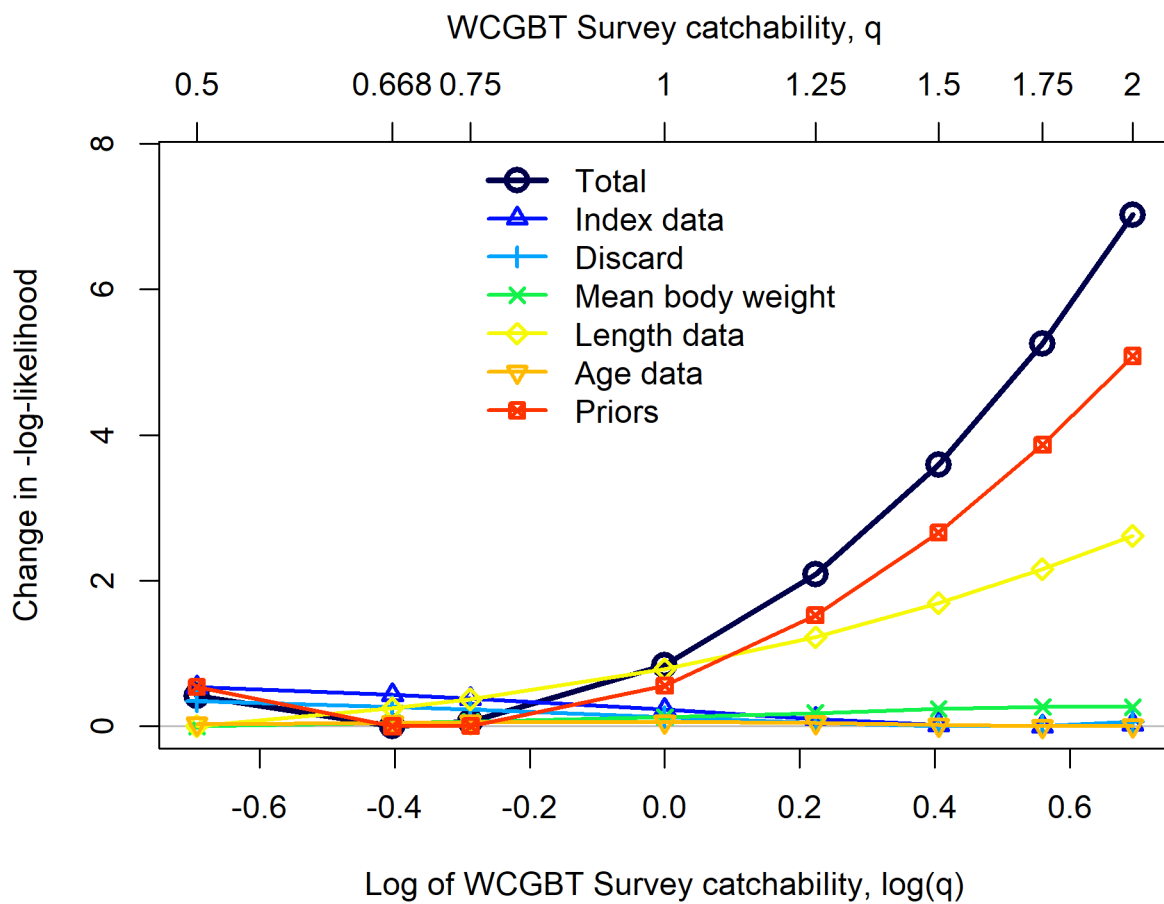


Figure 60: Likelihood profile over the catchability of the WCGBT survey (q) including the prior likelihood contribution.

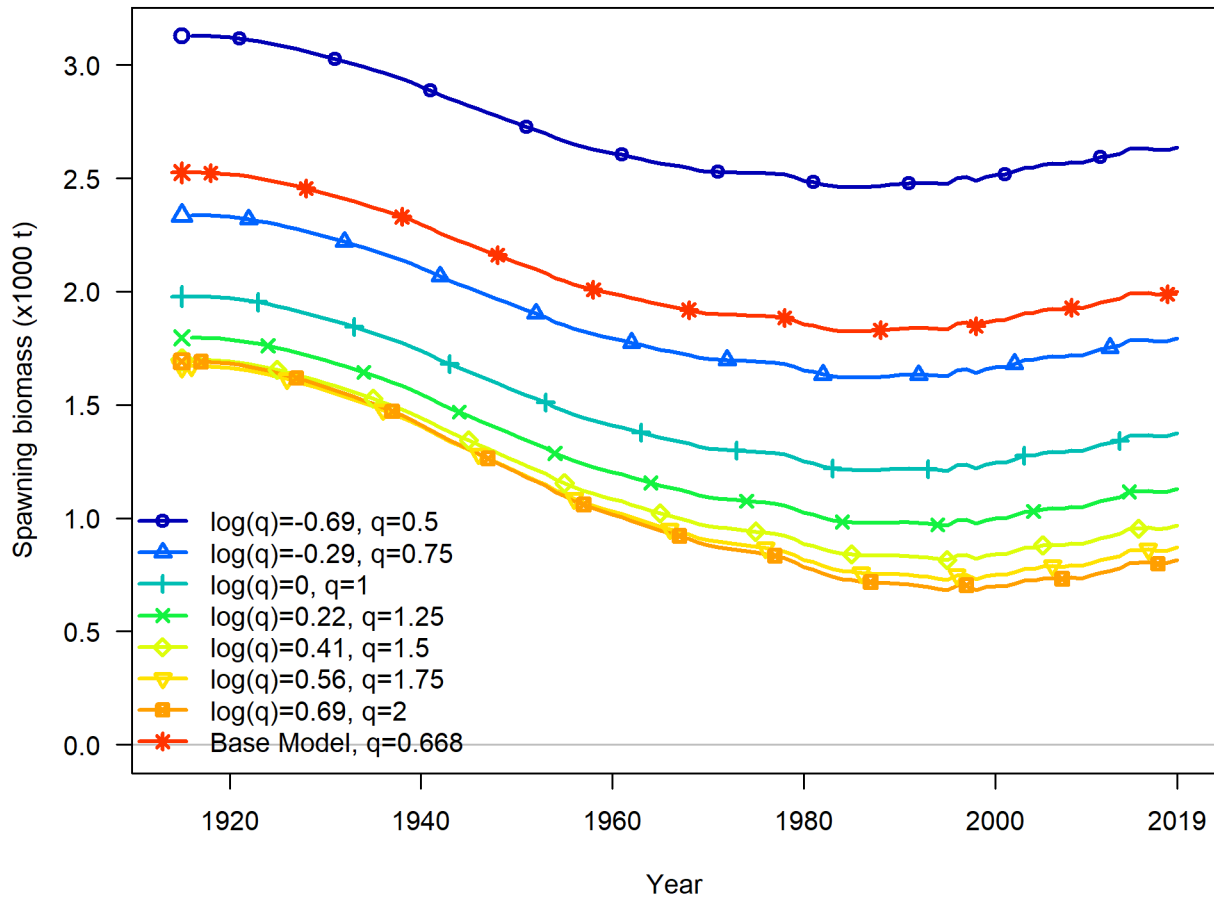


Figure 61: Time series of spawning biomass (mt) estimated for the models included in the profile over the catchability of the WCGBT Survey (q).

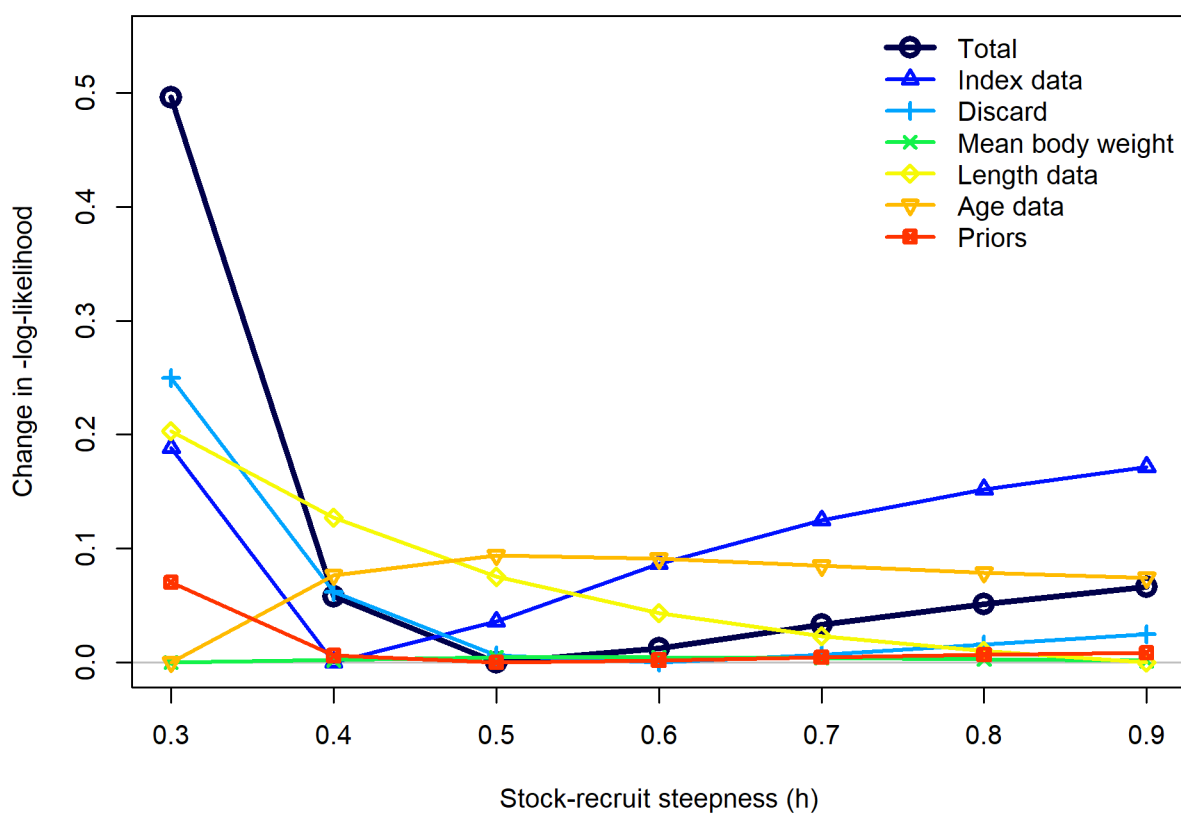


Figure 62: Likelihood profile over stock-recruit steepness (h).

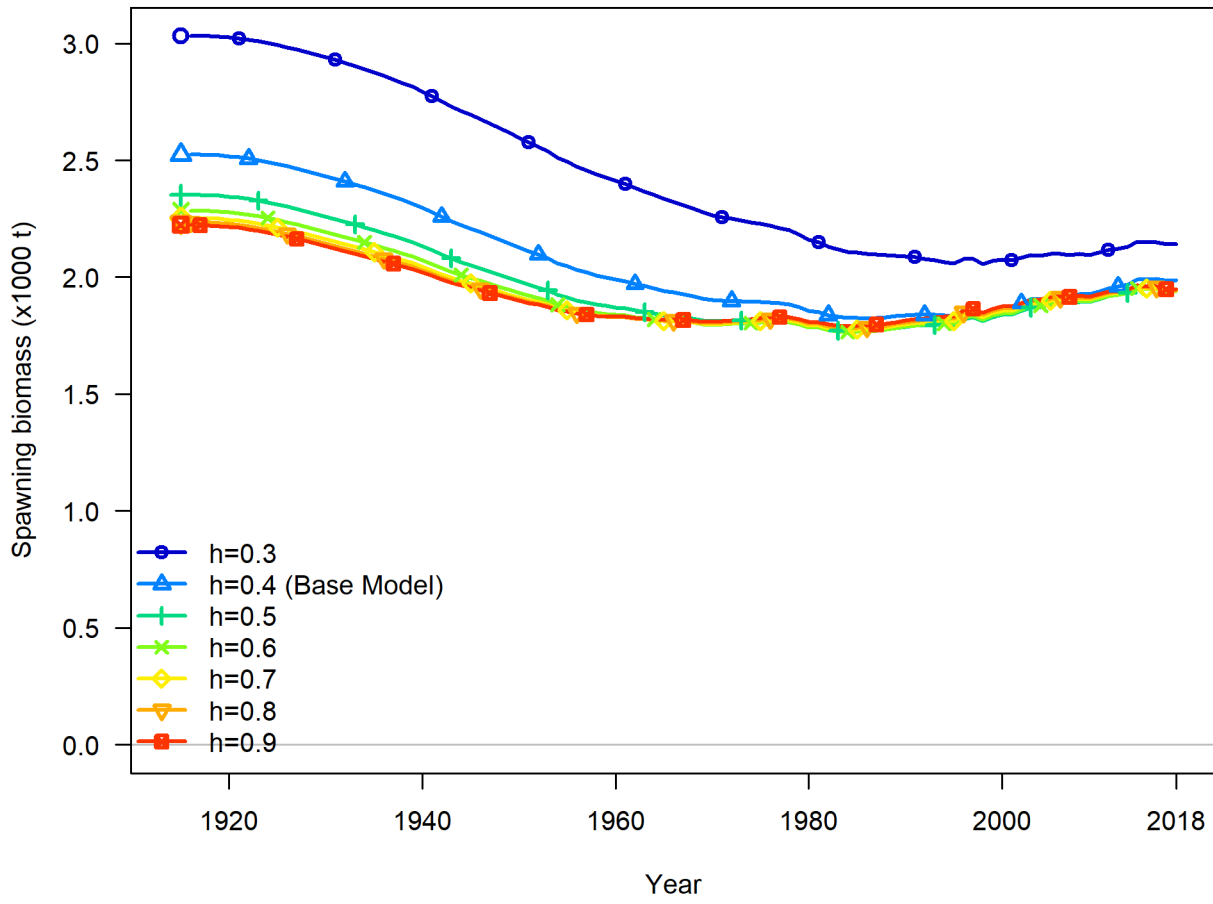


Figure 63: Time series of spawning biomass (mt) estimated for the models included in the profile over stock-recruit steepness (h).

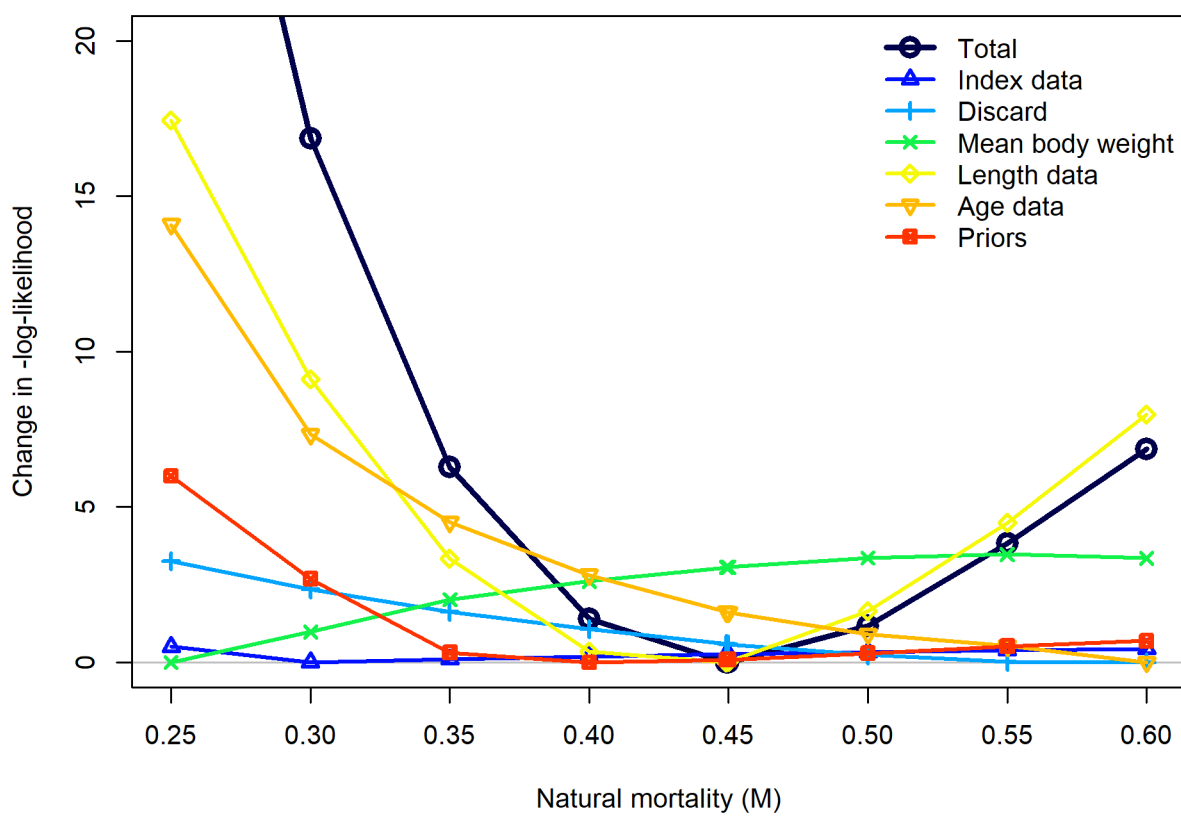


Figure 64: Likelihood profile over natural mortality (M).

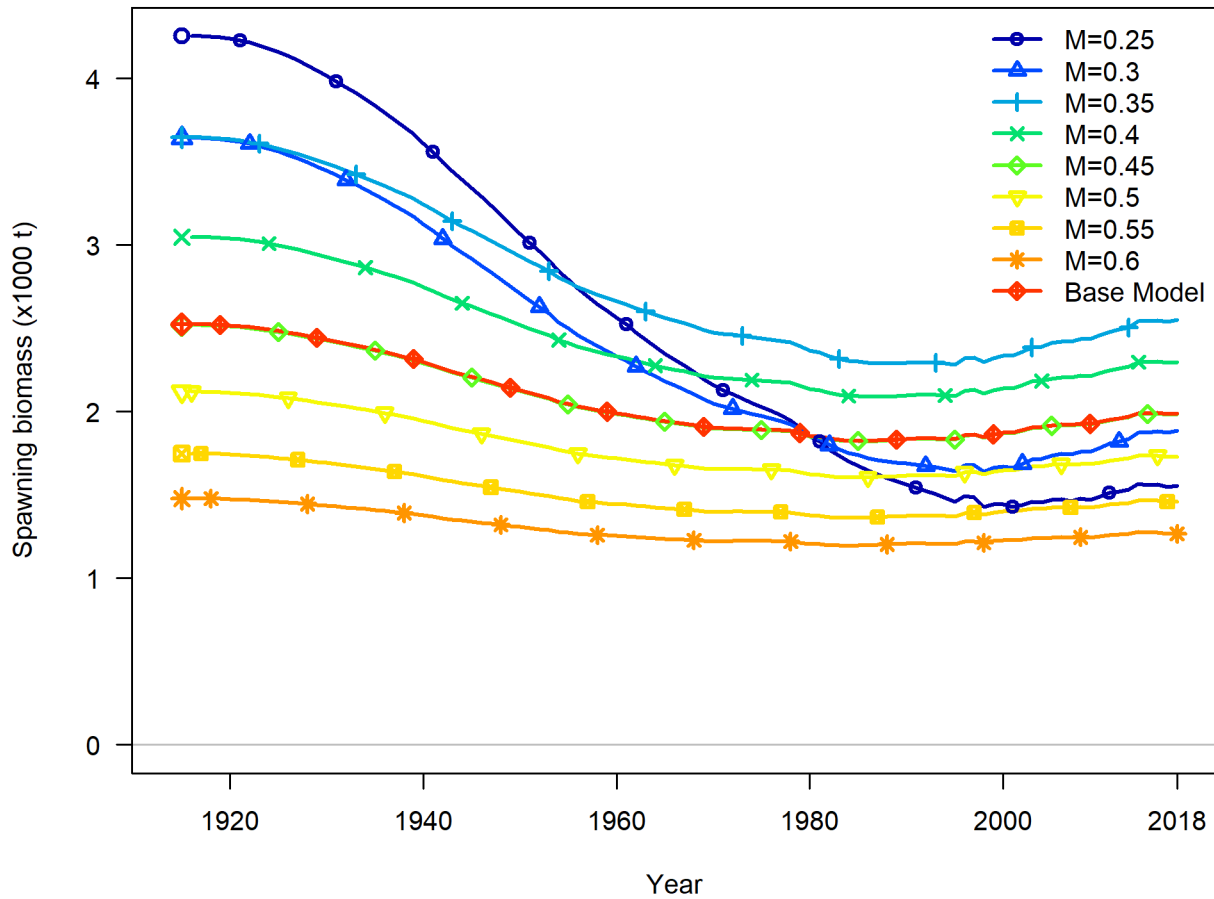


Figure 65: Time series of spawning biomass (mt) estimated for the models included in the profile over natural mortality (M).

12.3.6 Reference Points and Forecasts

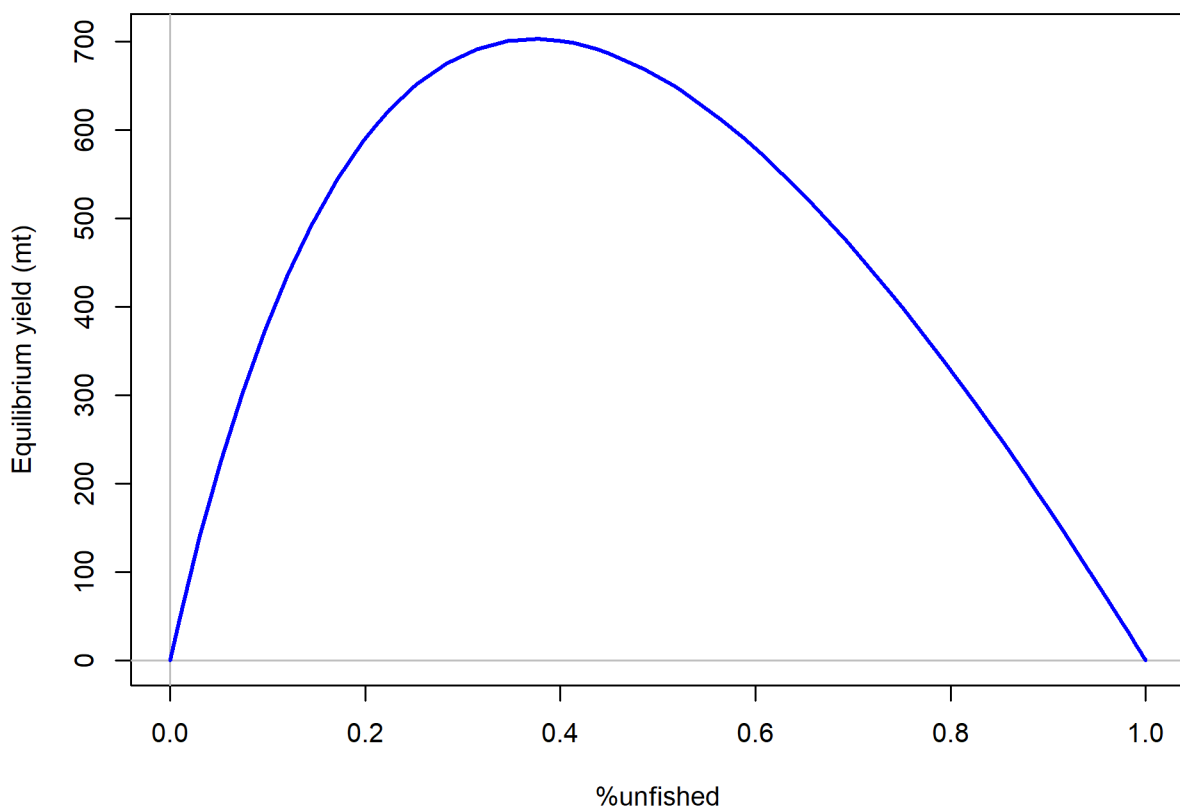


Figure 66: Equilibrium yield curve for the base case model. Values are based on the fishery selectivity and with steepness fixed at 0.4.

Appendix A. Detailed fits to length composition data

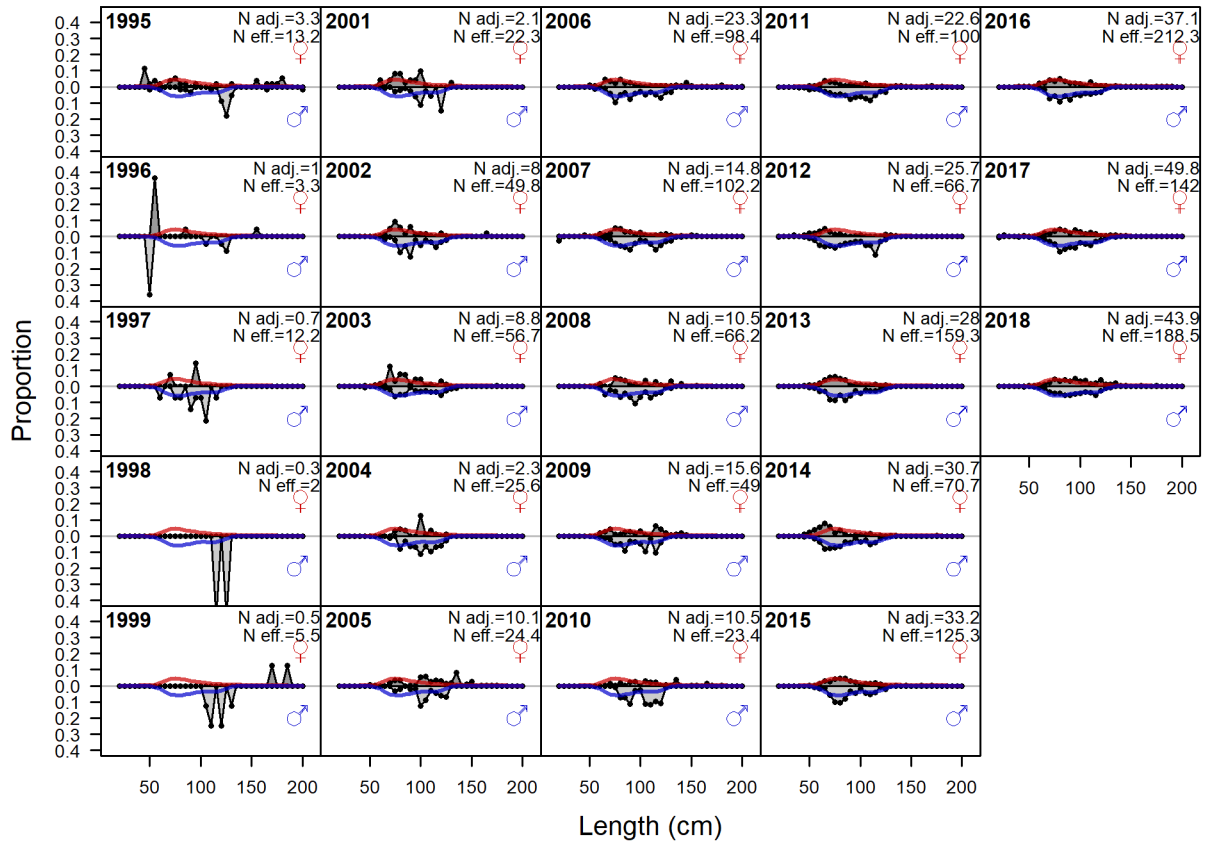


Figure A-1: Length comps, retained, Fishery. ‘N adj.’ is the input sample size after data weighting adjustment. N eff. is the calculated effective sample size used in the McAllister Iannelli tuning method.

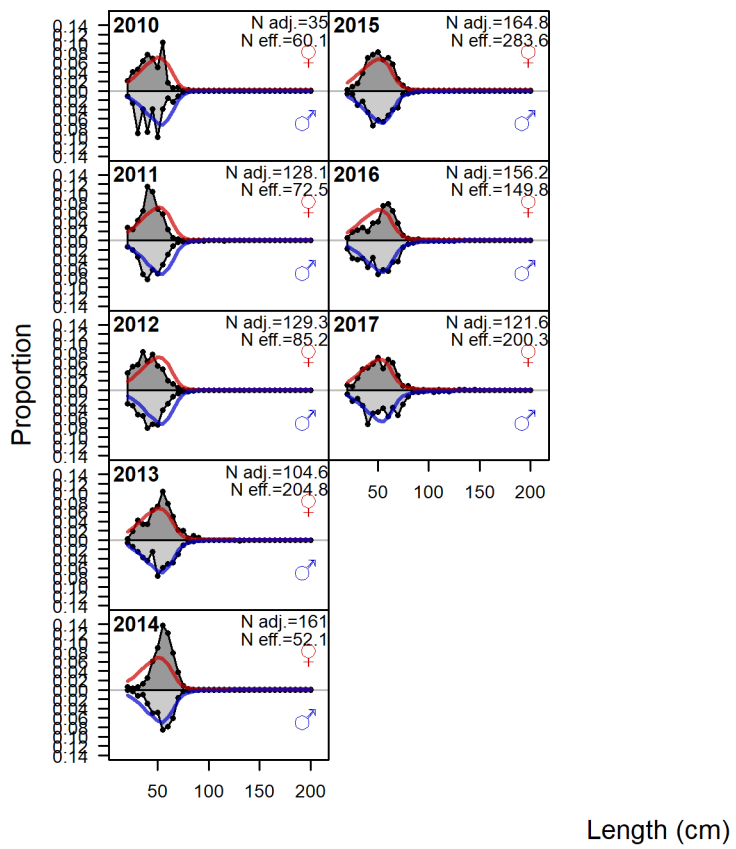


Figure A-2: Length comps, discard, Fishery. ‘N adj.’ is the input sample size after data_weighting adjustment. N eff. is the calculated effective sample size used in the McAlister_Iannelli tuning method.

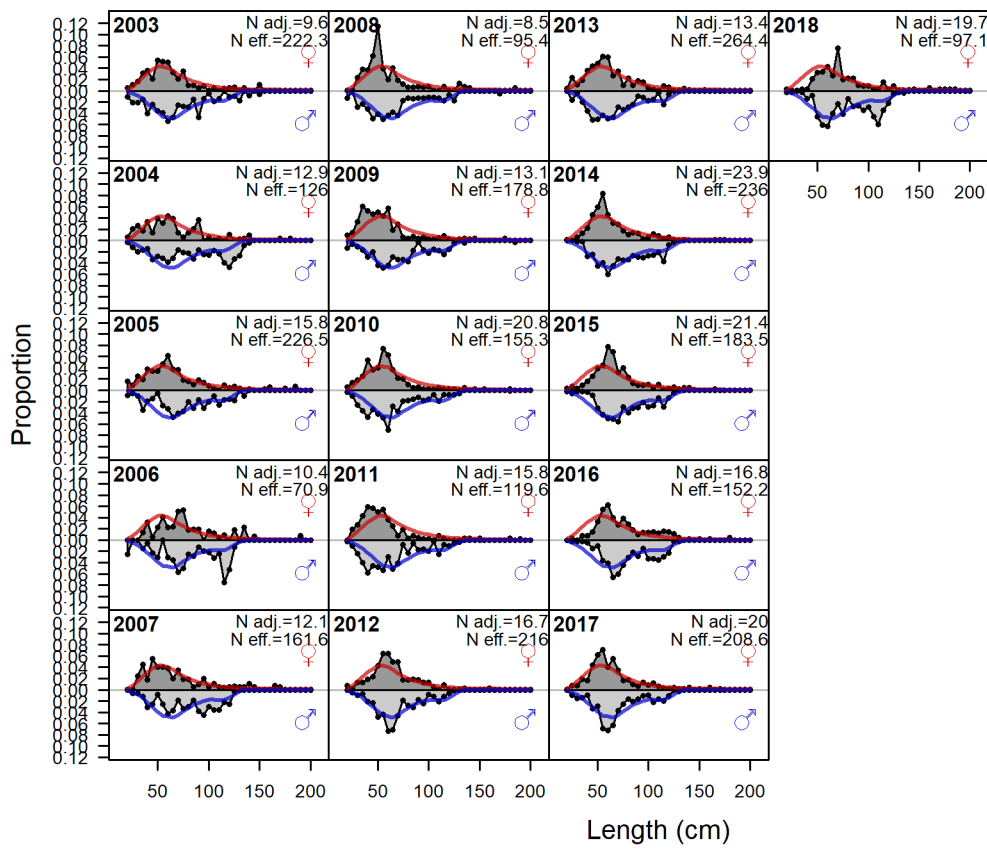


Figure A-3: Length comps, whole catch, WCGBT Survey. ‘N adj.’ is the input sample size after data_weighting adjustment. N eff. is the calculated effective sample size used in the McAllister_Iannelli tuning method.

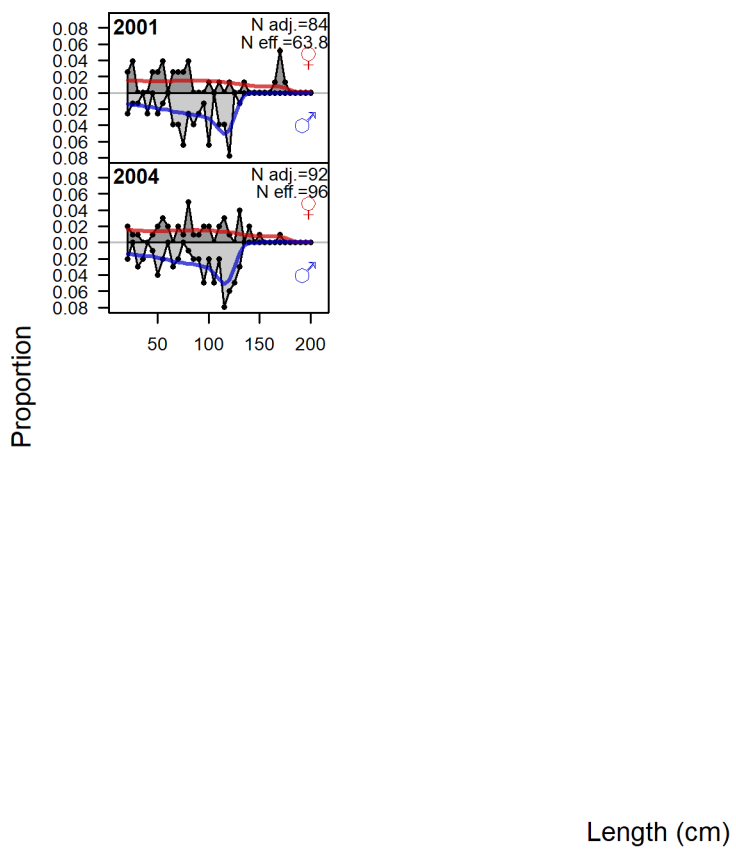


Figure A-4: Length comps, whole catch, Triennial Survey. 'N adj.' is the input sample size after data_weighting adjustment. N eff. is the calculated effective sample size used in the McAllister Iannelli tuning method.

Appendix B. Figures associated with responses to STAR Requests

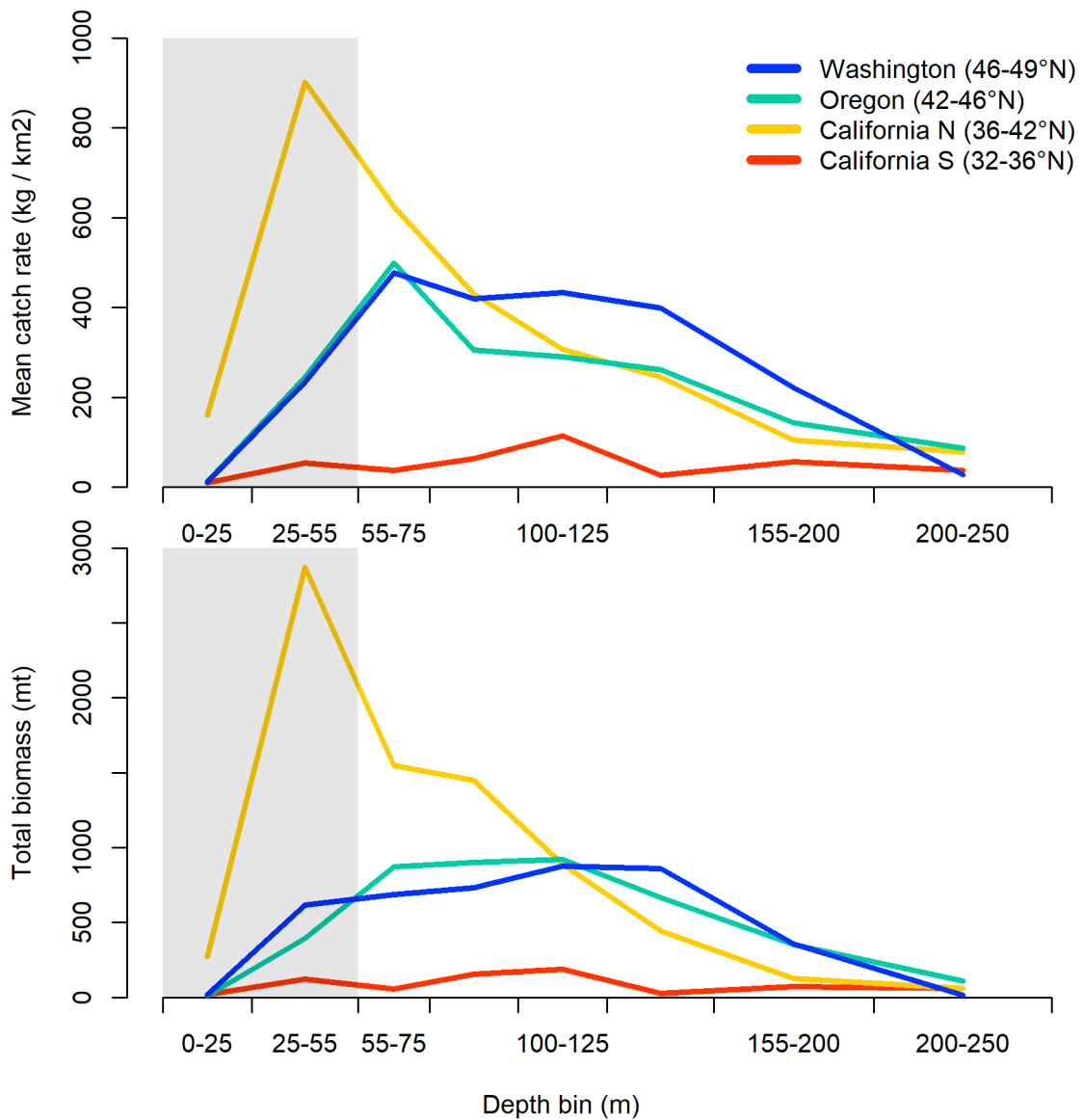


Figure B-1: Extrapolated catch rates (upper panel) and estimated biomass after adjustment for area of each bin (lower panel). The gray regions indicate those depths outside the survey range which were extrapolated based on catch rates from the commercial bottom trawl fishery. The extrapolated biomass is equal to 25.8% of the total biomass (extrapolated plus surveyed area).

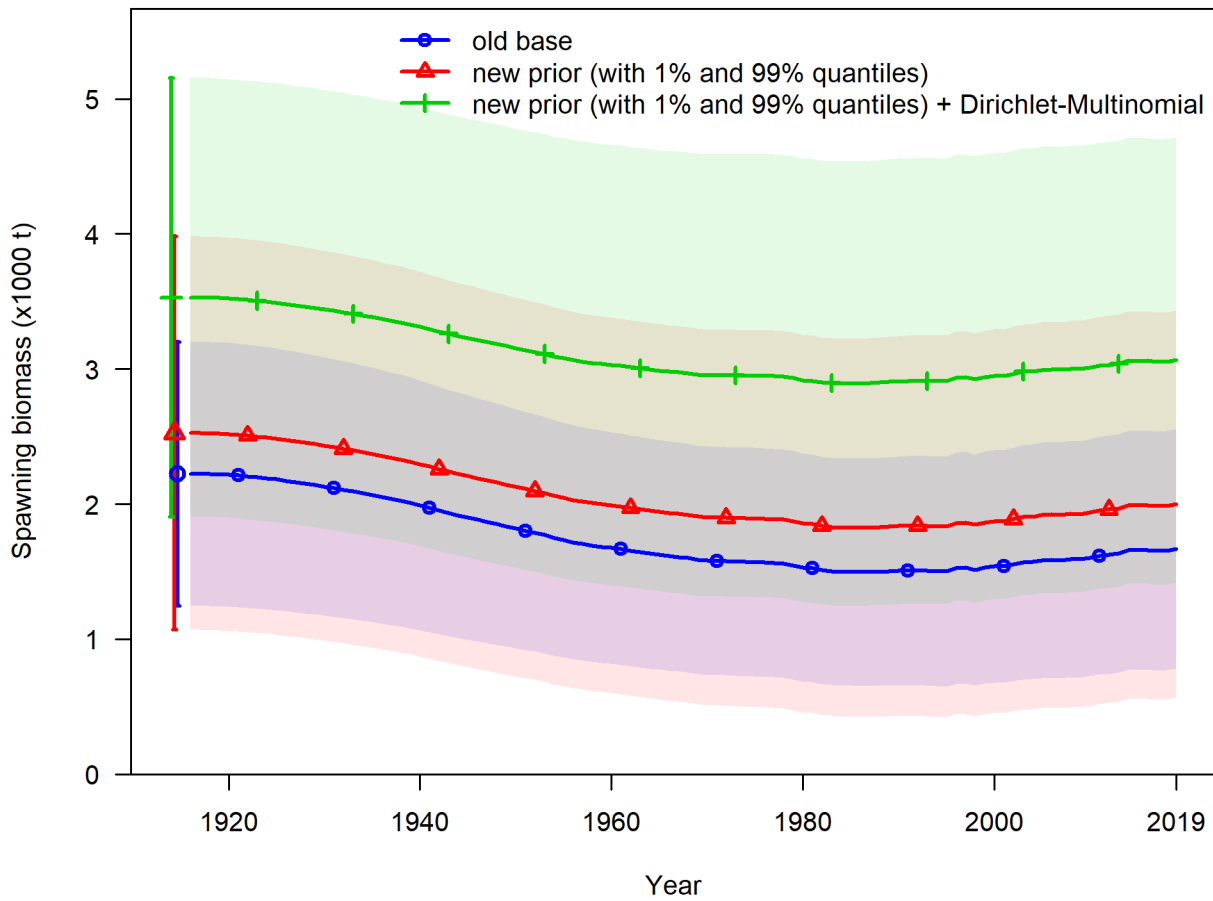


Figure B-2: Time series of spawning biomass with 95% uncertainty intervals for the pre-STAR (old) base model (blue) compared to two alternative models that used the revised catchability prior in combination with either the status-quo Francis data weighting (red) or the Dirichlet-Multinomial data weighting (green).

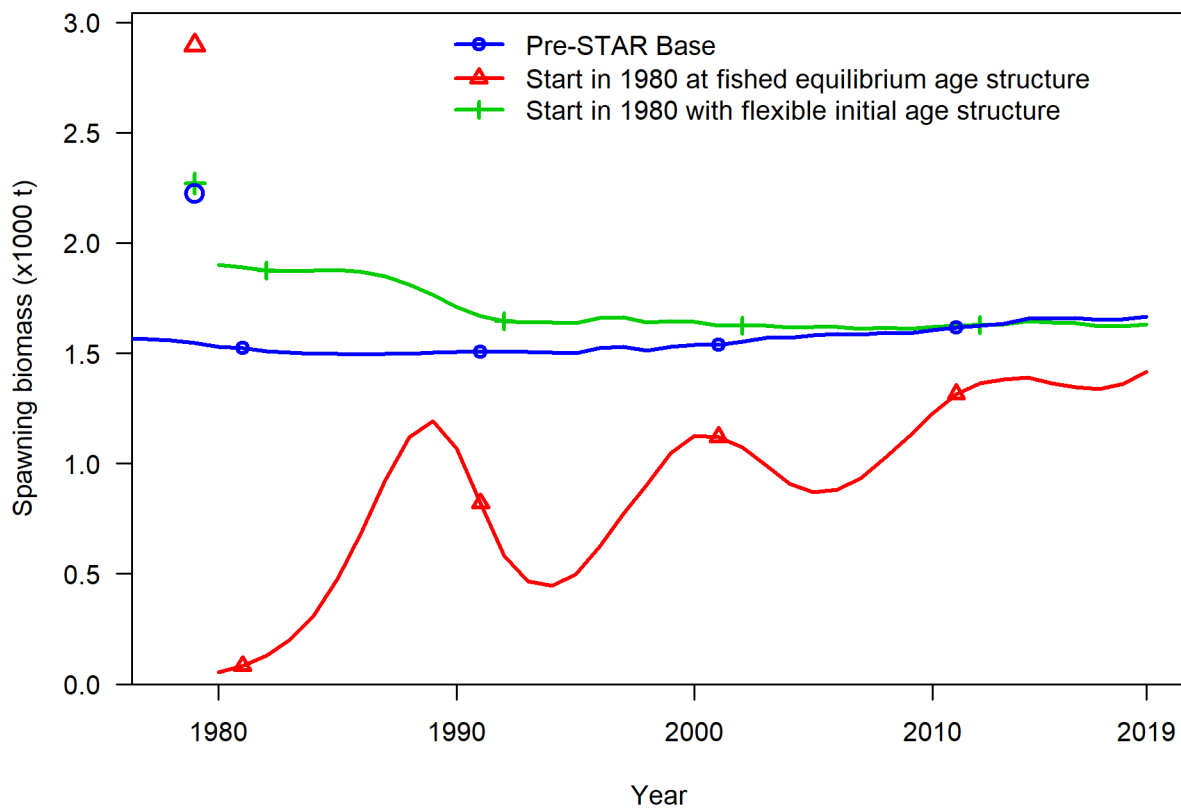


Figure B-3: Time series of spawning biomass for the pre-STAR base model compared to two alternative models that started in 1980 with either equilibrium or flexible initial age structure. Disconnected points prior to 1980 represent the unfished equilibrium in each case.

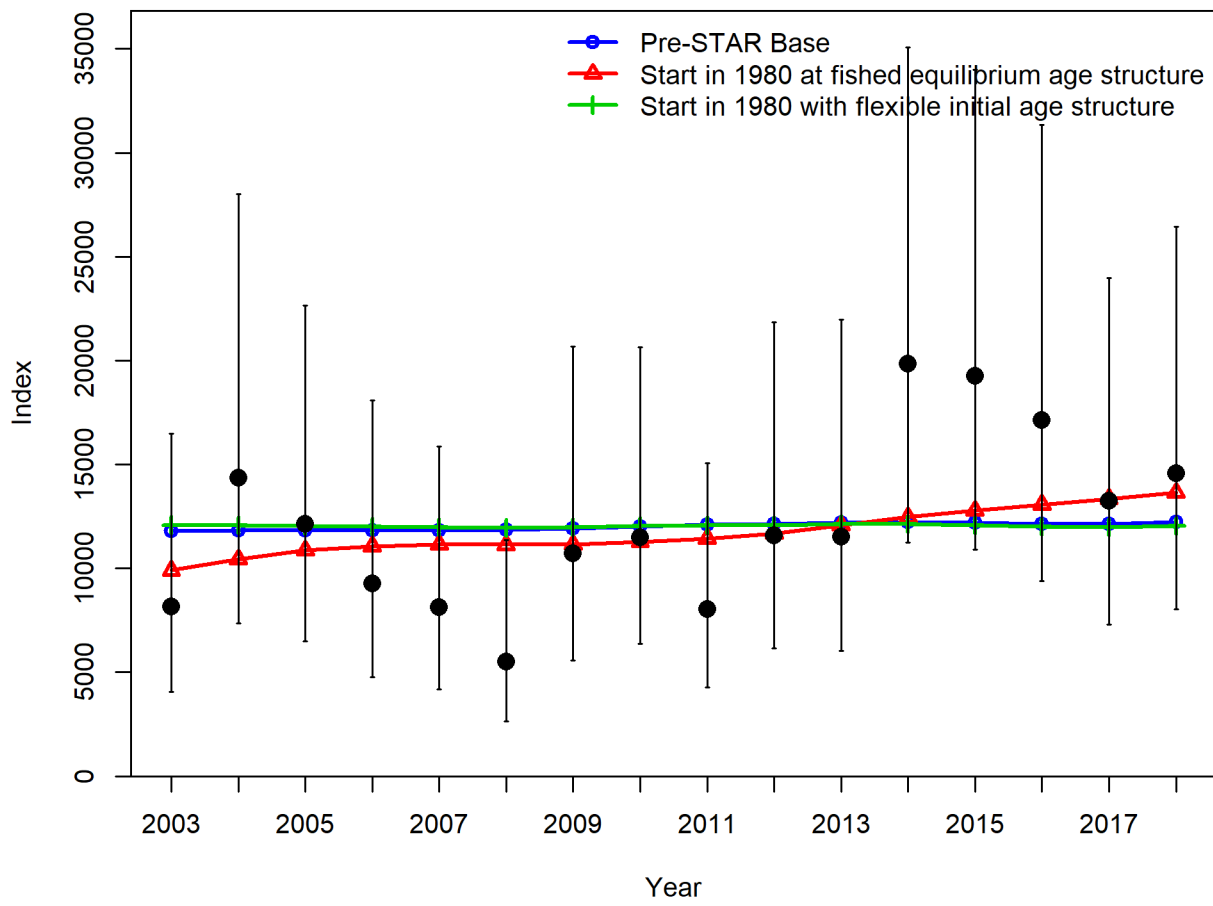


Figure B-4: Fit to WCGBT Survey index for the pre-STAR base model and the two alternative models that started in 1980. Uncertainty intervals include the extra standard deviation estimates from the pre-STAR base model.

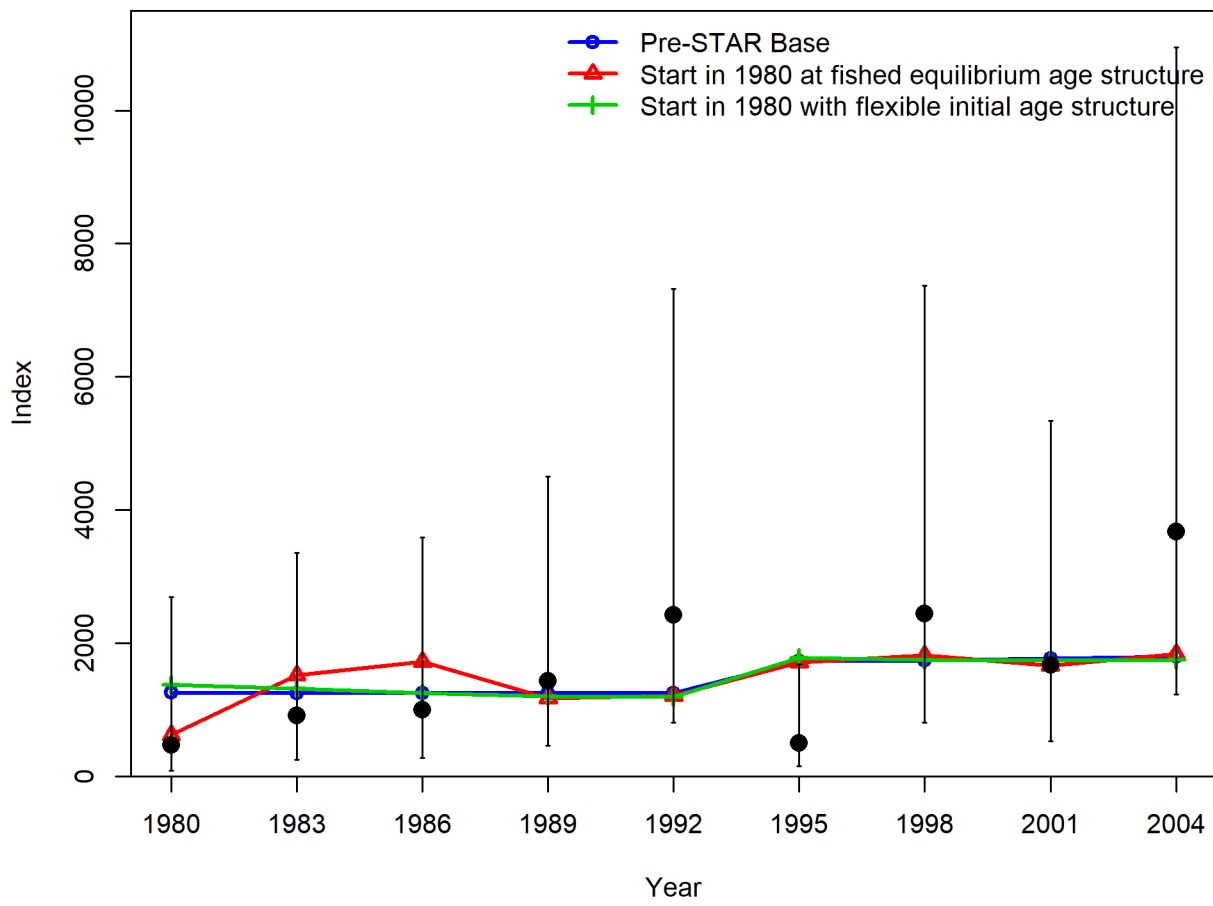


Figure B-5: Fit to Triennial Survey index for the pre-STAR base model and the two alternative models that started in 1980. Uncertainty intervals include the extra standard deviation estimates from the pre-STAR base model.

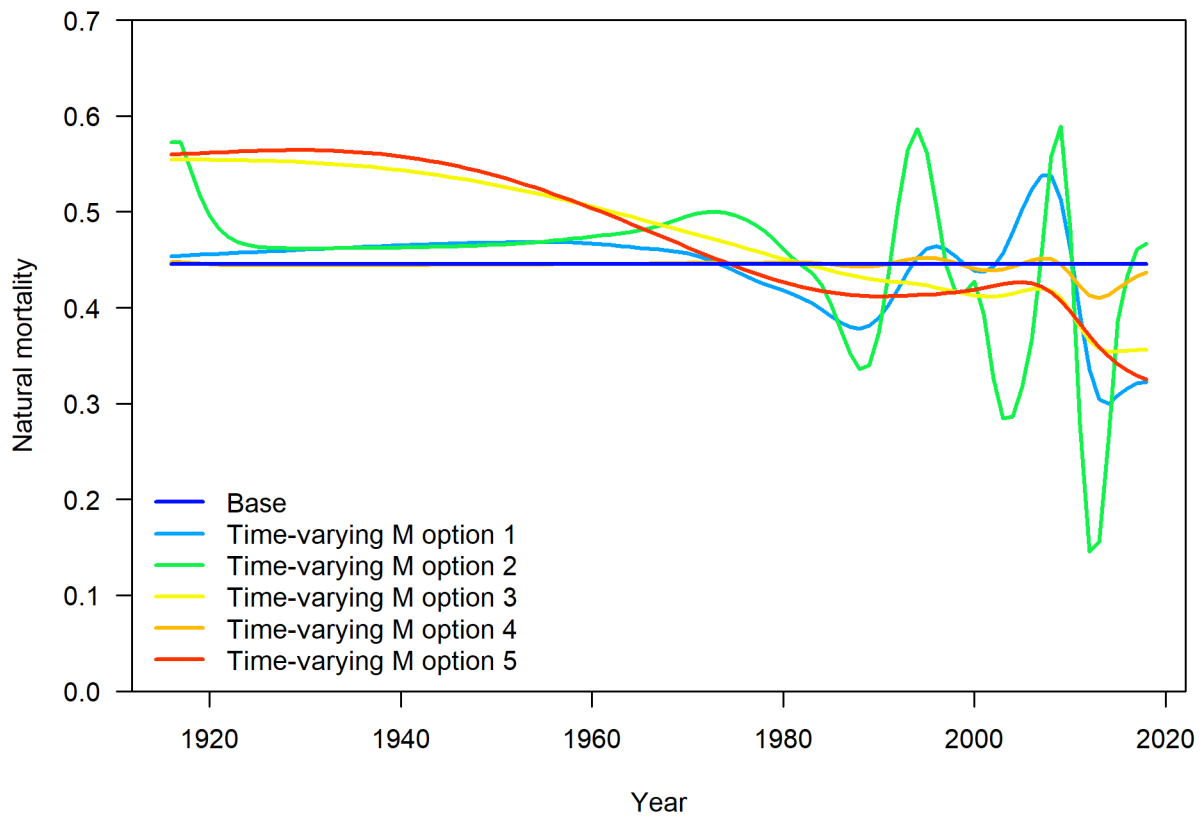


Figure B-6: Time series of time-varying natural mortality for sensitivity analyses associated with STAR request 3.

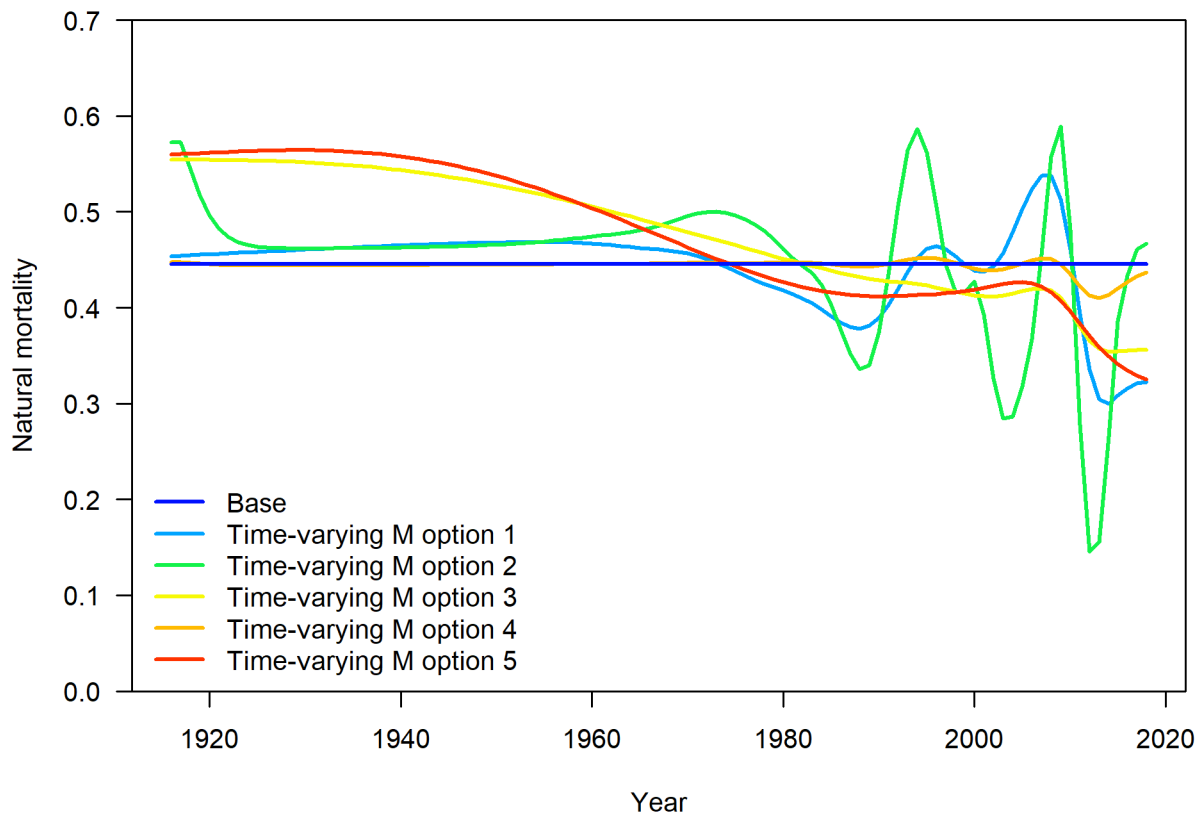


Figure B-7: Time series of time-varying natural mortality estimated in 5 models with different options for variability and autocorrelation associated with STAR request 3.

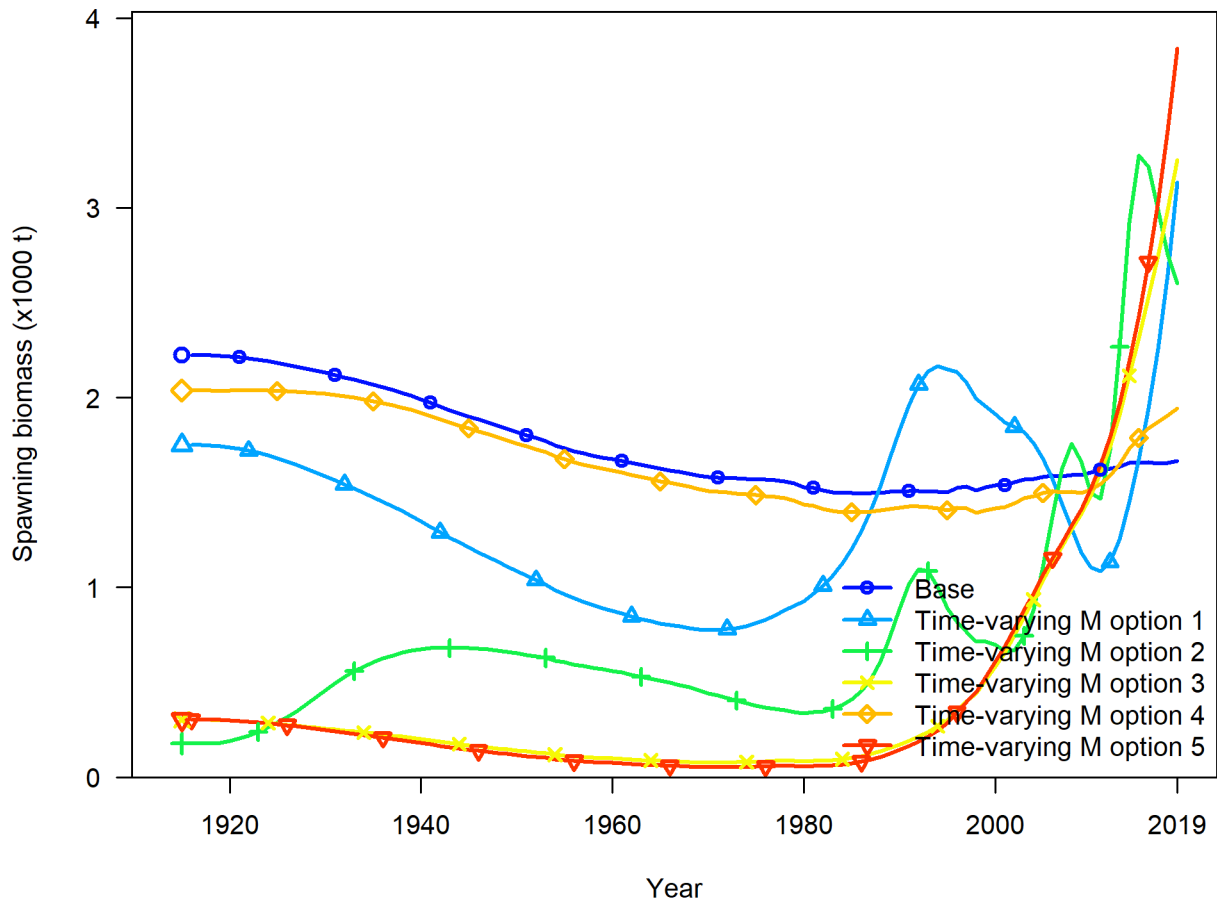


Figure B-8: Time series of spawning biomass estimated in the models with time-varying natural mortality associated with STAR request 3.

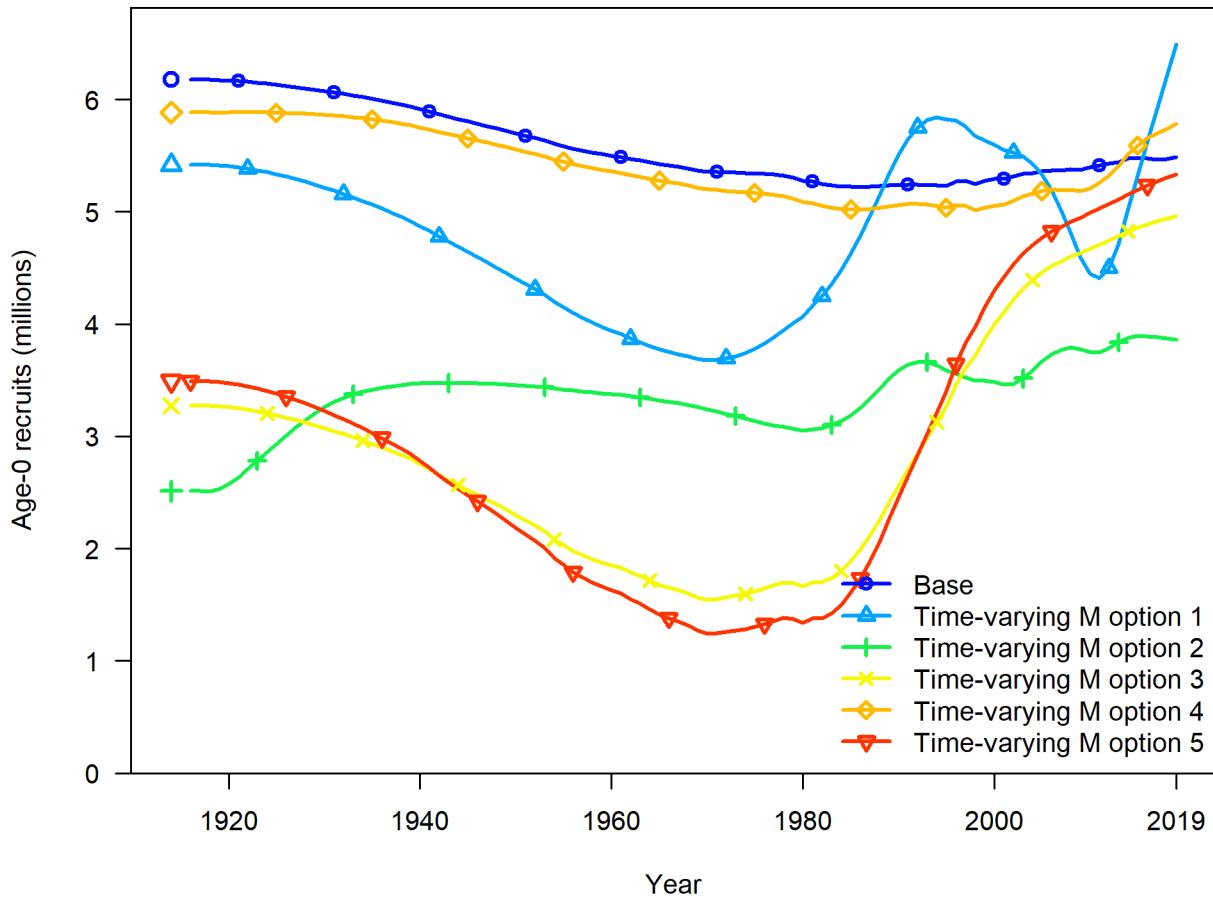


Figure B-9: Time series of recruitment estimated in the models with time-varying natural mortality associated with STAR request 3.

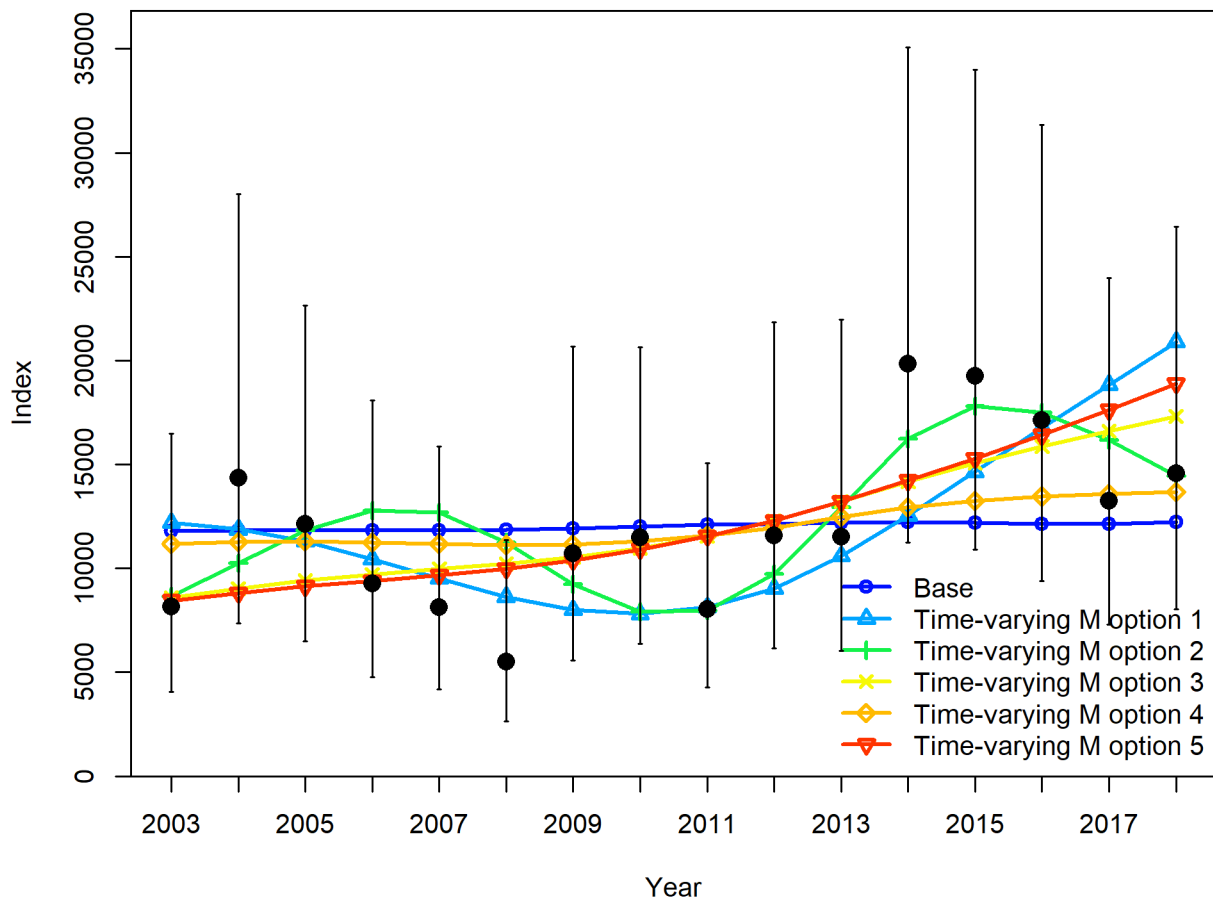


Figure B-10: Fit to WCGBT Survey index for the models with time-varying natural mortality. Uncertainty intervals include the extra standard deviation estimates from the pre-STAR base model.

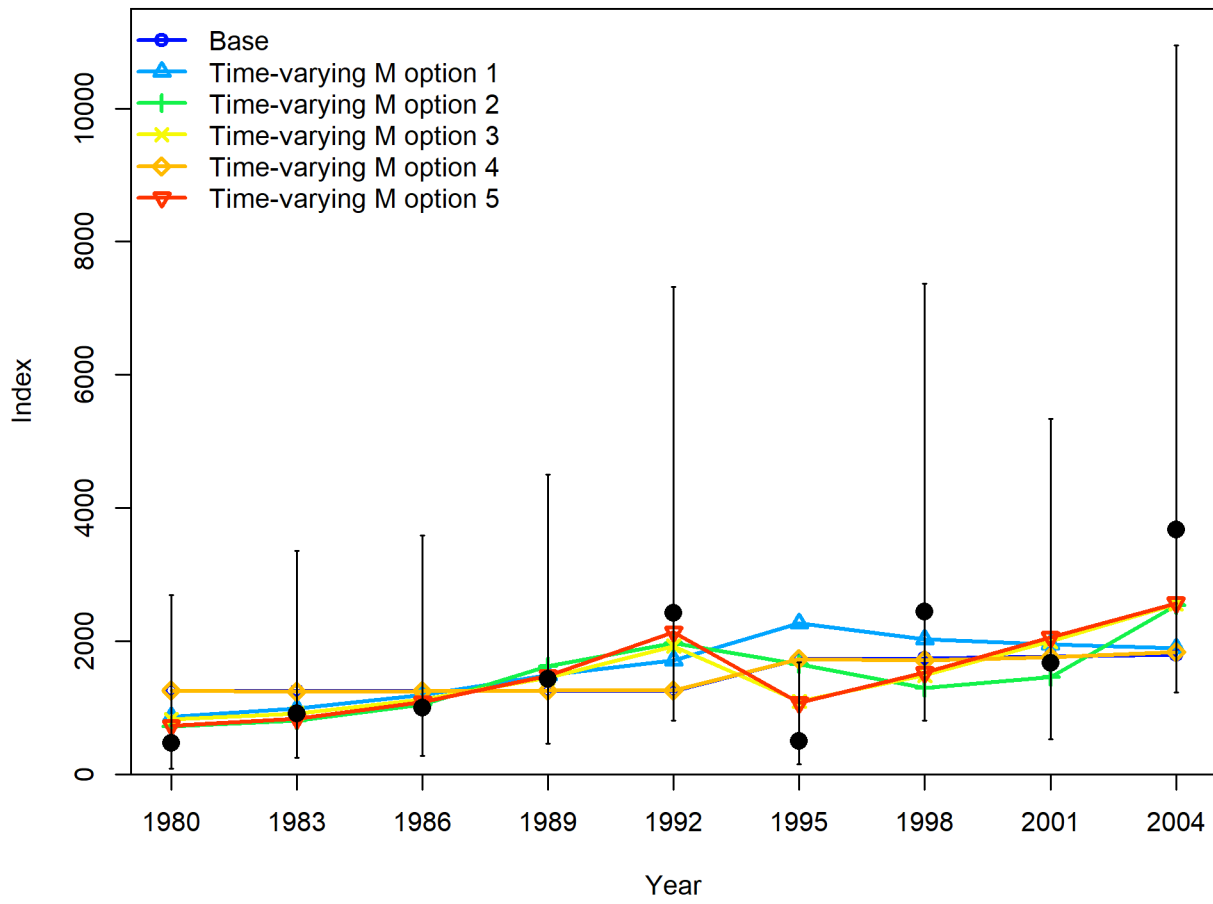


Figure B-11: Fit to Triennial Survey index for the models with time-varying natural mortality. Uncertainty intervals include the extra standard deviation estimates from the pre-STAR base model.

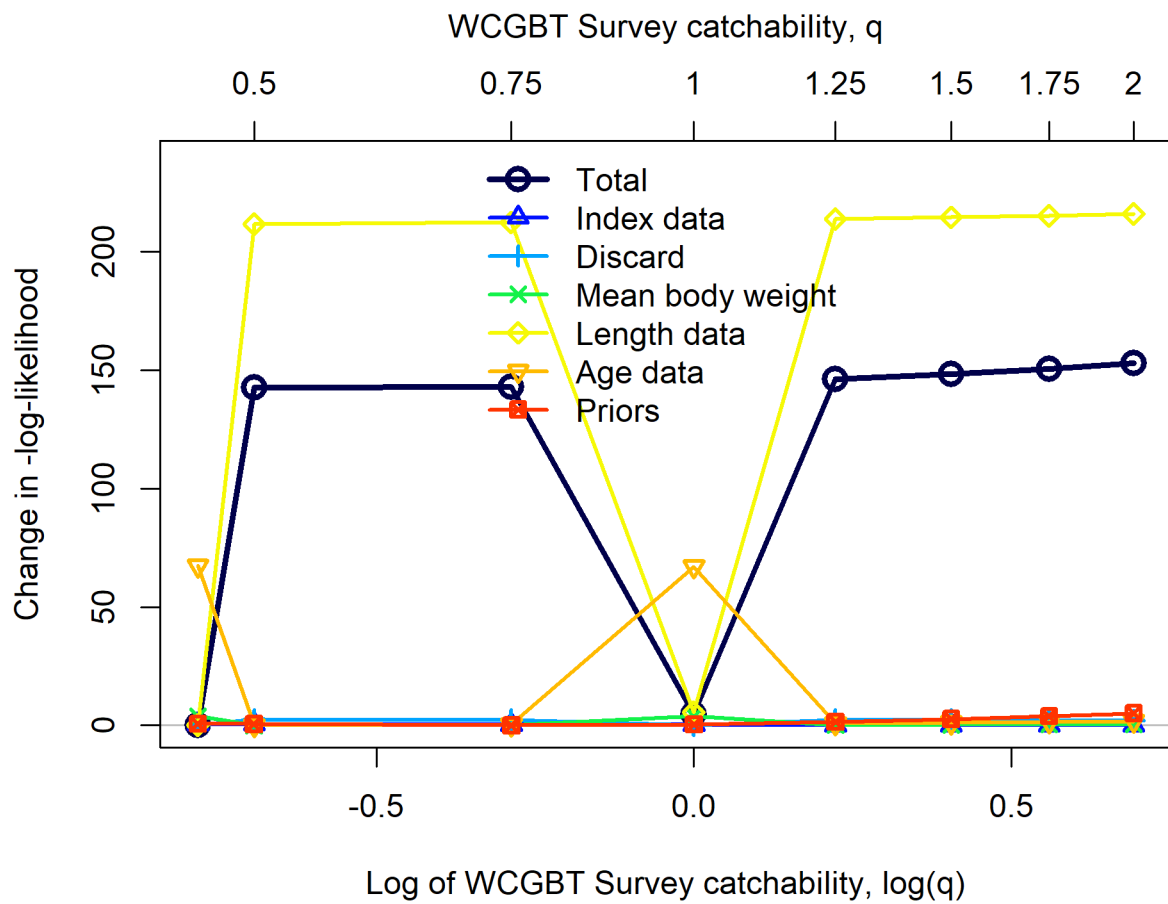


Figure B-12: Likelihood profile over the catchability of the WCGBT survey (q) for an alternative model with Dirichlet-Multinomial likelihood showing issues with convergence of some of the model runs.

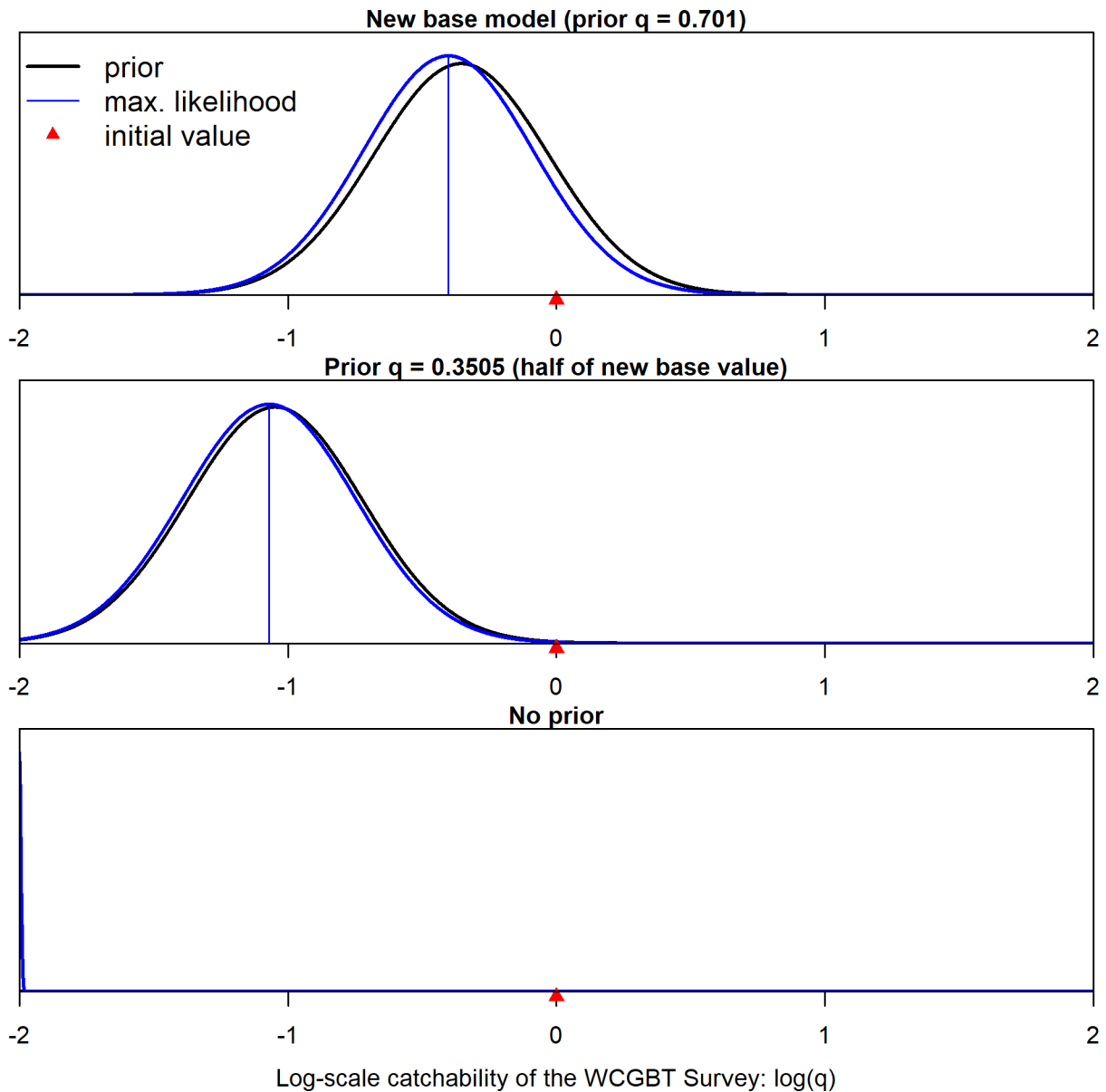


Figure B-13: Comparison of prior and maximum likelihood estimates with asymptotic approximation of uncertainty for the new prior and two alternative prior setups associated with STAR panel request 6.

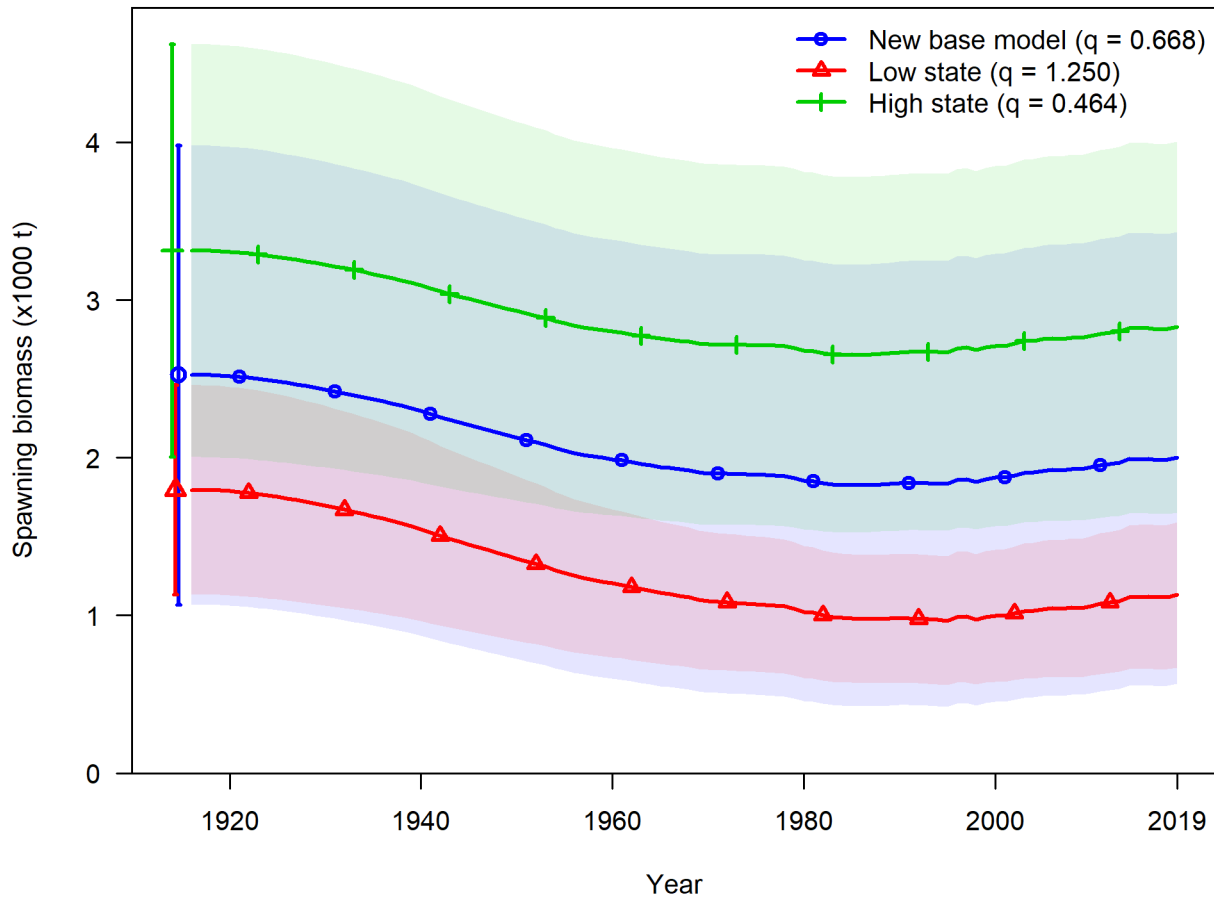


Figure B-14: Time series of spawning biomass with approximate 95% asymptotic intervals for the low and high states of nature compared to the base model.

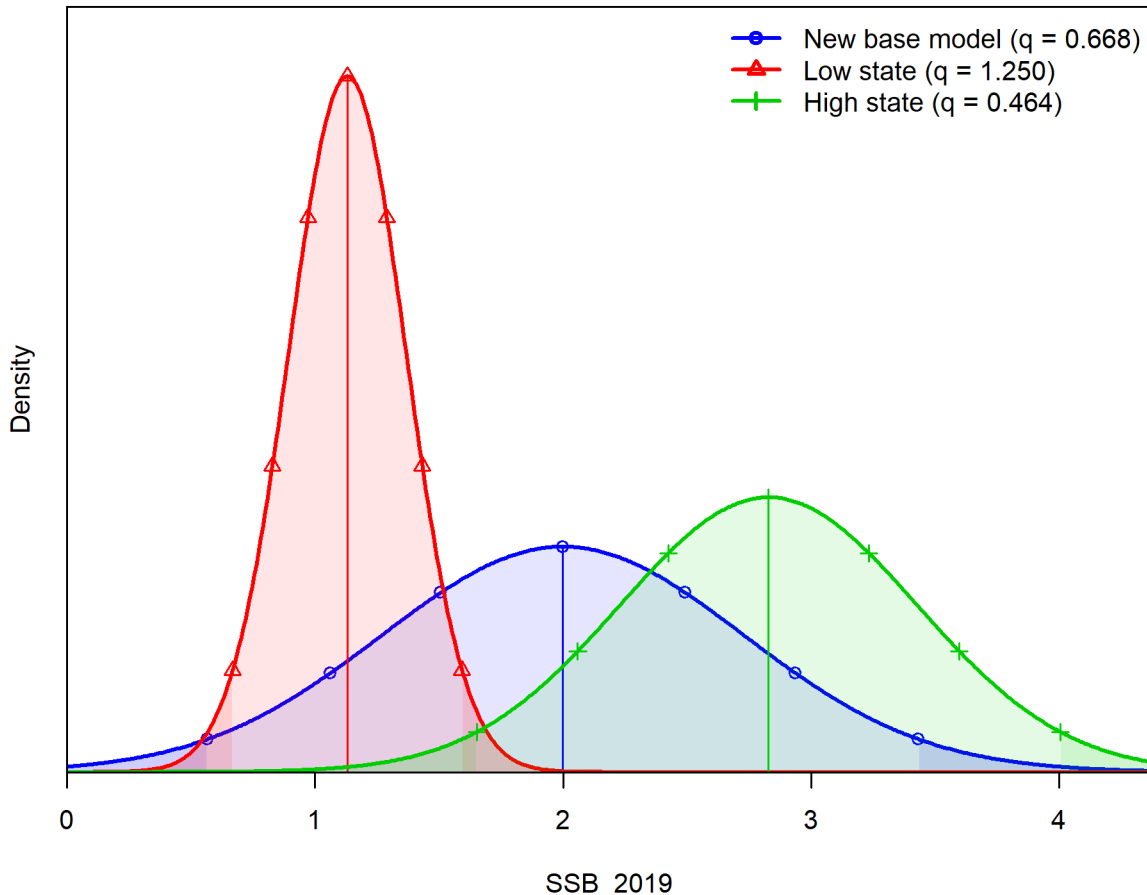


Figure B-15: Maximum likelihood estimates and approximate asymptotic uncertainty for 2019 spawning biomass from the low and high states of nature compared to the base model. The symbols on each curve indicate the 2.5%, 10%, 25%, 50%, 75%, 90%, and 97.5% quantiles and the low and high MLE estimates are just inside the 10% and 90% quantiles.

Appendix C. Auxiliary files

Links to model input files and supplementary tables will be provided here in the final version of this document.